Ollscoil na hÉireann, Corcaigh

The National University of Ireland, Cork

University College Cork

School of Food and Nutritional Sciences

Head: Professor Paul L.H. McSweeney

Supervisors: Doctor Mark A. E. Auty, Professor Alan Kelly, and Doctor James A. O'Mahony

Effect of Phytosterol Enrichment on the Crystallisation, Physiochemical, and Interfacial Behaviour of Bulk and Emulsified Milk Fat Triacylglycerol Matrices

Thesis presented by

Lisa M. Zychowski

teagasc
Agriculture and Food Development Authority

B.Sc. Food Science and Technology, University of Wisconsin, Madison

for the degree of

Doctor of Philosophy

in

Food Science and Technology

January, 2018

Table of Contents

Declaration

I hereby declare that the work submitted is entirely my own and has not been submitted to any other university or higher education institute, or for any other academic award in this university.

Signature: _____ Date: _____

Lisa Zychowski

Acknowledgements

I gratefully acknowledge the financial support of Teagasc, the Walsh Fellowship program, and RMIT for funding my research in Ireland and Australia. I would also like to thank CSIRO Food and Nutrition for aiding in experimental costs during my studies in Australia.

I would like to sincerely thank my main supervisor, Dr. Mark Auty, for providing me with the opportunity to pursue my doctoral degree in his research group. I would also like to acknowledge my academic supervisors, Professor Alan Kelly and Dr. Seamus O' Mahony, for their encouragement and support during the last 4 years. As I conducted a lot of my research abroad, I was very privileged to have the guidance of Dr. Amy Logan, Dr. Mary Ann Augustin, and Dr. Charlotte Conn. Thank you for your time and willingness to help me conduct my synchrotron work.

I am also very thankful for the numerous people I have been fortunate enough to work with in both Ireland and Australia. I would like to thank everyone at Moorepark, UCC, CSIRO, Melbourne University, and RMIT. Specifically, I would like to thank Lisa Blazo, Kamil Drapala, Grace Kelly, Patrick Maher, Mattia Bioiani, Meng Li, Anne Marie Mc Auliffe, Aoife Buggy, Stephen Homer, Tamar Greaves, Jared Raynes, Phil Muller, Li Day, and Mi Xu. Thank you all for your kindness, advice, and enthusiasm during my studies.

Finally, I would like to express my deepest gratitude to my father and mother for their unfaltering commitment to my education. To my siblings for their optimism and humour, thank you, it was certainly needed some days. To Javier thank you for your kindness and reassurance, especially during the last couple of months my Ph.D.

This experience has completely changed my outlook on life in both a personal and professional content. I am extremely grateful for everyone who has been involved. Thank you all for your support.

Introduction

In the last twenty years, there has been a rapid increase in the types of commercially available functional foods. Phytosterols have been one of the longest and most widely utilised bioactives in food, due to their well-studied ability to lower LDL cholesterol levels. Extensive research has been conducted on phytosterols and on their various health benefits; however, very little work has explored how phytosterols behave and interact when incorporated into different food matrices, nor on how the presence of phytosterols influences the physicochemical properties of the food system.

In this work, phytosterols were studied in milk fat matrices in either a bulk or emulsified system, with whey protein as the emulsifier. Milk fat was chosen to create a model dairy matrix, as dairy products are often used for phytosterol encapsulation and due to the proven bioaccessibility of functional dairy products. Phytosterols were enriched into the various milk fat matrices and these were examined to determine the underlying mechanisms of phytosterol crystallisation, how phytosterol enrichment influences milk fat crystallisation, and how phytosterols can influence the overall physicochemical properties of a food system. In addition, the research reported in this thesis sought to understand how the presence of the o/w interfacial layer influenced the crystallisation behaviour of the system both with and without phytosterols and whey proteins.

Information gathered during this study provides important fundamental information on the crystallisation behaviour of phytosterols within milk fat systems. In addition, physicochemical changes resulting from phytosterol addition and crystallisation were documented to understand the influence of phytosterol enrichment on the given food system. Knowledge gained during this study is useful in the understanding of phytosterol within food systems, and regarding the enrichment of milk fat with bioactives. This information can be applied to not only dairy products but also to other functional food systems.

Abstract

Phytosterols possess the ability to significantly lower levels of low-density lipoprotein (LDL) cholesterol in the blood, but their bioaccessibility is dependent upon the solubility of the phytosterol in the consumable food or pharmaceutical product. Phytosterols are one of the most commonly used groups of bioactive compounds in the functional food industry. However, very little research has examined how phytosterols crystallise within food systems or how the physiochemical properties of the food system change upon phytosterol addition. The studies in this thesis investigated phytosterol addition in bulk and emulsified milk fat matrices, as dairy products are a common matrix for phytosterol enrichment. The main objectives of the thesis were to: (i) characterise the collective crystalline behaviour of both milk fat and phytosterols; (ii) quantify how phytosterol enrichment influences the physiochemical properties of the food system; (iii) investigate how an oil-in-water (o/w) interface influences phytosterol and milk fat crystalline behaviour; and (iv) develop and assess the means by which phytosterol solubility could be improved in milk fat matrices. In both the emulsion and bulk milk systems employed, the level of phytosterol-enrichment in milk fat was either 0 (the control), 3, or 6%. In phytosterol-enriched emulsions, whey protein (1%) was employed as the emulsifier in emulsions with 10% oil and 89% water. During cooling, phytosterols addition altered the nucleation temperature of emulsions, but no such effect was identified in bulk milk fat. During the crystallisation process, emulsified milk fat triacylglycerols (TAG) packing expanded upon phytosterol enrichment, which was observed as an increase in the triple-chain length (3L). In bulk milk fat, both double-chain length (2L) and 3L TAG packing was seen during cooling; the 3L spacing also increased with phytosterol enrichment, but no differences were seen in the 2L packing. These results suggest that phytosterols can insert themselves into the milk fat TAG network during cooling; however, the overall polymorphic form did not change. After storage, the milk fat TAG network developed into more structured polymorphic forms, and phytosterols were no longer found within the TAG packing. Phytosterols were also found to be able to decrease the average size of droplets in an emulsion and participate in a synergistic interaction with whey protein at the emulsion interface. In addition, phytosterol enrichment was found to have no

negative effect on the creaming behaviour of the emulsions. Phytosterol crystallisation was altered by the addition of low molecular weight surfactants, lecithin and monoacylglycerol (MAG), and by changing the average droplet size from 1.0 to 0.2 μm. Lecithin and MAG addition significantly decreased phytosterol crystallisation in the bulk form, but changes in phytosterol crystallisation behaviour in the emulsified form were mainly driven by the decrease in droplet size. The lecithin-containing emulsions with the smaller droplets, however, showed the greatest potential for improved phytosterol solubility; in addition, they possessed better emulsion stability, as compared to the control and MAG-enriched emulsions. As the crystallisation properties of an emulsion are greatly affected by the o/w interface, two purified milk fat TAG lipids without surfactants or emulsifiers were studied in a grazing incidence synchrotron system. Differences between the lipid droplets were distinguishable, but further work is needed on the droplet deposition. In conclusion, the studies conducted in this thesis provide important insight on the behaviour of phytosterols in a model TAG-based system and can be utilised by the functional food or pharmaceutical industries to improve the bioaccessibility of phytosterols and possibility other lipophilic bioactives.

Publications and conference contributions

Publications

Zychowski, L. M., Logan, A., Augustin, M. A., Kelly, A. L., Zabara, A., O'Mahony, J. A., Conn, C. E., Auty, M. A. (2016). Effect of phytosterols on the crystallization behavior of oil-in-water milk fat emulsions. *Journal of Agricultural and Food Chemistry, 64*(34), 6546–6554.

Submitted manuscripts

Zychowski, L. M., Logan, A., Augustin, M. A., Kelly, A. L., O'Mahony, J. A., Conn, C. E., Auty, M. A. (2017). Phytosterol crystallisation within bulk and dispersed triacylglycerol matrices as influenced by oil droplet size and low molecular weight surfactant addition. *Food Chemistry.*

Manuscripts prepared for submission

Zychowski, L. M., Mettu, S., Dagastine, R. R., O'Mahony, J. A., & Auty, M. A. (2017). Physical and interfacial characterization of phytosterols in oil-in-water triacylglycerol-based emulsions. *Food Structure.* .

Zychowski, L. M., Logan, A., Augustin, M. A., Kelly, A. L., O'Mahony, J. A., Conn, C. E., Auty, M. A. (2017). The crystallisation behaviour of phytosterols in bulk milk fat. *Food Research International.*

Oral presentations

Zychowski, L.M., Logan, A., Augustin, M.A., Kelly, A.L., Zabara, A., O'Mahony, J.A., Greaves, T., Conn, C. and Auty, M.A.E. Structuring emulsion interfaces to control phytosterol crystallization in dispersed systems. *30th Australian Colloid and Surface Science Student Conference,* Kioloa, Australia (1st-4th February 2016).

Zychowski, L.M., Logan, A., Augustin, M.A., Kelly, A.L., O'Mahony, J.A., Conn, C. and Auty, M.A.E. Crystallization of phytosterols in dispersed systems. *2nd Food Structure and Functionality Forum Symposium,* Singapore, Singapore (28th February- 2nd March 2016).

Zychowski, L.M., Logan, A., Augustin, M.A., Boyd, B., Kelly, A.L., O'Mahony, J.A., Greaves, T., Conn, C. and Auty, M.A.E. The use of synchrotron X-ray scattering in designing functional food matrices with improved bioavailability. *2nd Food Structure Design Conference,* Antalya, Turkey (26th-28th October 2016).

Zychowski, L.M., Logan, A., Augustin, M.A., Kelly, A.L., O'Mahony, J.A., Conn, C. and Auty, M.A.E. Interfacial interactions within emulsified systems containing phytosterols and whey proteins**.** *Australian Colloid and Interface Symposium,* Coffs Harbour Australia (29th Januaray-2nd February 2017).

Poster presentations

Zychowski, L.M., Logan, A., Augustin, M.A., Kelly, A.L., Zabara, A., O'Mahony, J.A., and Auty, M.A.E. Encapsulation of plant sterols with whey protein in milk fat based emulsions. *Australian Institute of Food Science and Technology Summer Conference,* Melbourne, Australia (28th-30th January 2015).

Zychowski, L.M., Logan, A., Augustin, M.A., Kelly, A.L., Zabara, A., O'Mahony, J.A., and Auty, M.A.E. Plant sterols affect the crystallization behavior of milk fat in emulsified system. *Institute of Food Technologists (IFT) Annual Meeting*. Chicago, Illinois. (11th-14th July 2015).

Zychowski, L.M., Logan, A., Augustin, M.A., Kelly, A.L., Zabara, A., O'Mahony, J.A., Greaves, T., Conn, C., and Auty, M.A.E. Phytosterol crystallisation in dispersed systems. *Australasian Soft Matter Scattering Workshop,* Melbourne, Australia (11th-12th February 2016).

Zychowski, L.M., Logan, A., Augustin, M.A., Kelly, A.L., Zabara, A., O'Mahony, J.A., Greaves, T., Conn, C., and Auty, M.A.E. Controlling the crystallisation behaviour of phytosterols in functional dairy systems. *IuFOST International Union of Food Science and Technology Conference (IUFoST),* Dublin, Ireland (21st-25th August 2016).

Abbreviations and nomenclature

$D_{4,3}$=Volume-weighted mean diameters

2L=Double-chain length

3L=Triple-chain length

CLSM=Confocal laser scanning microscopy

Cryo-SEM= Cryogenic scanning electron microscopy

DSC=Differential scanning calorimetry

FAMES= Fatty acid methyl esters

FWHM =Full-width at half-maximum

GISAXS=Grazing incident small-angle X-ray scattering

MAG=Monoacylglycerol

PE=Phytosterol-enriched

SAXS=Small-angle X-ray scattering

TAG=Triacylglycerol

WAXS=Wide-angle X-ray scattering

WPI=Whey protein isolate

Chapter 1

Literature review

Lisa M. Zychowski[†§]

[†] Food Chemistry and Technology Department, Teagasc Food Research Centre, Moorepark, Fermoy, Co. Cork, Ireland

[§] School of Food and Nutritional Sciences, University College Cork, Cork, Ireland

Table of Contents- Chapter 1-Literature Review

1.1 Milk fat

Milk is a naturally occurring emulsion comprising a complex mixture of lipids dispersed within an aqueous serum phase. The lipid phase in milk is distributed in the form of droplets ≤ 1 to ~10 μm in diameter that are surrounded by an amphiphilic membrane, known as the milk fat globule membrane (MFGM; El-Loly, 2011). Milk fat provides the main source of energy for the new-born calf, along with essential fatty acids, fat-soluble nutrients, and other bioactive compounds, such as sphingolipids and cholesterol (Fox & McSweeney, 2006; Lopez, 2011).

Table 1.1 The classes of lipids in milk

Lipid Class	Average Amount (%, w/w)
Triacylglycerols	98.3
Diacylglycerols	0.3
Monoacylglycerols	0.03
Free fatty acids	0.1
Phospholipids	0.8
Sterols	0.3
Carotenoids	Trace
Fat-soluble vitamins	Trace
Flavour compounds	Trace

Adapted from Jenness &Walstra (1989) and MacGibbon & Taylor (2006).

Bovine milk typically contains 3-5% wt/wt milk fat but this can vary in quantity and composition, depending on the phenotype of the cow, season, and lactation stage (Fredrick, 2011). As milk fat influences many of the functional aspects of milk and its products, it is important to study milk fat and its compositional changes to understand how biological variation can influence the final functionality. The physicochemical properties of milk fat are mainly determined by triacylglycerols (TAG), which account for 95-98% of the total fat fraction (Fox & McSweeney, 2006). Even a slight change in the compositional profile of the triacylglycerols has been known to alter the rheological and crystallisation properties of dairy products (Shi et al., 2001).

Although TAG dictate many of the physical properties of milk, it is the minor components, i.e., phospholipids, monoacylglycerols and diacylglycerols that construct the actual MFGM (El-Loly, 2011). Without the amphiphilic nature of the MFGM

components, milk fat could not disperse in a stable manner in the aqueous phase of milk. Additional minor components found in the MFGM, include sterols, glycolipids, and free fatty acids, which aid in the dispersion of milk fat (Singh, 2006). The composition of the major and minor types of lipids are listed in Table 1.1.

1.1.1 Biological function of milk

The production of milk fat is initiated in the secretory cells of the mammary glands. The TAG are produced on, or inside, the surfaces of rough endoplasmic reticulum and accumulate as microlipid droplets (diameter < 0.5 μm to 2 μm) in the cytoplasm (Heid & Keenan, 2005). The droplets are coated with an interfacial layer composed of phospholipids, glycosphingolipids, cholesterol, and proteins, and grow in volume over time fusing together to form cytoplasmic lipid droplets ≥8 μm in diameter (Lopez, 2011). Fused droplets migrate to the apical pole of the cell and are secreted from the epithelial cell through progressive envelopment by the plasma membrane (Heid & Keenan, 2005). Secretion from the cell leaves the droplets with a layer of apical plasma membrane, which comprises the majority of the final MFGM composition (Wooding, 1971).

The MFGM helps to disperse the unstable milk fat globules within the milk for energy and nutrient delivery to the calf. Milk fat provides 9 kcal of energy for the calf for every gram of fat consumed (Smith, S. & Abraham, 1975). The essential fatty acids in milk fat are critical for neonatal development, as they cannot be synthesised by the calf (Hendricks & Guo, 2006). Milk fat is also important for the transport of lipid-soluble substances to the calf, such as vitamins A, E, D, and K, and carotenoids. Phytosterols can also be found within milk in trace amounts, along with cholesterol, the main sterol in milk at ≈3 mg/g (Baldi & Pinotti, 2008). Essential fatty acids, vitamins, and sterols are embedded in the milk fat fraction, which influences their bioaccessibility and bioavailability from milk (German & Dillard, 2006). The bioaccessibility being the potential for a substance to interact with and be absorbed by an organism, while the bioavailability refers to the amount of the compound which reaches the site of physiological activity after administration (Rodriguez- Amaya, 2015).

The ability of milk fat to deliver nutrients is not a coincidence, as milk is a unique food for neonates and is critical for early development. For example, intake of high-fat colostrum within the first 24 h of life is essential for supplying lipid-soluble compounds such as carotene, retinol, and α-tocopherol necessary for the first week of life (Kehoe et al., 2007). Mechanistically, this is most likely due to the fact that during digestion, bovine and other mammalian milk fats form what is known as a bicontinuous cubic phase (Salentinig et al., 2013). The large surface area and hydrophilic/hydrophobic nature of cubic phases results in a high uptake of the bioactives encapsulated therein (Barauskas et al., 2005). Lipids can form numerous other structures during digestion, such as hexasomes, sponges, and micelles, but the bicontinuous cubic phase has been shown to be one of the most effective for improving the bioaccessibility of bioactive compounds (Sagalowicz et al., 2006).

Hence, the bicontinuous cubic phase is after the most desired structure in pharmaceutical applications and it occurs naturally within mammalian milk fats, making them ideal for bioactive delivery (Salentinig et al., 2013). This principle also seems to apply across different species, as results from a human study have shown improved α-tocopherol absorption in enriched whole cow's milk, as opposed to soy milk (Cilla et al., 2012). Bovine milk enriched with oleic acid and long-chain omega-3 fatty acids also were also found to be effective in promoting absorption of unsaturated fatty acid; a review of nine previous studies showed decreased low density lipoprotein (LDL) cholesterol levels in the blood and an overall improvement in the cardiovascular health of patients who consumed fatty acid-enriched bovine milks (Lopez-Huertas, 2010).

1.1.2 Industrial applications of milk fat

Milk fat has an important functional role in butter, whipped cream, ice creams and numerous other dairy products. For example, in cheese milk fat influences the melting properties, microstructure, yield, texture, and flavour (Guinee et al., 1999). In cheese, milk fat globules disrupt the continuous casein protein matrix and change the microstructure of the final product. In higher fat cheeses, the milk fat globules tend to aggregate, while in lower fat cheeses the fat globules are smaller and more uniform;

this alters the texture of cheeses, such as low-fat Mozzarella, where the smaller fat globules enable the casein protein strands to separate as the curd forms, leading to the stringy texture of low-fat mozzarella (Guinee & McSweeney, 2006).

The way lipids crystallise within milk fat is also important, as crystallisation changes the physio-chemical properties of the system. In native milk fat globules, milk fat crystallisation within droplets leads to coalescence and eventual creaming (Huppertz & Kelly, 2006). This is in fact advantageous in ice cream, where partially crystalline milk fat droplets are essential for optimal fat structure formation during the freezing process (Fig. 1.1; Goff, 2003). In butter, the three-dimensional crystalline network formed by milk fat is responsible for the yield stress and viscoelastic behaviour of the final spread, so much so that even slight changes in the composition of milk fat between seasons (i.e., more saturated fatty acids in the winter months) can lead to a firmer butter (Palmquist et al., 1993).

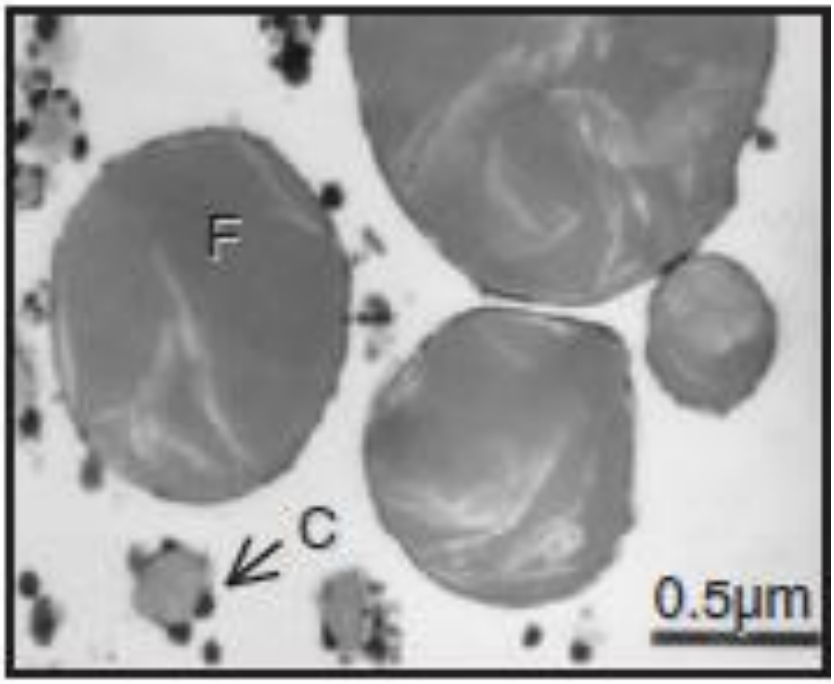

Figure 1.1 *Milk fat crystals in ice cream mix showing fat globules (F) in mix with crystalline fat within the globule and (C) adsorbed casein micelle, as viewed by thin section transmission electron microscopy (TEM; Goff., 2003).*

1.1.3 Chemical composition of milk fat

Milk fat is an extremely complex lipid composed mainly of TAG, with minor components including diacylglycerols, phospholipids, sterols, and free fatty acids (Table 1.1; Fredrick, 2011). The composition and variety of these components influences the final functional properties of the milk fat and are explained in detail below.

1.1.3.1 Major components

Milk fat is mainly composed of TAG, which are constructed from a glycerol backbone with 3 fatty acids attached through ester bonds (Fig. 1.2). The 3 hydroxyl groups on the glycerol backbone are 3 potential positions for fatty acid attachment. As there are over 400 fatty acids in milk fat, the variation in milk fat TAG composition is quite diverse, making it one of the most complex biological lipids (Jensen, 2000; Fredrick, 2011). While there are numerous different recorded fatty acids in milk, only 14 fatty acids make up ≥ 1.0% of the total fat fraction (Table 1.2). The different chain lengths and degrees of saturation in fatty acids not only contribute to the compositional complexity but also produce a broad melting range for milk fat (Fredrick, 2011).

In milk fat, 70-75% of the fatty acids are saturated, generally linear, and possess an even number of carbons (Fig. 1.2.a). The saturated fatty acids are considered either short chain (4-6 carbon chain), medium chain (8-12 carbons chain), or long chain (≥ 13 carbon chain). The short and medium chain fatty acids are present in milk fat at ≥ 14% wt/wt help lower the melting point, as milk fat needs to be liquid at physiological temperatures (Table 1.2). In addition, the short and medium chain fatty acids are metabolised quickly by the liver and provide rapid energy for the calf (Van Aken et al., 1999). However, the longer-chain saturated fatty acids make up the majority of the fatty acids found within milk. The most common saturated fatty acid within bovine milk fat is palmitic, as it makes up 23.6-32.34% wt/wt of the total milk faction.

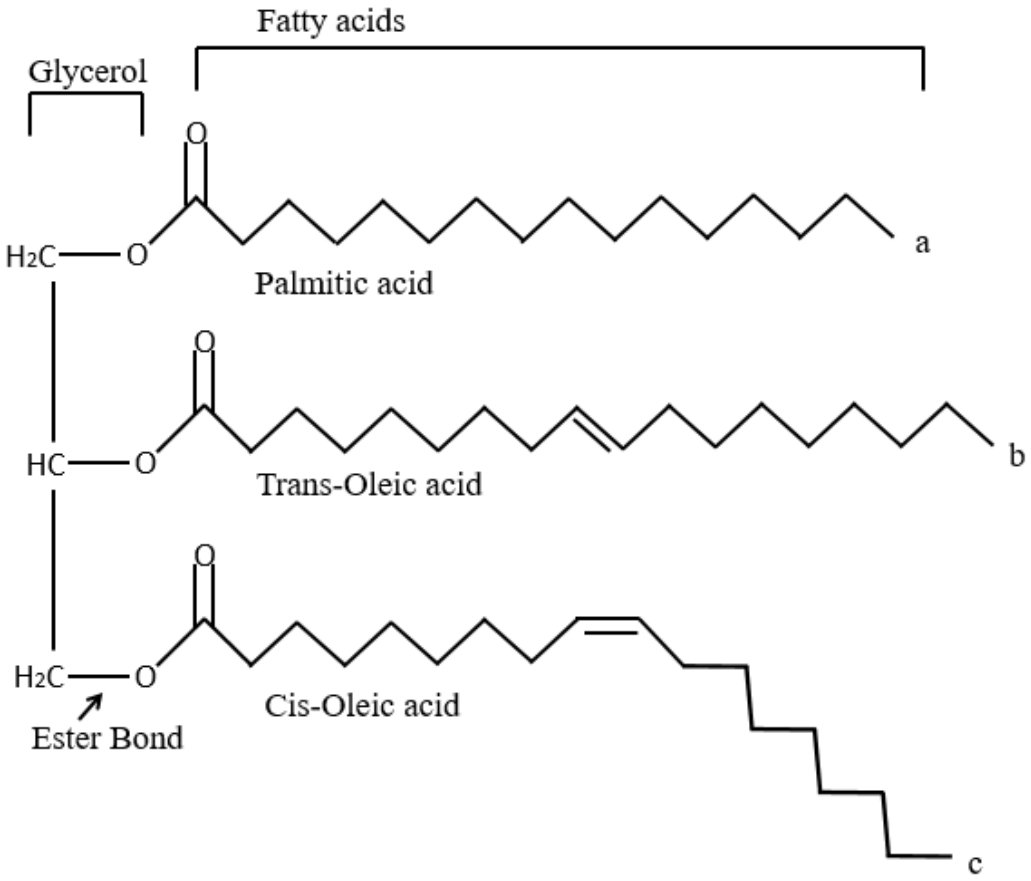

Figure 1.2 *Schematic representation of sample triacylglycerol molecule with 3 fatty acid moieties attached to a glycerol backbone; (a) palmitic fatty acid (b) trans-oleic acid, and (c) cis-oleic acid.*

Unsaturated fatty acids are also found within milk, meaning the carbon chain contains double bonds (Fig. 1.2. b-c). Most of these unsaturated fatty acids have double bonds in what is known as a cis-configuration, meaning the hydrogen atoms are adjacent to the double bond (Fig. 1.2.c). This *cis*-formation causes the carbon chain to bend, as opposed to the linear trans-configuration, where the hydrogen atoms are on the opposite side of the double bond (Damodaran et al., 2007). The most prevalent unsaturated fatty acid in milk is oleic acid at 14.9-20.0%, but the most studied fatty acid in milk is conjugated linolenic acid. Conjugated linolenic acid (CLA) possesses a double *cis*- and a *trans*-bond. Trans-fat consumption in the diet has been well documented to negatively influence blood plasma ratios by lowering high-density lipoprotein (HDL) and increasing LDL lipoprotein (Kummerow, 2009). However,

CLA is an extremely unique fatty acid, as it has been found to possess antiatherogenic, antidiabetic, and anticargenic properties (Nagao & Yanagita, 2005).

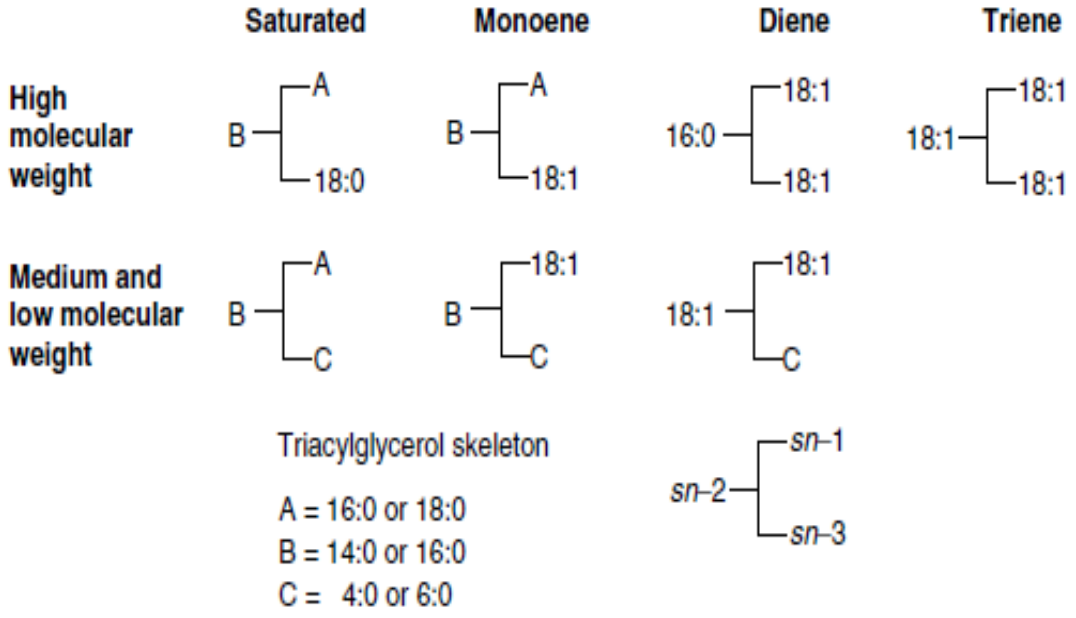

Figure 1.3 *Probable composition of the major triacylglycerols of milk fat (MacGibbon & Taylor, 2006).*

These fatty acids along with the glycerol backbone constitute the molecular structure of TAG (Fig. 1.2). Although the variety of TAG within milk fat is diverse, the fatty acid molecules are not randomly distributed. Typically, short-chain fatty acids are present on the sn-3 position within the TAG molecule, while 12:0 and 14:0 fatty acids are preferentially esterified at the sn-2 position (Jensen, 2002). Palmitic (16:0) can be found either at the sn-1 or sn-2 position. Saturated fatty acids tend to be found at either the sn-1 or sn-3 position (MacGibbon & Taylor, 2006).

As milk fat possess many TAG species, quantifying the composition and position of the fatty acids within milk fat has proven difficult. The most likely position of the majority of TAG is given in Figure 1.3, which has been hypothesised based on a combinations of separations and chromatographic methods (Kuksis et al., 1973; MacGibbon & Taylor, 2006). In a study by Gresti et al. (1993), employing high performance liquid chromatography (HPLC) and capillary gas chromatography, individual triglycerides were quantified with only 55% of the milk fat TAG consisting

of ≥0.5% of the total TAG profile. The most prevalent TAG were 4:0, 16:0, 18:1 (4.2%) and 4:0, 16:0, 16:0 (3.2%). Despite numerous studies, there is still not a method which can definitively quantify and identify the position of all the TAG components of milk fat (MacGibbon & Taylor, 2006).

1.1.3.2 Minor components

Minor components of milk fat consist of all non-TAG molecules (Table 1.1). The most important among these minor components are phospholipids (Fredrick, 2011). phospholipids possess a hydrophilic head with two hydrophobic fatty acid tails, which give them an amphiphilic nature; thus, phospholipids are crucial for milk fat stability within milk and are mostly derived from the MFGM (MacGibbon & Taylor, 2006).

The second most prevalent minor lipid components are sterols, which consist mainly of cholesterol (95%). Trace amounts of phytosterols such as campesterol, stigmasterol, and β-sitosterol are also present in milk fat (Parodi, 1973; Fox & McSweeney, 2006). Free fatty acids, diacylglycerols, and monoacylglycerols are also present due to incomplete TAG synthesis or the action of lipases. The production of excess free fatty acids can contribute to noticeable off flavours in dairy products, such as rancidity (Fredrick, 2011). Carotenoids give milk fat its amber pigment and are mostly composed of β-carotene. β-carotene in milk fat is dependent on the cow variety and feed, with grass-fed cows producing more β-carotene (Marino et al., 2012). Finally, fat-soluble vitamins A, E, D, and K are also present, which are crucial for the development of the new born calf.

1.4 Factors influencing milk fat composition

As milk fat is a biological material, it can be highly variable based on lactation stage, feed (type and seasonal changes), and breed of cow. The most important factor is the feed of the cow, as diet greatly influences the type of fatty acids that are produced. The most well-known example is that during the summer months, bovine milk fat includes more unsaturated fatty acids due to an increase in consumption of fresh grass (Fredrick, 2011). Bovine diet variations have been studied extensively to understand how diet influences the fatty acid profile of milk fat and its final functionality within dairy products (Wright & Marangoni, 2006). In a study performed by Gonzalez et al.

(2003), the fatty acid profile of milk fat was altered by adding high-oleic or high-linoleic sunflower oil into the diets of cows; this diet alteration significantly decreased the quantity of saturated palmitic acid produced and increased the percentage of the two unsaturated fatty acids, oleic and linoleic. The change in the fatty acid profile of the milk due to sunflower oil enrichment, produced less viscous ice cream and butter with a lower firmness.

The lactation stage also influences the fatty acid profile of milk, along with its minor components. During the early stages of lactation, the cow is in a negative energy balance and must utilise its fat reserves, which are mostly composed of longer chain fatty acids. As lactation progresses, so does the proportion of short chain fatty acids, as less fat is taken from reserves (Palmquist et al., 1993). Early lactation is intended to quickly deliver nutrients to the calf and tends to also have higher levels of fat-soluble vitamins and phospholipids (Ostersen et al., 1997; Kehoe et al., 2007).

The breed of the cow can also alter the quantity and compositional profile of the milk fat produced. Jersey cows have been found to produce higher fat milks than Holstein cows, and variations in fatty acid can also occur between breeds (Soyeurt et al., 2006). As milk fat is complex and can be influenced by many genetic and environmental factors, it has been extensively studied throughout the years. However, still today, there are many opportunities to study milk fat, as the lipid component of milk is crucial in the development of many dairy products.

Table 1.2 Major fatty acids in bovine milk fat

		Range	Typical
	Common name	%(wt/wt)	%(wt/wt)
4:0	Butyric	3.1-4.4	3.9
6:0	Caproic	1.8-2.7	2.5
8:0	Caprylic	1.0-1.7	1.5
10:0	Capric	2.2-3.8	3.2
12:0	Lauric	2.6-4.2	3.6
14:0	Myristic	9.1-11.9	11.1
14:1	Myristoleic	0.5-1.1	0.8
15:0	---	0.9-1.4	1.2
16:0	Palmitic	23.6-31.4	27.9
16:1	Palmitoleic	1.4-2.0	1.5
18:0	Stearic	10.4-14.6	12.2
18:1 Trans11	Rumenic	14.9-22.0	17.2
18:1 Cis 9	Cis-oleic		3.9
18:2	Linoleic	1.2-1.7	1.4
18:2 Cis 9 trans 11	Conjugated Linoleic	0.8-1.5	1.1
18:3	α Linolenic	0.9-1.2	1
	Minor Acids	4.8-7.5	6

Adapted from MacGibbon & Taylor (2006).

1.2 Phytosterols

Phytosterols are naturally occurring compounds found within the plant cell wall membrane. There are over 200 identified types of phytosterols, the most abundant being β-sitosterol (Moreau et al., 2002; Berger et al., 2004). In plants, phytosterols are the substrates for synthesis of various secondary metabolites (i.e., cardenolides, glycoalkaloids, pregnane) and are part of different signalling pathways (Hartmann, 1998). Most importantly, phytosterols regulate fluidity and stability of the plant cell membranes (Hartmann, 1998).

When ≥ 1.5 g of phytosterols are consumed by humans a decrease (≥ 10%) in LDL cholesterol level can be observed (Cusack et al., 2013). Phytosterols also possess anti-carcinogenic and anti-inflammatory properties and have no associated negative side-effects (Berger et al., 2004; Chawla & Goel, 2016). Phytosterols are present within

foods of plant origins, such as vegetables, fruits, cereals, nuts, and plant-based oils but only in limited concentrations. The average consumption of phytosterols is between 160-400 mg per day, and thus supplementation is required to achieve a significant reduction in LDL-cholesterol levels (Berger et al., 2004).

A common way to consume phytosterols is with enriched functional foods, as research has demonstrated that solubilised phytosterols within lipid matrices are more effective at lowering LDL-cholesterol than crystalline phytosterol tablets (Ostlund et al., 1999; Rossi et al., 2010). Despite phytosterol solubility being crucial in the development of functional foods, very little research has been performed on how phytosterol solubility is influence by different food compounds.

1.2.1 Chemical composition of phytosterols, phytostanols, and their fatty acid esters

Phytosterols, which encompass both plant sterols and stanols, are composed of steroid-based structures with hydroxyl groups attached to the C-3 atom and side chain attached to the C-17 atom (Fig. 1.4). Phytosterols are structurally similar to human cholesterol but possess different side chains at the C-22 position and, in the case of stanols lack a double bond at the C-5 position (Fig. 1.4c; Moreau et al., 2002). The side chains differentiate between some of the major phytosterol varieties with sitosterol, stigmasterol, and campesterol being the most common (Jones & AbuMweis, 2009).

Phytosterols can also have different conformations with the addition of an alkyl group at the C-24 position. Soy beans, for instance, have both 24-methylcholesterol isomers: campesterol (24-α-configuration) and dihydrobrassicasterol (24-β-configuration; Nes et al., 1976). Generally the α configuration for phytosterols is more commonly found in plants, whereas the β configuration is often found in algae (Goodwin, 1985).

Other variations in phytosterol structure can be found at the C-3 position, with the addition of either a glycoside group, long-chain fatty acid ester, or ferulate ester. Phytosterols with a glycoside group are more rare in nature but can occur in significant amounts in some foods such as potatoes (Jonker et al., 1985). However, phytosterol with esters are more common and can be found in grains such as wheat or spelt (Fig

1.3e; Lagarda et al., 2006). Natural esterified phytosterols can also account for over 50% of the phytosterols found within corn oil (Ostlund et al., 2002).

However, in general, esterified phytosterols are not as abundant in nature as non-esterified phytosterols and these are usually industrially processed from free phytosterols. Processing is used to produce esterified phytostanols that have approximately 10 times better solubility in oil, than non-processed phytosterols. Hence, esterified phytostanols tend to be favoured in food products, as they are less likely to crystallise out of the lipid matrix (Zawistowski, 2010).

Due to the lower solubility of free phytosterols, the majority of studies on phytosterols have been performed on esterified phytosterols. However, esterified phytosterols must be hydrolysed before absorption can occur, which is subject to inter-individual variability among human digestive systems. This variation can cause free phytosterol absorption rates to vary between 40-96% (Carden et al., 2015). In addition, results from 60 clinical trials have shown that, when comparing phytosterols to esterified phytosterol, free phytosterols can lower LDL-cholesterol levels more than their esterified counterparts (Normén et al., 2004; Franchetti, 2016). Although free phytosterols require more research in terms of final solubility in the product, they have lower processing costs and improved bioaccessibility when solubilised (Franchetti, 2016).

1.2.2 Sources of phytosterols

Phytosterols can be found within the lipid component of plant materials. The most common phytosterols in plants are 4-demethylsterols such as sitosterol (≥ 90%), campesterol, stigmasterol, 5-avenasterol and 7-avenasterol (Lagarda, M. et al., 2006). Cereal products are also good sources of phytosterols, with the majority of the phytosterols generally being found within the bran fraction. This also applies to un-milled brown rice, as it contains a higher concentration of phytosterols than polished white rice (Piironen et al., 2000). Due to the high quantity of lipids present, nuts and seeds can also be a good source of phytosterols. For example, sesame seeds were found to have a high quantity of phytosterols, at 400–413 mg/100 g, while on the other hand Brazil nuts were found to contain only 95 mg/100 g (Phillips et al., 2005).

A typical diet includes of 160-400 mg per day of phytosterols, but on a vegetarian diet this quantity can easily double (Ling & Jones, 1995) However, this is still not a sufficiently high concentration of phytosterols to result in a decrease in LDL-cholesterols (Berger et al., 2004). Thus, phytosterols are typically extracted from either vegetable or tall oil (by-product from wood pulping) and enriched into food products to create functional foods.

In the case of oil extraction, the oil is first extracted from the seeds and minor components are removed. During the deodorisation process, volatiles are separated with a vapor condenser. This distillate is comprised mainly of free fatty acids but also contains a significant amount of phytosterols (8-20%). This distillate is further processed and phytosterols are removed *via* solvent crystallisation (Cantrill, 2008). This process produces free phytosterols, mainly β-sitosterol, which then must be further processed to create the esterified variety (Zawistowski, 2010).

1.2.3 Physical and crystalline behaviour of phytosterols

Phytosterols and phytosterol esters are insoluble in water and have limited solubility in non-polar solvents, like hexane. Phytosterols have some solubility in hydrophobic media, such as fats and oils, but their solubility is dependent on the extraction method and type of phytosterol. For example, stanols tend to be less soluble than plant sterols and, by esterifying the steroid, its solubility in lipid bases can be improved 10 fold (Jones et al., 1997; Vaikousi et al., 2007). Without esterification, phytosterol solubility in corn oil is limited to around 2-3% (wt/wt; Daels et al.,2017).

Hence, the use of solubility aids have been employed for phytosterol systems along with encapsulation techniques to improve phytosterol solubility (Engel & Schubert, 2005). For example, in a study by Ostlund et al. (1999), Sitostanol was solubilised in lecithin rich micelles. Formulations containing these micelles were able to reduce LDL cholesterol level ~25% more effectively in humans than the powdered crystalline Sitostanol, highlighting the importance of managing the crystallisation of the phytosterol. In another study, phytosterols were encapsulated into a medium chain TAG oil with a Tween emulsifier and either lecithin or monoacylglycerol was added. Results demonstrated both encapsulation and lecithin were the most effective at

improving phytosterol solubility, as emulsions with 30% lecithin and phytosterol did not crystallise even after 60 d of storage (Engel & Schubert, 2005).

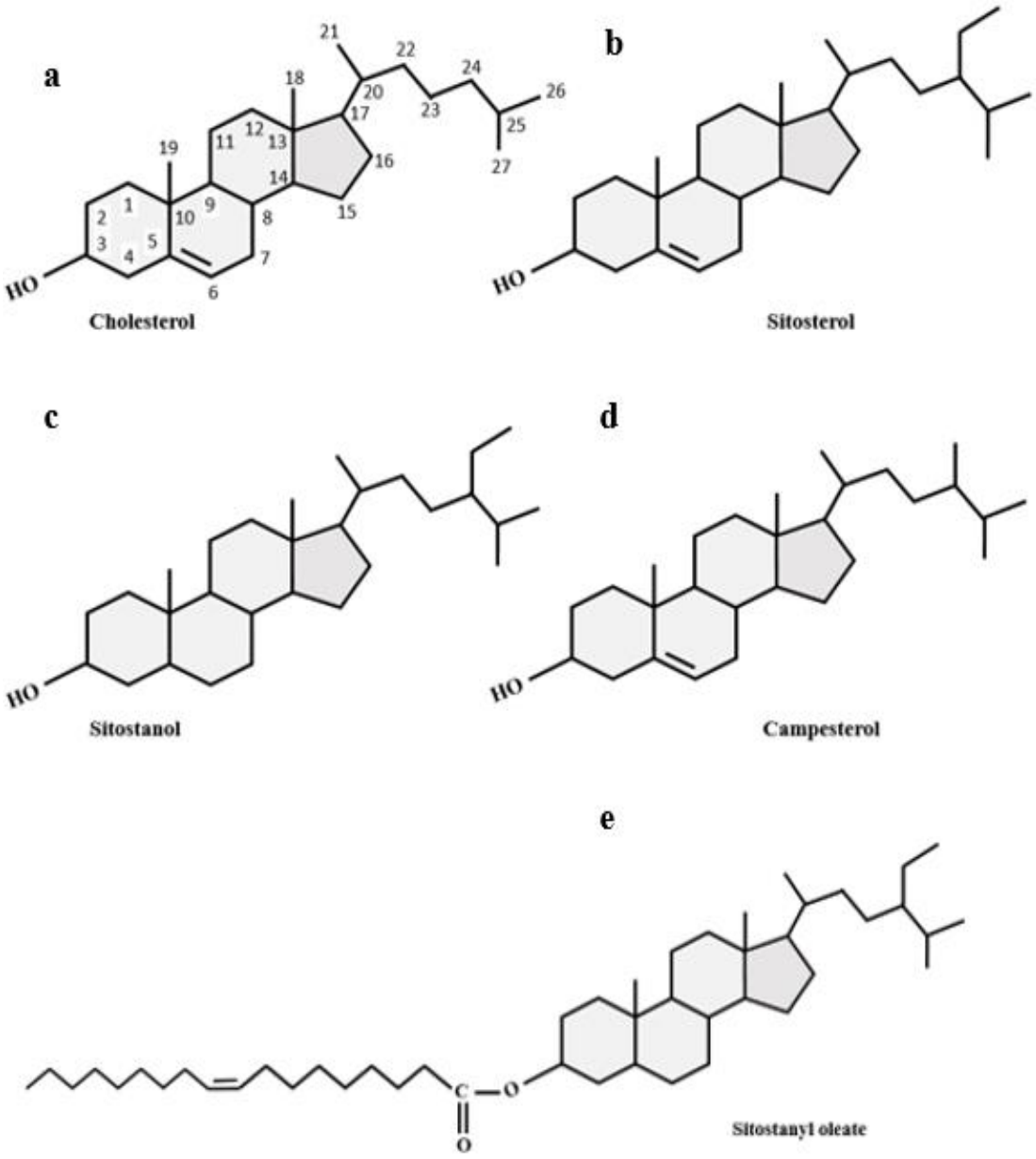

Figure 1.4 *Molecular structure of (a) cholesterol, (b) phytotsterol (sitosterol),(c) phytostanol (sitostanol),(d) another phytosterol (campesterol), and (e) a phytosterol fatty acid ester adapted from Cantrill, 2008.*

Phytosterols crystallise in numerous different polymorphs, for example β-sitosterol can form either hemihydrate, anhydrous or monohydrate crystals (Moreno-Calvo et al., 2014). The size, shape, and type of crystalline phytosterol polymorphs are influenced by changes in phytosterol, water, and oil concentrations. All three parameters were altered in a β-sitosterol oil suspension in a study by Christiansen et al. (2002). The addition of water into the oil suspension was found to convert the plate-like β-sitosterol anhydrous crystals into needle-like monohydrated crystals (Fig. 1.5). A higher concentration of phytosterols was found to supersaturate the solution and create smaller phytosterol crystals.

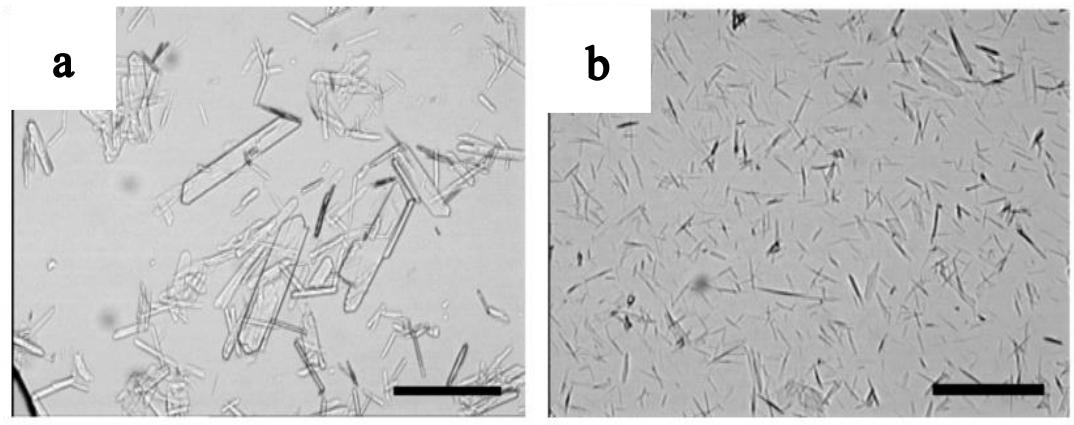

Figure 1.5 *Micrographs showing phytosterols (a) in bulk oil at 20% wt/wt and (b) at 20% wt/wt with 15% wt/wt water added into the system. Bar represents 100 µm (von Bonsdorff-Nikander et al., 2003).*

Crystalline phytosterols are not as bioaccessible as solubilised phytosterols, but can be used as food-grade structuring agents (Ostlund et al., 1999; Shaghaghi et al., 2014). For example, phytosterols have been extracted using an anti-solvent technique and have been employed to stabilise emulsion interfaces as a Pickering stabiliser (Liu & Tang, 2014). Phytosterols can also be combined with γ-Orgzanol to create tubules for organogel applications (Bot et al., 2009). Crystalline phytosterols on their own can also increase the viscosity of a lipid-based solution or the firmness of a food spread (Christiansen et al., 2002; Giri et al., 2014).

The thermal behaviour of crystalline phytosterol material is also important when considering possible food applications. Interestingly, in a study by Vaikousi et al.

(2007), phytosterol blends all tended to broadly melt between 138 to 144.56 °C, despite their different plant origins. However, purified phytosterols have been found to have slightly different melting temperatures. For example, β-sitosterol crystals were recorded to melt around 133.1 °C, while sitostanol crystals were found to melt at 141.3 °C (Melnikov et al., 2004). Most importantly for food applications, the melting behaviour of phytosterols can change depending on the chosen dispersion lipid. For example, in a study by Acevedo & Franchetti (2016), phytosterols melted at a much lower temperatures when dispersed within hydrogenated soy bean oil, as compared to the bulk phytosterol powder, 63.02 ± 2.00 °C as opposed to 137.78 ± 0.79 °C, respectively.

1.2.4 Potential health benefits of phytosterol dietary enrichment

Elevated LDL cholesterol level is a key risk factor in the development of coronary heart disease, cerebrovascular accidents or strokes, and gallbladder stone disease (Moreau et al., 2002; Jiang et al., 2004). In the USA, alone one third of adults have high cholesterol levels and blood pressure, with similar numbers being recorded in other countries such as England, Germany, Japan, Jordan, and Mexico (Health, 2011). Often statins are used to treat high cholesterol but they have various side effects such as muscle pain, increased risk of diabetes, and decreased muscle function (Golomb & Evans, 2008).

Phytosterols can also be used to decrease LDL-cholesterol levels and have no noted sides effects (Chawla & Goel, 2016). In a meta-analysis by Abumweis et al. (2008), 59 randomised clinical trials were compared to evaluate how phytosterol consumption influences LDL cholesterol levels. Data gathered from the studies showed that, overall, phytosterols can decrease LDL cholesterol levels by 5-15%. The authors speculated that variations in studies were most likely caused from some patients experiencing a greater effect of LDL reduction due to a higher baseline LDL cholesterol level baseline. Trautwein and Demony (2007) came to a similar conclusion but also discussed that age could have an effect, as older patients experienced larger decreases in LDL-cholesterol levels with phytosterol consumption.

When comparing studies, patient age and baseline LDL cholesterol level are important to consider, however, phytosterol solubility in the dose matrix must be noted (Berger et al., 2004). For example, in a study performed by Pouteau et al. (2003), 1.8 g of non-esterified phytosterols were solubilised in a milk matrix and consumed. The solubilised phytosterol ester resulted in a 29.1 ± 4.1% reduction in LDL-cholesterol levels. On the other hand, 3 g of crystallised phytosterols administered in a crystallised tablet were only able to decrease LDL-cholesterol levels by a 11.0% (Carr et al., 2009). In a side by side study, solubilised phytosterols in micelles were ~25% more effective in reducing LDL cholesterol levels than the powdered crystalline dose response (Ostlund et al., 1999). The discrepancy between the results highlights the need for further research on what factors influence phytosterol solubility within different food matrices.

The mechanism behind LDL cholesterol level reduction from phytosterols is a widely disputed topic among health experts. The most well-known and accepted theory is that phytosterols participate in competitive solubilisation within the (LDL) chylomicrons, which are absorbed by the enterocyte cells within the small intestine. By blocking absorption of cholesterol into these chylomicrons, LDL-cholesterol absorption is limited (Rozner & Garti, 2006; Smet et al., 2012; Yi et al., 2016). Another possible mechanism is that phytosterols inhibit cholesterol esterification at the cholesterol acyl transferase level, which encourages cholesterol secretion out of the intestinal cells (Ling & Jones, 1995). It has also been suggested the phytosterols activate a liver receptor that controls ABCG5/8 expression, which increases the transport of cholesterol from enterocytes back into the intestinal lumen (Plat & Mensink, 2002).

Although the mechanism of action is still unclear, the ability of phytosterols to lower LDL cholesterol is undisputed (Jones et al., 1997; Zawistowski, 2010). Besides the effect on LDL cholesterol, phytosterols have also been found to possess anti-inflammatory and anti-carcinogenic properties (Jones et al., 1997; Bouic, 2001; Engel & Schubert, 2005). In a study by Raicht et al. (1980), a 60% reduction in the number of chemically induced colon cancer tumours was observed in rats fed with 0.2% β-sitosterol. Phytosterols consumption has also been found to block cartilage degradation and decrease pain in patients with rheumatoid arthritis (Bouic, 2001;

Gabay et al., 2010). However, more research is needed to understand what levels of phytosterols are required to experience the other associated health benefits.

1.2.5 Phytosterol fortification in food matrices

Many products exist in the market place, such as yogurt drinks, milk, and table spreads made by Benecol™ or Flor pro-active™ of Unilever (Clifton, 2007). Several more examples of products and brands are listed in Table 1.3. Many of the current products in the market employ phytosterol esters instead of free phytosterols, due to the improved solubility of the esterified phytosterols. However, as mentioned previously, free phytosterols have the potential to be more effective at lowering LDL-cholesterol in the blood than esterified phytosterol, if they are properly solubilised (Ostlund et al., 1999; Pouteau et al., 2003).

Phytosterol solubility is crucial to manage in whatever food product it is enriched into. Chocolate muffins, brownies, chews, and juices have all been employed as functional food matrices for phytosterol enrichment (Cargill, 2008). However, the most popular products for phytosterols have been spreads or dairy-based products, such as milk, drinks or yogurts (Clifton, 2007). When compared side-by-side, phytosterol-enriched (PE) milk and yogurts lowered LDL-cholesterol more than cereals or bread (Clifton et al., 2003).

Although PE-enriched milks are not as common as PE spreads, milk fat is potentially an interesting matrix to use for phytosterol enrichment. To the author's knowledge no product currently exists that formulates phytosterols directly into the milk fat. The products currently on the market suspend phytosterol esters into milk with an emulsifier and sometimes use an oil to suspend the phytosterol, such as vegetable oil. Milk fat is a semi-solid lipid at refrigeration temperatures, which means it could potentially entrap the bioactive, preventing crystallisation, as seen in solid lipid nanoparticle technology (Weiss et al., 2008). In addition, as mentioned, milk fat forms bicontinuous cubic phases when digested, which can improve bioaccessibility of the bioactive components (Sagalowicz et al., 2006; Salentinig et al., 2013).

Table 1.3 Phytosterol-enriched food products

Company/distributors	Brand Name	Product	Type of Sterol
Benecol-McNeil (Europe, USA)	Benecol™	Milk, butter milk, yoghurt & single shot beverage	Vegetable tall oil ester
Unilever (Europe, Australia)	Flora Pro.activ™	Milk & yoghurt	Vegetable sterol ester
Forbes Meditech (U.S.A)	Heartfelt+™	Cheese, yoghurt & probiotic drinks	Tall oil free sterol
Archer Daniel Midland (Europe)	Cardioaid™	Milk & yoghurts	Vegetable oil sterols/ester
Cargill (U.S.A)	Lifetime™, Corowise™, Smart blance™	Low fat cheese, muffins, brownies, orange juice & cardio chews	Vegetable sterol esters (corowise)
Cognis (Europe, S. America, Japan)	Heart Choice™	Yoghurts & milk	Vegetable sterol esters (vegapure)

Table adapted from Clifton et al. (2004)

1.3 Emulsions

An emulsion is a dispersed system consisting of at least two immiscible liquid phases. The dispersed liquid is usually in the form of droplets and is referred to as the dispersed, discontinuous, or internal phase. The liquid surrounding these droplets is the continuous or external phase (McClements, 2015). These dispersions can be of two main formats, oil-in-water (o/w) or water-in-oil (w/o); most food systems are o/w

emulsions, such as milk, soup, or salad dressing, but there are some instances of o/w, such as margarine or butter (Dickinson, 1999; Widlak et al., 2001). Although not as commonly utilised, multiple emulsions can be prepared that are composed of larger droplets that contain another dispersed phase such as oil-in-water-in-oil (o/w/o), or vice versa (w/o/w; Fig 1.5). These can be used for controlled release or protecting certain ingredients, such as probiotics (Akoh & Min, 2008).

All emulsions are inherently unstable systems due to the thermodynamic incompatibility of the oil and water phases at the interface (McClements, 2015). The unfavourable interaction between oil and water drives the droplets to merge and inevitably separate into different phases. Factors such as emulsifiers used, droplet size, type of emulsion and fat or water concentration all influence emulsion stability (McClements, 2004a).

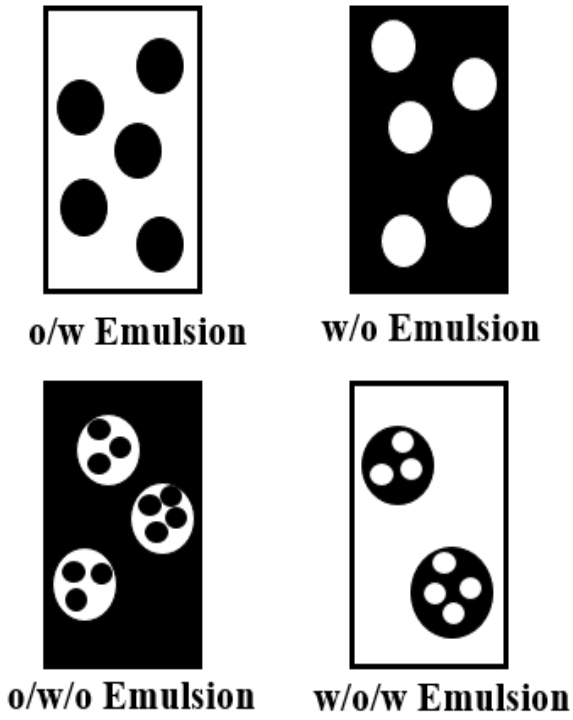

Figure 1.6 *The two-main single (top) and double emulsion varieties (bottom).*

The type of emulsifier employed is one of the most important factors to consider when developing an emulsion. Emulsifiers are typically amphiphilic molecules, which means they have both polar and nonpolar regions. This chemical structure gives them the ability to absorb to an interface and create a protective membrane around the dispersed phase. The most common types in the food industry are lipid-based and can range from small low molecular weight compounds, such as lecithin and tween compounds, to larger biopolymers like proteins. Emulsions can also be employed to encapsulate functional ingredients such as probiotics, vitamins, phytonutrients,

carotenoids or even flavours (McClements, 2012). In many cases, emulsifying the functional ingredients within an oil or water phase can protect it from physical or chemical degradation (McClements, 2004a). In the case of bioactives, emulsification can sometimes even prevent the encapsulated compound from crystallising (Shahidi & Han, 1993; McClements, 2004a, 2012; Pool et al., 2013). Thus, emulsions are commonly employed in the food industry to aid in shelf-life and bioaccessibility of functional food products.

1.3.1 Emulsion formation and stability

When the immiscible phases of an emulsion are mixed, they generally separate, as this is the most thermodynamically stable state. Thus, in order to mix the liquids, a mechanical force is required to combine the two phases into an emulsion. Often a two-step process, emulsion formation requires mixing by means of high shear mixing, homogenisation, membrane processing, and/or ultrasonication. First, a course emulsion is typically created to mix the two phases, which is followed by a second phase to reduce the size of the dispersed droplets (Dickinson, 1999).

The quantity and time of the shear applied influences the size and stability of the dispersed droplets (Damodaran et al., 2007). For example, in a study by Desrumaux and Marcand (2002), the average size of an emulsion droplet before final homogenisation (coarse emulsion) was 30 µm. When 50 MPa of pressure was applied to the emulsion from homogenisation, the average emulsion droplet size decreased to 0.7 µm, and with a higher homogenisation pressure (250 MPa) the droplet size decreased further to 0.25 µm. While shear is needed to create an emulsion to prevent the droplets from merging during formation, a sufficient quantity of an emulsifier must be present to absorb onto the droplet surface. The emulsifier will interact with both the dispersed and continuous phase to create a barrier between the two liquids. This barrier could consist of one or more emulsifiers but needs to be effective in preventing the dispersed droplets from interacting (Palanuwech & Coupland, 2003; McClements, 2004b).

Droplet interactions can result in several different types of emulsion destabilisation, such as coalescence, Oswald ripening, flocculation, phase inversion, sedimentation,

and/or creaming (Fig. 1.7). Coalescence is the process by which two droplets merge during contact to form a larger droplet (Damodaran et al., 2007). Partial coalescence can also occur and is normally seen in food emulsions when a crystallised fat crystal from one droplet pierces the lipid phase of another droplet (Dickinson, 1999). Flocculation is the process in which droplets make contact but do not merge. Oswald ripening can occur when both phases are not completely immiscible and there are different droplet sizes present in the system; here, larger droplets will form at the expense of smaller droplets (Damodaran et al., 2007). Creaming, sedimentation, and phase inversion also result in noticeable physical changes in the emulsion structure and, in food emulsions can result in the end of shelf-life. Food emulsion instability can also come in the form of chemical degradation of the dispersed phase, such as lipid oxidation or microbial processes (McClements, 2004a).

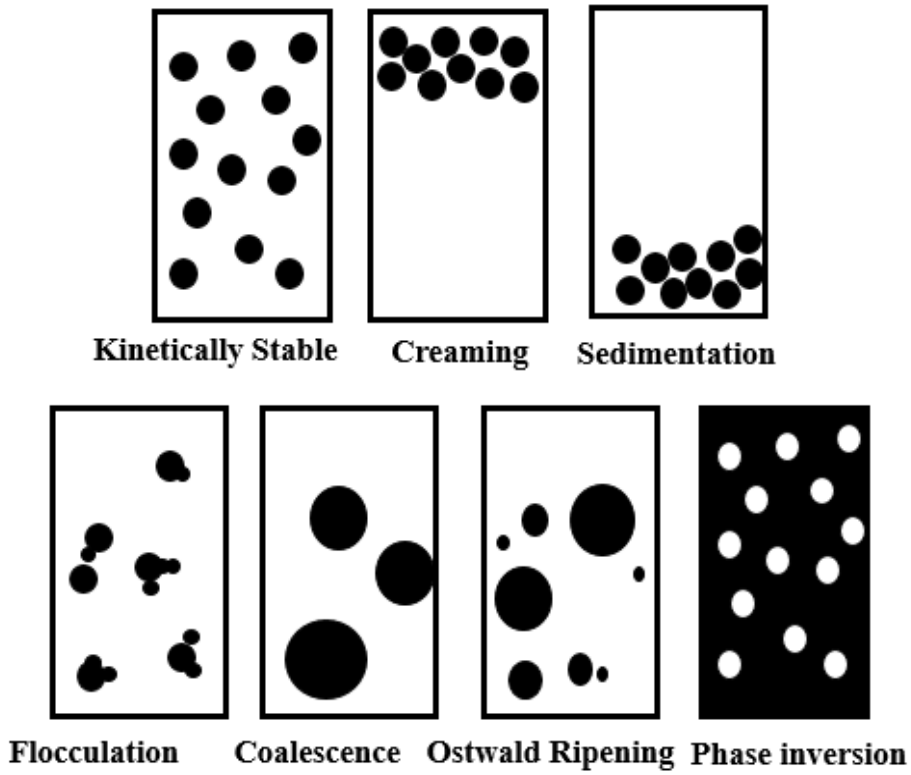

Figure 1.7 *Physical mechanisms of emulsion destabilisation adapted from McClements, 2007.*

Hence, when creating a food emulsion, several factors are crucial to consider, such as shear/heat treatment and formulation (McClements, 2015). In the case of food emulsions with encapsulated bioactives, special care needs to be taken to monitor emulsion and bioactive stability. For example, many bioactive compounds are highly lipophilic, crystalline at room temperature, and have poor solubility in water (McClements, 2012). Once emulsified, the bioactive could crystallise again, which could lead to partial coalescence and eventual emulsion destabilisation (Fredrick et al., 2010). To create an optimal formulation bioactives are often studied under a number of conditions, as seen in a study of polymethoxyflavones (PMFs) emulsions by Zheng et al. (2012). Here numerous oils (corn, MCT, orange) and emulsifiers (β-lactoglobulin, lecithin, tween, and DTAB) were trialled to see which type of formulation would be best suited for PMFs. In this study, lecithin was found to be the best emulsifier for the system, and DTAB resulted in complete emulsion destabilisation and the formation of large PMFs crystals. Bioactive crystallisation can also result in decrease bioaccessibility of the bioactive and, thus, it is important to monitor and understand the mechanisms behind bioactive crystallisation in emulsion systems.

1.3.2 Methods to measure emulsion stability

The perceivable quality attributes of an emulsion system are strongly influenced by their physicochemical characteristics such as droplet size, charge, droplet-droplet interactions and pH. If destabilisation occurs, obvious sensory and bulk physicochemical defects can be detected. In a food emulsion system, emulsion destabilisation often results in the end of shelf-life and, thus, it is crucial to quantify how and why changes are occurring within the food system (Dickinson, 1999).

To characterise a colloidal food system multiple different analytical instruments are used to quantify emulsion characteristics, i.e., droplet size, morphology, and charge. It can also be equally important to quantify changes in the continuous phase, such as crystallisation or changes in viscosity. Often, combinations of techniques are used to elucidate the main mechanisms behind emulsion destabilisation, which in the future could aid in the creation of emulsions with improved physio-chemical properties.

1.3.2.1 Light Scattering

The size of the dispersed droplets is a major factor in quantifying the stability of an emulsion system. Droplet size is often evaluated using light-scattering techniques, which are related to the intensity of light from a laser. Larger particles will scatter light at a narrow angles, as opposed to the smaller particles that scatter light at wider angles (Fig. 1.8b). This information is processed by a laser diffraction instrument such as a Mastersizer (Malvern Instruments Ltd., Malvern, UK; Fig. 1.8a) and the range of particle sizes present in the sample is calculated (Sprow, 1967). The most commonly utilized information from the Malvern is the $D_{(4,3)}$ value, which is the volume-based mean diameter, and the particle size distribution. This average is based on the volume of the dispersed phase instead of the number of particles. The effect of this is to increase the sensitivity of larger particles (McClements, 2007).

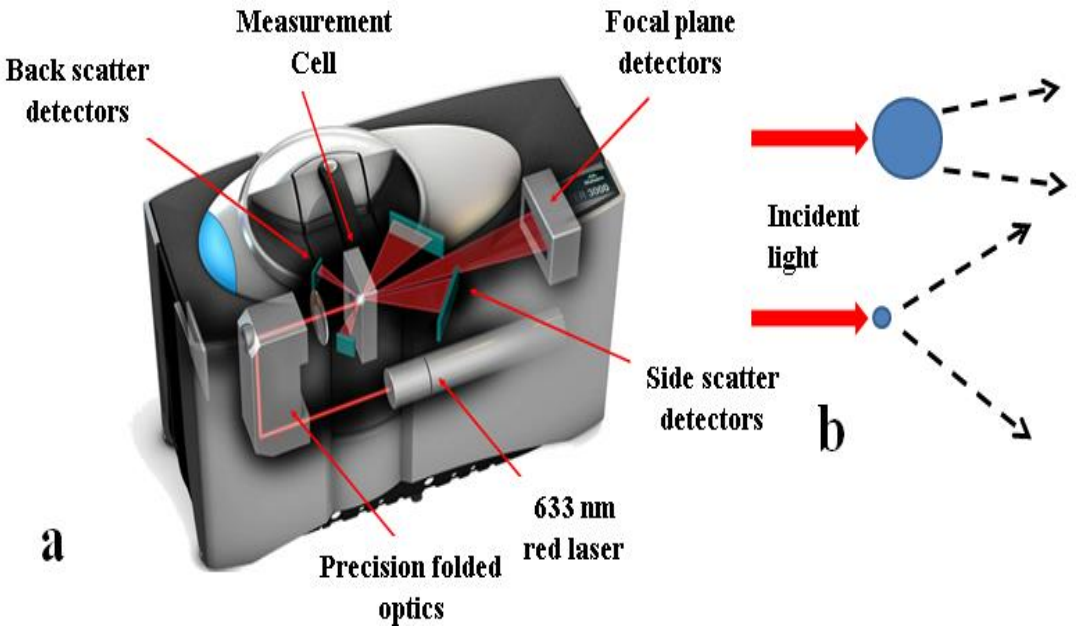

Figure 1.8 *(a) Diagram of light scattering device (Malvern Mastersizer) utilised to measure particle size. Red laser light is first bent by precision folded optics and is then passed through the measurement cell. Here the laser light is scattered by (b) different particles, which is then interrupted by the different detectors. The focal plane detector is mainly used for small angle scattering (larger particles), while the other detectors (side and back scatter) capture larger angle scattering (smaller particles; Malvern 2017)*

Light scattering is often used to measure emulsion droplet sizes and can be used when evaluating the response of emulsions to different treatments. In a study by Drapala et al. (2016), sunflower oil emulsions with whey protein and maltodextrins were evaluated for heat stability. Light scattering data showed changes in the fat globule size distribution (FGSD) after heat treatments and demonstrated that whey proteins conjugated with maltodextrins had the best heat stability, as minimal changes in the FGSD were observed. Light scattering can also be used in a similar way to measure the size of powder particles or protein aggregates. For example, laser light scattering is often used to quantify the sizes of different dairy powders, as results are a better representation of the different powder sizes than other techniques, such as microscopy (Silva & O'Mahony, 2017).

Light scattering can also be used to measure emulsion creaming or sedimentation, with systems, such as the Turbiscan (Turbiscan MA2000, Formulaction, France) or Lumifuge (Adaptive Instruments, West Sussex, UK). During creaming in o/w emulsions, the lower density droplets will move upwards, which also results in a clearing of droplets from the bottom of the tube (McClements, 2007). The Turbiscan can measure this change in the stability o/w emulsion by backscattering photons along the length of a tube containing the emulsion. This is then picked up and interrupted by an infrared diode and compared against the emulsion before storage. A LUMiFuge functions in a similar way but uses centrifugation to accelerate the aging process (McClements, 2015).

1.3.2.2 Zeta potential

Depending on the system, electrostatic charge (zeta potential, ζ) can also give an indication of colloid stability. The ζ-potential is the highest when the pH of the system is far from the isoelectric point of the compounds present at the emulsion interface. Other factors such a concentration of salts can also influence the ζ-potential and, thus, it important to establish the electrostatic charge of the emulsifier (Drapala, 2016). ζ-potential information is also useful in understanding the general behaviour of proteins and other dispersible compounds at various pHs and conditions (Hunter, 2013).

To measure ζ-potential, an instrument such as the Zetasizer (Malvern Instruments Ltd., Malvern, UK) is used, which sends an electrical current through a diluted colloidal sample. The electrical potential of the samples at the "shear plane" can give an indication of the attraction/repulsion forces present on the dispersed droplet (McClements, 2007). Often this is used, along with other techniques such as light scattering and microscopy, to gauge the mechanism of emulsion destabilisation in a system. For example ζ-potential was utilised in a study evaluating the emulsion stability in a high salt ($CaCl_2$) system with lactoferrin and/or β-casein emulsions. ζ-potential decreased in emulsions with a mixture of lactoferrin and β-casein or β-casein alone at the interface but no change was observed with $CaCl_2$ addition in emulsions with just lactoferrin. This information was combined with light scattering data, which showed that emulsions made with lactoferrin or both β-casein and lactoferrin had no significant change in particle size, while emulsions with β-casein alone had a large increase in emulsion droplet size. From this information the authors were able to conclude that lactoferrin can protect β-casein-stabilised emulsions from calcium-induced flocculation, as it electrostatically interacts with the negative phosphates groups on β-casein and can block calcium phosphate interactions (McCarthy et al., 2014).

1.3.2.3 Confocal laser scanning microscopy

Confocal laser scanning microscopy (CLSM) offers a unique opportunity to visualise different emulsion components, such as proteins, surfactants, and lipids. This is achieved through specific fluorescent probes emitting different wavelengths of light from pre-labelled samples. Separate channels then process the intensity emitted from the sample and images are created and overlapped to give insight into the multi-component microstructure of the sample. While CLSM can be a powerful tool, care must be taken to minimise sample disturbance, i.e., emulsion destabilisation from fluorescent dye addition (Auty et al., 2001).

Emulsion characteristics, such as droplet morphology and size, can be elucidated from CLSM images, along with protein distribution and interfacial thickness. Often, CLSM visualisation makes it easier to identify the causes of emulsion destabilisation, and it is often employed along with other techniques in fundamental emulsion studies.

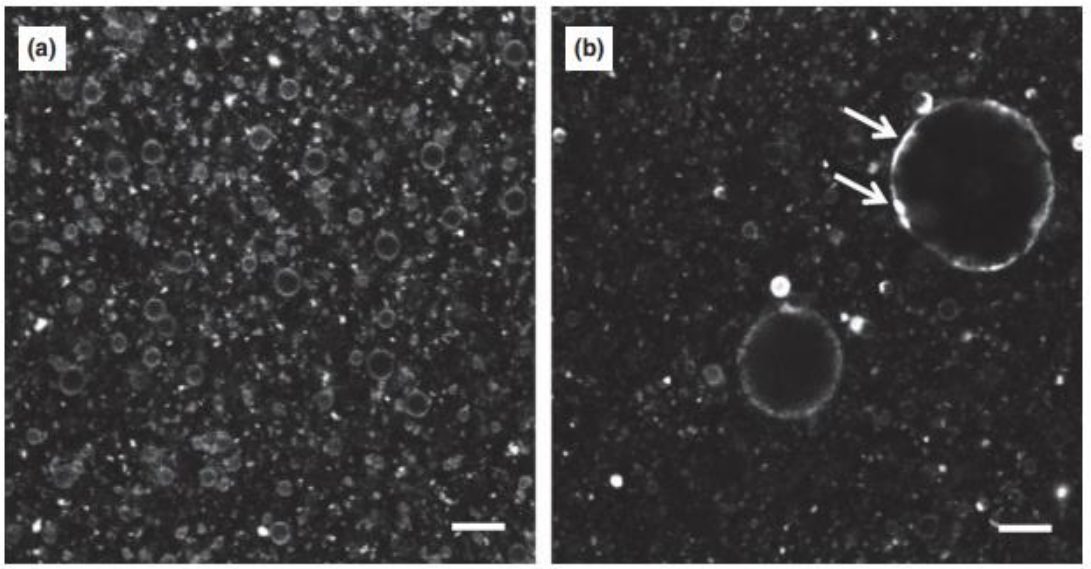

Figure 1.9 *High-magnification confocal micrographs of emulsions showing the uneven protein coverage in emulsions with (a) 0% lecithin and (b) 1% lecithin. Scale bar = 5 µm. Arrows highlight the variable thickness of protein at the oil droplet interface (Drapala et al., 2015).*

For example, in a study by Drapala et al. (2015), model infant formula emulsions were produced with protein hydrolysate and varying levels of lecithin. The addition of lecithin into the system was found to decrease interfacial tension and to decrease the fat globule size. However, at lower levels of lecithin (1-3%), coalescence occurred and a bimodal fat globule distribution was detected. Images of coalesced droplets captured using CLSM showed an uneven distribution of protein at the droplet interfaces of the emulsion suggesting possible partial displacement of the whey protein by lecithin (Fig. 1.9).

1.3.2.4 Cryogenic scanning electron microscopy

Cryogenic scanning electron microscopy (Cryo-SEM) is another useful technique in directly visualising the microstructure of emulsions. As emulsions are typically liquid systems, the sample is first rapidly frozen using liquid nitrogen. After freeze-fracturing, the sample is placed under a vacuum, sublimated, and coated with a conductive metal such as platinum. The sample can be imaged in the frozen hydrated state using a focused electron beam. During imaging, primary electrons penetrate the sample and incident electron scattered from the sample are interrupted by detectors as images.

Similar to CLSM, Cyro-SEM can be a helpful tool in visualising structure but expertise is need to minimise ice crystal development in high-moisture systems, such as o/w emulsions (Auty et al., 2001; Kelly, 2015). Cryo-SEM is often useful for visualising crystal development in emulsion systems, as this is difficult to see using CLSM. In a study by Norton et al. (2009), cocoa-butter emulsion systems were successfully imaged using Cyro-SEM, showing that in tempered emulsions a smooth layer of crystalline fat on the surface aided in emulsion stability. Fat-based Pickering emulsions, that exploit crystalline fat for interfacial stability, are often characterised by Cryo-SEM (Frasch-Melnik, Norton, et al., 2010; Frasch-Melnik, Spyropoulos, et al., 2010). It can also be noted that Cryo-SEM has previously proved useful in examining emulsion destabilisation in milk fat and whey-protein-based emulsions, as emulsion destabilisation was found to be due to flocculation instead of coalescence, which was apparent from Cyro-SEM images but not from data gathered on the particle size distribution (Rosenberg & Lee, 1993).

1.3.3 Emulsifiers and surfactants

During emulsion formation, emulsifiers and/or surfactants present in the formulation will move to the oil/water interface and align. These surface-active molecules are typically amphiphiles, with polar and non-polar portions of the molecule and are able to interact with both emulsion phases (Hill, 1998).

Smaller compounds, known as surfactants, have a greater mobility than emulsifiers and tend to dominate the emulsion interface initially. Surfactants can help produce

small droplets during emulsion formation, but are unable to provide long-term stability to an emulsion. Examples of surfactants utilised in the food industry are tweens, lecithin (phospholipids), and mono-and di-glycerides (Akoh & Min, 2008). Emulsifiers, on the other hand, impart long-term stability to an emulsion system, although they typically take longer to reach an emulsion interface, as they tend to be larger molecules than surfactants. Commonly utilised emulsifiers in the food industry include various proteins, such as whey, caseinates, or soy (Foegeding & Davis, 2011).

Non-ionic surface-active compounds are categorised by their hydrophilic-lipophilic balance (HLB). The calculation of HLB is as follows:

$$\mathrm{HLB} = 20\left(\frac{Mh}{M}\right) \tag{1.1}$$

where M_h = molar mass of the hydrophilic portion of the molecules and M = molecular mass of the whole molecule (Griffin, 1954; O' Dwyer, 2012). HLB values can be used to predict the surface activity of a compound and are useful when formulating an emulsion. For example in an o/w emulsion it would be advantageous to select a surface-active compound that has a higher HLB value (8-18; Table 1.4), as the compound needs to dispersible within the continuous phase but still be able to interact with the oil droplets (Bos & van Vliet, 2001).

Table 1.4 Ranges of applications of surfactants with different hydrophilic-lipophilic balance (HLB) values

HLB value	Application
3-6	Emulsifiers of w/o emulsions
7-9	Wetting agents
8-18	Emulsifiers of o/w emulsions
13-15	Detergents
15-18	Solubilisers

Table adapted from Bos & van Vliet, 2001.

1.3.3.1 Milk proteins as emulsifiers

Proteins are powerful emulsifiers as they are able to form a protective membrane around the dispersed droplet phase (usually o/w emulsions). When at an emulsion

interface, proteins can generate repulsive interactions (i.e., steric and electrostatic), which aid in maintaining the colloid dispersion, although not all food proteins are sufficiently surface-active to enable creation of emulsions or foams (i.e., air as the dispersed phase). A surface-active protein generally possesses the following characteristics: (1) it can rapidly absorb at an interface, (2) it can rapidly unfold and reorientate at an interface and (3) it is able to form a strong viscoelastic film once at the interface (Damodaran et al., 2007).

Milk proteins are typically surface-active, as they contain both polar and non-polar residues, which enables them to interact with both the oil and water phases of an emulsion (Dickinson, 1999). For example, casein proteins from milk contain clusters of phosphoserine residues that are substantially amphiphlic, as they possess a high proportion of accessible non-polar residues (O' Dwyer, 2012). These residues have a negative charge at a neutral pH, which aids in maintaining an electrostatic repulsion between oil droplets. However, too much non-absorbed casein protein can result in emulsion de-stabilisation through depletion flocculation, so emulsifier concentration should be monitored (Dickinson & Golding, 1997; Srinivasan et al., 2002). Sodium caseinate, in particular, is widely utilised in food products such as ice cream and whipped topping, as it is an extremely flexible protein and can move quickly to air/water or oil/water interfaces (O' Dwyer, 2012).

Whey proteins can also be used to stabilise o/w emulsion systems. Whey protein molecules have both hydrophobic and hydrophilic regions and are able to rapidly absorb at an oil/water interface to form a protective film. Although whey proteins are not as heat-stable as caseins, they are able to function over a large pH range. Whey protein has also been found to be more stable against emulsion destabilisation in dispersed systems containing crystals than sodium caseinate or tween 20 (Thanasukarn et al., 2004). In addition, whey proteins have demonstrated antioxidant properties, which is important in maintaining lipid integrity in o/w emulsions (Hu et al., 2003). This property is believed to be due to the sulfhydryl groups present in whey proteins, which can interact with peroxyl radicals (Taylor & Richardson, 1980; O' Dwyer, 2012).

1.3.4 Interfacial tension

When emulsifiers or surfactants align and interact at an emulsion interface, a decrease in the free energy of the system occurs. This decrease in free energy makes emulsion formation possible and can be quantified through interfacial tension measurements (Kim & Burgess, 2001). Interfacial tension is commonly utilised to quantify the surface activity of a compound. Traditionally performed with a Langmuir tray, interfacial tension measurements have become possible with optical devices, du Noüy rings, and Wilhelmy plates. The Wilhelmy plate (Krüss GmbH, Hamburg, Germany) is useful for emulsion systems as dynamic interfacial tension can be recorded over time. Thus, it is possible to quantify how quickly a compound can move to the interface, changes in interfacial tension over time, and if the compound is stable at the interface (Drapala, 2016).

The Wilhelmy plate is a thin vertical plate, which first operates by making contact with the heaviest (higher density) immiscible phase. The second phase (typically the lighter oil phase) is then added to cover the plate and the plate begins to pull against the interface (Fig. 1.10). The tension or force present at the interface is quantified using a microbalance (equation 1.2). If a surface-active compound is present, that force will be lower than for a clean interface (Drelich et al., 2002).

$$\gamma = \frac{F}{L \cos \theta} \tag{1.2}$$

where γ is the interfacial tension (mN/m), F is the pull force (mN) acting on the plate, L is the plate length (i.e., 2 × plate width; mm) and θ is the contact angle between liquid meniscus and the plate (Drapala, 2016).

By measuring interfacial tension, is it also possible to observe how different compounds behave at an emulsion interface. For example, Li et al. (2016) used dynamic interfacial tension measurements to demonstrate that mixtures of whey protein isolate (WPI) and β-casein were able to lower interfacial tension to a greater extent than WPI alone;these results, along with CLSM images, which showed both proteins co-localised at the emulsion interface, suggest a potential interaction with the two proteins at the emulsion interface. Similar results have been observed in emulsion

systems with proteins and other surfactants, such as lecithin (Sünder et al., 2001; Drapala et al., 2015).

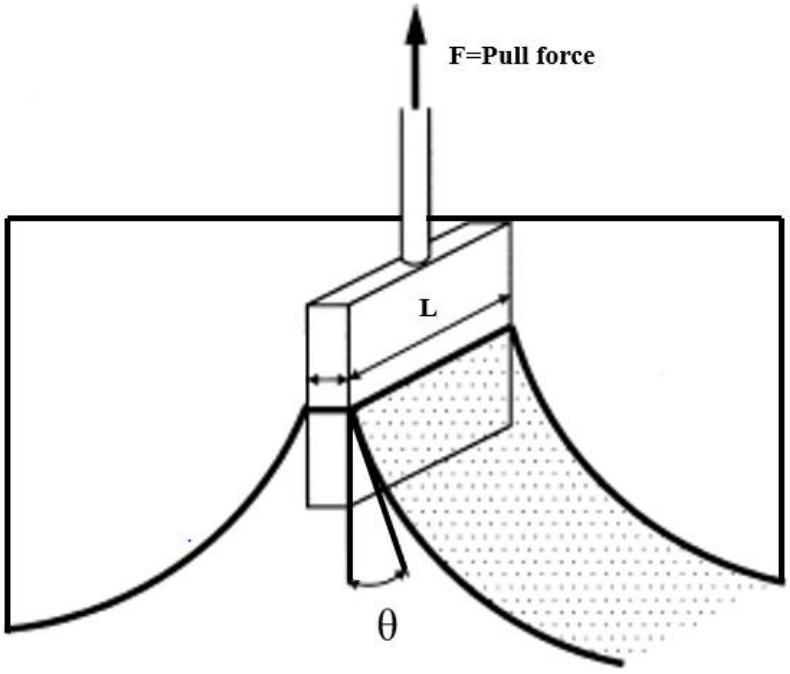

Figure 1.10 *Schematic of Wilhelmy plate geometry used for interfacial tension measurements (Drelich et al., 2002, Drapala, 2016).*

1.3.5 Emulsion-based delivery systems

Emulsion-based delivery systems are often employed in both the food and pharmaceutical industry. Emulsions, especially o/w emulsions, can improve the bioaccessibility and dispersibility of a compound within different matrices (McClements et al., 2007). For example, lipophilic bioactive compounds, such as phytosterols, carotenoids and antioxidants, are not soluble in hydrophilic environments. Functional foods need to be consumed in high doses and, thus, large portions of oil-based foods are not always desirable due to the accompanying high-calorie content. Hence, foods with a higher water content are often utilised in functional food matrices, such as yoghurts, orange juice, or milk and, by utilising an o/w emulsion, enrichment of these matrices is possible (Torre & Pinho, 2015).

Several different types of bioactive-enriched emulsions can be employed, which should be selected based on the intended matrix and bioactive (Fig. 1.11). The most common type is the conventional o/w emulsion, as discussed above, which consists of an oil phase surrounded by an interfacial layer, dispersed in an aqueous phase. Conventional o/w emulsions offer several advantages as they can easily incorporate bioactive compounds if the bioactive is added prior to homogenisation. For example, if the bioactive is an omega-3 oil, incorporation into the oil phase involves simple mixing but, in the case of bioactives with higher melting points, the oil phase is first combined with the bioactive and then must heated beyond the melting point of the bioactive. After heating, the emulsion is usually subjected to homogenisation or another form of shear before the bioactive has the opportunity to re-crystallise (McClements & Li, 2010). Typical o/w emulsions are also usually low in cost when compared to other more sophisticated systems as discussed below, as they require less research and development and usually use less expensive, easy to source food-grade ingredients. They are also customisable, as they can be tailor designed to release at pre-determined stages of digestion.

Conventional o/w emulsions have been able to successfully incorporate many different types of bioactive compounds, such as lycopene, β-carotene, astaxanthin and phytosterols (Tyssandier et al., 2001; Yuan et al., 2008). However, there are disadvantages to using simpler o/w emulsions, as sometimes the bioactive components can degrade. For example, in a study by Clark et al. (2000), stable o/w emulsions with the β-carotene were created using soy bean polysaccharides; however, they were susceptible to β-carotene oxidation. Chitosan was added to create a multilayer emulsion system, which decreased β-carotene oxidation in the emulsion. Multiple layer emulsions can be useful in other similar situations when the bioactive requires extra protection but are difficult to prepare, as flocculation can easily occur when adding polyelectrolytes to an emulsion surface (McClements et al., 2007). Spray-drying multiple layer emulsions has also been proven effective to slow bioactive degradation, as work by Lim et al. (2016) has shown that carotenoid retention improved significantly in multiple layer spray-dried emulsion made with trehalose and WPI, as opposed to single layer emulsions.

Another option for bioactive encapsulation is multiple emulsion systems such as w/o/w. These emulsions are perhaps the most difficult to make but can be beneficial in novel applications, such as controlled release, to protect bioactives/oil matrices that are very susceptible to degradation, or in systems with encapsulated bioactives with different hydrophilicities. For example w/o/w have been used to encapsulate polyunsaturated fatty acid, docosahexaenoic acid (DHA; oil phase) and insulin (aqueous inner phase) to improve insulin absorption in the intestinal membrane (Onuki et al., 2003).

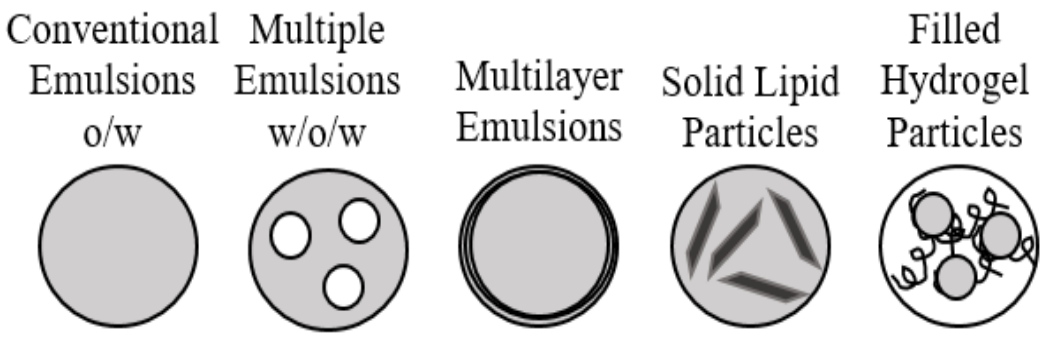

Figure 1.11 *Different types of possible emulsion system adapted from McClements et al. (2007).*

Filled hydrogels are another emulsion type that can be used for bioactive delivery. These emulsions are used extensively in the pharmaceutical industry and consist of bioactive-enriched oil droplets which are confined by hydrogel particles, dispersed in an aqueous continuous phase (McClements et al., 2007; Ahmed, 2015). Hydrogels have been successful in encapsulating compounds such as drug compounds (i.e., 4-vinylpyridine and *N*-(3-aminopropyl), ω-3 fatty acids, and flavour oils (McClements et al., 2007; Xinming et al., 2008). However, hydrogels are more difficult to prepare than the more basic o/w or multiple layer emulsions and have not been used extensively in food (Shewan & Stokes, 2013).

Another type of emulsion matrix that is used commonly in the pharmaceutical industry are solid lipid particles (SLP) emulsions. In these emulsions, a fully or semi-solid lipid matrix is chosen to encapsulate a bioactive compound. This matrix can be a disordered

or ordered crystalline matrix, which will in turn stop bioactive crystallisation or limit bioactive crystal growth. Preventing bioactive crystal growth in emulsion systems is important, as it can lead to emulsion destabilisation and possibly decrease the bioactivity of the active component (Ostlund et al., 1999; McClements, 2012). The solid lipid matrix can also improve bioactive stability, as radicals and other compounds have limited mobility in the matrix. For example, milk fat-based emulsions (semi-solid lipid participles) with β-carotene were found to have less bioactive degradation than similar emulsions made with corn oil (Zhang et al., 2013). Sometimes just the addition of a solid lipid, such as monoacylglycerols (MAG), can sufficiently immobilise a compound. In soybean emulsions MAG added at 0.5% into the lipid phase had significantly higher flavour retention than emulsions with no added MAG. Increasing the MAG to 2% in the lipid phase, further decrease flavour loss demonstrating the ability of solid lipid particles to confine encapsulated compounds (Mao et al., 2014).

Thus, when choosing a bioactive-enriched emulsion system, several factors should be considered for emulsion and bioactive stability. Firstly, it is crucial to understand and manage the mechanism of chemical degradation of the bioactive (i.e., hydrolysis or oxidation). Also, the loading capacity of the system is important, as excessively high bioactive addition could result in emulsion destabilisation and bioactive degradation in the aqueous phase. The delivery mechanism needs to also be considered as some bioactives might degrade in the stomach and must be released in the intestine. Finally, the bioactive must be compatible in the food material and bioaccessible (McClements et al., 2007).

1.4 Lipid crystallisation

Lipid crystallisation is an important process which dictates the functionality of many food, cosmetic and pharmaceutical products. In foods, lipid crystallisation is often responsible for the perceivable sensorial and physical attributes of the food product. For example, cocoa butter in chocolate needs to be tempered during the cooling process. When controlled properly the cocoa butter crystals contribute to the desired shiny appearance of chocolate and its melt-down rate upon consumption. If the

chocolate cools too rapidly, chocolate bloom occurs and the chocolate takes on a moulted whitish appearance, which is undesirable (Bricknell & Hartel, 1998).

In most food systems containing natural fats, the crystallisation of the TAG molecules is the most important factor in determining product quality but other types of food lipids should be considered, i.e., monoacylglycerols, diacylglycerols, and phospholipids (Metin & Hartel, 2005). Natural fats are made up of ~98% TAG molecules, which explains why lipid crystallisation varies from other types of crystallisation in food like sugar or salt. The molecular structure of TAG molecules favours the formation of a crystal lattice during cooling. These crystal lattices are dependent on lipid cooling/heating parameters and the presence of other compounds/minor lipids. The packing or orientation of the TAG lattice structures will determine the overall structure of the lipid, or its polymorph. The structures created during crystallisation determine the functionality of the lipid and its performance within a given food matrix and, thus, are important to characterise and understand.

1.4.1 General principles of primary crystallisation

Lipid crystallisation can be described by three main phases: super-cooling, nucleation, and crystal growth. Super-cooling is the process before nucleation, where a sufficient quantity of energy must be introduced into the system before TAG arrangement can occur. After this activation energy has been met, nucleation can ensue in either a homogenous or heterogeneous fashion. After nuclei form, the molecules begin to form crystal lattices and polymorphs are created. The following sections explain in further detail the outlined events.

1.4.1.1 Supercooling

Before primary nucleation can commence, the lipid must be in a liquid state, free from any molecular organisation from past heating/cooling regimes. During cooling, the solid or crystalline form of the lipid is thermodynamically favoured; however, the activation energy associated with nuclei creation must be overcome before molecular organisation can occur. In many cases, the liquid form can exist for some time in a metastable state, if the activation energy is high compared to the thermal energy of the system (Damodaran et al., 2007). Depending on the system, the amount of energy or

degree of super-cooling observed can vary. In purified lipids, the energy required to initiate nucleation is greater than in mixed TAG systems (Du, 2015). This driving force for nucleation can be described by a difference in chemical potential (Δμ) by the following equation:

$$\Delta\mu = \Delta H_m \frac{T_m - T}{T_m} \quad (1.3)$$

where T_m is the melting temperature of the lipid, ΔH_m is the melting enthalpy, and T is the temperature, at which nucleation begins (Fredrick, 2011).

1.4.1.2 Nucleation

Once the activation energy is reached, the TAG molecules start to arrange into what is known as a "chair" or "tuning fork configuration" and create a crystal nucleus (Fig. 1.12). There is a negative free energy change associated with the formation of these nuclei, but the nucleus cannot remain stable unless it reaches a critical radius (r*), which is defined by the following equation:

$$r^* = \Delta Hm \frac{2\gamma_i - T_m}{\Delta H_{fus} \Delta T} \quad (1.4)$$

where ΔH_{fus} is the enthalpy change per unit volume associated with crystallisation and γ_i is the interfacial tension between the crystalline solid and the lipid. The degree of super-cooling in the equation is defined as $\Delta T = T - T_m$, where T is the temperature of crystallisation and T_m is the melting point of the lipid. If the nucleus is sufficiently large, nucleation will continue from the surface of the formed crystal. If not, the crystal will dissociate and the process repeats until the critical radius is reached.

In homogenous nucleation, there is only one nucleus in the system, but in TAG-diverse food systems nucleation is heterogenous, as more than one nucleus is present. Heterogenous nucleation can also occur if any foreign particles are present in the lipid system, such as dust or other non-lipid compounds. These particles act as nucleation sites and lower the activation energy required for nucleation (Widlak et al., 2001; Damodaran et al., 2007).

Homogenous nucleation is quite rare, as the lipid system must be pure and free from any foreign particles. As there are no foreign surfaces to start nucleation, often a large

degree of supercooling is required. Temperature differences as low as 30 ºC have been recorded for super-cooling within purified systems, as opposed to 1-3ºC in mixed systems (Kloek, 1998; Fredrick, 2011). Once a stable nucleus is present in either system, the crystals will then begin the final stage, known as crystal growth.

1.4.1.3 Crystal growth

Crystal growth begins on a stable nuclei that meets the critical radius (equation 1.4). Molecules from the liquid lipid oil organise around a crystal nucleus, and upon contact with the nucleus, become incorporated into the crystal. Crystals grow at different rates, especially in food lipids, with a large variety of TAG molecules (Akoh & Min, 2008). The shape of the nuclei crystal is one of the most important factors that influences growth rate. Crystals are characterised as having either a smooth or rough surface (Ghotra et al., 2002; Himawan et al., 2006; Fredrick, 2011), where by smooth surfaces on a crystal typically have slower TAG attachment, while rough surfaces are able to grow faster as the crystal is in contact with more molecules (Fredrick, 2011). Crystal growth rate also depends on mass transfer of the molecules from the liquid to solid state and the removal of heat generated from crystallisation at the crystal/liquid interface. Environmental factors can also influence growth rate, such as thermal profile (time/temperatures), viscosity and shear rate (Damodaran et al., 2007). In products like ice cream the thermal profile is critical, as slow cooling results in larger ice crystals, with rapid cooling resulting in smaller crystals and a smoother texture. Crystal coarsening and growth can also result in deleterious effects on the texture of ice cream and can be minimised by decreasing the residence time in the ice cream freezer (Russell et al., 1999).

Viscosity and growth rate are interrelated variables, as high initial viscosity samples tend to crystallise at a slower rate, i.e., honey, but different growth rates can also influence the viscosity during and after crystallisation (Bhandari et al., 1999). For example, in a study by Martini et al. (2008), milk fat samples that crystallised faster upon high intensity ultrasound application possessed a higher final viscosity, than samples without the application of ultrasound; however, this difference was only observed at lower temperatures (22, 24 & 26 ºC). Samples that were crystallised at higher temperatures (28 & 30 ºC) had a longer induction time, and the effect of

ultrasound application was not observed, as it was only applied at the beginning of the hold time (Martini et al., 2008).

Shear rate should also be considered as it influences crystal growth and is commonly utilised during the tempering process of chocolate. Synchrotron X-ray scattering (see below) was employed to monitor cocoa butter crystallisation and it was discovered that shearing during cooling not only increases the nucleation temperature but also increases the temperature at which the different cocoa butter polymorphs are observed (MacMillan et al., 2002). When performed correctly, the shearing process in cocoa butter encourages crystal growth of the more stable β form, which is needed for long-term chocolate stability (Widlak et al., 2001).

In general, growth rate in food lipids is a slow process, as TAG molecules are large and require time to reach the proper conformation. When compared to nucleation, the thermodynamic driving force for crystal growth is much lower. Hence, when a system is supersaturated or supercooled, nucleation will dominate and a large number of small crystals will be present (Fredrick, 2011).

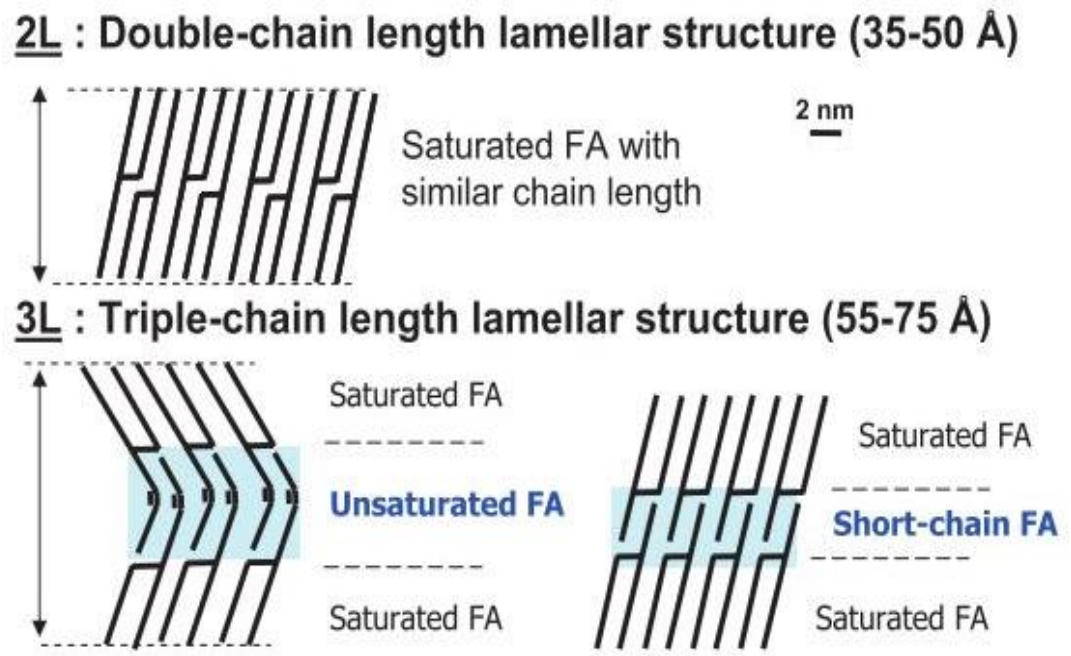

Figure 1.12 *TAG longitudinal organisation of TAG molecules in crystal lattices (Lopez et al., 2007).*

1.4.2 Polymorphism of lipids

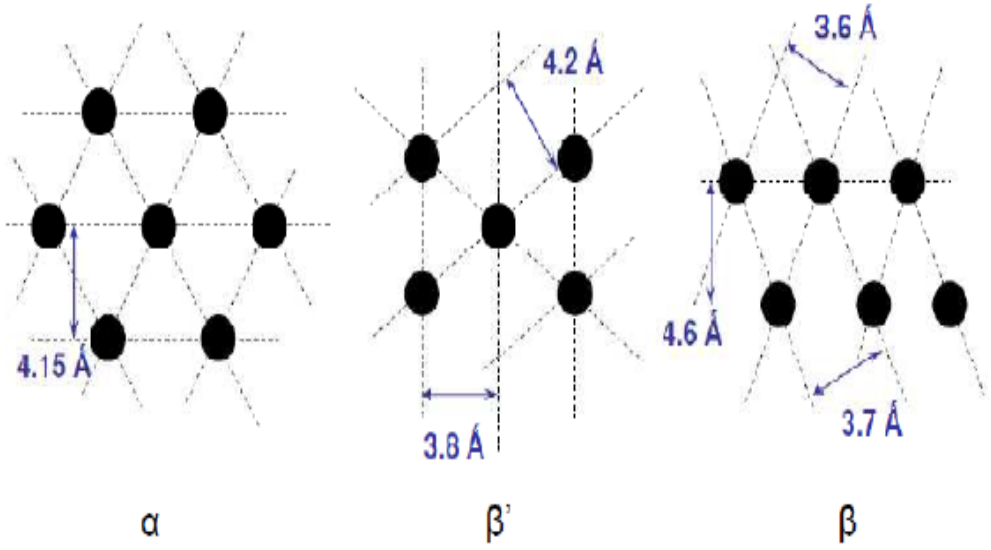

Figure 1.13 *Cross sectional view of the subcell packing of the different polymorphs. The lengths of some of the short spacing are also given (Fredrick, 2011).*

Polymorphism is the ability of a molecule to possess more than one crystalline form and is dependent on the crystal lattice arrangement. As TAG molecules crystallise, they form repeating lattice structures (Sato, 1999) and the longitudinal stacking of the TAG in the lattice structures is dictated by the length of the repeating lamellar units (Fig. 1.13). The lateral cross section of these repeating units gives information on the polymorphism (Widlak et al., 2001).

Several polymorphisms can be present at one time depending on the lipid and are reliant on a multitude of factors (Fig. 1.12). Rate of crystallisation, temperature of crystallisation, impurities, pressure, and shear rate can all influence the type of polymorphism formed. Likewise, the polymorphs created have different physical properties, i.e., melting point, density, and functionality in foods (Sato, 2001).

In food lipids, three main polymorphic forms are observed frequently: hexagonal (α form), orthorhombic perpendicular (β' form), and triclinic parallel (β form; Fig. 1.12; Lopez et al., 2007). The α polymorph has perpendicular hydrocarbon chains with a

high degree of molecular freedom. The β' and β polymorph have less freedom and possess zigzag hydrocarbon chains with a tighter packing density. The hydrocarbon chain of the β polymorph are all on one plane, while the β' polymorph has chains on different planes (Fredrick, 2011).

The most stable polymorph is generally the β polymorph, as it has the highest packing density and the lowest Gibbs free energy. To create a β polymorph, the cooling rate must be slow enough, so that the matrix has time to rearrange the TAG molecules, which are already in a less stable polymorph. With faster cooling rates, the α polymorph is typically the first one observed, as it has the lowest activation energy (Damodaran et al., 2007). The α form is also the most unstable polymorph and has the lowest melting point and melting enthalpy. Interestingly, rapid cooling in sugar or starch systems often results in the glassy state, which also possess little structure and no long-term ordering (Metin & Hartel, 2005). In between the two polymorphs is the β', which is more stable than α but not as stable as β (Sato, 2001; Fredrick, 2011).

Over time, most lipid systems rearrange to be in the β form, as this is the most stable state. However, β crystals tend to be larger and are not always preferred over the finer β' crystals in foods. Smaller β' are often found in margarine or spreads, while β lipid crystals are functional for bakery shortening to create "flakiness" or in chocolate for stability (Damodaran et al., 2007). The α form also has some novel applications, as it has been extensively studied for the inclusion of drugs, since it possesses a lower packing density (Rosenblatt & Bunjes, 2009; Joseph et al., 2015).

1.4.3 Crystallisation in bulk and emulsion matrices

Bulk lipid crystallisation generally transpires as outlined above, with supercooling, nucleation, and crystal growth occurring in sequence. In a bulk system, impurities can easily catalyse the system to nucleate. This differs from an emulsion system, where the impurities of the bulk system are divided among the droplets. Impurities generally cause heterogeneous nucleation to begin in bulk phases at higher temperatures. Thus,

in droplets, a larger activation energy and amount of supercooling is needed to begin the crystallisation process, as opposed to in bulk systems (McClements, 2012).

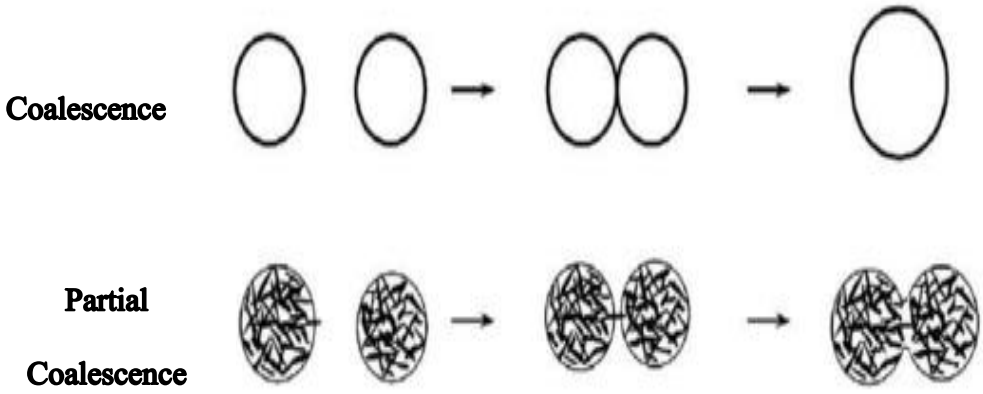

Figure 1.14 *Image of emulsion droplets undergoing going normal and partial coalescence (Fredrick et al., 2010).*

The effect of supercooling between bulk and emulsion systems has been observed in numerous studies and can even be observed between larger and smaller droplets (Skoda & Van den Tempel, 1963; Vanapalli et al., 2002; Sato & Ueno, 2011). However, emulsifiers present at the interface can also influence when the emulsion crystallises. For example, in a study by Gulseren and Coupland (2007), smaller emulsions (0.15 vs 3.45 μm) required more supercooling than larger emulsions in samples stabilised with Tween 20. On the other hand, emulsions with sodium caseinate at the interface, showed no difference in nucleation temperature, which is most likely due to the presence of the protein at the interface. Often it is assumed that homogenous nucleation is the cause of supercooling in emulsion systems. However, homogenous nucleation can only be observed when the droplets are so small that only one nucleus is present in each one. This is dependent on the purity of the fat and structure of the emulsion and is not often seen in food emulsions (Coupland, 2002).

In addition, small lipid droplets have a high surface-to-volume ratio and, thus, during crystallisation, there is the potential for surface effects to influence crystallisation (Coupland, 2002). For example, monoglyceridess are often added to o/w emulsions for their emulsifying capability. As monoglycerides are typically crystalline at room

temperature, they are heated to liquid state, along with the oil/dispersed phase before homogenisation. When emulsion formation occurs, the liquid monoglyceride molecules move to the surface and, during cooling, crystallise to create a crystalline interfacial layer; this can subsequently nucleate crystallisation of the dispersed lipid as well (Dickinson et al., 1993). Other non-crystalline molecules at the interface, such as surfactants, as discussed further below, can also influence crystallisation rates of emulsion systems (Smith, K. W. et al., 2011).

Another difference between bulk and emulsion crystallisation is the potential for partial coalescence to occur. During partial coalescence, crystals orientate towards the surface of the emulsion droplet and can puncture another colliding droplet. Any remaining liquid oil in the lipid volume phase flows out between the crystal linkage and the two droplets become joined. In partial coalescence, the strength of the crystal network maintains the droplet shape, as opposed to complete coalescence where one full larger droplet is created (Fig. 1.14; Coupland, 2002). Partial coalescence is crucial to the development of an air cell structure in products such as whipped and ice cream (Fredrick et al., 2010)

1.4.4 Crystallisation in milk fat systems

As mentioned previously, milk fat is composed of a diverse range of TAG's and therefore has a complex melting and crystallisation behaviour. Milk fat typically participates in heterogenous nucleation, with the possibility of secondary nucleation to also occur (Fredrick, 2011). Secondary nucleation is the result of nuclei formation upon contact with existing crystals and is promoted by agitation. In butter, secondary nucleation is critical for structural development of the phase inverted milk fat. If a higher level of agitation is used, a firmer butter is created with finer crystals (Wright, 2003).

Milk fat has a large melting range from -40 to 40 ºC, due to its TAG composition. This composition means that during cooling, milk fat initially forms less stable polymorphs. The TAG must form into mixed crystals, which leads to a lower packing density (Wright & Marangoni, 2006). Stable polymorphs can still be formed in milk fat after cooling, if the cooling rate is sufficiently slow. Lopez et al. (2002) showed that, by

cooling at -0.15 ºC/min, a β' polymorph can be formed after temperature stabilisation. However, if given sufficient time at a low enough temperature, milk fat crystallised at a faster rate can form stable polymorphs (Lopez et al., 2006).

It is also worth noting that the main differences between natural cream and bulk milk fat system during crystallisation. Unprocessed cream tends to have a slower transition between polymorphic forms than bulk milk and nucleates at lower temperatures. Additionally, the milk fat is more disordered in nature and possess smaller crystals (Lopez et al., 2002; Fredrick, 2011). This has been attributed to the high amount of supercooling needed to induce nucleation and the crystal packing constraints of the curved interface (Michalski et al., 2004; Fredrick, 2011).

1.4.4.1 Effect of low molecular weight surfactants on milk fat crystallisation

Low molecule weight surfactants can also influence the crystallisation behaviour of milk fat. Some low molecular weight surfactants are already present in milk fat, such as monoacylglycerols, diacylglycerols, and lecithin (phospholipids). However, a higher concentration of these compounds can often produce different effects in milk fat. Previous work on mixtures of milk fat and lecithin showed that lecithin is able to delay milk fat nucleation. This was attributed to the phospholipids molecules, from the lecithin, incorporating themselves into the milk fat crystalline nuclei. This subsequently slowed the crystal growth of the milk fat, as TAG attachment was delayed by phospholipids steric hindrance (Vanhoutte et al., 2002). Similar results were seen in a processed cream system, where added lecithin at 0.5% wt/wt decreased the solid fat fraction of the system, compared to samples without lecithin (Mutoh et al., 2007).

Monoacylglycerols, on the other hand, can induce milk fat nucleation, as they can act as seed crystals. Milk fat and monoacylglycerol combinations have been found to induce nucleation and increase the crystal growth rate, as opposed to milk fat alone (Foubert et al., 2004; Fredrick, 2011). Ambiguously, diacylglycerols when combined with milk fat at 0.1 % wt/wt were found to delay the onset of crystallisation (Wright & Marangoni, 2002). Although the mechanism behind this is not quite fully

understood, this relationship suggests that monoacylglycerols can more easily be incorporated into milk fat crystals than diacylglycerols (Fredrick, 2011).

1.4.5 Methods to observe lipid crystallisation

To characterise lipid crystallisation, multiple different analytical techniques can be used: X-ray diffraction, nuclear magnetic resonance, calorimetry or microscopy. X-ray diffraction is one of the most powerful tools for elucidating the crystal structure of a given lipid. However, access to and X-ray diffraction facility is often limited. Nuclear magnetic resonance (NMR) is also a useful technique, as it is often employed to measure the rate of crystallisation, as it can differentiate between crystalline and liquid lamellar state in liquids. Differential scanning calorimetry measurements are more difficult to interpret but can also give insightful information about the thermal behaviour of a lipid, particularly if coupled with other types of measurements (Lopez et al., 2007). Finally, microscopy is also beneficial to use when trying to understand crystal morphology and behaviour. Mostly, polarised light microscopy is used for investigating crystal structures but cryogenic transmission electron, atomic force, or even confocal microscopy can be employed (Korlach et al., 1999).

1.4.5.1 Small- and wide-angle X-ray scattering

X-ray scattering is an essential method for identifying the type of TAG structure that is created during the crystallisation process. The longitudinal spacing of the TAG units can be calculated from the peaks present from small-angle X-ray scattering (SAXS) diffraction patterns. Wide-angle X-ray scattering (WAXS) can be used to understand the resulting lipid polymorph or chain packing. Often SAXS and WAXS can be used together, at a high resolution, if a synchrotron is employed as a light source. The use of a synchrotron also allows systems to be studied in "real time," as scans can be taken quickly as a function of heating, cooling or shear treatment (Lopez & Ollivon, 2009).

The application of synchrotron analysis has allowed milk fat to be studied during numerous different cooling and heating regime, whereas without this technology only the final polymorphic form created could be studied (Lopez et al., 2006; Lopez et al., 2007). Synchrotron radiation can also be used to study crystallisation of bioactives. In a recent study by Daels et al. (2017), phytosterol ester crystallisation in palm oil was

evaluated during the crystallisation process. Diffraction patterns showed the development of different phytosterol ester crystals during the cooling process and how palm oil structure was influenced by phytosterol addition.

There are over 60 synchrotron instruments in the world, with the most renowned being the CERN Large Hadron Collider (LHC) near Geneva, Switzerland. Synchrotron instruments are particle accelerators, which harness the power of charge particles to create synchrotron light (Fig. 1.15; Zychowski et al., 2016). This light can then be utilised at different frequencies, such as X-ray or Near Infrared. When the sample is irradiated with X-rays, the atoms inside of the sample scatter the radiation in different directions. The difference between the background radiation and the excess scattering of the sample makes it possible to draw conclusions about lattice structure (Lopez & Ollivon, 2009; Schnablegger & Singh, 2013)

This difference can be thought of as constructive and destructive waves being emitted from the sample. All diffraction patterns are presented as a function of the scattering vector (q), which is measured relative to the applied radiation wave length (λ) by the following equation:

$$q=\frac{4\pi}{\lambda}\sin\theta \tag{1.5}$$

When the particles are close to each other like in a crystal lattice, the interference pattern multiplies with the form factor and defined peaks can be seen in the diffraction pattern. These defined peaks are known as Bragg peaks and can be interrupted into distances (Å) using the following law, with q peak representing the position of the peak q ($Å^{-1}$):

$$dbragg = \frac{2\pi}{qpeak} \tag{1.6}$$

In densely packed systems the position and orientation of these molecules can be derived from the diffraction patterns. This in turn can be used to understand the how the polymorphic and packing behaviour of lipids are affected by changes in the crystallisation environment, like changes in cooling rate or shear application (Schnablegger & Singh, 2013).

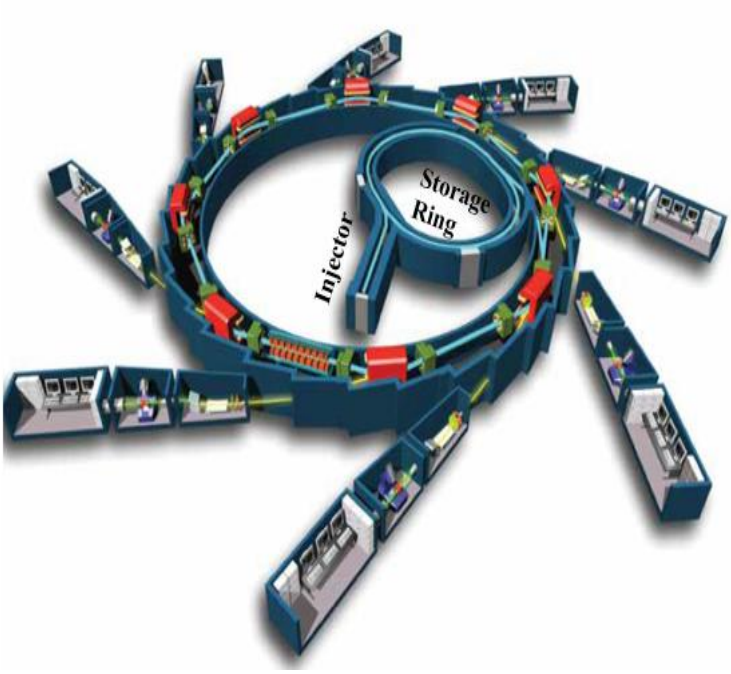

Figure 1.15 *Schematic diagram of a synchrotron. Charged particles, such as electrons, are produced in the injector and are pre-accelerated in the booster ring. After the particles are injected into the storage ring, bending magnets (as shown in green) facilitate the movement of the particles around the ring, while a radio frequency generator holds the particles at a constant speed. Energy from accelerated particles is harvested as 'synchrotron light' in various beamlines. Image courtesy of EPSIM 3D/JF Santarelli, Synchrotron Soleil.*

1.4.5.2 Nuclear Magnetic Resonance

Another technique that is often employed to measure bulk and emulsified crystallisation is NMR. To obtain information regarding the structure of the lipid using NMR, a magnetic field is first applied to the sample, which is absorbed, and electromagnetic radiation is then emitted by the sample. An increase in the crystalline phase of the lipid results in a decrease in the oil resonance intensity and the liquid to crystalline fat ratios can thus be calculated. The advantage of NMR is that it is a non-

evasive measurement and it requires very little sample for a measurement to be taken (Simoneau et al., 1992).

In a study with emulsified trilaurin and/or trimyristin, the combination of both components in the oil phase, as opposed to a singular TAG, was found to significantly lower the rate of crystallisation (Simoneau et al., 1993). The use of NMR allows one to easily quantify reaction rates, which is not always possible with DSC or X-ray diffraction in complex food lipids system. For example, the crystallisation of cream has also been quantified using NMR, as well as cocoa butter (Miquel & Hall, 1998; Bertram et al., 2005). Information from NMR is useful as kinetics can be calculated, as well as the nucleation temperature of the lipid.

1.4.5.3 Differential scanning calorimetry

Differential scanning calorimetry (DSC) can also be utilised to study and monitor the crystallisation of lipids. This thermoanalytical technique measures the exothermic and endothermic events that occur in a sample during a given temperature treatment, by gauging the heat flow of the sample and comparing this against the control. In food lipids, crystallisation and melting temperature ranges can be broad, with several different crystallisation and melting events occurring during any one treatment. Measurements from DSC allow one to capture the specific heat capacity changes of the sample during this period (Cebula & Smith, 1991).

DSC is also very useful when comparing the actual induction time of nucleation at a certain temperature rate (Vanhoutte et al., 2002; Shukat et al., 2011). Although not as conclusive as X-ray diffraction, DSC can also help distinguish between the types of polymorphic forms present in a sample (Bunjes & Unruh, 2007). For example, DSC measurements have been able to detect the melting of the initial melting of the α polymorph during heating; which if present, will be followed by a second endothermic event of a more stable polymorphs, such as β or β' (Kellens et al., 1991; Widlak et al., 2001). However, as mentioned, DSC data is typically used as more of a confirmatory tool in food lipids with other techniques, as the melting/crystallisation profile typically contain multiple peaks.

1.4.5.4 Polarised light microscopy

Polarised light microscopy is another technique that is often utilised to visualise crystallisation. Polarised light is created by blocking light with a polariser that is orientated at 90º to the illumination source. Any crystalline material present in the sample will double-refract this light and stand out against the dark background.

This is because non-cubic crystals possess what is known as birefringence, which can be exploited to confirm the presence of crystalline material. Birefringence is an optical property of material, which gives it the ability to refract polarised light. As it is a simple and non-evasive tool, polarised light has been used extensively to study the crystallisation of not only lipids but also lactose and starch crystals in food (Baldwin et al., 1994; Toro- Vazquez et al., 2005; Maher et al., 2015).

1.5 Conclusion

There is significant knowledge in existence regarding milk fat in terms of its composition, production, and crystallisation behaviour. However, milk fat has not been studied extensively as a potential encapsulation matrix. Phytosterols have been found to be effective when dispersed within milk using lecithin (Ostlund et al., 1999); however, no research known to the authors, has explored utilising milk fat to encapsulate phytosterols (Pouteau et al., 2003; Thomsen et al., 2004). Further research is required in this area, as phytosterol bioaccessibility is limited by its solubility within its carrier matrix (Ostlund et al., 1999). In particular, the mechanism responsible for phytosterol crystallisation in milk fat has not been studied, nor has the effects of phytosterol crystallisation on the physicochemical properties of a milk fat system. Knowledge gained in this area would be useful to both the functional foods and dairy industry in the production of new phytosterol-enriched products.

References

Acevedo, N. C., & Franchetti, D. (2016). Analysis of co-crystallized free phytosterols with triacylglycerols as a functional food ingredient. *Food Research International, 85*, 104-112. doi:http://dx.doi.org/10.1016/j.foodres.2016.04.012

Ahmed, E. M. (2015). Hydrogels: Preparation, characterization, and applications: A review. *Journal of Advanced Research, 6*(2), 105-121.

Akoh, C. C., & Min, D. B. (2008). *Food lipids: Chemistry, nutrition, and biotechnology*: CRC press.

Auty, M. A. E., Twomey, M., Guinee, T. P., & Mulvihill, D. M. (2001). Development and application of confocal scanning laser microscopy methods for studying the distribution of fat and protein in selected dairy products. *Journal of Dairy Research, 68*(3), 417-427.

Baldi, A., & Pinotti, L. (2008). Lipophilic microconstituents of milk. *Advances in Experimental Medicine and Biology, 606*, 109.

Baldwin, P. M., Adler, J., Davies, M. C., & Melia, C. D. (1994). Holes in starch granules: Confocal, sem and light microscopy studies of starch granule structure. *Starch - Stärke, 46*(9), 341-346.

Barauskas, J., Johnsson, M., Joabsson, F., & Tiberg, F. (2005). Cubic phase nanoparticles (cubosome†): Principles for controlling size, structure, and stability. *Langmuir, 21*(6), 2569-2577.

Berger, A., Jones, P. J. H., & Abumweis, S. S. (2004). Plant sterols: Factors affecting their efficacy and safety as functional food ingredients. *Lipids Health and Disease, 3*(5), 907-919.

Bertram, H. C., Wiking, L., Nielsen, J. H., & Andersen, H. J. (2005). Direct measurement of phase transitions in milk fat during cooling of cream—a low-field nmr approach. *International Dairy Journal, 15*(10), 1056-1063. doi:https://doi.org/10.1016/j.idairyj.2004.10.005

Bhandari, B., D'Arcy, B., & Kelly, C. (1999). Rheology and crystallization kinetics of honey: Present status. *International Journal of Food Properties, 2*(3), 217-226.

Bos, M. A., & van Vliet, T. (2001). Interfacial rheological properties of adsorbed protein layers and surfactants: A review. *Advances in Colloid and Interface Science, 91*(3), 437-471.

Bot, A., Den Adel, R., Roijers, E., & Regkos, C. (2009). Effect of sterol type on structure of tubules in sterol + γ-oryzanol-based organogels. *Food Biophysics, 4*(4), 266-272. doi:10.1007/s11483-009-9124-9

Bouic, P. J. (2001). The role of phytosterols and phytosterolins in immune modulation: A review of the past 10 years. *Current Opinion in Clinical Nutrition & Metabolic Care, 4*(6), 471-475.

Bricknell, J., & Hartel, R. (1998). Relation of fat bloom in chocolate to polymorphic transition of cocoa butter. *Journal of the American Oil Chemists' Society, 75*(11), 1609-1615.

Bunjes, H., & Unruh, T. (2007). Characterization of lipid nanoparticles by differential scanning calorimetry, x-ray and neutron scattering. *Advanced Drug Delivery Reviews, 59*(6), 379-402. doi:http://dx.doi.org/10.1016/j.addr.2007.04.013

Cantrill, R. (2008). *Phytosterols, phytostanols and their esters* Paper presented at the Joint FAO/WHO Expert Committee on Food Additives Rome.

Carden, T. J., Hang, J., Dussault, P. H., & Carr, T. P. (2015). Dietary plant sterol esters must be hydrolyzed to reduce intestinal cholesterol absorption in hamsters. *The Journal of Nutrition*.

Cargill. (2008). Corowise-where to buy. Retrieved from http://www.corowise.com/wheretobuy/

Carr, T. P., Krogstrand, K. L. S., Schlegel, V. L., & Fernandez, M. L. (2009). Stearate-enriched plant sterol esters lower serum ldl cholesterol concentration in normo- and hypercholesterolemic adults. *The Journal of nutrition, 139*(8), 1445-1450.

Cebula, D. J., & Smith, K. W. (1991). Differential scanning calorimetry of confectionery fats. Pure triglycerides: Effects of cooling and heating rate variation. *Journal of the American Oil Chemists' Society, 68*(8), 591-595.

Chawla, R., & Goel, N. (2016). Phytosterol and its esters as novel food ingredients: A review. *Asian Journal of Dairy & Food Research, 35*(3).

Christiansen, L. I., Rantanen, J. T., von Bonsdorff, A. K., Karjalainen, M. A., & Yliruusi, J. K. (2002). A novel method of producing a microcrystalline β-sitosterol suspension in oil. *European Journal of Pharmaceutical Sciences, 15*(3), 261-269.

Cilla, A., Alegría, A., de Ancos, B. a., Sánchez-Moreno, C. n., Cano, M. P., Plaza, L., Clemente, G., Lagarda, M. J., & Barberá, R. (2012). Bioaccessibility of tocopherols, carotenoids, and ascorbic acid from milk-and soy-based fruit beverages: Influence of food matrix and processing. *Journal of Agricultural and Food Chemistry, 60*(29), 7282-7290.

Clark, R. M., Yao, L., She, L., & Furr, H. C. (2000). A comparison of lycopene and astaxanthin absorption from corn oil and olive oil emulsions. *Lipids, 35*(7), 803-806.

Clifton, P. (2007). Plant sterols and stanols as functional ingredients in dairy products. In M. Saarela (Ed.), *Functional dairy products* (Vol. 2, pp. 255-261): Woodhead Publishing.

Clifton, P., Noakes, M., Sullivan, D., Erichsen, N., Ross, D., Annison, G., & Nestel, P. (2003). Cholesterol-lowering effects of plant sterol esters differ in milk, yoghurt, bread and cereal. *European Journal of Clinical Nutrition, 58*(3), 503-509.

Coupland, J. N. (2002). Crystallization in emulsions. *Current Opinion in Colloid & Interface Science, 7*(5), 445-450.

Cusack, L. K., Fernandez, M. L., & Volek, J. S. (2013). The food matrix and sterol characteristics affect the plasma cholesterol lowering of phytosterol/phytostanol. *Advanced Nutrition 4*(6), 633-643.

Daels, E., Foubert, I., & Goderis, B. (2017). The effect of adding a commercial phytosterol ester mixture on the phase behavior of palm oil. *Food Research International*. doi:http://dx.doi.org/10.1016/j.foodres.2017.08.015

Damodaran, S., Parkin, K. L., & Fennema, O. R. (2007). *Fennema's food chemistry*. Boca Raton, FL: CRC press.

Desrumaux, A., & Marcand, J. (2002). Formation of sunflower oil emulsions stabilized by whey proteins with high-pressure homogenization (up to 350 mpa): Effect of pressure on emulsion characteristics. *International Journal of Food Science & Technology, 37*(3), 263-269. doi:10.1046/j.1365-2621.2002.00565.x

Dickinson, E. (1999). *Food emulsions and foams*. Witney, UK: Elsevier Applied Science Publishers Ltd.

Dickinson, E., & Golding, M. (1997). Depletion flocculation of emulsions containing unadsorbed sodium caseinate. *Food Hydrocolloids, 11*(1), 13-18.

Dickinson, E., Kruizenga, F.-J., Povey, M. J., & van der Molen, M. (1993). Crystallization in oil-in-water emulsions containing liquid and solid droplets. *Colloids and Surfaces A: Physicochemical and Engineering Aspects, 81*, 273-279.

Drapala, K. P. (2016). *Processing and stability of infant formula-based emulsions as affected by emulsifier type.* (Doctor of Philosophy), University College Cork.

Drapala, K. P., Auty, M. A. E., Mulvihill, D. M., & O'Mahony, J. A. (2015). Influence of lecithin on the processing stability of model whey protein hydrolysate-based infant formula emulsions. *International Journal of Dairy Technology, 68*(3), 322-333.

Drelich, J., Fang, C., & White, C. (2002). Measurement of interfacial tension in fluid-fluid systems. *Encyclopedia of Surface and Colloid Science, 3*, 3158-3163.

Du, H. (2015). *Physico-chemical properties of tristearin-oil blends.* (Masters of Science), Rutgers The State University of New Jersey, New Brunswick, NJ.

El-Loly, M. M. (2011). Composition, properties and nutritional aspects of milk fat globule membrane-a review. *Polish Journal of Food and Nutrition Sciences, 61*(1), 7-32.

Engel, R., & Schubert, H. (2005). Formulation of phytosterols in emulsions for increased dose response in functional foods. *Innovative Food Science & Emerging Technologies, 6*(2), 233-237. doi:http://dx.doi.org/10.1016/j.ifset.2005.01.004

Foegeding, E. A., & Davis, J. P. (2011). Food protein functionality: A comprehensive approach. *Food Hydrocolloids, 25*(8), 1853-1864.

Foubert, I., Vanhoutte, B., & Dewettinck, K. (2004). Temperature and concentration dependent effect of partial glycerides on milk fat crystallization. *European Journal of Lipid Science and Technology, 106*(8), 531-539.

Fox, P. F., & McSweeney, P. L. H. (2006). Composition and structure of bovine milk lipids. In Third (Ed.), *Advance dairy chemistry: Lipids* (3 ed., Vol. 2, pp. 1-35). New York, NY: Springer Science and Business Media.

Franchetti, D. (2016). Analysis of co-crystallized free phytosterols with triacylglycerols as a functional food ingredient. *Food Research International, 85*, 104–112.

Frasch-Melnik, S., Norton, I. T., & Spyropoulos, F. (2010). Fat-crystal stabilised w/o emulsions for controlled salt release. *Journal of Food Engineering, 98*(4), 437-442.

Frasch-Melnik, S., Spyropoulos, F., & Norton, I. T. (2010). W 1/o/w 2 double emulsions stabilised by fat crystals–formulation, stability and salt release. *Journal of Colloid and Interface Science, 350*(1), 178-185.

Fredrick, E. (2011). *Fat crystallization and partial coalescence in dairy creams: Role of monoacylglycerols.* (Doctor of Philosophy), Ghent University, Ghent University, Belgium. Retrieved from https://biblio.ugent.be/publication/1923936/file/4335708.pdf

Fredrick, E., Walstra, P., & Dewettinck, K. (2010). Factors governing partial coalescence in oil-in-water emulsions. *Advances in Colloid and Interface Science, 153*(1), 30-42.

Gabay, O., Sanchez, C., Salvat, C., Chevy, F., Breton, M., Nourissat, G., Wolf, C., Jacques, C., & Berenbaum, F. (2010). Stigmasterol: A phytosterol with potential anti-osteoarthritic properties. *Osteoarthritis and Cartilage, 18*(1), 106-116. doi:http://dx.doi.org/10.1016/j.joca.2009.08.019

German, J. B., & Dillard, C. J. (2006). Composition, structure and absorption of milk lipids: A source of energy, fat-soluble nutrients and bioactive molecules. *Critical Reviews in Food Science and Nutrition, 46*(1), 57-92.

Ghotra, B. S., Dyal, S. D., & Narine, S. S. (2002). Lipid shortenings: A review. *Food Research International, 35*(10), 1015-1048.

Giri, A., Kanawjia, S. K., & Rajoria, A. (2014). Effect of phytosterols on textural and melting characteristics of cheese spread. *Food Chemistry, 157*, 240-245. doi:http://dx.doi.org/10.1016/j.foodchem.2014.01.127

Goff, H. (2003). Ice cream. In P. L. H. McSweeney (Ed.), *Advanced dairy chemistry—proteins* (4 ed., Vol. 2, pp. 1063-1082): Springer.

Golomb, B. A., & Evans, M. A. (2008). Statin adverse effects. *American Journal of Cardiovascular Drugs, 8*(6), 373-418.

Goodwin, T. (1985). Biosynthesis of plant sterols. *New Comprehensive Biochemistry, 12*, 175-198.

Gresti, J., Bugaut, M., Maniongui, C., & Bezard, J. (1993). Composition of molecular species of triacylglycerols in bovine milk fat. *Journal of Dairy Science, 76*(7), 1850-1869. doi:https://doi.org/10.3168/jds.S0022-0302(93)77518-9

Griffin, W. C. (1954). Calculation of hlb values of non-ionic surfactants. *Journal of Cosmetic Science, 5*, 249-256.

Guinee, T. P., Auty, M. A. E., & Mullins, C. (1999). Observations on the microstructure and heat-induced changes in the viscoelasticity of commercial cheeses. *Australian Journal of Dairy Technology, 54*(2), 84.

Guinee, T. P., & McSweeney, P. L. H. (2006). Significance of milk fat in cheese *Advanced dairy chemistry lipids* (Vol. 2, pp. 377-440). New York, NY: Springer.

Gülseren, İ., & Coupland, J. N. (2007). The effect of emulsifier type and droplet size on phase transitions in emulsified even-numbered n-alkanes. *Journal of the American Oil Chemists' Society, 84*(7), 621-629. doi:10.1007/s11746-007-1093-x

Hartmann, M. (1998). Plant sterols and the membrane environment. *Trends in Plant Science, 3*(5), 170-175. doi:http://dx.doi.org/10.1016/S1360-1385(98)01233-3

Heid, H. W., & Keenan, T. W. (2005). Intracellular origin and secretion of milk fat globules. *European Journal of Cell Biology, 84*(2), 245-258. doi:http://dx.doi.org/10.1016/j.ejcb.2004.12.002

Hendricks, G., & Guo, M. (2006). Significance of milk fat in infant formulae *Advanced dairy chemistry lipids* (Vol. 2, pp. 467-477). New York, NY: Springer.

Hill, S. E. (1998). Functional properties of food macromolecules. In S. E. L. Hill, D.A.; Mitchell, J.R. (Ed.), *Food emulsions and foams*. Gaithersburg, MD: Aspen Publishers.

Himawan, C., Starov, V., & Stapley, A. (2006). Thermodynamic and kinetic aspects of fat crystallization. *Advances in Colloid and Interface Science, 122*(1), 3-33.

Hu, M., McClements, D. J., & Decker, E. A. (2003). Impact of whey protein emulsifiers on the oxidative stability of salmon oil-in-water emulsions. *Journal of Agricultural and Food Chemistry, 51*(5), 1435-1439.

Hunter, R. J. (2013). *Zeta potential in colloid science: Principles and applications* (Vol. 2). London, UK: Academic press.

Huppertz, T., & Kelly, A. (2006). Physical chemistry of milk fat globules *Advanced dairy chemistry lipids* (Vol. 2, pp. 173-212). New York, NY: Springer.

Jenness, R., & Walstra, P. (1984). *Dairy chemistry and physics-a wiley-interscience publication* (1 ed.): Wiley Subscription Services, Inc., A Wiley Company.

Jensen, R. G. (2000). Fatty acids in milk and dairy products. In C. K. Chow (Ed.), *Fatty acids in foods and their health implications* (Vol. 2, pp. 109-124). New York, Bastel: Marcel Dekker, Inc.

Jensen, R. G. (2002). The composition of bovine milk lipids: January 1995 to december 2000. *Journal of Dairy Science, 85*(2), 295-350. doi:https://doi.org/10.3168/jds.S0022-0302(02)74079-4

Jiang, Z.-Y., Han, T.-Q., Suo, G.-J., Feng, D.-X., Chen, S., Cai, X.-X., Jiang, Z.-H., Shang, J., Zhang, Y., et al. (2004). Polymorphisms at cholesterol 7α-hydroxylase, apolipoproteins b and e and low density lipoprotein receptor genes in patients with gallbladder stone disease. *World Journal of Gastroenterology, 10*(10), 1508.

Jones, P. J. H., & AbuMweis, S. S. (2009). Phytosterols as functional food ingredients: Linkages to cardiovascular disease and cancer. *Current Opinion in Clinical Nutrition & Metabolic Care, 12*(2), 147-151.

Jones, P. J. H., MacDougall, D. E., Ntanios, F., & Vanstone, C. A. (1997). Dietary phytosterols as cholesterol-lowering agents in humans. *Canadian Journal of Physiology and Pharmacology, 75*(3), 217-227. doi:10.1139/y97-011

Jonker, D., Van der Hoek, G., Glatz, J., Homan, C., Posthumus, M., & Katan, M. (1985). Combined determination of free, esterified and glycosilated plant sterols in foods. *Nutrition Reports International, 32*, 943-952.

Joseph, S., Rappolt, M., Schoenitz, M., Huzhalska, V., Augustin, W., Scholl, S., & Bunjes, H. (2015). Stability of the metastable α-polymorph in solid triglyceride drug-carrier nanoparticles. *Langmuir, 31*(24), 6663-6674.

Kehoe, S. I., Jayarao, B. M., & Heinrichs, A. J. (2007). A survey of bovine colostrum composition and colostrum management practices on pennsylvania dairy farms1. *Journal of Dairy Science, 90*(9), 4108-4116. doi:http://dx.doi.org/10.3168/jds.2007-0040

Kellens, M., Meeussen, W., Hammersley, A., & Reynaers, H. (1991). Synchrotron radiation investigations of the polymorphic transitions in saturated monoacid triglycerides. Part 2: Polymorphism study of a 50:50 mixture of tripalmitin and tristearin during crystallization and melting. *Chemistry and Physics of Lipids, 58*(1), 145-158. doi:http://dx.doi.org/10.1016/0009-3084(91)90120-Z

Kelly, G. M. (2015). *The effects of formulation and processing on surface characteristics and functional properties of dairy powders.* (Doctor of Philosophy), University College of Cork.

Kim, H., & Burgess, D. J. (2001). Prediction of interfacial tension between oil mixtures and water. *Journal of Colloid and Interface Science, 241*(2), 509-513.

Kloek, W. (1998). *Properties of fats in relation to their crystallization.* (Doctor of Philosophy), Wageningen University, Wageningen, Netherlands.

Korlach, J., Schwille, P., Webb, W. W., & Feigenson, G. W. (1999). Characterization of lipid bilayer phases by confocal microscopy and fluorescence correlation spectroscopy. *Proceedings of the National Academy of Sciences, 96*(15), 8461-8466.

Kuksis, A., Marai, L., & Myher, J. J. (1973). Triglyceride structure of milk fats. *Journal of the American Oil Chemists Society, 50*(6), 193-201. doi:10.1007/bf02640489

Kummerow, F. A. (2009). The negative effects of hydrogenated trans fats and what to do about them. *Atherosclerosis, 205*(2), 458-465. doi:http://dx.doi.org/10.1016/j.atherosclerosis.2009.03.009

Lagarda, M., García-Llatas, G., & Farré, R. (2006). Analysis of phytosterols in foods. *Journal of Pharmaceutical and Biomedical Analysis, 41*(5), 1486-1496.

Lagarda, M. J., García-Llatas, G., & Farré, R. (2006). Analysis of phytosterols in foods. *Journal of Pharmaceutical and Biomedical Analysis, 41*(5), 1486-1496. doi:http://dx.doi.org/10.1016/j.jpba.2006.02.052

Lim, A. S., Burdikova, Z., Sheehan, J. J., & Roos, Y. H. (2016). Carotenoid stability in high total solid spray dried emulsions with gum arabic layered interface and trehalose–wpi composites as wall materials. *Innovative Food Science & Emerging Technologies, 34*, 310-319.

Ling, W. H., & Jones, P. J. H. (1995). Dietary phytosterols: A review of metabolism, benefits and side effects. *Life Sciences, 57*(3), 195-206.

Liu, F., & Tang, C.-H. (2014). Phytosterol colloidal particles as pickering stabilizers for emulsions. *Journal of Agricultural and Food Chemistry*.

Lopez-Huertas, E. (2010). Health effects of oleic acid and long chain omega-3 fatty acids (epa and dha) enriched milks. A review of intervention studies. *Pharmacological Research, 61*(3), 200-207. doi:http://dx.doi.org/10.1016/j.phrs.2009.10.007

Lopez, C. (2011). Milk fat globules enveloped by their biological membrane: Unique colloidal assemblies with a specific composition and structure. *Current Opinion in Colloid & Interface Science, 16*(5), 391-404. doi:http://dx.doi.org/10.1016/j.cocis.2011.05.007

Lopez, C., Bourgaux, C., Lesieur, P., Bernadou, S., Keller, G., & Ollivon, M. (2002). Thermal and structural behavior of milk fat: 3. Influence of cooling rate and droplet size on cream crystallization. *Journal of Colloid and Interface Science, 254*(1), 64-78. doi:http://dx.doi.org/10.1006/jcis.2002.8548

Lopez, C., Bourgaux, C., Lesieur, P., & Ollivon, M. (2007). Coupling of time-resolved synchrotron x-ray diffraction and dsc to elucidate the crystallisation properties and polymorphism of triglycerides in milk fat globules. *Le Lait, 87*(4-5), 459-480.

Lopez, C., Bourgaux, C., Lesieur, P., Riaublanc, A., & Ollivon, M. (2006). Milk fat and primary fractions obtained by dry fractionation: 1. Chemical composition and crystallisation properties. *Chemistry and Physics of Lipids, 144*(1), 17-33. doi:http://dx.doi.org/10.1016/j.chemphyslip.2006.06.002

Lopez, C., & Ollivon, M. (2009). Crystallisation of triacylglycerols in nanoparticles. *Journal of Thermal Analysis and Calorimetry, 98*(1), 29-37. doi:10.1007/s10973-009-0183-4

MacGibbon, A., & Taylor, M. (2006). Composition and structure of bovine milk lipids *Advanced dairy chemistry: Lipids* (Vol. 2, pp. 1-42). New York, NY: Springer.

MacMillan, S., Roberts, K., Rossi, A., Wells, M., Polgreen, M., & Smith, I. (2002). In situ small angle x-ray scattering (saxs) studies of polymorphism with the associated crystallization of cocoa butter fat using shearing conditions. *Crystal Growth & Design, 2*(3), 221-226.

Maher, P. G., Auty, M. A. E., Roos, Y. H., Zychowski, L. M., & Fenelon, M. A. (2015). Microstructure and lactose crystallization properties in spray dried nanoemulsions. *Food Structure, 3*(0), 11. doi:http://dx.doi.org/10.1016/j.foostr.2014.10.001

Malvern, I. (2017). The masterclass 1: Laser diffraction explained. *Webinars*.

Mao, L., Roos, Y. H., & Miao, S. (2014). Flavour release from monoglyceride structured oil-in-water emulsions through static headspace analysis. *Food Biophysics, 9*(4), 359-367.

Marino, V. M., Schadt, I., La Terra, S., Manenti, M., Caccamo, M., Licitra, G., & Carpino, S. (2012). Influence of season and pasture feeding on the content of α-tocopherol and β-carotene in milk from holstein, brown swiss and modicana cows in sicily. *Dairy Science & Technology, 92*(5), 501-513. doi:10.1007/s13594-012-0069-2

Martini, S., Suzuki, A., & Hartel, R. W. (2008). Effect of high intensity ultrasound on crystallization behavior of anhydrous milk fat. *Journal of the American Oil Chemists' Society, 85*(7), 621-628.

McCarthy, N. A., Kelly, A. L., O'Mahony, J. A., & Fenelon, M. A. (2014). Sensitivity of emulsions stabilised by bovine β-casein and lactoferrin to heat and cacl 2. *Food Hydrocolloids, 35*, 420-428.

McClements, D. J. (2004a). *Food emulsions: Principles, practices, and techniques*: CRC press.

McClements, D. J. (2004b). Protein-stabilized emulsions. *Current Opinion in Colloid & Interface Science, 9*(5), 305-313. doi:http://dx.doi.org/10.1016/j.cocis.2004.09.003

McClements, D. J. (2007). Critical review of techniques and methodologies for characterization of emulsion stability. *Critical Reviews in Food Science and Nutrition, 47*(7), 611-649.

McClements, D. J. (2012). Crystals and crystallization in oil-in-water emulsions: Implications for emulsion-based delivery systems. *Advances in Colloid and Interface Science, 174*, 1-30.

McClements, D. J. (2015). *Food emulsions: Principles, practices, and techniques*. Boca Raton, FL: CRC press.

McClements, D. J., Decker, E. A., & Weiss, J. (2007). Emulsion- based delivery systems for lipophilic bioactive components. *Journal of Food Science, 72*(8), R109-R124.

McClements, D. J., & Li, Y. (2010). Structured emulsion-based delivery systems: Controlling the digestion and release of lipophilic food components. *Advances in Colloid and Interface Science, 159*(2), 213-228.

Melnikov, S. M., Seijen ten Hoorn, J. W. M., & Bertrand, B. (2004). Can cholesterol absorption be reduced by phytosterols and phytostanols via a cocrystallization mechanism? *Chemistry and Physics of Lipids, 127*(1), 15-33. doi:https://doi.org/10.1016/j.chemphyslip.2003.08.007

Metin, S., & Hartel, R. W. (2005). *Crystallization of fats and oils* (Vol. 1). Hoboken, NJ: Wiley Subscription Services, Inc., A Wiley Company.

Michalski, M.-C., Ollivon, M., Briard, V., Leconte, N., & Lopez, C. (2004). Native fat globules of different sizes selected from raw milk: Thermal and structural behavior. *Chemistry and Physics of Lipids, 132*(2), 247-261.

Miquel, M. E., & Hall, L. D. (1998). A general survey of chocolate confectionery by magnetic resonance imaging. *LWT - Food Science and Technology, 31*(2), 93-99. doi:https://doi.org/10.1006/fstl.1997.0329

Moreau, R. A., Whitaker, B. D., & Hicks, K. B. (2002). Phytosterols, phytostanols, and their conjugates in foods: Structural diversity, quantitative analysis, and health-promoting uses. *Progress in Lipid Research, 41*(6), 457-500. doi:http://dx.doi.org/10.1016/S0163-7827(02)00006-1

Moreno-Calvo, E., Temelli, F., Cordoba, A., Masciocchi, N., Veciana, J., & Ventosa, N. (2014). A new microcrystalline phytosterol polymorph generated using co2-expanded solvents. *Crystal Growth & Design, 14*(1), 58-68. doi:10.1021/cg401068n

Mutoh, T.-A., Kubouchi, H., Noda, M., Shiinoki, Y., & Matsumura, Y. (2007). Effect of oil-soluble emulsifiers on solidification of thermally treated creams. *International Dairy Journal, 17*(1), 24-28. doi:https://doi.org/10.1016/j.idairyj.2006.01.004

Nagao, K., & Yanagita, T. (2005). Conjugated fatty acids in food and their health benefits. *Journal of Bioscience and Bioengineering, 100*(2), 152-157. doi:http://dx.doi.org/10.1263/jbb.100.152

Nes, W. R., Krevitz, K., & Behzadan, S. (1976). Configuration at c-24 of 24-methyl and 24-ethylcholesterol in tracheophytes. *Lipids, 11*(2), 118-126.

Normén, L., Frohlich, J., & Trautwein, E. (2004). Role of plant sterols in cholesterol lowering *Phytosterols as functional food components and nutraceuticals* (pp. 243-315). New York, NY: Marcel Dekker, Inc.

O' Dwyer, S. (2012). *Stabilisation of omega-3 oils in food and emulsion systems* (Doctor of Philosophy), University of Limerick.

Onuki, Y., Morishita, M., Watanabe, H., Chiba, Y., Tokiwa, S., Takayama, K., & Nagai, T. (2003). Improved insulin enteral delivery using water-in-oil-in-water multiple emulsion incorporating highly purified docosahexaenoic acid. *Sciences Techniques et Pratiques Pharmaceutiques Sciences 13*(4), 231-235.

Ostersen, S., Foldager, J., & Hermansen, J. E. (1997). Effects of stage of lactation, milk protein genotype and body condition at calving on protein composition and renneting properties of bovine milk. *Journal of Dairy Research, 64*(2), 207-219. doi:undefined

Ostlund, R. E., Racette, S. B., Okeke, A., & Stenson, W. F. (2002). Phytosterols that are naturally present in commercial corn oil significantly reduce cholesterol absorption in humans. *The American Journal of Clinical Nutrition, 75*(6), 1000-1004.

Ostlund, R. E., Spilburg, C. A., & Stenson, W. F. (1999). Sitostanol administered in lecithin micelles potently reduces cholesterol absorption in humans. *The American Journal of Clinical Nutrition, 70*(5), 826-831.

Palanuwech, J., & Coupland, J. N. (2003). Effect of surfactant type on the stability of oil-in-water emulsions to dispersed phase crystallization. *Colloids and Surfaces A: Physicochemical and Engineering Aspects, 223*(1), 251-262.

Palmquist, D., Beaulieu, A. D., & Barbano, D. (1993). Feed and animal factors influencing milk fat composition. *Journal of Dairy Science, 76*(6), 1753-1771.

Parodi, P. (1973). The sterol content of milkfat, animal fats, margarines and vegetable oils. *Australian Journal of Dairy Technology, 28*(3), 135.

Phillips, K. M., Ruggio, D. M., & Ashraf-Khorassani, M. (2005). Phytosterol composition of nuts and seeds commonly consumed in the united states. *Journal of Agricultural and Food Chemistry, 53*(24), 9436-9445.

Piironen, V., Toivo, J., & Lampi, A. M. (2000). Natural sources of dietary plant sterols. *Journal of Food Composition and Analysis, 13*(4), 619-624. doi:http://dx.doi.org/10.1006/jfca.2000.0898

Plat, J., & Mensink, R. P. (2002). Increased intestinal abca1 expression contributes to the decrease in cholesterol absorption after plant stanol consumption. *The FASEB Journal, 16*(10), 1248-1253.

Pool, H., Mendoza, S., Xiao, H., & McClements, D. J. (2013). Encapsulation and release of hydrophobic bioactive components in nanoemulsion-based delivery systems: Impact of physical form on quercetin bioaccessibility. *Food & Function, 4*(1), 162-174.

Pouteau, E. B., Monnard, I. E., Piguet-Welsch, C., Groux, M. J. A., Sagalowicz, L., & Berger, A. (2003). Non-esterified plant sterols solubilized in low fat milks inhibit cholesterol absorption. *European Journal of Nutrition, 42*(3), 154-164. doi:10.1007/s00394-003-0406-6

Raicht, R. F., Cohen, B. I., Fazzini, E. P., Sarwal, A. N., & Takahashi, M. (1980). Protective effect of plant sterols against chemically induced colon tumors in rats. *Cancer Research, 40*(2), 403-405.

Rodriguez- Amaya, D. B. (2015). *Food carotenoids: Chemistry, biology, and technology*.

Rosenberg, M., & Lee, S. (1993). Microstructure of whey protein/anhydrous milkfat emulsions. *Food Structure, 12*(2), 14.

Rosenblatt, K. M., & Bunjes, H. (2009). Poly(vinyl alcohol) as emulsifier stabilizes solid triglyceride drug carrier nanoparticles in the α-modification. *Molecular Pharmaceutics, 6*(1), 105-120. doi:10.1021/mp8000759

Rossi, L., ten Hoorn, J. W. S., Melnikov, S. M., & Velikov, K. P. (2010). Colloidal phytosterols: Synthesis, characterization and bioaccessibility. *Soft Matter, 6*(5), 928-936.

Rozner, S., & Garti, N. (2006). The activity and absorption relationship of cholesterol and phytosterols. *Colloids and Surfaces A: Physicochemical and Engineering Aspects, 282*, 435-456.

Russell, A., Cheney, P., & Wantling, S. (1999). Influence of freezing conditions on ice crystallisation in ice cream. *Journal of Food Engineering, 39*(2), 179-191.

Sagalowicz, L., Leser, M. E., Watzke, H. J., & Michel, M. (2006). Monoglyceride self-assembly structures as delivery vehicles. *Trends in Food Science & Technology, 17*(5), 204-214. doi:http://dx.doi.org/10.1016/j.tifs.2005.12.012

Salentinig, S., Phan, S., Khan, J., Hawley, A., & Boyd, B. J. (2013). Formation of highly organized nanostructures during the digestion of milk. *American Chemical Society Nano, 7*(12), 10904-10911.

Sato, K. (1999). Solidification and phase transformation behaviour of food fats—a review. *European Journal of Lipid Science and Technology, 101*(12), 467-474.

Sato, K. (2001). Crystallization behaviour of fats and lipids — a review. *Chemical Engineering Science, 56*(7), 2255-2265. doi:http://dx.doi.org/10.1016/S0009-2509(00)00458-9

Sato, K., & Ueno, S. (2011). Crystallization, transformation and microstructures of polymorphic fats in colloidal dispersion states. *Current Opinion in Colloid & Interface Science, 16*(5), 384-390.

Schnablegger, H., & Singh, Y. (2013). *The saxs guide*. Austria: Anton Paar GmbH.

Shaghaghi, M. A., Harding, S. V., & Jones, P. J. H. (2014). Water dispersible plant sterol formulation shows improved effect on lipid profile compared to plant sterol esters. *Journal of Functional Foods, 6*, 280-289.

Shahidi, F., & Han, X. Q. (1993). Encapsulation of food ingredients. *Critical Reviews in Food Science & Nutrition, 33*(6), 501-547.

Shewan, H. M., & Stokes, J. R. (2013). Review of techniques to manufacture micro-hydrogel particles for the food industry and their applications. *Journal of Food Engineering, 119*(4), 781-792. doi:https://doi.org/10.1016/j.jfoodeng.2013.06.046

Shi, Y., Smith, C. M., & Hartel, R. W. (2001). Compositional effects on milk fat crystallization. *Journal of Dairy Science, 84*(11), 2392-2401. doi:http://dx.doi.org/10.3168/jds.S0022-0302(01)74688-7

Shukat, R., Bourgaux, C., & Relkin, P. (2011). Crystallisation behaviour of palm oil nanoemulsions carrying vitamin e: Dsc and synchrotron x-ray scattering studies. *Journal of Thermal Analysis and Calorimetry, 108*(1), 153-161.

Silva, J. V. C., & O'Mahony, J. A. (2017). Flowability and wetting behaviour of milk protein ingredients as influenced by powder composition, particle size and microstructure. *International Journal of Dairy Technology, 70*(2), 277-286. doi:10.1111/1471-0307.12368

Simoneau, C., McCarthy, M. J., Reid, D. S., & German, J. B. (1992). Measurement of fat crystallization using nmr imaging and spectroscopy. *Trends in Food Science & Technology, 3*, 208-211. doi:https://doi.org/10.1016/0924-2244(92)90192-Y

Simoneau, C., McCarthy, M. J., Reid, D. S., & German, J. B. (1993). Influence of triglyceride composition on crystallization kinetics of model emulsions. *Journal of Food Engineering, 19*(4), 365-387. doi:https://doi.org/10.1016/0260-8774(93)90026-G

Skoda, W., & Van den Tempel, M. (1963). Crystallization of emulsified triglycerides. *Journal of Colloid Science, 18*(6), 568-584.

Smet, E. D., Mensink, R. P., & Plat, J. (2012). Effects of plant sterols and stanols on intestinal cholesterol metabolism: Suggested mechanisms from past to present. *Molecular Nutrition & Food Research, 56*(7), 1058-1072.

Smith, K. W., Bhaggan, K., Talbot, G., & van Malssen, K. F. (2011). Crystallization of fats: Influence of minor components and additives. *Journal of the American Oil Chemists' Society, 88*(8), 1085-1101.

Smith, S., & Abraham, S. (1975). The composition and biosynthesis of milk fat. *Advanced Lipid Research, 13*, 195-239.

Soyeurt, H., Dardenne, P., Gillon, A., Croquet, C., Vanderick, S., Mayeres, P., Bertozzi, C., & Gengler, N. (2006). Variation in fatty acid contents of milk and milk fat within and across breeds. *Journal of Dairy Science, 89*(12), 4858-4865. doi:http://dx.doi.org/10.3168/jds.S0022-0302(06)72534-6

Sprow, F. (1967). Distribution of drop sizes produced in turbulent liquid—liquid dispersion. *Chemical Engineering Science, 22*(3), 435-442.

Srinivasan, M., Singh, H., & Munro, P. (2002). Formation and stability of sodium caseinate emulsions: Influence of retorting (121 c for 15 min) before or after emulsification. *Food Hydrocolloids, 16*(2), 153-160.

Sünder, A., Scherze, I., & Muschiolik, G. (2001). Physico-chemical characteristics of oil-in-water emulsions based on whey protein–phospholipid mixtures. *Colloids and Surfaces: Biointerfaces, 21*(1), 75-85.

Taylor, M., & Richardson, T. (1980). Antioxidant activity of skim milk: Effect of heat and resultant sulfhydryl groups. *Journal of Dairy Science, 63*(11), 1783-1795.

Thanasukarn, P., Pongsawatmanit, R., & McClements, D. (2004). Influence of emulsifier type on freeze-thaw stability of hydrogenated palm oil-in-water emulsions. *Food Hydrocolloids, 18*(6), 1033-1043.

Thomsen, A. B., Hansen, H. B., Christiansen, C., Green, H., & Berger, A. (2004). Effect of free plant sterols in low-fat milk on serum lipid profile in

hypercholesterolemic subjects. *European Journal of Clinical Nutrition 58*(6), 860-870.

Toro- Vazquez, J. F., Rangel- Vargas, E., Dibildox- Alvarado, E., & Charó- Alonso, M. A. (2005). Crystallization of cocoa butter with and without polar lipids evaluated by rheometry, calorimetry and polarized light microscopy. *European Journal of Lipid Science and Technology, 107*(9), 641-655.

Torre, L. G., & Pinho, S. C. (2015). Lipid matrices for nanoencapsulation in food: Liposomes and lipid nanoparticles. In H. Hernández-Sánchez & G. F. Gutiérrez-López (Eds.), *Food nanoscience and nanotechnology* (pp. 99-143). New York, NY: Springer International Publishing.

Trautwein, E. A., & Demonty, I. (2007). Phytosterols: Natural compounds with established and emerging health benefits. *Oléagineux, Corps gras, Lipides, 14*(5), 259-266.

Tyssandier, V., Lyan, B., & Borel, P. (2001). Main factors governing the transfer of carotenoids from emulsion lipid droplets to micelles. *Biochimica et Biophysica Acta (BBA)-Molecular and Cell Biology of Lipids, 1533*(3), 285-292.

Vaikousi, H., Lazaridou, A., Biliaderis, C. G., & Zawistowski, J. (2007). Phase transitions, solubility, and crystallization kinetics of phytosterols and phytosterol−oil blends. *Journal of Agricultural and Food Chemistry*, *55*(5), 1790-1798. doi:10.1021/jf0624289

Van Aken, G. A., Ten Grotenhuis, E., Van Langevelde, A. J., & Schenk, H. (1999). Composition and crystallization of milk fat fractions. *Journal of the American Oil Chemists' Society, 76*(11), 1323-1331. doi:10.1007/s11746-999-0146-8

Vanapalli, S. A., Palanuwech, J., & Coupland, J. N. (2002). Stability of emulsions to dispersed phase crystallization: Effect of oil type, dispersed phase volume fraction, and cooling rate. *Colloids and Surfaces A: Physicochemical and Engineering Aspects, 204*(1), 227-237.

Vanhoutte, B., Dewettinck, K., Foubert, I., Vanlerberghe, B., & Huyghebaert, A. (2002). The effect of phospholipids and water on the isothermal crystallisation of milk fat. *European Journal of Lipid Science and Technology, 104*(8), 490-495.

von Bonsdorff-Nikander, A., Karjalainen, M., Rantanen, J., Christiansen, L., & Yliruusi, J. (2003). Physical stability of a microcrystalline β-sitosterol suspension in oil. *European Journal of Pharmaceutical Sciences, 19*(4), 173-179.

Weiss, J., Decker, E., McClements, D. J., Kristbergsson, K., Helgason, T., & Awad, T. (2008). Solid lipid nanoparticles as delivery systems for bioactive food components. *Food Biophysics, 3*(2), 146-154. doi:10.1007/s11483-008-9065-8

Widlak, N., Hartel, R. W., & Narine, S. (2001). *Crystallization and solidification properties of lipids*. Champaign, IL: The American Oil Chemists Society.

Wooding, F. (1971). The mechanism of secretion of the milk fat globule. *Journal of Cell Science, 9*(3), 805-821.

Wright, A. J. (2003). Spreading the word on butter. *Food Structure 14*(10), 613-614.

Wright, A. J., & Marangoni, A. G. (2002). Effect of dag on milk fat tag crystallization. *Journal of the American Oil Chemists' Society, 79*(4), 395-402.

Wright, A. J., & Marangoni, A. G. (2006). Crystallization and rheological properties of milk fat *Advanced dairy chemistry lipids* (Vol. 2, pp. 245-291). New York, NY: Springer.

Xinming, L., Yingde, C., Lloyd, A. W., Mikhalovsky, S. V., Sandeman, S. R., Howel, C. A., & Liewen, L. (2008). Polymeric hydrogels for novel contact lens-based ophthalmic drug delivery systems: A review. *Contact Lens and Anterior Eye, 31*(2), 57-64. doi:http://dx.doi.org/10.1016/j.clae.2007.09.002

Yi, J., Knudsen, T. A., Nielsen, A.-L., Duelund, L., Christensen, M., Hervella, P., Needham, D., & Mouritsen, O. G. (2016). Inhibition of cholesterol transport in an intestine cell model by pine-derived phytosterols. *Chemistry and Physics of Lipids, 200*, 62-73. doi:http://doi.org/10.1016/j.chemphyslip.2016.06.008

Yuan, Y., Gao, Y., Zhao, J., & Mao, L. (2008). Characterization and stability evaluation of β-carotene nanoemulsions prepared by high pressure homogenization under various emulsifying conditions. *Food Research International, 41*(1), 61-68.

Zawistowski, J. (2010). 17 tangible health benefits of phytosterol functional foods. *Functional Food Product Development, 2*.

Zhang, L., Hayes, D. G., Chen, G., & Zhong, Q. (2013). Transparent dispersions of milk-fat-based nanostructured lipid carriers for delivery of β-carotene. *Journal of Agricultural and Food Chemistry, 61*(39), 9435-9443.

Zychowski, L. M., Logan, A., Kelly, A. L., & Auty, M. A. E. (2016). Synchrotron application in functional foods. *Teagasc Research Autumn 2016*, 26-27.

Objectives

This thesis investigated a series of interrelated topics on the behaviour of phytosterol-enriched bulk and emulsified milk fat matrices. Milk fat-based systems were developed and examined to establish how phytosterol enrichment influenced the crystalline behaviour of the milk fat. Another objective was to quantify crystalline behaviour of phytosterols in these systems and to see if the solubility of phytosterols could be improved, for greater bioaccessibility in future applications. Furthermore, this work studied how the o/w interface influenced the behaviour of milk fat, phytosterols, and phytosterols/whey protein combinations (used in the emulsion systems); since the structure of interface is directly linked to interfacial phytosterol crystallisation and the observed physicochemical behaviour of the system. The work is presented in the following experimental chapters as outlined in Figure 1.16.

The specific aims of the work presented in this thesis are as follows:

- To characterise the crystallisation behaviour of milk fat in both bulk and emulsified matrices following phytosterol enrichment;
- To establish how phytosterols crystallise in milk fat in both bulk and emulsified matrices at different levels of phytosterol enrichment;
- To access the physicochemical changes of emulsified milk fat systems upon the addition of phytosterols into the dispersed oil phase;
- To investigate if phytosterol crystallisation behaviour/solubility can be influenced by the presence of low molecular weight surfactants or by changes in the droplet size in milk fat systems;
- To develop a system to investigate the influence of interfacial components on the crystallisation behaviour of TAG emulsions.

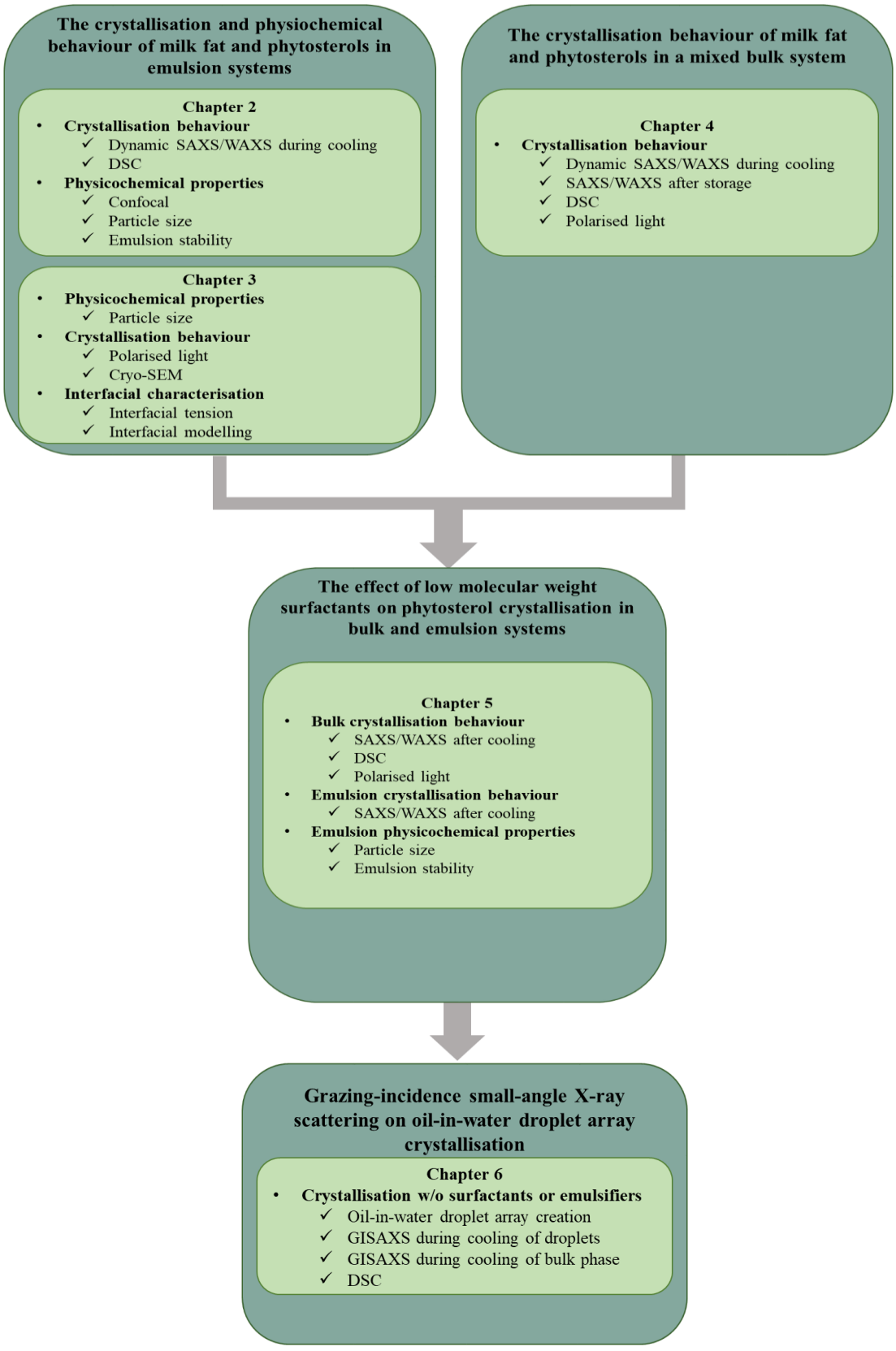

Figure 1.16 *Schematic representation of the experimental design of the thesis*

Chapter 2

Effect of phytosterols on the crystallisation behaviour of oil-in-water milk fat emulsions

Lisa M. Zychowski[†§‡#], Amy Logan*[‡], Mary Ann Augustin[‡], Alan L. Kelly[§], Alexandru Zabara[#], James A. O'Mahony[§], Charlotte E. Conn[#], Mark A. E. Auty*[†]

[†] Food Chemistry and Technology Department, Teagasc Food Research Centre, Moorepark, Fermoy, Co. Cork, Ireland

[§] School of Food and Nutritional Sciences, University College Cork, Cork, Ireland

[‡] CSIRO Food and Nutrition, Werribee, Victoria 3030, Australia

[#] School of Applied Science, RMIT University, Melbourne, Victoria 3000, Australia

Published as: Zychowski, L. M., Logan, A., Augustin, M. A., Kelly, A. L., Zabara, A., O'Mahony, J. A., Conn, C. E., Auty, M. A. (2016). Effect of Phytosterols on the Crystallization Behavior of Oil-in-Water Milk Fat Emulsions. *Journal of Agricultural and Food Chemistry, 64*(34), 6546–6554.

Declaration: DSC data collection was performed by Amy Logan. All other measurements were collected and analysed by the first author.

Abstract

Milk has been used commercially as a carrier for phytosterols, but there is limited knowledge on the effect of added plant sterols on the properties of the system. In this study, phytosterols dispersed in milk fat at levels of 0.3 or 0.6% were homogenised with an aqueous dispersion of whey protein isolate (WPI). The particle size, morphology, ζ-potential, and stability of the emulsions were investigated. Emulsion crystallisation properties were examined through the use of differential scanning calorimetry (DSC) and synchrotron X-ray scattering at both small and wide angles. Phytosterol enrichment influenced the particle size and physical appearance of the emulsion droplets, but did not impact the stability or charge of the dispersed particles. DSC data demonstrated that, at the higher level of phytosterol addition, crystallisation of milk fat was delayed whereas, at the lower level, phytosterol enrichment induced nucleation and emulsion crystallisation. These differences were attributed to the formation of separate phytosterol crystals within the emulsions at the high phytosterol concentration, as characterised by synchrotron X-ray measurements. X-ray scattering patterns demonstrated the ability of the phytosterol to integrate within the milk fat triacylglycerol matrix, with a concomitant increase in longitudinal packing and system disorder. Understanding the consequences of adding phytosterols, on the physical and crystalline behaviour of emulsions may enable the functional food industry to design more physically and chemically stable products.

2.1 Introduction

Phytosterols are naturally occurring compounds found in cereals, nuts, vegetables, and fruits. There are over 200 identified types of phytosterols, the most abundant being β-sitosterol, campesterol, and stigmasterol (Berger et al., 2004). They are chemically similar to human cholesterol, differing only in the presence or absence of a double bond and a side chain at the C-24 position (MacKay & Jones, 2012). This similarity enables phytosterols to effectively reduce serum cholesterol by preventing its absorption in the intestinal tract. Mechanistically, this is achieved through competitive solubilisation between cholesterol and plant sterols in the bile salt and acid micelles. The result is an increase in endogenous cholesterol synthesis, which mediates removal of low-density lipoproteins (LDL) from the blood (Ostlund, 2002; Plat, Jogchum & Mensink, 2005; Rozner et al., 2007; Plat, J. et al., 2012; Smet et al., 2012).

To significantly lower LDL-cholesterol levels, it is recommended to consume > 1.5 grams of plant sterols daily (Cusack et al., 2013). In order to achieve these levels, dietary supplementation is needed, as the average intake of plant sterols is between 160-400 mg per day (Lagarda et al., 2006). Due to a global rise in diet-related chronic diseases, there has been an increased interest in using phytosterols in functional foods. However, successful incorporation of these molecules within food matrices has been challenging because of their low solubility, lipophilic nature, and high melting point (Clifton, P., 2007; Dickinson & Leser, 2007; Vaikousi et al., 2007).

To overcome these challenges, the functional food industry traditionally esterified phytosterols to solubilise them into high fat matrices such as plant margarines. Although esterified phytosterols are more soluble in oil than their non-esterified counterparts, their application is not preferred due to higher processing costs and unpredictable adsorption rates (Clifton, P., 2007; Franchetti, 2016). Ester varieties need to be hydrolysed prior to absorption, which is subject to interindividual variability among human digestive systems, resulting in absorption rates varying between 40-96% (Mattson et al., 1982; Clifton, P., 2007; Smet et al., 2012; Lubinus et al., 2013; Carden et al., 2015). In order to enhance the solubility of unesterified phytosterols, emulsion-based delivery systems have been employed and proven successful in lowering LDL cholesterol (Ostlund et al., 1999; Gremaud et al., 2002; Alexander et al., 2012; Rondanelli et al., 2013).

Although phytosterol-enriched emulsion systems are effective at lowering LDL cholesterol, their success is still highly dependent upon the physical state and location of the phytosterols in the emulsion system. It has been demonstrated that solubilised phytosterols are more effective at lowering LDL cholesterol levels than dispersed nonsolubilised phytosterols (Ostlund et al., 1999; Pouteau et al., 2003; Engel & Schubert, 2005; Shaghaghi et al., 2014). In the design of an appropriate carrier matrix, functional performance of the bioactive in the chosen matrix is crucial to ensuring the success of the final functional food (McClements, 2015).

In this study, a milk fat-based emulsion was chosen as the carrier matrix. Milk has become a popular carrier for phytosterols, as it has been reported to be more effective at lowering LDL cholesterol than bread or cereals (Clifton, P et al., 2003). In a previous study, a 29.1 ± 4.1% reduction in LDL-cholesterol levels was observed when subjects ingested milk enriched with emulsified phytosterols using a proprietary crystal-retardation method (Pouteau et al., 2003). In addition, the diverse blend of triacylglycerols (TAG) in milk fat has been found to be more effective than soybean oil, for the encapsulation of the bioactive β-carotene (Zhang et al., 2013). Milk fat contains up to 400 different types of fatty acids, which generates a complex crystalline TAG network upon cooling (MacGibbon & Taylor, 2006). Milk fat has the potential to encapsulate other types of bioactives, but limited knowledge exists about how the physical and chemical properties of the milk fat are affected by this or what type of compounds can be incorporated.

Thus, this study aimed to develop knowledge regarding the use of milk fat-based emulsions for the delivery of phytosterols. The crystallisation and melting properties of phytosterols within emulsified milk fat systems was investigated through thermal and structural analysis. The stability, particle size, and ζ-potential of the emulsions were also monitored to understand how phytosterol incorporation impacts the physical properties and stability of the emulsion systems. This knowledge will enable the functional food industry to optimise the bioaccessibility and functional performance of phytosterol-enriched dairy products.

2.2 Materials and methods

2.2.1 Chemicals and ingredients

Crystalline phytosterol, a mixture of β-sitosterol (≥70%) with residuals of campesterol and β-sitostanol, was purchased from Sigma Aldrich (Wicklow, Ireland). Commercial grade anhydrous milk fat was obtained from Marsh Dairy Product (Appendix 1; Footscray, Australia). Whey protein isolate (WPI) (ALACEN© 895, protein content 92.0%) was purchased from Fonterra (Maungaturoto, New Zealand). Sodium azide was purchased from Sigma Aldrich (Castle Hill, Australia). Emulsions prepared for imaging in Ireland utilised anhydrous milk fat purchased from Corman Miloko (Carrick on Suir, Ireland) and WPI (BiPro© protein content 92.7%) sourced from Danisco Food International (Eden Prairie, Minnesota).

2.2.2.1 Preparation of emulsions

Oil-in-water emulsions (10% oil: 1% protein: 89% H_20) were prepared on a wt/wt basis with or without added phytosterols in the oil fraction (0.3 or 0.6% wt/wt). The aqueous phase was prepared by reconstituting WPI at 11.11% protein for 2 hours (h) in an ice bath with Milli-Q water. The solution was then stored overnight at 4 ˚C to allow for complete hydration. Before homogenisation, aliquots of WPI solution needed to create 1% protein in the final emulsion were removed and heated to 55 ˚C for 20 minutes (min). After heating, the WPI solution was diluted with distilled water at 70 ˚C and then subsequently added to the oil phase. This process was employed to minimise denaturation of the whey protein by high temperatures or excessive heat exposure (McClements, 2004).

The oil phase was prepared by heating the milk fat to 110 ˚C and holding the sample at this temperature for 2 min while stirring with a magnetic hot plate at 300 rpm. If phytosterols were added, they were included at the start of the 2 min hold time. After the hold time, the oil phase was added to aqueous phase and the mixture was sheared with a Silverson rotor-stator mixer for 1 min at 3200 rpm and 65 ˚C to form a pre-emulsion. The pre-emulsion was then homogenised using an EmulsiFlex-C5 (Avestin, Mannheim, Germany) operating at 300 bar pressure at 60 ˚C in a single pass. The control emulsion (without added phytosterol) and phytosterol-enriched (PE) emulsions were then statically cooled and stored at 25 °C. After cooling, 0.01%

sodium azide was added to prevent microbial growth during storage and samples were analysed within 24 h of production.

In total, three different levels of enrichment were chosen for the PE emulsions: 0.0%, 0.3%, and 0.6%. The 0.0% PE emulsion functions as the control sample as it contains only milk fat in the dispersed phase. The next two levels of enrichment, 0.3% and 0.6%, are expressed in this study based on weight by weight percentage of the total phytosterol in the emulsion. The 0.6% PE emulsion was chosen as the highest level of enrichment, as the emulsion at 0.8% enrichment was not stable and separated immediately upon pre-homogenisation. It can be noted that all formulated emulsions had a pH of 6.8, independent of phytosterol enrichment.

2.2.2.2 Particle size

The particle size of the emulsions was measured by laser light scattering using a Mastersizer 2000 instrument (Malvern Instruments Ltd., Worcestershire, UK). The emulsions were measured at room temperature in a Hydro SM cell with an obscuration of ~10%. A differential refractive index of 1.095 (1.462 for milk fat/1.33 for water) and an absorption of 0.001 were used as optical parameters for the measurements. Particle size distributions and volume-weighted mean diameters ($D_{4,3}$)

$$D_{4,3} \left(= \sum n_i d_i^4 / \sum n_i d_i^3 \right) \quad (2.1)$$

were calculated based on a spherical geometry, where *ni* is the number of droplets with diameter *di* (Equation 2.1). Measurements were averaged from two replicates and trials were repeated in triplicate.

2.2.2.3 Emulsion ζ-potential

The ζ-potential of each emulsion was determined using a Malvern Nano ZS. Before analysis each emulsion was diluted to 1:200 in Milli-Q water. An electric field was then applied to each sample in a folded capillary cell held at 25 ˚C. Using the Smoluchowski model, the direction and velocity of the droplet was used to calculate the ζ-potential of the particles present. The results and standard deviations are reported as the average of two measurements on three individual emulsion preparations.

2.2.2.4 Optical characterisation of emulsion stability

Emulsion stability was assessed using a light-scattering optical analyser (Turbiscan MA2000, Formulaction, France) as a function of time. After cooling, 6 mL of emulsion samples were placed into glass holding cells to be measured at day (d) 0. Samples were then held at 25 °C and measured again on d 1, 3, 5, and 7 to compare the amount of destabilisation between treatments. Maximum backscattering values for each treatment were used to compare the percentage difference between d 0 and 7 during storage. Light photons were backscattered along the length of the tube containing a near infrared diode. Scattering data was then collected and interpreted for emulsion destabilisation.

2.2.2.5 Differential scanning calorimetry

Thermal analysis of onset temperatures and peaks was conducted on emulsion samples using a DSC 1 STARe System (Mettler Toledo, Port Melbourne, Australia) and software (version 12.10). Samples were stored at room temperature prior to analysis, for which aliquots (~19-21 mg) were weighed into a 40 µL aluminium pan (Mettler Toledo, part number ME-27331) and hermetically sealed. MilliQ was used in the reference pan. Thermal history of the phytosterols and milk fat was found to be erased by heating samples from 25-60 °C at 10 °C/min and holding the samples at this temperature for 5 min (Appendix 2). After holding, the samples were cooled from 60 to 4 °C at a rate of 3 °C/min and held at 4 °C for 5 min. Samples were then heated to 60 °C at a rate of 10 °C/min. Analysis was conducted in triplicate.

2.2.2.6 Synchrotron X-ray analysis

The Australian Synchrotron SAXS/WAXS beamline in Clayton, Australia was used to perform scattering experiments at a flux of 14 keV and a camera length of 0.9 m. Diffraction patterns were recorded in the small angle ($q = 0.03\text{-}1.4$ Å^{-1}) and wide angle regions ($q = 0.9 – 3.5$ Å^{-1}) using a Dectris Pilatus 1M and a Pilatus 200K detector, respectively. Detailed information regarding the beamline systems and parameters can be found elsewhere (Kirby et al., 2013). Emulsion samples of 20 µL were decanted into quartz capillaries of 1.5 mm diameter (GLAS Muller, Berlin, Germany) and subjected to a temperature ramp. The heating/cooling element for the melting and cooling stages was an adapted Linkam microscope stage with a steel holder designed to hold the capillary upright in the X-ray beam. Samples were heated from 25° C to

above 60 °C at 10 ˚C/min and held at that temperature for 5 min. All samples were found to be in a liquid crystalline lamellar state prior to cooling. Cooling was conducted at 3˚C/min until 4 ˚C was reached. Small-angle X-ray scattering (SAXS) and wide-angle X-ray scattering (WAXS) patterns were collected once the sample reached the isothermal period. The machine scanned for 3 seconds (s) of live time with a subsequent 7 s of dead time over a 15 mm gap in series to avoid overexposing the sample. After 5 min of holding at 4 ˚C, the stage was re-equilibrated to room temperature before loading the next sample. SAXS and WAXS snapshots of material references were collected on the crystalline phytosterol, with and without MiliQ water, and the aqueous phase with WPI after storage at 4 ˚C for 24 h.

Baseline correction was performed using the Australian Synchrotron SAXS/WAXS software (ScatterBrain, V2.71, Australia). Diffraction peaks were analysed, as a function of time and phytosterol concentration, in terms of the maximum intensity and the full-width at half-maximum (FWHM) using MatLab (Math Works Inc., Matlab R2014b, USA). The Gaussian peak analysis

$$f(x) = ae^{-\frac{(x-b)^2}{2c^2}} \tag{2.2}$$

Function (Equation 2.2) was used to analyse the multiple peaks in each pattern. In this equation, *a* is the height of the diffracted peak, *b* is the center position of the peak, and *c* is the peak's full-width at half of its maximum intensity. The FWHM can provide structural information on the level of ordering within a TAG system (Lopez, Bourgaux, Lesieur, Bernadou, et al., 2002).

2.2.2.7 Confocal laser scanning microscopy

Visualisation of the emulsion droplets was carried out at the National Food Imaging Centre at Teagasc (Fermoy, Ireland). Emulsions were prepared in the same manner and pressure but utilised an APV1000 homogeniser instead (SPX flow, Germany). Imaging was carried out using a Leica TCS SP5 Confocal Laser Scanning Microscope (CLSM; Leica Microsystems CMS GmbH, Wetzlar, Germany) using 63x oil immersion objective at 3 and 5 times zoom factor. Dual confocal illumination was created by using an Argon laser at 488nm and a Helium/Neon laser at 633nm to show lipids and proteins, respectively. Samples were prepared for imaging by adding 10 µL

of Nile Blue (0.1g/100 µL) into 1 mL of emulsion and vortexing for 10 s. Approximately 50 µL of labeled emulsion was placed on a microscope slide and a coverslip placed on top. Images (8-bit, 512x512 pixels) were obtained using simultaneous dual-channel imaging, and were pseudo-colored to show protein (red) and lipids (green). Emulsions were evaluated 24 h after preparation to evaluate the microstructure of the droplets after equilibration.

2.2.2.8 Statistical analysis

Mean values ± standard deviations were reported for each employed treatment. Results were analysed for statistical significance utilising SAS® 9.3 software for Windows. A Tukey's Post Hoc Difference Test with a level of probability at $p<0.05$ was utilised to analyse significant differences between treatments.

2.3. Results

2.3.1 Physical properties of emulsions

Particle sizes were expressed as the volume-weighted distributions of emulsions made with varying amount of phytosterol added to the fat phase (0.0, 0.3, and 0.6% wt/wt). The droplet distribution of the PE emulsions ranged from 0.035 µm to 28.25 µm, and were visualised base on a logarithmic scale (Fig. 2.1). Phytosterol addition resulted in a shift in the droplet size distribution and a reduction in the mean droplet diameter, reflected in the ($D_{4,3}$) values (Table 2.1). The particle size decreased significantly ($p<0.05$) from an average of 1.17 ± 0.13 µm for the control emulsion to 0.99 ± 0.07 and 0.90 ± 0.04 µm for the 0.3% and 0.6% PE emulsions, respectively.

Emulsions (pH 6.8) were found to range in ζ-potential from -53.62 ± 4.53 to -47.34 ± 1.78 mV (Table 2.1), in agreement with previous research utilising whey protein at an oil-in-water interface (Ye et al., 2012; Mao et al., 2014). Emulsions were not found to have statistically different ζ-potential values ($p>0.05$) following the addition of phytosterols, but these values tended to be less negative with phytosterol addition.

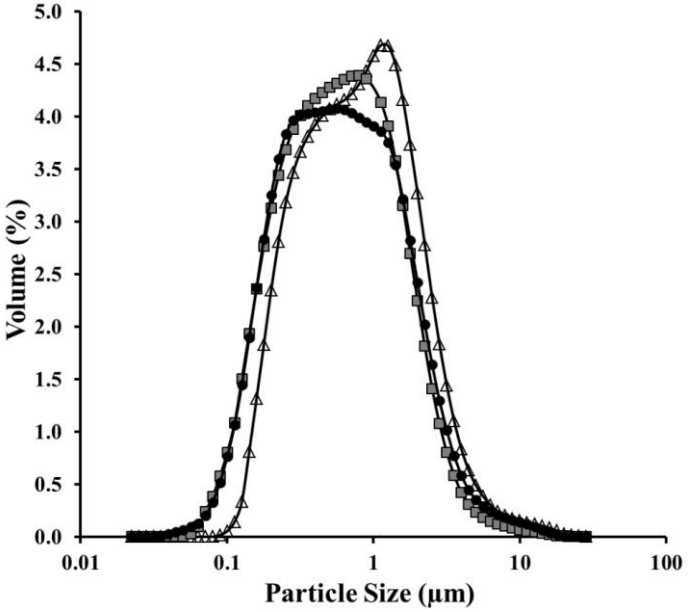

Figure 2.1 *Particle size distribution of 10% milk fat: 1% protein: 89% H_2O emulsions with different phytosterol-enrichment (PE) levels: (△) 0.0% PE emulsion (the control), (▬) 0.3% PE emulsion, (●) 0.6% PE emulsion.*

Emulsion stability was examined by assessment of creaming as a function of time. Droplet creaming is demonstrated by a decrease in the initial slope of the pattern and an increase in the backscattering at the top of the tube (Fig. 2.2). Creaming was observed in all samples, increasing over time from d 1 to d 7. Samples did not differ greatly between each other in terms of destabilisation with the addition of phytosterols (Fig. 2.2a & b). The extent of creaming was quantified by subtracting the maximum backscattering percentages between d 0 and 7; the difference in percentage is reported as an absolute value in Table 2.1 and was not significantly different ($p>0.05$) between treatments.

The microstructures of the emulsions were recorded using confocal laser scanning microscopy (CSLM) within 24 h of homogenisation (Fig. 2.3). All of the emulsions contained relatively small droplets with a range of different diameters ($d \approx$ 0.1–10 μm), consistent with the particle size measurements (Table 2.1) and distributions shown in Fig. 2.1. There were no visible differences between the control and the 0.3% PE emulsion at 3 and 5 times magnification. However, in the 0.6% PE emulsion, visible crystals were present in larger droplets by negative contrast, creating an altered interface on the droplets and changing their shape (Fig. 2.3).

Table 2.1
Volume-weighted mean diameters of emulsions ($D_{4,3}$), ζ-potential and change in max backscattering percentages on d 0 and 7 as a function of phytosterol enrichment (PE) level

Formulation	$D_{4,3}$ (μm)	ζ-potential (mV)	Δ in BS (d 0 7) (%)
0.0% PE Emulsion	1.17 ± 0.13^{a}	-53.62 ± 4.53^{a}	$8.28 + 1.11^{a}$
0.3% PE Emulsion	0.99 ± 0.07^{b}	-51.07 ± 3.24^{a}	7.48 ± 1.79^{a}
0.6% PE Emulsion	0.90 ± 0.04^{b}	-47.34 ± 1.78^{a}	6.80 ± 2.04^{a}

Δ in BS=Difference between backscattering maximums between day 0 and day 7
Superscript letters denote significant differences in Tukey's Post Hoc Test with a $p<0.05$

2.3.2. Crystallisation properties

2.3.2.1 Differential scanning calorimetry

Emulsion samples consisting of different levels of phytosterol enrichment were heated to erase the previous thermal history and subjected to cooling at 3 ˚C/min until holding at 4 ˚C. During cooling, the start of crystallisation (Tonset) differed significantly ($p<0.05$) between all PE emulsions. The 0.3% PE emulsion nucleated first at 14.92 ± 0.12 ˚C (Fig. 2.4a & Table 2.2). The control emulsion begun crystallising at 13.35 ± 0.16 ˚C followed by the 0.6% sample at 11.36 ± 0.03 ˚C. Subsequently, the thermal output of each emulsion peaked at significantly ($p<0.05$) different temperatures in the same order as initial nucleation.

During heating at 10 ˚C/min, the Tonset or melting of 0.3% PE sample began at 7.06 ± 0.60 ˚C (Fig. 2.4b & Table 2.2). This was followed by the control at 8.16 ± 0.52 ˚C and the 0.6% PE emulsion at 8.84 ± 0.16 ˚C. The order of melting between samples was similar to the exhibited Tonset order during cooling. During melting, the 0.3% PE emulsion peaked first at 12.22 ± 0.09 ˚C, then exhibited a second peak at 17.33 ± 0.17 ˚C, to create a different pattern than the other two samples.

Thermodynamic changes in enthalpy were also measured during the heating and cooling regime. During cooling, the change in enthalpy between emulsions was not significantly different between the 0.0%, 0.3%, and 0.6% PE emulsions. However, it should be noted that the 0.6% emulsion released 1.36 ± 0.02 Jg^{-1}, even though its nucleation temperature was lower than that of the other PE emulsions. In addition,

during the isothermal period, the 0.6% PE emulsion released more energy than both the control and the 0.3% PE emulsions in order to reach equilibrium at 4 °C (Fig. 2.5b). During melting, there was no significant difference in the change in enthalpy among the samples.

2.3.2.2 Synchrotron SAXS and WAXS

Synchrotron X-ray scattering data, obtained under isothermal conditions, measured at small (SAXS) and wide (WAXS) angles, provided structural information such as the lamellar spacing, polymorphic forms, and the presence of phytosterol crystals adopted by the PE emulsions after cooling at -3 °C/min. The isothermal evolution at 4 °C for 5 min of the 0.6% PE emulsion is shown in Figure 2.5a. The triple-chain length (3L) second and third reflection, denoted as 3L(002) and 3L(003), were observed first, which is expected as these are typically the most intense peaks (Lopez, Bourgaux, Lesieur, Bernadou, et al., 2002). After 1 min, the $3L_{(001)}$ peak at 76.6 Å appears, along with the $3L_{(005)}$ reflection at 15.1 Å. This transition is not a 2L to 3L transition, due to the early peak heights matching those of scans taken at the end of the isotherm; this has also been observed in other dispersed milk fat systems (Lopez, Bourgaux, Lesieur, Bernadou, et al., 2002). During the isotherm of the 0.6% sample, development of the phytosterol crystals can be observed (Fig. 2.5a). At 0 min, the phytosterol crystalline peak at 5.9 Å was already present, but the phytosterol crystalline peak at 17.7 Å began to develop only after 1 min of holding at 4˚C. This crystal formation is accompanied by a large exothermic release in the DSC results (Fig. 2.5b). The occurrence of phytosterol crystals were confirmed by diffraction patterns corresponding to the material references of the dry and aqueous dispersed phytosterol crystalline powder (Fig. 2.6). It can also be noted that the lamellar phase of the dispersed milk fat in the 0.0% and the 0.3% samples developed identically to the 0.6%, but no additional crystal presence was recorded (data not shown).

Averaged diffraction patterns and values of the last ten scans of all PE emulsions at the end of the isothermal period are displayed in Figure 2.7. The 1^{st}, 2^{nd}, 3^{rd}, and 5^{th} reflections of a characteristic lamellar phase were observed for all three samples. The lamellar packing of the emulsified milk fat crystals in the 0.0% and the 0.3% PE emulsions was within the range of 55-75 Å, consistent with a 3L structure (Widlak et al., 2001; Lopez et al., 2007). The 0.6% PE emulsion falls slightly outside of this

generally accepted range (75.6 Å), but is still considered to be a 3L system, as seen previously in milk fat with added polyunsaturated fatty acids (Bugeat et al., 2015). All PE emulsions contained the characteristic 3L reflections at approximately 37 Å, 25 Å, and 15 Å denoted as 3L(002), 3L(003), and 3L(005), respectively. The 3L(004) reflection was absent as it is mainly observable within bulk milk fat systems (Bugeat et al., 2015). The TAG lamellar spacing of the milk fat increased with higher levels of phytosterols in the emulsion. The control had the smallest 3L(001) D-spacing among samples at 74.0 Å, with the 0.3% sample and the 0.6% PE emulsion expanded to 74.9 Å and 75.6 Å, respectively (Fig. 2.7a).

The largest and most intense reflection, 3L(002), was evaluated for its full-width at half-maximum expressed as $Å^{-1}$ (FWHM). The FWHM provides an indication of the level of disorder within the lamellar phase (Lopez, Bourgaux, Lesieur, Bernadou, et al., 2002). Here as phytosterol was added, the FWHM increased from 0.013 $Å^{-1}$ in the control sample to 0.014$Å^{-1}$ in the 0.3% PE sample, and widened further to 0.016 $Å^{-1}$ in the 0.6% PE sample (Fig. 2.7a). This is indicative of increased disorder within the lamellar structure as the phytosterol was incorporated. An α-packing type was observed throughout the samples at the same short spacing distance of 4.1 Å (Lopez, Bourgaux, Lesieur, & Ollivon, 2002). Phytosterols also crystallised separately in the 0.6% sample and were identified in both SAXS and WAXS patterns at 17.7 Å and 5.9 Å, respectively (Fig. 2.7).

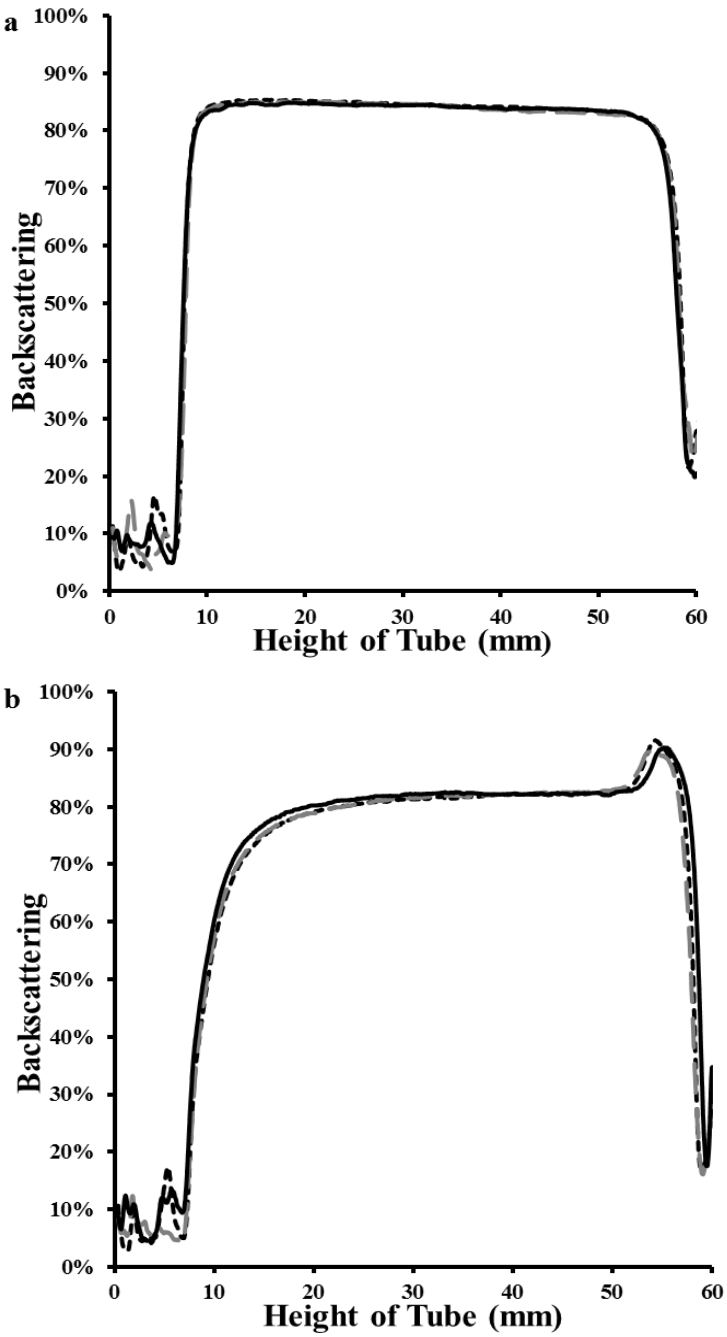

Figure 2.2 *Turbiscan backscattering results of phytosterol-enriched (PE) emulsions during stability testing on (a) d 0 and (b) d 7. Emulsions are depicted as (----) 0.0% PE emulsion (the control), (— -) 0.3% PE emulsion, (──) 0.6% PE emulsion.*

Table 2.2 Thermal parameters calculated from DSC thermographs recorded during heating and cooling cycle of phytosterol-enriched (PE) emulsions.

Temp Cycle	Sample	Tonset (˚C)	Peak 1 (˚C)	Peak 2 (˚C)	Peak 3 (˚C)	Peak 4 (˚C)	$\Delta H(Jg^{-1})$
Cooling	0.0% PE Emulsion	13.35 ± 0.16^{a}	7.08 ± 0.03^{a}	---	---	---	1.39 ± 0.04^{a}
	0.3% PE Emulsion	14.92 ± 0.12^{b}	9.57 ± 0.09^{b}	---	---	---	1.32 ± 0.04^{a}
	0.6% PE Emulsion	11.36 ± 0.03^{c}	6.80 ± 0.08^{c}	---	---	---	1.36 ± 0.02^{a}
Heating	0.0% PE Emulsion	8.16 ± 0.52^{ab}	---	16.60 ± 0.54^{a}	21.88 ± 0.82^{a}	34.50 ± 0.01^{a}	-2.93 ± 0.74^{a}
	0.3% PE Emulsion	7.06 ± 0.60^{a}	12.22 ± 0.09	17.33 ± 0.17^{b}	24.72 ± 0.09^{a}	34.38 ± 0.49^{a}	-2.95 ± 0.35^{a}
	0.6% PE Emulsion	8.84 ± 0.16^{b}	---	15.96 ± 0.29^{a}	24.86 ± 0.10^{b}	34.13 ± 0.34^{a}	-3.22 ± 0.42^{a}

Tonset corresponds the start of both crystallisation and melting profiles for emulsions, ΔH corresponds to the total change in enthalpy during the heating or cooling profile, Superscript letters denote significant differences in Tukey's Post Hoc Test with a $p<0.05$

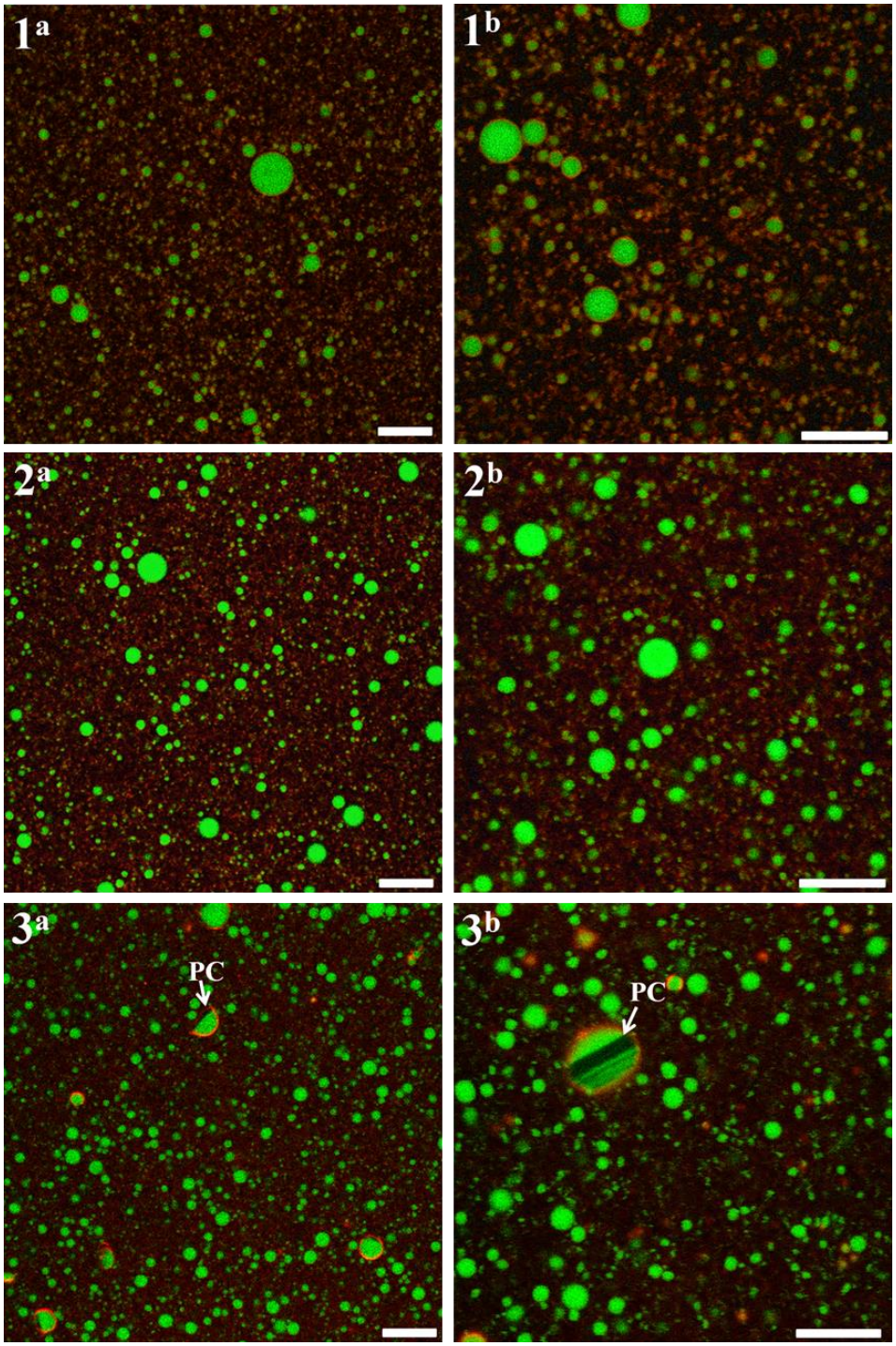

Figure 2.3 *Confocal laser scanning micrographs of phytosterol-enriched (PE) emulsions at 3 and 5 times magnification superscripted as "a" and "b", respectively. Emulsions are labelled as (1) 0.0% PE emulsion (the control), (2) 0.3% PE emulsion, (3) 0.6% PE emulsion. Micrographs show size distribution of milk fat droplets with fat represented in green and protein in red. Scale bar = 10 µm. Note: crystalline phytosterols both at the interface and within fat droplets are made visible by negative contrast (white arrows). PC = phytosterol crystal.*

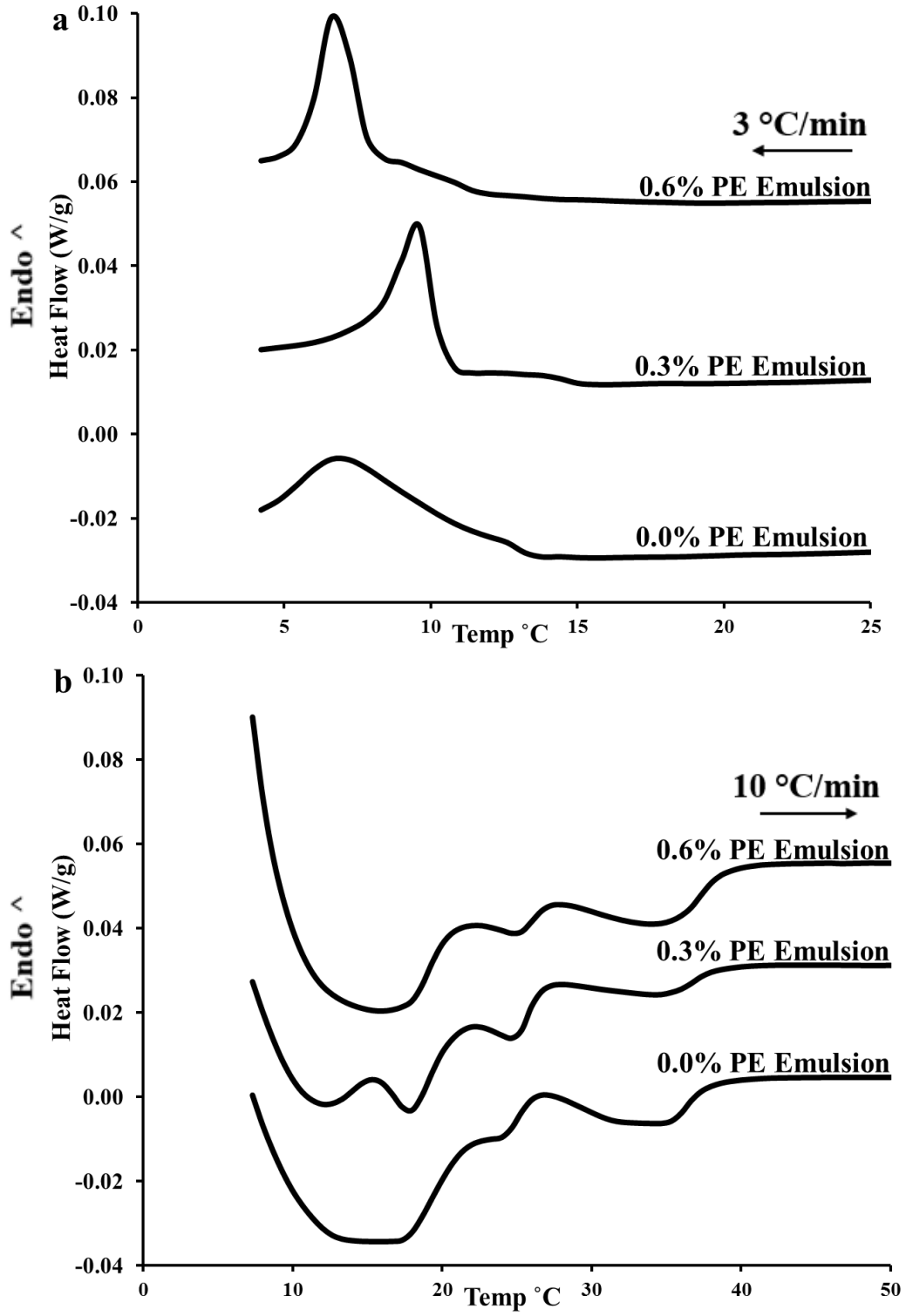

Figure 2.4 *DSC thermographs of PE emulsions during (a) the cooling cycle at -3 ˚C/min and (b) the heating cycle at 10 ˚C/min.*

2.4. Discussion

2.4.1 Influence of physical properties on the emulsion system

Particle size, ζ-potential, stability, and confocal micrographs were used to evaluate the effect of phytosterol addition on the emulsion's physical properties. The particle size and appearance of the PE emulsion droplets were altered after phytosterols were dispersed within the lipid phase, whereas emulsion stability and ζ-potential were not affected. Phytosterols dispersed with a non-ionic surfactant at a similar pH have been reported to have a ζ-potential of -45 mV, but in this system the protein's electrostatic repulsion at the droplet interface might have been too strong for the phytosterols to significantly influence the system (Rossi et al., 2010). The addition of phytosterols also did not contribute to creaming or destabilisation within the emulsion systems.

Phytosterol addition decreased the $D_{4,3}$ of the emulsion droplets and the appearance of droplets at 0.6% enrichment. It has been found previously that phytosterols possess the ability to lower interfacial tension and can pack together tightly at an oil-water interface (Cercaci et al., 2007). The presence of water has been found to produce large monohydrated needle-shaped phytosterol crystals (Christiansen et al., 2002). Thus, it is hypothesised that the elongated shapes observed in the confocal micrographs of our work were phytosterol crystals. This confirmation of an interfacial presence and crystallisation supports the possibility that interfacial phytosterol interactions occurred within the emulsion systems. It is theorised that these surface interactions resulted in the decreased particle size observed within the 0.3 and the 0.6% PE emulsions. To confirm these findings, more work was performed in Chapter 3 to characterise this type of interfacial phytosterol behaviour in dispersed systems.

2.4.2 Thermal analysis of phytosterol-enriched emulsions

Differences in the thermal profiles of PE emulsions may be explained by understanding the concentration-dependent mechanism of phytosterol crystallisation within the milk fat TAG matrix. In both the 0.3% and the 0.6% PE emulsions, the dispersed phytosterols acted as an impurity, forming nucleation sites within the oil droplets; this resulted in volume-heterogeneous nucleation. Volume-heterogeneous nucleation describes an emulsion with a higher number of impurities than available droplets. These impurities function as nuclei during cooling, and thus initiate the

crystallisation of the dispersed fat (Skoda & Van den Tempel, 1963; Coupland, 2002; Fredrick et al., 2011). In accordance with this mechanism, crystallisation occurred in the 0.3% PE emulsion at 14.92 ± 0.12 ˚C, before the control at 13.35 ± 0.16 ˚C, as expected.

Thus, the 0.6% PE emulsion should have nucleated before the 0.3% PE emulsion, due to the higher concentration of impurities. It is hypothesised that the delayed nucleation was a result of the differences between how the phytosterols were partitioned between the 0.3% and the 0.6% PE emulsions. In the 0.6% PE emulsion, separate phytosterol crystals formed and 3L longitudinal packing increased (Fig. 2.7). Additional evidence for crystal formation was demonstrated by the higher energy released during the isothermal period in the 0.6% PE emulsion (Fig. 2.5b). The phytosterols within 0.3% PE emulsion inserted themselves within the milk fat TAG network, but no large phytosterol crystals were detected (Fig. 2.7). It is hypothesised that the higher activation energy observed within the 0.6% PE emulsion is the result of phytosterol crystal formation. Thus, supercooling is required to overcome this activation energy, which in turn delays the overall nucleation in the 0.6% PE emulsion. This type of concentration-dependent crystalline behaviour has been observed in other systems with catalytic impurities, such as phospholipid-based lecithin. In an earlier study by Miskandar et al, soy lecithin was dispersed into palm oil blends at 0.03, 0.06, and 0.09% wt/wt and monitored for solid fat content through nuclear magnetic resonance; the blends with the lowest concentration of soy lecithin, at 0.03%, were found to promote crystallisation, through an increase in the solid fat content of the palm oil blends, compared to blends with 0.06–0.09% lecithin (Miskandar et al., 2006; Ribeiro et al., 2014).

Similarly, during the heating cycle, the 0.6% PE emulsion began melting (Tonset) at a higher temperature than both the control and the 0.3% PE emulsion. This can possibly be explained by the higher energy required to melt the phytosterol crystals formed during the isothermal holding period (Fig 2.5b). Additionally, the presence of these phytosterol crystals may have slowed the lamellar devolution of the TAG matrix through steric hindrance (Aronhime et al., 1987; Ribeiro et al., 2014). A similar response can be seen in delayed transitions between polymorphic phases such as α, β, and β’ when different additives have been incorporated into the lipophilic carriers (Sato & Kuroda, 1987; Bunjes et al., 2002; Ribeiro et al., 2014; Joseph et al., 2015).

This was also supported by the synchrotron results, where the highest amount of disorder was observed in samples with added phytosterols (Fig. 2.7a). These results will be further discussed in the following section on emulsion crystallisation.

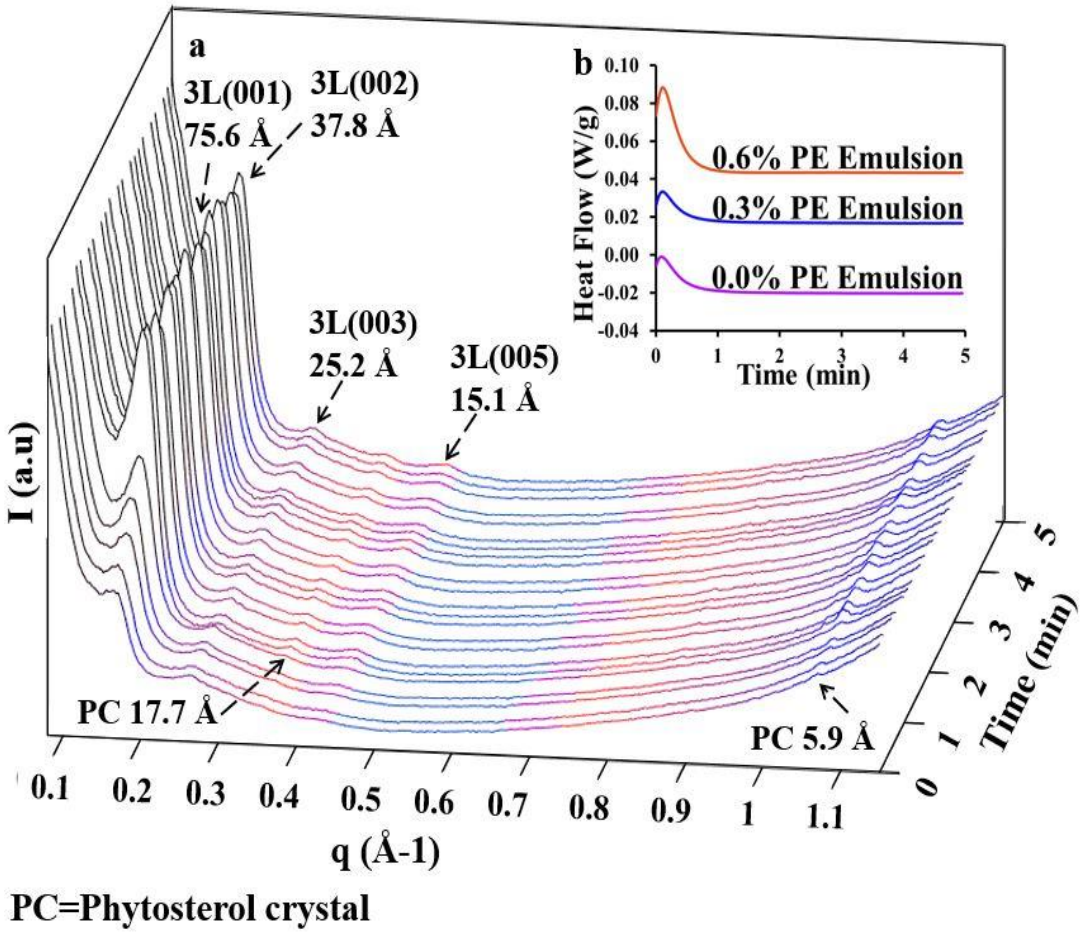

Figure 2.5 *Structural evolution of 0.6% PE emulsion during the isothermal holding period at 4 °C after cooling at -3 °C/min. Graph includes SAXS diffraction pattern with WAXS overlap to demonstrate the development of phytosterol crystals (a). Corresponding DSC recordings during the 5 min hold are plotted with all of the PE emulsions to demonstrate the differences in thermal responses (b). PC = Phytosterol Crystal*.

2.4.3 Crystalline structures and morphologies of phytosterol-enriched emulsions

Milk fat is composed of a complex mixture of TAG and can adopt lamellar structures in either a 3L or a 2L configuration (Lopez, Bourgaux, Lesieur, Bernadou, et al., 2002; Cisneros et al., 2006; Bugeat et al., 2015). All emulsions were found to demonstrate 3L crystalline packing, which is well recognised in dispersed milk fat systems cooled at 3 ˚C/min (Fig. 2.7a) (Lopez, Bourgaux, Lesieur, Bernadou, et al., 2002; Lopez et al., 2007; Bugeat et al., 2015). The 0.6% PE emulsion is graphed for reference, during the isothermal evolution at 4 ˚C for 5 min, to exhibit the development of the milk fat TAG lamellar structure within the PE emulsions (Fig. 2.5a). A 3L lamellar structure is observed within the sample, with the 3L(002) and 3L(003) diffracting first, followed by less intense reflections at 3L(001) and 3L(005). These results indicate that 3L packing had already developed within the dispersed phase at the start of the isothermal period, and the increase in intensity over time confirms these findings. Similar studies on milk fat have also recorded a slight delay between the development of all the 3L reflections (Lopez, Bourgaux, Lesieur, Bernadou, et al., 2002; Lopez et al., 2006).

Most importantly, during the isothermal evolution of the 0.6% sample, it is possible to observe the development of the phytosterol crystals (Fig. 2.5a). The graph includes a slight overlap with the WAXS region, allowing the presence of phytosterol crystals in the WAXS region at 5.9 Å at time zero to be clearly seen. After 1 min of holding at 4 ˚C, the second phytosterol crystal peak became apparent in the SAX region at 17.7 Å. As discussed previously, this development was accompanied by a large exothermic event in the 0.6% sample (Fig. 2.5b). The 0.6% PE sample had a large heat of fusion during cooling as well, even though it crystallised later than the control and the 0.3% PE samples. It is possible that the development of these phytosterol crystals would have required a large activation energy. Thus, delayed nucleation was observed as more energy was needed for crystallisation of the phytosterols.

Differences were observed in the internal packing of the 3L crystal structures in the PE emulsions, which relates to the thickness of the laminar layers (Fig. 2.7a). As such, an increase in long-spacing indicates that the distance between the repeated TAG units, i.e. the spacing within the 3L laminar layers, is larger. The control sample had the shortest long-spacing at 74.0 Å. In contrast, the 3L structure of the 0.3% and the 0.6%

PE samples had a thickness of 74.9 Å and 75.6 Å, respectively. This progressive increase in long-spacing suggests that, during lipid crystallisation, phytosterols molecules are able to incorporate themselves within the complex milk fat TAG matrix. This insertion enlarges the internal spacing between the laminar layers, but does not affect the spacing between the individual 3L units; thus, the same α-packing is retained throughout the samples. The 0.3% and 0.6% PE emulsions both influenced the lamellar packing of the milk fat TAG, but the 0.6% PE emulsion contains additional separate crystal peaks at 17.7 Å and 5.9 Å. These separate crystals are most likely outside of the α-repeating units, as the TAG lamellar layers did not expand sufficiently to encompass a large phytosterol crystal. However, it is hypothesised that phytosterol molecules and not crystals are within the TAG lamellar layers, as an expansion was observed. A potential model for this system is demonstrated in Figure 2.8, which depicts how the phytosterols might be incorporated into the system.

Similar changes in the lamellar thickness have been seen in studies with different milk fat compositions (Bugeat et al., 2015). An increase in the unsaturated fatty acids content of milk has been shown to result in an augmentation of long-spacing, similar to the observations from our work with phytosterol addition (Bugeat et al., 2015). Upon adding polyunsaturated fatty acids into the bovine diet, Lopez et al. (2015) showed that there was an increase in the 3L(001) spacing in milk fat from 71.5 Å to 75.5 Å. The bent-chain morphology of the unsaturated fatty acids within the TAG matrix of the enriched samples expanded the long-spacing during crystallisation, but did not change the initial α-packing at 4.10 Å(Bugeat et al., 2015).

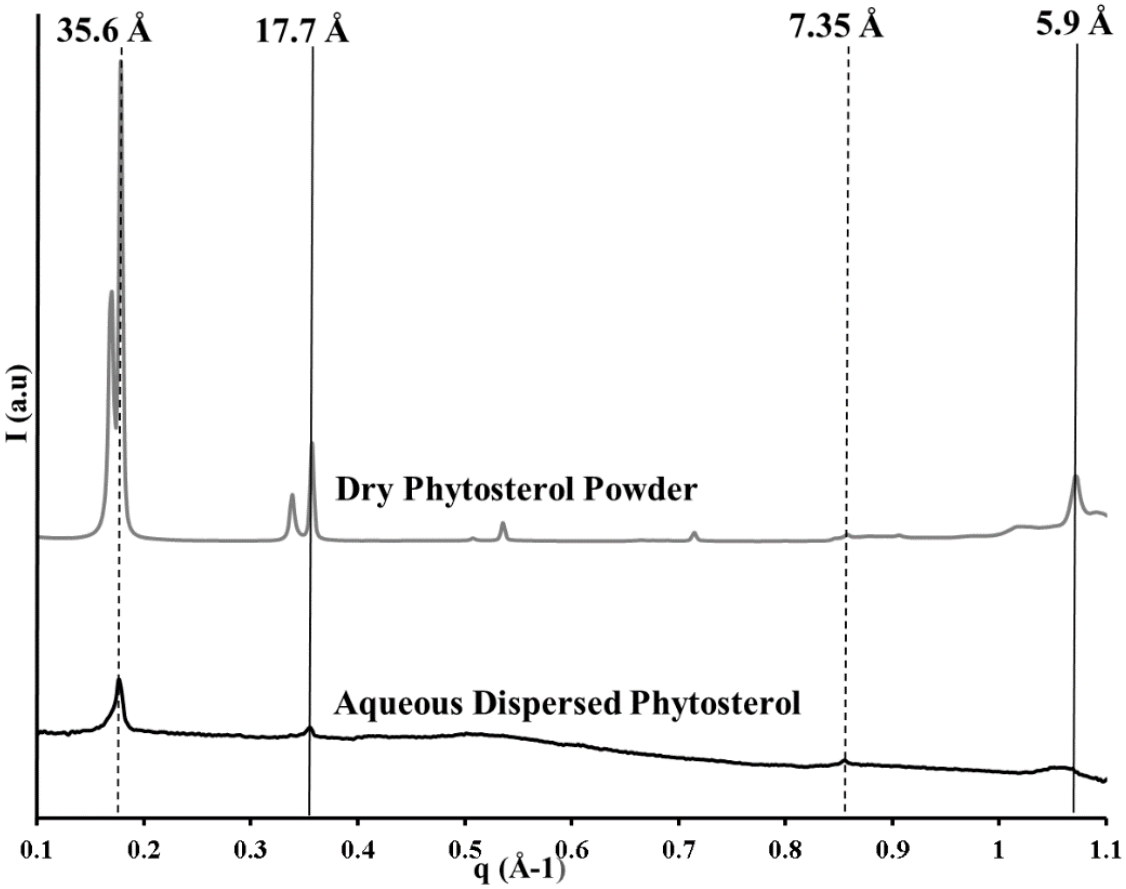

Figure 2.6 *Diffraction patterns of material references; 5% wt/wt phytosterol dispersed in water and dry phytosterol powder after storage at 4 °C for 24 h. Graph includes SAXS with WAXS overlap to show the phytosterol crystals present within both references. The solid line ( ) represents phytosterol peaks present in the PE emulsions after crystallisation and are used for comparison. The dashed line ( ) marks phytosterol peaks that only appear after 24 h at 4 °C and are therefore not relevant.*

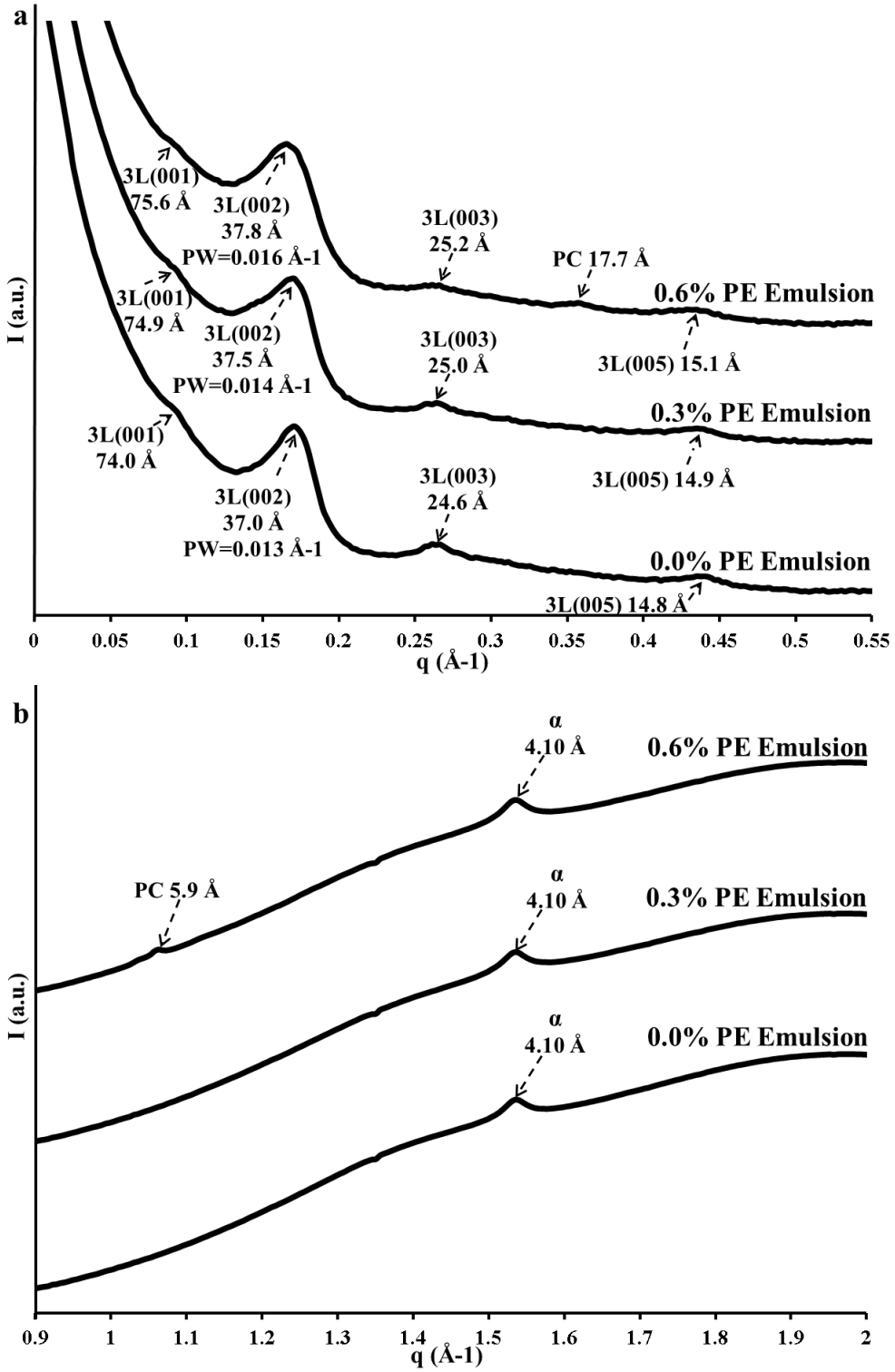

Figure 2.7 *(a) Small and (b) wide-angle synchrotron diffraction patterns captured at 4 °C after cooling at -3 °C/min. Values are averaged from the last minute of the 5 min isotherm after equilibrium was reached. PC = Phytosterol Crystal.*

The FWHM of the diffracted synchrotron peaks can be an additional tool to understand the lamellar packing, indicating the internal organisation of the system. In milk fat systems a larger FWHM is associated with a higher degree of disorder within the 3L or 2L TAG packing (Lopez, Bourgaux, Lesieur, Bernadou, et al., 2002). Larger FWHM have been shown previously in milk fat fractions with a larger diversity of fatty acids. For example, Lopez and Ollivon (2006) reported that the olein milk fat fraction, consisting of more unsaturated fatty acids but with a lower diversity of TAG, has a smaller FWHM than that of unfractionated milk fat. Similarly, in the conducted study, the control emulsion had the smallest FWHM at 0.013 $Å^{-1}$. When phytosterol concentration increased, so did the FWHM; to 0.014 $Å^{-1}$ in the 0.3% PE emulsion and 0.016 Å-1 in the 0.6% PE emulsion. In the emulsion, the insertion of phytosterol molecules into the dispersed phase further disordered the already complex TAG matrix, which in turn increased the FWHM.

2.5 Conclusion

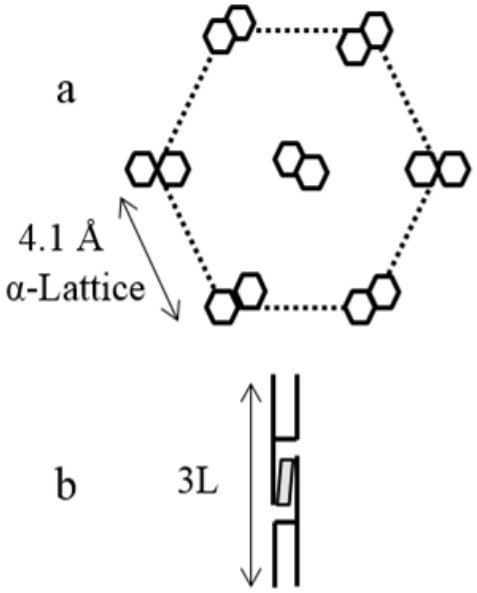

Figure 2.8 *Lamellar structures of the dispersed fat phase in phytosterol-enriched PE emulsions, detailing the lateral chain packing in image a. Image b details the 3L structure of the TAG molecules. The ( ) represents a phytosterol molecule in its proposed position between TAG units.*

The use of phytosterols in milk fat emulsions is of significant interest in the dairy and functional food industries. In this study, the physical, thermal, and structural consequences of adding these bioactives into dispersed milk fat systems were examined. These results demonstrated that phytosterols can be added at levels up to 0.6% with little impact on the emulsion stability or ζ-potential. The addition of these molecules into a dispersed system was found to decrease the average mean particle size and distribution along with changing the physical appearance of some droplets, with large phytosterol crystals forming near the droplet interface at 0.6% enrichment. Phytosterol addition was also found to impact crystallisation properties of the system and was concentration dependent. In the 0.6% PE emulsion, nucleation was delayed and a larger amount of energy was released during the cooling and isothermal period than in the 0.3% and the control emulsions. These DSC results coincided with the formation of nonsolubilised phytosterol crystal growth. Phytosterol enrichment in emulsions also changed the long-spacing of the observed lamellar structure, expanding the structure, but not changing the overall α-packing of this system. This indicates that, during crystallisation, while phytosterols could integrate between TAG units, they could not influence the polymorphic form created. Little work has been done to characterise milk fat emulsions enriched with bioactive compounds. Thus, the results of this fundamental study can be used to further develop this area of research, as well as provide valuable information to the functional food industry regarding the effects of adding phytosterols into milk fat systems.

Acknowledgements

The authors would like to thank the Teagasc Food Research Centre for its support (Teagasc Project RMIS6412) and assistance in organising this collaborative project and the Australian Synchrotron for beamline access (proposal number M8476). The authors would also like to thank Christelle Lopez (INRA Rennes, France) and Nigel Kirby (Australian Synchrotron, Melbourne, Australia) for invaluable guidance in setting up the synchrotron experiment. Additionally, we would like to thank Mi Xu, Sofia Oiseth and Li Day (CSIRO, Melbourne, Australia), and Dale Osborn and Tamar Greaves (RMIT, Australia) for their assistance in this project.

References

Alexander, M., Acero Lopez, A., Fang, Y., & Corredig, M. (2012). Incorporation of phytosterols in soy phospholipids nanoliposomes: Encapsulation efficiency and stability. *Food Science and Technology, 47*(2), 427-436. doi:http://dx.doi.org/10.1016/j.lwt.2012.01.041

Aronhime, J. S., Sarig, S., & Garti, N. (1987). Mechanistic considerations of polymorphic transformations of tristearin in the presence of emulsifiers. *Journal of the American Oil Chemists Society, 64*(4), 529-533.

Berger, A., Jones, P. J. H., & Abumweis, S. S. (2004). Plant sterols: Factors affecting their efficacy and safety as functional food ingredients. *Lipids Health and Disease, 3*(5), 907-919.

Bugeat, S., Perez, J., Briard-Bion, V., Pradel, P., Ferlay, A., Bourgaux, C., & Lopez, C. (2015). Unsaturated fatty acid enriched vs. Control milk triacylglycerols: Solid and liquid tag phases examined by synchrotron radiation x-ray diffraction coupled with dsc. *Food Research International, 67*(0), 91-101. doi:http://dx.doi.org/10.1016/j.foodres.2014.10.029

Bunjes, H., Koch, M. H., & Westesen, K. (2002). Effects of surfactants on the crystallization and polymorphism of lipid nanoparticles *Molecular organisation on interfaces* (pp. 7-10): Springer.

Carden, T. J., Hang, J., Dussault, P. H., & Carr, T. P. (2015). Dietary plant sterol esters must be hydrolyzed to reduce intestinal cholesterol absorption in hamsters. *The Journal of Nutrition*.

Cercaci, L., Rodriguez-Estrada, M. T., Lercker, G., & Decker, E. A. (2007). Phytosterol oxidation in oil-in-water emulsions and bulk oil. *Food Chemistry, 102*(1), 161-167.

Christiansen, L. I., Rantanen, J. T., von Bonsdorff, A. K., Karjalainen, M. A., & Yliruusi, J. K. (2002). A novel method of producing a microcrystalline β-sitosterol suspension in oil. *European Journal of Pharmaceutical Sciences, 15*(3), 261-269.

Cisneros, A., Mazzanti, G., Campos, R., & Marangoni, A. G. (2006). Polymorphic transformation in mixtures of high-and low-melting fractions of milk fat. *Journal of Agricultural and Food Chemistry, 54*(16), 6030-6033.

Clifton, P. (2007). Plant sterols and stanols as functional ingredients in dairy products. In M. Saarela (Ed.), *Functional dairy products* (Vol. 2, pp. 255-261): Woodhead Publishing.

Clifton, P., Noakes, M., Sullivan, D., Erichsen, N., Ross, D., Annison, G., & Nestel, P. (2003). Cholesterol-lowering effects of plant sterol esters differ in milk, yoghurt, bread and cereal. *European Journal of Clinical Nutrition, 58*(3), 503-509.

Coupland, J. N. (2002). Crystallization in emulsions. *Current Opinion in Colloid & Interface Science, 7*(5), 445-450.

Cusack, L. K., Fernandez, M. L., & Volek, J. S. (2013). The food matrix and sterol characteristics affect the plasma cholesterol lowering of phytosterol/phytostanol. *Advanced Nutrition 4*(6), 633-643.

Dickinson, E., & Leser, M. E. (2007). *Food colloids: Self-assembly and material science* (Vol. 308): Royal Society of Chemistry.

Engel, R., & Schubert, H. (2005). Formulation of phytosterols in emulsions for increased dose response in functional foods. *Innovative Food Science & Emerging Technologies, 6*(2), 233-237. doi:http://dx.doi.org/10.1016/j.ifset.2005.01.004

Franchetti, D. (2016). Analysis of co-crystallized free phytosterols with triacylglycerols as a functional food ingredient. *Food Research International, 85*, 104–112.

Fredrick, E., Van de Walle, D., Walstra, P., Zijtveld, J. H., Fischer, S., Van der Meeren, P., & Dewettinck, K. (2011). Isothermal crystallization behaviour of milk fat in bulk and emulsified state. *International Dairy Journal, 21*(9), 685-695. doi:http://dx.doi.org/10.1016/j.idairyj.2010.11.007

Gremaud, G., Dalan, E., Piguet, C., Baumgartner, M., Ballabeni, P., Decarli, B., Leser, M., Berger, A., & Fay, L. (2002). Effects of non-esterified stanols in a liquid emulsion on cholesterol absorption and synthesis in hypercholesterolemic men. *European Journal of Nutrition, 41*(2), 54-60.

Joseph, S., Rappolt, M., Schoenitz, M., Huzhalska, V., Augustin, W., Scholl, S., & Bunjes, H. (2015). Stability of the metastable α-polymorph in solid triglyceride drug-carrier nanoparticles. *Langmuir, 31*(24), 6663-6674.

Kirby, N. M., Mudie, S. T., Hawley, A. M., Cookson, D. J., Mertens, H. D., Cowieson, N., & Samardzic-Boban, V. (2013). A low-background-intensity focusing small-angle x-ray scattering undulator beamline. *Journal of Applied Crystallography, 46*(6), 1670-1680.

Lagarda, M. J., García-Llatas, G., & Farré, R. (2006). Analysis of phytosterols in foods. *Journal of Pharmaceutical and Biomedical Analysis, 41*(5), 1486-1496. doi:http://dx.doi.org/10.1016/j.jpba.2006.02.052

Lopez, C., Bourgaux, C., Lesieur, P., Bernadou, S., Keller, G., & Ollivon, M. (2002). Thermal and structural behavior of milk fat: 3. Influence of cooling rate and droplet size on cream crystallization. *Journal of Colloid and Interface Science, 254*(1), 64-78. doi:http://dx.doi.org/10.1006/jcis.2002.8548

Lopez, C., Bourgaux, C., Lesieur, P., & Ollivon, M. (2002). Crystalline structures formed in cream and anhydrous milk fat at 4 c. *Le Lait, 82*(3), 317-335.

Lopez, C., Bourgaux, C., Lesieur, P., & Ollivon, M. (2007). Coupling of time-resolved synchrotron x-ray diffraction and dsc to elucidate the crystallisation properties

and polymorphism of triglycerides in milk fat globules. *Le Lait, 87*(4-5), 459-480.

Lopez, C., Bourgaux, C., Lesieur, P., Riaublanc, A., & Ollivon, M. (2006). Milk fat and primary fractions obtained by dry fractionation: 1. Chemical composition and crystallisation properties. *Chemistry and Physics of Lipids, 144*(1), 17-33. doi:http://dx.doi.org/10.1016/j.chemphyslip.2006.06.002

Lubinus, T., Barnsteiner, A., Skurk, T., Hauner, H., & Engel, K.-H. (2013). Fate of dietary phytosteryl/-stanyl esters: Analysis of individual intact esters in human feces. *European Journal of Nutrition, 52*(3), 997-1013. doi:10.1007/s00394-012-0407-4

MacGibbon, A., & Taylor, M. (2006). Composition and structure of bovine milk lipids *Advanced dairy chemistry: Lipids* (Vol. 2, pp. 1-42). New York, NY: Springer.

MacKay, D. S., & Jones, P. J. H. (2012). Phytosterols and cardiovascular. In R. Watson & V. Preedy (Eds.), *Bioactive food as dietary interventions for cardiovascular disease* (Vol. 1, pp. 171-181). London, UK: Elsevier.

Mao, L., Calligaris, S., Barba, L., & Miao, S. (2014). Monoglyceride self-assembled structure in o/w emulsion: Formation, characterization and its effect on emulsion properties. *Food Research International, 58*, 81-88.

Mattson, F. H., Grundy, S. M., & Crouse, J. R. (1982). Optimizing the effect of plant sterols on cholesterol absorption in man. *The American Journal of Clinical Nutrition, 35*(4), 697-700.

McClements, D. J. (2004). Protein-stabilized emulsions. *Current Opinion in Colloid & Interface Science, 9*(5), 305-313. doi:http://dx.doi.org/10.1016/j.cocis.2004.09.003

McClements, D. J. (2015). Enhancing nutraceutical bioavailability through food matrix design. *Current Opinion in Food Science, 4*, 1-6. doi:http://dx.doi.org/10.1016/j.cofs.2014.12.008

Miskandar, M., Che Man, Y., Abdul Rahman, R., Nor Aini, I., & Yusoff, M. (2006). Effects of emulsifiers on crystallization properties of low-melting blends of palm oil and olein *Journal of Food Lipids, 13*(1), 57-72.

Ostlund, R. E. (2002). Phytosterols in human nutrition. *Annual Review of Nutrition, 22*(1), 533-549.

Ostlund, R. E., Spilburg, C. A., & Stenson, W. F. (1999). Sitostanol administered in lecithin micelles potently reduces cholesterol absorption in humans. *The American Journal of Clinical Nutrition, 70*(5), 826-831.

Plat, J., Mackay, D., Baumgartner, S., Clifton, P., Gylling, H., & Jones, P. J. H. (2012). *Progress and prospective of plant sterol and plant stanol research: Report of the maastricht meeting.* Paper presented at the Atherosclerosis meeting.

Plat, J., & Mensink, R. P. (2005). Plant stanol and sterol esters in the control of blood cholesterol levels: Mechanism and safety aspects. *American Journal of Cardiology, 96*(1), 15-22.

Pouteau, E. B., Monnard, I. E., Piguet-Welsch, C., Groux, M. J. A., Sagalowicz, L., & Berger, A. (2003). Non-esterified plant sterols solubilized in low fat milks inhibit cholesterol absorption. *European Journal of Nutrition, 42*(3), 154-164. doi:10.1007/s00394-003-0406-6

Ribeiro, A. P. B., Masuchi, M. H., Miyasaki, E. K., Domingues, M. A. F., Stroppa, V. L. Z., de Oliveira, G. M., & Kieckbusch, T. G. (2014). Crystallization modifiers in lipid systems. *Journal of Food Science and Technology*, 1-22.

Rondanelli, M., Monteferrario, F., Faliva, M. A., Perna, S., & Antoniello, N. (2013). Key points for maximum effectiveness and safety for cholesterol-lowering properties of plant sterols and use in the treatment of metabolic syndrome. *Journal of the Science of Food and Agriculture, 93*(11), 2605-2610. doi:10.1002/jsfa.6174

Rossi, L., ten Hoorn, J. W. S., Melnikov, S. M., & Velikov, K. P. (2010). Colloidal phytosterols: Synthesis, characterization and bioaccessibility. *Soft Matter, 6*(5), 928-936.

Rozner, S., Aserin, A., Wachtel, E. J., & Garti, N. (2007). Competitive solubilization of cholesterol and phytosterols in nonionic microemulsions. *Journal of Colloid and Interface Science, 314*(2), 718-726. doi:http://dx.doi.org/10.1016/j.jcis.2007.05.091

Sato, K., & Kuroda, T. (1987). Kinetics of melt crystallization and transformation of tripalmitin polymorphs. *Journal of the American Oil Chemists' Society, 64*(1), 124-127. doi:10.1007/BF02546266

Shaghaghi, M. A., Harding, S. V., & Jones, P. J. H. (2014). Water dispersible plant sterol formulation shows improved effect on lipid profile compared to plant sterol esters. *Journal of Functional Foods, 6*, 280-289.

Skoda, W., & Van den Tempel, M. (1963). Crystallization of emulsified triglycerides. *Journal of Colloid Science, 18*(6), 568-584.

Smet, E. D., Mensink, R. P., & Plat, J. (2012). Effects of plant sterols and stanols on intestinal cholesterol metabolism: Suggested mechanisms from past to present. *Molecular Nutrition & Food Research, 56*(7), 1058-1072.

Vaikousi, H., Lazaridou, A., Biliaderis, C. G., & Zawistowski, J. (2007). Phase transitions, solubility, and crystallization kinetics of phytosterols and phytosterol−oil blends. *Journal of Agricultural and Food Chemistry, 55*(5), 1790-1798. doi:10.1021/jf0624289

Widlak, N., Hartel, R. W., & Narine, S. (2001). *Crystallization and solidification properties of lipids*. Champaign, IL: The American Oil Chemists Society.

Ye, A., Lo, J., & Singh, H. (2012). Formation of interfacial milk protein complexation to stabilize oil-in-water emulsions against calcium. *Journal of Colloid and Interface Science, 378*(1), 184-190. doi:http://dx.doi.org/10.1016/j.jcis.2012.04.042

Zhang, L., Hayes, D. G., Chen, G., & Zhong, Q. (2013). Transparent dispersions of milk-fat-based nanostructured lipid carriers for delivery of β-carotene. *Journal of Agricultural and Food Chemistry, 61*(39), 9435-9443.

Chapter 3

Physical and interfacial characterisation of phytosterols in oil-in-water triacylglycerol-based emulsions

Lisa M. Zychowski[†§], Srinivas Mettu[#‡], Raymond R. Dagastine[#‡], Alan L. Kelly[§], James A. O'Mahony[§], Mark A. E. Auty*[†]

[†] Food Chemistry and Technology Department, Teagasc Food Research Centre, Moorepark, Fermoy, Co. Cork, Ireland

[§] School of Food and Nutritional Sciences, University College Cork, Cork, Ireland

[#] Department of Chemical Engineering, Parkville, Victoria, Australia

[‡] Particulate Fluids Processing Centre (PFPC), Parkville, Victoria, Australia

Declaration: The first author completed all emulsion characterisation and interfacial tension measurements. Interfacial modelling was performed by Srinivas Mettu of Melbourne University.

Abstract

Phytosterols possess the ability to significantly lower low-density lipoprotein (LDL) cholesterol levels in the blood, but their bioaccessibility is highly dependent upon the solubility of the phytosterol within the carrier matrix. Currently, there is a limited amount of knowledge on how phytosterols interact at oil-water interfaces, despite research indicating that these interfaces could promote the crystallization of phytosterols and thus decrease bioaccessibility. In order to fill this knowledge gap, this work expands upon a previously studied emulsion system for encapsulating phytosterols and addresses whether phytosterols can crystalize at an oil-in-water emulsion interface. Images from multiple microscopic techniques suggest interfacial phytosterol crystallization in 0.6% phytosterol-enriched emulsions, while interfacial tension results and calculated models showed that whey protein and phytosterols had a synergistic effect on interfacial tension. A deeper understanding of the interfacial behavior of phytosterols in emulsions can provide the functional food and pharmaceutical industry with the knowledge needed to design more bioaccessible phytosterol-enriched products.

3.1 Introduction

Phytosterols, or plant sterols, are compounds found within plant-cell membranes and are well-known for their ability to lower low-density lipoprotein (LDL) cholesterol in the blood (Jones et al., 1997; Ostlund, 2002; Moruisi et al., 2006). Phytosterols are present in all foods of plant origins, such as fruits, cereals, and nuts, but only in limited concentrations. To significantly lower LDL-cholesterol levels, dietary supplementation is needed to achieve the recommended > 1.5 g of phytosterols per day (Berger et al., 2004). Therefore, as the incidence of heart disease increases and consumers become more health-conscious, so does the use of phytosterols within food products (Henson et al., 2010; Zawistowski, 2010). Phytosterol-enriched food products, or functional foods, can be utilized to lower cholesterol levels simply by regularly ingesting the food product. Despite their increased use within the functional food sector, little is known about how phytosterols interact with different food components.

On a molecular level, phytosterols are chemically similar to human cholesterol and possess the same tetracyclic-backbone; differences between the two compounds arise at the C-22 and C-5 positions, with the presence or absence of various side chains and/or a double bond. These various side chains also distinguish between phytosterol varieties, the most common being β-sitosterol, stigmasterol and campesterol (Ostlund, 2002; Jones & AbuMweis, 2009). The molecular similarities between phytosterols and human cholesterol enable phytosterols to successfully reduce serum cholesterol levels by preventing cholesterol absorption within the small intestine (Santas et al., 2013). Phytosterols also possess anti-inflammatory and anti-carcinogenic properties and have no associated negative side-effects (Jones et al., 1997; Engel & Schubert, 2005).

Despite these benefits, phytosterol enrichment of food systems is not common due to formulation difficulties associated with their insolubility and crystallinity at room temperature (Zawistowski, 2010). Thus, phytosterols are commonly esterified by the industry to improve their solubility and dispersibility within food matrices, such as margarine (Clifton, 2007). Addtionally esterification results in higher processing costs, as compared to using natural phytosterols and unpredictable absorption rates (Clifton, 2007). Phytosterol esters have to be hydrolyzed prior to absorption, which is

subject to inter-individual variability among human digestive systems, resulting in absorption rates varying between 40-96% (Carden et al., 2015).

Conversely, emulsion-based delivery systems can be utilized to enhance the solubility of non-esterified phytosterols, but the bioacessbility of the emulsion is dependent upon the physical state of the phytosterol (Ostlund, 2002). Previous studies have demonstrated that crystalline, non-solubilized phytosterols are not as effective at lowering LDL-cholesterol in the blood, as solubilized phytosterols (Pouteau et al., 2003; Jones & AbuMweis, 2009). Phytosterols can crystallize within the carrier oil, but it should be noted that the presence of water at the interface can also induce sterol crystallization (Jandacek et al., 1977; Engel & Schubert, 2005). Phytosterols possess the ability to lower interfacial tension, and thus their propensity to move to an interface could lead to crystallization and decreased bioaccessibility (Cercaci et al., 2007).

Despite phytosterol crystallization resulting in decreased bioaccessibility in functional food emulsions, very little research has been performed in analysing the mechanism by which phytosterols crystallize. Previously research conducted by the group highlighted how phytosterols crystallize within a triacylglycerol-based food emulsion, utilizing whey protein as the emulsifier; however, little emphasis was placed upon the possibility of phytosterol crystallization at the interface (Chapter 2). Thus, this work seeks to investigate the possibility of phytosterols crystallization at the interface and to characterize how phytosterols influence the morphology and physical properties of a food emulsion. The morphology of phytosterol-enriched emulsions (PE emulsions) were analyzed utilizing confocal laser scanning microscopy, cryo-scanning electron microscopy, polarized light microscopy, and a Malvern mastersizer to study droplet size distribution. Interfacial tension and modelling were used to understand phytosterol and whey protein behavior at the emulsion interface. By understanding how the interfacial behavior of phytosterols influences the properties of a food emulsion, the functional food industry can design more stable and bioaccessible, phytosterol-enriched products.

3.2 Materials and methods

3.2.1 Chemicals and ingredients

Crystalline phytosterols, glycerol, and sodium azide were purchased from Sigma Aldrich, Wicklow, Ireland. The main sterol present was β-sitosterol (≥70%) with residual campesterol and β-sitostanol. Commercial-grade anhydrous milk fat (AMF) was obtained from Corman Miloko, Tipperary, Ireland (Appendix 1). Whey protein isolate (WPI; BiPro®, of 92.7% protein) was purchased from Davisco Foods International Inc, Minnesota, USA. Medium Chain Triglyceride (MCT) oil was procured from Pure Vita labs (British Columbia, Canada) for interfacial measurements.

3.2.2 Preparation of emulsions

Oil-in-water emulsions (10% oil: 1% protein: 89% H_20) were prepared on a wt/wt basis with or without added phytosterols in the oil ratio (0.3% or 0.6% wt/wt), as detailed by in Chapter 2. Emulsions were prepared by homogenisation with an APV 1000 homogeniser (SPX flow, Germany) at 300 bars of pressure for 1 pass at 60 °C. Emulsions were allowed to statically cool and were stored at 20-25 °C with 0.1% sodium azide added to the final emulsion. All evaluations and images were carried out within 24 h on samples from three separate emulsion trials.

3.2.3 Particle size

The droplet size distribution of the emulsion was measured at 22 °C utilising a Malvern Mastersizer 3000 equipped with a Hydro R cell (Malvern Instruments Ltd, Worcestershire, UK). Distilled water was used as the dispersing medium with an obscuration between 4-10% and absorption level of 0.001. Refractive index values of 1.33 for water and 1.46 for milk fat were used in the optical parameters. The $D_{(4,3)}$ value was calculated by the Mastersizer 3000 software based on a spherical geometry, as performed in Chapter 2.

3.2.4 Polarised light microscopy

Polarised light images were captured using an Olympus BX51 microscope (Olympus Corporation, Tokyo, Japan) at 60X using a ProgRes CT3 camera with Prores 2.7.7 software (Jenoptik, Wiltshire, UK). Fifty microliters of emulsion samples were placed onto a glass slide with a coverslip. The glass slide was then placed directly onto the heating element of a linkam LNP heating/cooling stage (Linkam, Surry, UK). Images were taken at 20 °C and after heating to 50 °C at 3 °C/min; as 50 °C is above the melting point of milk fat but not of phytosterols within a TAG matrix (Lopez et al., 2007; Acevedo & Franchetti, 2016). Images were taken to characterise changes in emulsion morphology and the presence of crystals above the melting point of milk fat.

3.2.5 Confocal laser scanning microscopy

Imaging was performed utilising a confocal laser scanning microscope (CLSM; Leica Microsystems CMS GmbH, Wetzlar, Germany) with 63x oil immersion objective, at 3 and 5x zoom factor. Dual confocal illumination was produced with an Argon laser at 488 nm and a Helium/Neon laser at 633 nm to show lipids and proteins, respectively. After imaging, the protein channel was isolated for separate visualisation of the protein coverage around the emulsion droplets using LAS AF (Leica Mircosystems CMS GmbH, Wetzlar, Germany). Samples were prepared for microscopic analysis by adding 10 µl of Nile Blue (0.1 g/100 µl) to 1 ml of emulsion and vortexing the sample for 10 s, as detailed previously (Chapter 2). Nile blue has been found not to influence lipid crystallisation (Herrera & Hartel, 2000). After vortexing, 50 µl of the emulsion was pipetted onto a glass microscope slide and a coverslip was placed on top. Images were captured at 8-bit, 512x512 pixels resolution and were pseudo-coloured to show protein (red) and lipid (green).

3.2.6 Cryo-scanning electron microscopy

Cryo-scanning electron microscopy was performed using a Zeiss Supra 40VP field emission SEM (Carl Zeiss SMT Ltd., Cambridge, UK). Samples were prepared for imaging by adding 200 µl glycerol (cryo-protectant) into 1 ml of emulsion and vortexing for 10 s. Samples were then centrifuged for 5 min at 10,000 rpm in an eppendorf centrifuge (model 5417R; Eppendorf, Hauppauge, New York) at 20˚C to

concentrate the fat droplets. Afterwards, 400 µl of the solution was removed from the top of the tube and mounted onto a slotted aluminum sample holder. In order to cryofix the sample, the stage was then plunged immediately into melting liquid nitrogen slush (− 210 °C). The sample was then transferred under vacuum to the cryo-preparation chamber using the Alto 2500 cryo-transfer device (Gatan Ltd., Oxford, UK). Once inside the chamber, the sample was fractured at -195 °C, followed by sublimation at -90 °C for 2 min. After sublimation, the sample was sputter coated with platinum at -130 °C and transferred to the cold stage for imaging at -125 °C. Secondary electron images were obtained at an operating distance of 6 mm and an accelerating voltage of 2 kV.

2.2.7 Dynamic interfacial tension measurements

Interfacial tension (ϒI) was measured using a Kruss K12 tensiometer (Kruss GmbH, Hamburg, Germany) equipped with aWilhelmy plate, as described previously (Drapala et al., 2015). Dynamic ϒI data was collected continuously during the first 5 min at 60˚C and in subsequent 5 min intervals over 30 min; this was performed to simulate emulsion formation conditions and to capture initial changes in ϒI with the addition of phytosterols and whey proteins at the oil-water interface, respectively. Whey protein solutions were reconstituted at 0.5%, 1%, 2%, or 3% (wt/wt; % protein) in an ice bath with Milli-Q water and stirred at 300 rpm. Solutions were then stored overnight at 4˚C to allow for complete hydration. Phytosterols were added to the oil phase of MCT at 1% increments between 0.0-6.0% wt/wt as described previously (Chapter 2). Filtered water (Milli-Q system) with MCT (no WPI), without phytosterol, was used as a control sample.

Purified MCT oil was used to simulate melted AMF in these emulsions, as the commercial grade AMF used in this study produced inconsistent results between the water and lipid phase, most likely due to the presence of minor lipid components such as phospholipids and free fatty acids. MCT oil was chosen as it has been used previously to study the behaviour of milk proteins in other model milk systems (Waninge et al., 2005).

Before each measurement, the Wilhelmy plate was calibrated by submerging the plate within the light phase, consisting of MCT solution with or without phytosterol. After

calibration, 25 ml of the heavy phase, MCT or MCT with phytosterols, was added into the sample holder. The Wilhelmy plate was then lowered onto the interface and the light phase was added until the plate was completed submerged. The glass sample vessel and Wilhelmy plate were cleaned and annealed before each measurement. All glassware for sample preparation was acid-washed overnight with 1 M Nitric acid and washed 3 times with distilled water before drying. Measurements were completed in triplicate on each interface.

3.2.8 Surface modeling

In order to describe the interfacial interactions of the phytosterol and WPI interfaces at 60 °C, collected surface tension data was fitted utilising the Isofit® Software developed by Aksenenko and Miller (Möbius et al., 2001). As noted previously for other whey protein systems, the absorption of protein is different compared to other typical surfactants due to structural reorganisation and electrostatic or hydrophobic interactions between adsorbed molecules at the interface (Pradines et al., 2008). In this system, Langmuir best fit the protein only system, while the Frumkin model was employed on the phytosterol system. The following equations (3.2-3.7) describe the isotherm models employed (Möbius et al., 2001).

$$-\frac{\Pi\omega}{RT} = ln(1-\Gamma\omega) + \alpha(\Gamma\omega)^2 \tag{3.2}$$

where $\Pi = \gamma_{lvo} - \gamma_{lv}$ is the surface pressure, ω is the molar area, Γ is the surface excess and α is the interaction parameter between adsorbed adjacent surfactant molecules at the oil-water interface. Adsorption isotherm for Frumkin model is given by:

$$bc = \frac{\Gamma\omega}{1-\Gamma\omega}\exp(-2\alpha\Gamma\omega) \tag{3.3}$$

where b is the adsorption rate constant and c is the bulk concentration of surfactant. With surface coverage given by $\theta = \Gamma\omega$ equations 3.1 and 3.2 can be written as:

$$-\frac{\Pi\omega}{RT} = ln(1-\theta) + \alpha(\theta)^2 \tag{3.4}$$

$$bc = \frac{\theta}{1-\theta}\exp(-2\alpha\theta) \tag{3.5}$$

There are three model parameters, *b*, ω and α. When α=0, i.e. when there is no interaction between adsorbed surfactant molecules, the Frumkin equation limits to a Langmuir isotherm.

$$-\frac{\Pi\omega}{RT} = ln(1-\theta) \tag{3.6}$$

$$bc = \frac{\theta}{1-\theta} \tag{3.7}$$

These models were used to calculate the interfacial concentration of phytosterol and whey protein at different concentrations necessary for the employment of regular solution theory, which will be described in detail in the upcoming sections.

3.2.9 Statistical analysis

Mean values ± standard deviations of the data were reported for each emulsion formulation. Results were analysed for statistical significance utilising SAS® 9.3 software for Windows. A *Tukey's Post Hoc* Difference Test with a level of probability at $p < 0.05$ was used to analyse significant differences between treatments.

3.3 Results

3.3.1 Shape, size, and morphology

3.3.1.1 Particle size

The particle size of emulsions enriched with 0.0% (control), 0.3%, and 0.6%, wt/wt, of phytosterol were expressed as the mean of volume-weighted distributions ($D_{(4,3)}$). Phytosterol addition resulted in a significant decrease ($p<0.05$) in $D_{(4,3)}$ values of all the emulsions, from 0.85 ± 0.02 μm in the control emulsion to 0.78 ± 0.03 μm or 0.70 ± 0.01 μm in the 0.3% and 0.6% PE emulsions, respectively. Decreased particle size was also observed in Chapter 2, yet, these emulsions were generated uses a different homogeniser and milk fat/whey protein source.

3.3.1.2 Polarised light microscopy

Figure 3.1 shows polarised light microscopy (PLM) images of the 0.6% PE emulsion with milk fat as the carrier matrix at 20˚C and 50˚C. Crystalline material can be identified by its optical response to polarisation through light birefringence and is commonly used to establish the presence of crystalline material within food matrices (Toro-Vazquez et al., 2005; Thivilliers et al., 2008; Maher et al., 2015; Chen et al., 2016). Birefringence within the 0.6% PE emulsion appeared at both temperatures and confirmed the presence of crystalline material above the melting point of AMF, 50˚C, but below that of phytosterols within a TAG matrix (Lopez et al., 2007; Acevedo & Franchetti, 2016). Micrographs are consistent with results obtained from confocal microscopy showing evidence of crystals within and at the surface of emulsion droplets (Fig. 3.2). Birefringence within the 0.0% and 0.3% PE emulsion was not seen in emulsion droplets and is discussed in more detail below (data not shown).

3.1.3 Confocal laser scanning microscopy

Confocal laser scanning microscopy (CSLM) with fluorescent staining was performed to examine the lipid and protein distribution within PE emulsions (Fig. 3.2). Images were captured at 3 and 5x magnification with protein and lipid components labelled as red and green, respectively. Protein and lipid fluorescent channels were overlapped in all CLSM images, except the zoomed in protein image for the 0.6% PE emulsion at 5x magnification. No differences were observed between the control and 0.3% PE emulsion. Conversely, in the 0.6% PE emulsion, detectable crystals, identified by negative contrast as straight edges, were present within and at the surface of larger emulsion droplets, as observed in Chapter 2. Separated protein scans of the 0.6% PE emulsion demonstrated how crystalline material is distributed within the emulsion and appears to disrupt protein coverage on the lipid droplets.

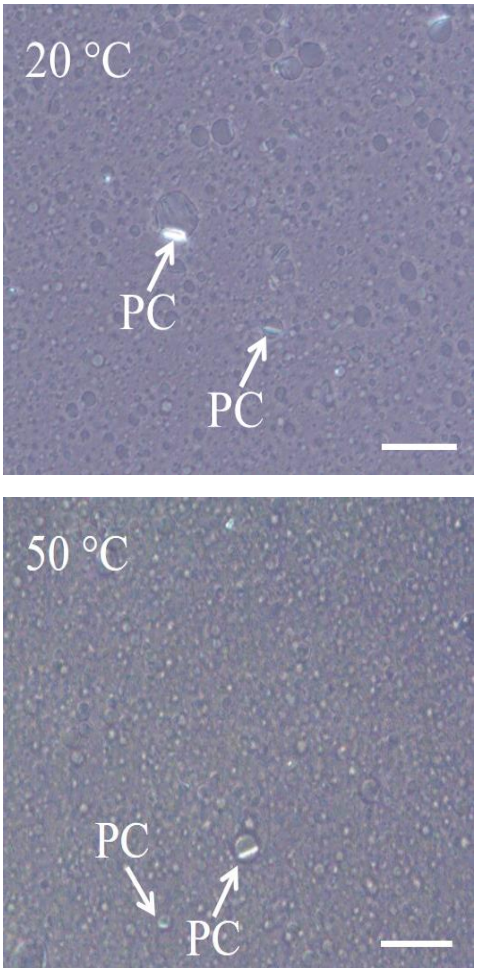

Figure 3.1 *Polarised light micrograph (partially uncrossed polar filters) of 0.6% w/w phytosterol emulsion showing elongated birefringent crystals associated with fat droplets (arrows) at 20 °C and 50 °C. Scale bar = 10 µm. PC = phytosterol crystal.*

3.3.1.4 Cryo-scanning electron microscopy

Droplet surface and fracture morphology was visualised utilising cryo-scanning electron microscopy (Cryo-SEM; Fig. 3.3). Cryogenic fracturing enabled the visualisation of cross-sections of the emulsion samples. The control emulsion contained relatively smooth droplets, as seen in the confocal images (Fig. 3.2). The 0.3% and 0.6% emulsion both contained droplet cross sections showing straight-edged and angular/needle-like structures within the emulsions droplets, consistent with PLM micrographs (Fig. 3.1) and other cryo-images of fat crystals (Heertje, 1993). Besides having droplets containing crystalline material, the 0.6% PE emulsion sample had

some larger coalesced droplets, which altered and roughened surfaces, suggestive of crystalline material at the droplet interface (Rousseau, 2000). A similar surface morphology has been observed in other food systems, such as margarine or cocoa butter emulsions, which exploit surface crystals to stabilise the interface (Heertje, 1993; Norton & Fryer, 2012).

3.3.2 Interfacial tension and modeling of emulsion systems

3.2.2.1 Interfacial tension

Interfacial tension was measured at 60ºC to understand the interactions of phytosterols and whey protein at the interface during initial emulsion formation and homogenisation (Table 3.1, Fig. 3.4 & 3.5). In agreement with previous research, the initial interfacial tension (γI 0 min) of water with medium chain triglyceride (MCT) oil (water/MCT), was found to be 20.4 ± 0.5 mN/m (Jumaa & Müller, 1998; Mao et al., 2009). Upon the addition of just 2% phytosterol to the oil phase, there is a significant decrease in observed initial γI, as compared to the water/MCT sample. Correspondingly, every 1% increase in phytosterol, with a water-only aqueous phase, resulted in a further significant decrease in initial γI. The water/0.6% phytosterol sample, which had a value of 9.3 ± 0.3 mN/m, was the lowest of all of the water/phytosterol interfaces and was similar to that of the 1% protein/MCT sample with an initial γI value of 10.0 ± 0.4 mN/m (Table 3.1). The water/0.6% phytosterol sample also had a slight increase in interfacial tension values at 5 and 30 min but, since these values all fall within the samples standard deviation, this was not deemed significant.

When phytosterol and protein addition were added separately both decreased initial interface tension, interfaces with ≥ 0.3% phytosterol and whey protein combined had a significantly lower initial γI ($p < 0.05$) than all other samples. The lowest initial γI was the 1% protein/5% phytosterol and 1% protein/6% phytosterol interfaces, at 3.6 ± 0.5 mN/m and 2.7 ± 0.5 mN/m, respectively (Table 3.1). These results for initial γI describe the ability of both phytosterols and whey protein to move to the interface and influence the interfacial tension at an oil/water surface both separately and synergistically. Both phytosterols and whey protein possess an amphiphilic molecular structure and their ability to influence interfacial tension separately is expected

(McClements, 2004; Rouimi et al., 2005; Rossi et al., 2010; Chen et al., 2016). However, a synergistic effect between these two molecules has not been recorded previously and will be further explained in the discussion section.

The interfaces were continuously monitored for 5 min, then in subsequent 5 min intervals for 30 mins. Final values at 5 min (γI 5 min) and 30 min (γI 30 min) were compared against the initial γI (Δ 0-5 min and Δ 0-30 min, respectively), as a quantitative means of evaluation (Table 3.1, Fig. 3.4, & Fig.3.5). By comparing changes within these two time points, several features regarding interface formation can be described. Firstly, 1% phytosterols and whey protein separated at the interface had a statistically similar Δ 0-5 min values, but the 1% whey protein sample had a larger Δ 0-30 min value (Table 3.1). This demonstrated that whey protein can decrease interfacial tension more than phytosterols, but during initial emulsion formation their ability is relatively equal. Secondly, the largest initial change in interfacial tension occurred on the 1% protein/4% phytosterol sample but at 30 min the overall change in tension was similar to other samples (Table 3.1; Fig. 3.5). Thus, this multicomponent interface demonstrated that this synergistic interfacial effect acts quickly upon the oil/water interface.

Table 3.1 Interfacial tension for oil and water systems containing different concentrations of whey protein (pro) and phytosterol (ps). All interfaces contained water and MCT but some interfaces were respectively enriched with either/both pro and/or ps.

	Interfacial tension (γI) (mN/m)				
Interface	0 min	5 min	30 min	Δ (0-5 min)	Δ (0-30min)
Water/mct	20.4 ± 0.5^{a}	19.9 ± 0.4^{a}	19.6 ± 0.3^{a}	0.5 ± 0.6^{abcd}	0.9 ± 0.6^{abc}
Water/1% ps	20.3 ± 0.2^{a}	19.5 ± 0.2^{a}	18.6 ± 0.5^{a}	0.8 ± 0.3^{abe}	1.7 ± 0.6^{bc}
Water/2% ps	17.4 ± 0.4^{b}	17.2 ± 0.5^{b}	16.6 ± 0.6^{b}	0.2 ± 0.6^{abcdf}	0.8 ± 0.7^{abc}
Water/3% ps	15.6 ± 0.1^{c}	15.6 ± 0.1^{c}	15.5 ± 0.2^{b}	0.1 ± 0.2^{bcdf}	0.1 ± 0.2^{de}
Water/4% ps	13.6 ± 0.4^{d}	13.6 ± 0.4^{d}	13.6 ± 0.4^{c}	0.0 ± 0.6^{df}	0.0 ± 0.7^{de}
Water/5% ps	11.2 ± 0.5^{e}	11.2 ± 0.5^{e}	10.8 ± 0.5^{d}	0.0 ± 0.8^{cdf}	0.4 ± 0.7^{ad}
Water/6% ps	9.3 ± 0.3^{f}	9.6 ± 0.3^{f}	10.2 ± 0.7^{d}	-0.3 ± 0.4^{f}	-0.9 ± 0.7^{e}
0.5% pro/mct	$10.0 \pm 0.5e^{f}$	9.3 ± 0.6^{gf}	6.8 ± 0.4^{e}	0.8 ± 0.8^{abce}	3.3 ± 0.7^{fg}
1% pro/mct	10.0 ± 0.4^{ef}	9.1 ± 0.3^{gf}	6.3 ± 0.3^{ef}	0.9 ± 0.5^{ace}	3.7 ± 0.5^{gh}
1.5% pro/mct	9.2 ± 0.5^{f}	8.7 ± 0.4^{gf}	6.2 ± 0.5^{ef}	0.6 ± 0.6^{abcd}	3.0 ± 0.7^{fg}
2% pro/mct	9.7 ± 0.4^{f}	8.2 ± 0.3^{gh}	5.8 ± 0.1^{efg}	1.5 ± 0.5^{ghe}	3.9 ± 0.4^{gh}
3% pro/mct	9.6 ± 0.6^{f}	8.3 ± 0.5^{gh}	5.9 ± 0.7^{efg}	1.3 ± 0.8^{egh}	3.8 ± 0.9^{gh}
1% pro/1% ps	9.1 ± 0.2^{f}	8.3 ± 0.1^{gh}	6.9 ± 0.2^{e}	0.8 ± 0.2^{abe}	2.2 ± 0.2^{cf}
1% pro/2% ps	9.4 ± 0.2^{f}	7.5 ± 0.1^{h}	5.4 ± 0.1^{fg}	1.9 ± 0.2^{h}	4.1 ± 0.2^{ghi}
1% pro/3% ps	7.3 ± 0.5^{g}	5.8 ± 0.3^{i}	3.5 ± 0.2^{hi}	1.5 ± 0.6^{egh}	3.8 ± 0.6^{gh}
1% pro/4% ps	5.9 ± 0.6^{h}	2.7 ± 0.2^{j}	2.2 ± 0.4^{j}	3.2 ± 0.6^{i}	3.6 ± 0.7^{gh}
1% pro/5% ps	3.6 ± 0.5^{i}	2.7 ± 0.1^{j}	2.3 ± 0.3^{j}	0.9 ± 0.5^{ace}	1.3 ± 0.6^{abc}
1% pro/6% ps	2.7 ± 0.5^{i}	2.5 ± 0.5^{j}	2.6 ± 0.3^{ij}	0.2 ± 0.7^{abcdf}	0.1 ± 0.6^{de}

Within a column, values with different superscript letters are significantly different ($p < 0.05$). Δ Difference between γI values at different time points.

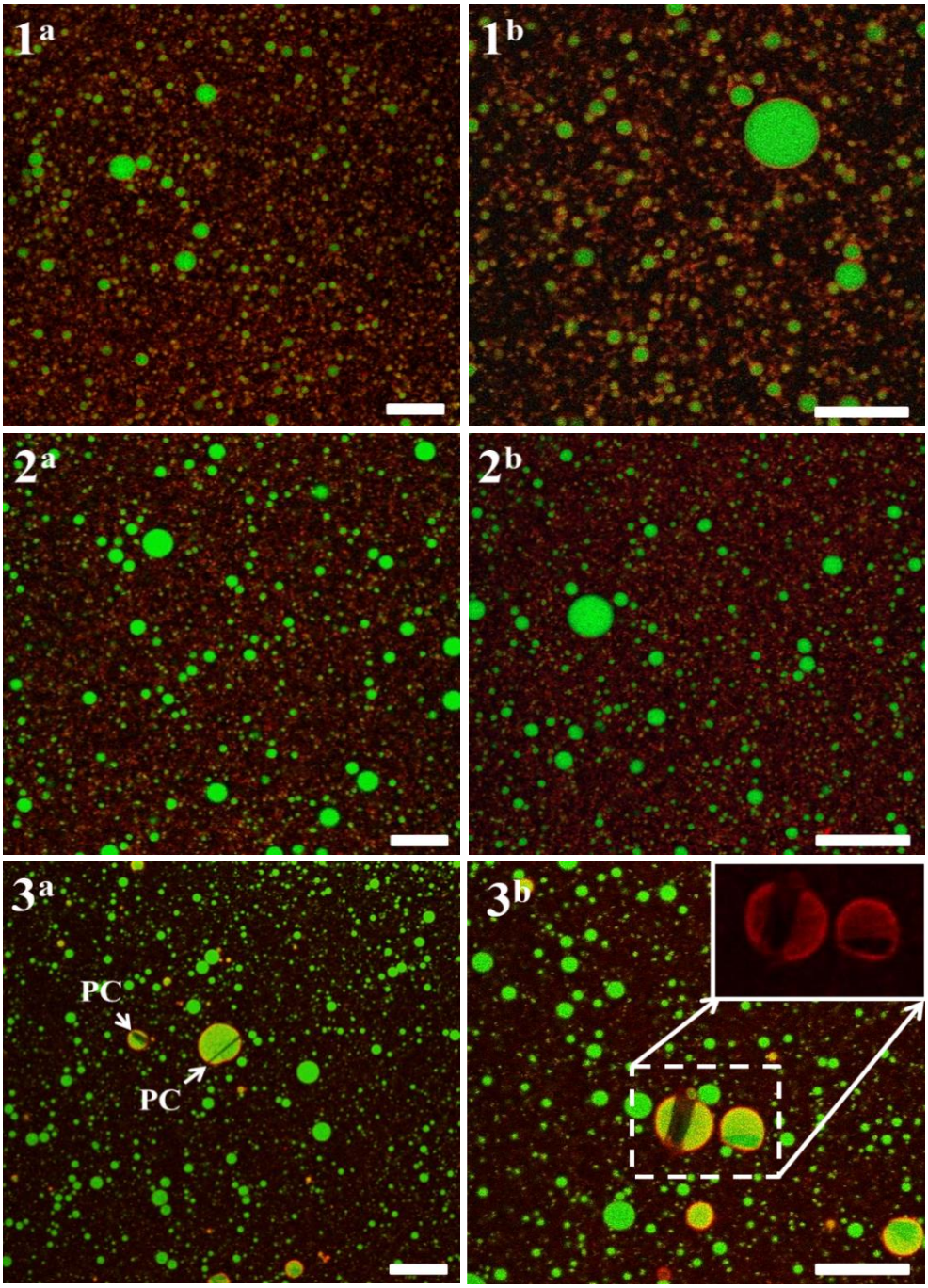

Figure 3.2 *Confocal images of phytosterol-enriched (PE) emulsions at 3 and 5x magnification, superscripted as 'a' and 'b', respectively. Emulsions are labelled as (1) 0.0% PE emulsion (control), (2) 0.3% PE emulsion, and (3) 0.6% PE emulsion. Images show the distribution of fat and protein, with fat represented in green and protein in red. Image 3b shows an enlarged section of a protein only-scan of PE emulsion droplets with phytosterol crystals. Scale bar = 10 µm. Note: crystalline phytosterols both at the interface and within fat droplets are made visible by negative contrast (white arrows). PC = phytosterol crystal.*

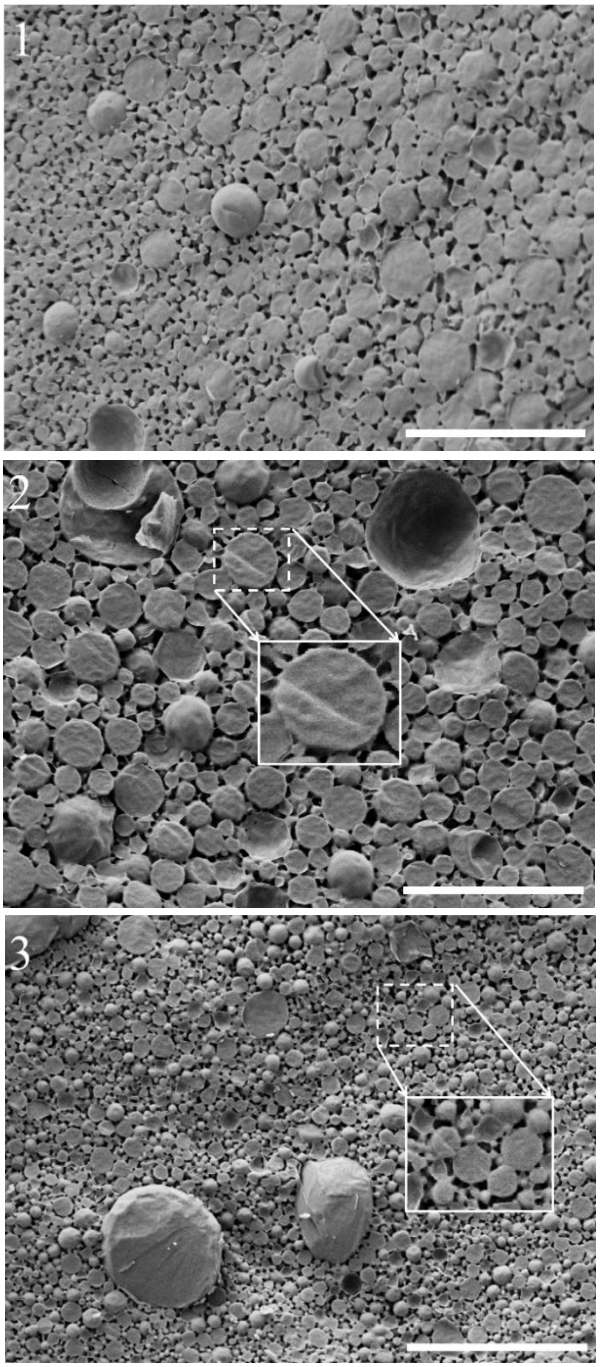

Figure 3.3 *Cryo-scanning electron micrographs of cross sections of emulsions with different levels of phytosterol enrichment. Emulsions are labelled as (1) 0.0% PE emulsion (control), (2) 0.3% PE emulsion and (3) 0.6% PE emulsion. Enlarged section highlights the presence of crystal-like material inside of emulsion droplets. Scale bar = 10 µm.*

3.2.2.2 Interfacial modeling

The ability of surfactants to synergistically influence interfacial tensions has been previously studied by several authors (Rosen & Zhou, 2001; Zhou & Rosen, 2003; Reddy & Ghosh, 2010). To model this relationship, final interfacial tension results were graphed on wt/wt % of each component and the mixed phytosterol and whey protein interfaces (Fig. 3.6). A synergic relationship between whey protein and phytosterols was apparent, as phytosterol concentrations higher than 3% at 1% protein possessed a lower final γI values than the two components separately. This data was then processed by the regular solution theory (RST) developed by Rubingh and altered by Rosen and Hau to account for surfactant mixtures (Rubingh, 1979; Rosen & Hua, 1982). The approach by Rosen and Hua takes the non-ideality of mixing into consideration through a molecular interaction parameter, β (eq 8) (Rosen & Hua, 1982). The magnitude of the interaction parameter corresponds to the deviation from ideal solution behaviour. Negative values of the interaction parameter signify that the attractive interaction between the surfactants in the mixture is greater than the self-attraction of each surfactant. Positive values indicate repulsive interactions between the surfactants. The molecular interaction parameter, β, is defined by equation 3.8.

$$\beta = \frac{ln\left(C_s / x_s C_s^o\right)}{(1-x_s)^2} \tag{3.8}$$

Where, Cs is the bulk concentration of surfactant (phytosterols) in the mixture, xs is the interfacial composition of surfactant, and C_s^o is the bulk concentration of pure surfactant required to achieve the same interfacial tension of the mixture.

Rosen and Hua showed that the interfacial composition (xs) can be calculated by utilising equation 3.9 (Rosen & Hua, 1982). Here Cs and xs refer to the phytosterols concentrations, while Cp and xp correspond to the protein bulk concentration and interfacial composition, respectively.

$$\frac{x_s^2 ln\left(C_s / x_s C_s^o\right)}{(1-x_s)^2 ln\left(C_p / (1-x_s) C_p^o\right)} = 1 \tag{3.9}$$

To solve for xs, C_s^o and C_p^o are needed, which are the bulk concentrations of pure surfactants (phytosterols and WPI) required to achieve the same interfacial tension of that of the mixture. Values for C_s^o and C_p^o were derived from the adsorption isotherm, Langmuir and Frumkin for whey protein and phytosterol, respectively (Fig. 3.7).

For a fixed bulk protein concentration of 1 wt%, with increasing phytosterol concentration, the interaction parameter and the interfacial composition were calculated to better understand the synergistic effect of protein and phytosterols at the interface (eq 8-9; Table 3.2). The interaction parameter was negative, suggesting attractive behaviour between the adsorbed proteins and phytosterols at the interface (Rosen & Hua, 1982; Zhou & Rosen, 2003). However, after surface tension of the systems reaches its lower limit at 4% sterol and 1% protein, the interaction parameter remains relatively constant, even decreasing slightly upon phytosterol addition (Table 3.2).

As seen previously within other whey protein-surfactant complexes, once the interface is saturated with the complex, additional surfactant can lead to less surface-active complexes, which then have to compete with free surfactant molecules (Wüstneck et al., 1996). Subsequently, as the concentration of phytosterol increased from 2-6 wt%, the calculated interfacial composition of phytosterols increased from 54 to 88% (Table 3.2). This indicates that during emulsion formation, phytosterols can outcompete whey protein/whey protein complexes for space at the oil/water interface. Preliminary results showed that it was not possible to form emulsions consisting of ≥ 8% phytosterol and 1% protein or phytosterols alone; confirming that, at higher levels of phytosterol addition, the interfacial composition is indeed different and dominated by phytosterols.

Even though the RST approach is strictly only valid when both the surfactants are present in a single phase, it is surprising that the theory gives a qualitative picture of the interfacial composition when the surfactants adsorb from two different phases, which is the case for proteins and phytosterols that are dispersed within the oil and aqueous phase, respectively. The calculations presented in this section are intended for a qualitative explanation of synergistic behaviour of phytosterols and proteins at the oil/water interface.

Table 3.2 Interfacial composition of phytosterols (xs) and protein (xp) as a function of phytosterol concentration in bulk oil phase

Bulk Total Concentration (wt%)	Bulk Phytosterols Concentration Ws (wt%)	Bulk Protein Concentration Wp (wt%)	Surface Tension (mN/m)	Interfacial composition phytosterols xs (mol%)	Interfacial Composition Protein xp (mol%)	Interaction parameter (β)
3	2	1	5.4	0.54	0.46	-2.90
4	3	1	3.5	0.69	0.31	-5.05
5	4	1	2.2	0.77	0.23	-6.74
6	5	1	2.3	0.82	0.18	-5.64
7	6	1	2.6	0.88	0.12	-4.42

The interface with 1% phytosterol and 1% bulk protein was not included as it did not converge with the Rosen and Hau model (Rosen & Hua, 1982). Surface tension measurements are taken after 30 min at 60 °C.

3.4 Discussion

3.4.1 Influence of phytosterol addition on the morphology and physical properties of the emulsions.

Particle size and images captured using PLM, CSLM, and cryo-SEM demonstrated the effect of phytosterol enrichment on the emulsion system. Particle size of the PE emulsion decreased consistently with the addition of phytosterols in the oil phase between separate emulsion trials. Although the trend was similar, the extent of difference between trials was less than what was observed previously using a different homogenizer and mastersizer (Zychowski et al., 2016). A decrease in emulsion droplet size was also recorded in a study which analyzed the stability of oil-in-water loaded $MgCl_2$ emulsions with phytosterols enriched into the continuous phase. Emulsion droplets dispersed within the phytosterol containing lipid were found to be smaller upon initial formation and were able to resist coalescence unlike the control sample without phytosterols. This was further investigated by studying the o/w interface with and without the presence of phytosterols and results demonstrated that phytosterols presence was able to significantly influence the absorption behaviour of the both of the emulsifiers used, polyglycerol polyricinoleate (PGPR) and sodium caseinate (Andrade & Corredig, 2016). Phytosterols have also been documented to decrease interfacial tension, as observed within the current and previous studies (Table 1 & Figure 5; Cercaci, et al., 2007). Thus, it is possible that the recorded particle size decrease could be due phytosterols presence at the oil-in-water interface.

PLM images were captured at 20˚C and 50˚C, as AMF melts completely at ~40˚C and phytosterol within TAG systems at around ~60˚C (Fig. 1; Acevedo et al., 2016; Lopez et al., 2007; Zychowski et al.,2016). Birefringence in the images was used to distinguish the presence of crystalline material within the emulsion systems. Thus, the birefringence observed at 50 ˚C, above the melting point of AMF, confirms that the observed crystals in images are indeed composed of phytosterols. No crystalline AMF was observed in the 0.0% and 0.3%, despite the sample being held at 20˚C for 24 h. This was most likely due to an insufficient quantity or potentially smaller sized milk fat crystals that were produced during the holding period. Similar results have been observed in lard based emulsions where fine crystals could not be observed via

polarised light and only after holding could larger protruding lard crystals be observed in some emulsion droplets (Campbell et al., 2001).

Images captured using CSLM differentiated between the lipid and protein components of the PE emulsions. Previous CSLM images published by Zychowski et al. (2016) showed an altered interface present within 0.6% PE emulsion, as seen in this study, but did not clearly capture the protein layer distribution around fat droplets. In Figure 2, all PE emulsions can be visualized, along with the images taken from the separated protein and lipid channels for the 0.6% PE emulsion. The separated channel images show protein coverage around the lipid droplet of the 0.6% PE emulsion, except where phytosterol interfacial crystals were present (Fig. 2; Image 3b). This gap in protein coverage supports the hypothesis of phytosterols being present at the interface and suggests that possibility phytosterols can stabilize the interface of an emulsion droplet. Phytosterol stabilization at the interface was also observed in PE sunflower oil emulsions with octenyl succinic anhydride starch as the main emulsifier. Phytosterols were able to co-crystallize with the starch and this complex formed a strong barrier around the dispersed oil droplets. After 90 d emulsions containing phytosterols were ~8 times smaller than the control emulsion with starch alone, which had coalesced, demonstrating the ability of crystalline phytosterols to successfully stabilize an interface (Chen et al., 2016).

Cross-sectional images taken using cryo-SEM highlight how phytosterol crystallization influences the surface morphology of emulsion droplets (Fig. 3). Micrographs of the control and 0.3% PE emulsions show droplets with a relatively smooth surface, as compared to the coalesced droplets present in the 0.6% PE emulsion. These larger droplets facilitate the visualization of the presence of phytosterol crystals but, in line with previous studies, did not result in significant destabilization of the PE emulsion system (Zychowski et al., 2016).

Crystallization within emulsions usually results in partial coalesce, which leads to particle aggregation and eventual emulsion destabilization (McClements, 2012). As mentioned, phytosterols have been previously documented to crystallize at the interface but not destabilize the emulsion. Although phytosterol crystallization might not result in emulsion destabilization, it can decrease bioaccessibility within the

functional food systems (Jones & AbuMweis, 2009). For example, in a study performed by Nestec, 1.8 g of non-esterified phytosterols were solubilised in a milk matrix and consumed. The solubilised phytosterol ester resulted in a 29.1 ± 4.1% reduction in LDL-cholesterol levels (Pouteau et al., 2003). Conversely, 3 g of crystallised phytosterols administered in a crystallised tablet were only able to decrease LDL-cholesterol levels by a 11.0% (Carr et al., 2009). In a side by side study, 0.7 g solubilised phytosterols in micelles were ~25% more effective in reducing LDL cholesterol level than the 1 g of powdered crystalline phytosterols (Ostlund et al., 1999). The discrepancy between the results highlights the need for further research on what factors influence phytosterol solubility food matrices.

3.4.2 The influence of phytosterols and whey protein on interfacial tension

Dynamic γI values were evaluated under several different concentrations of phytosterols and whey protein to understand the influence of each component individually and with various combinations of emulsion formations (Table 1, Figs. 4 & 5). The unadulterated surface for all measurements is the initial γI of the interface with MCT oil and water, as adjustments to this interface were completed with the addition of either phytosterol to the oil phase and/or whey protein isolate to the water phase (Drapala et al., 2015). When ≥ 2% phytosterols were added to the oil phase initial γI values significantly decreased ($p < 0.05$; Table 1). The ability of phytosterols to lower γI has been observed previously in an experiment employing hexane, as the lipid phase, with dissolved phytosterols. Results demonstrated that even low phytosterol concentrations(1 mmol/kg) in hexadecane were able to significantly decrease γI, while higher phytosterol concentrations could further decrease γI (Cercaci et al., 2007). Phytosterols such as β-sitosterol, campesterol and sigmasterol possess a hydrophobic, tetracyclic, fused-ring skeleton and a polar, hydroxyl group. The differing polarities within their chemical structure give phytosterols a slightly amphiphilic nature, allowing them to interact with both the aqueous and lipid phases at oil-water interfaces (Rossi et al., 2010; Chen et al., 2016).

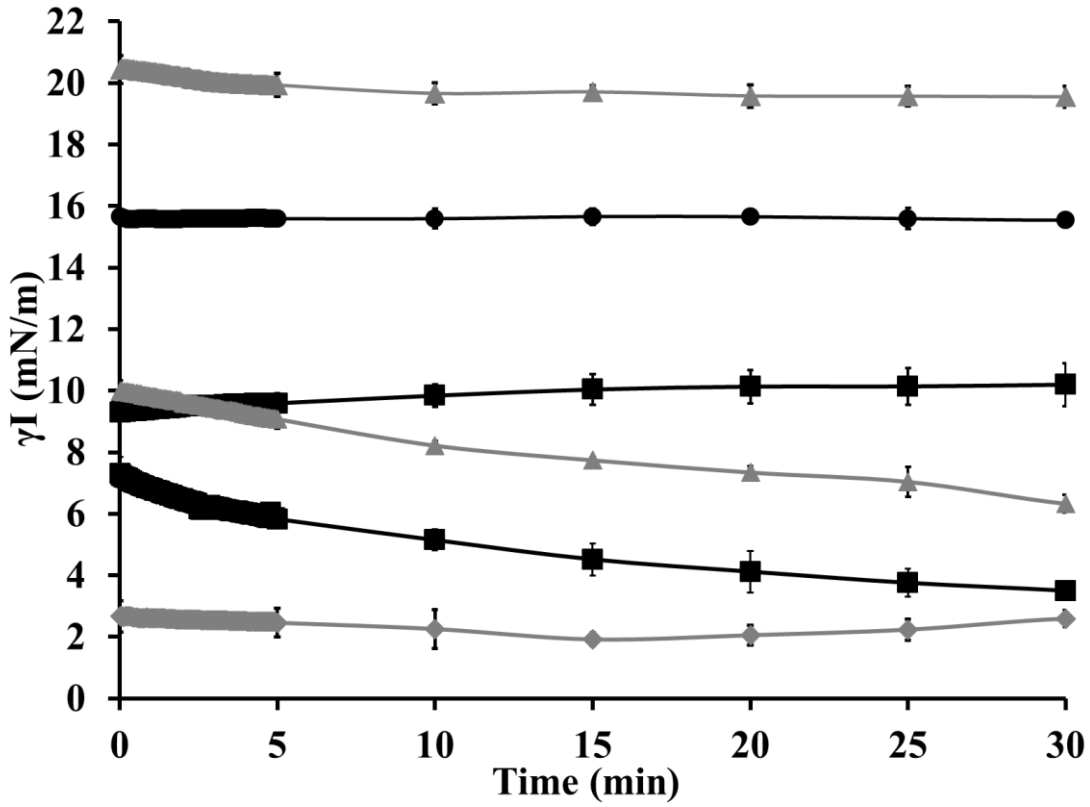

Figure 3.4 *Dynamic interfacial tension measurements of samples over 30 min at 60 °C. All interfaces contained water (aqueous phase) and MCT (oil) but some phases were enriched with either/both whey protein and phytosterol, respectively. Interfaces are denoted as (▲) water/MCT, (●) water/3% phytosterol, (■) water/6% phytosterol, (▲) 1% protein/MCT, (■) 1% protein/3% phytosterol, and (◆) 1% protein/6% phytosterol.*

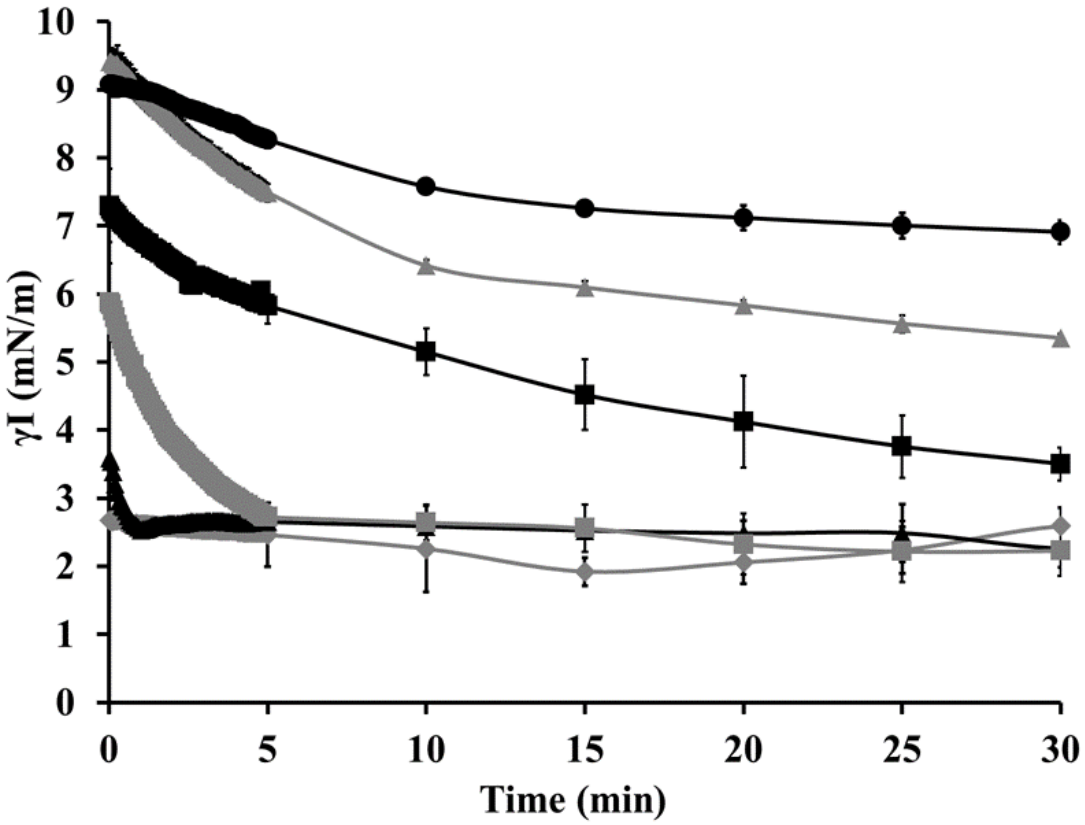

Figure 3.5 *Dynamic interfacial tension measurements of samples at 60 °C containing 1% protein and different concentrations of phytosterols dissolved into MCT; (●) 1% phytosterol, (▲) 2% phytosterol, (■) 3% phytosterol, (■) 4% phytosterol, (▲) 5% phytosterol, (◆) 6% phytosterol.*

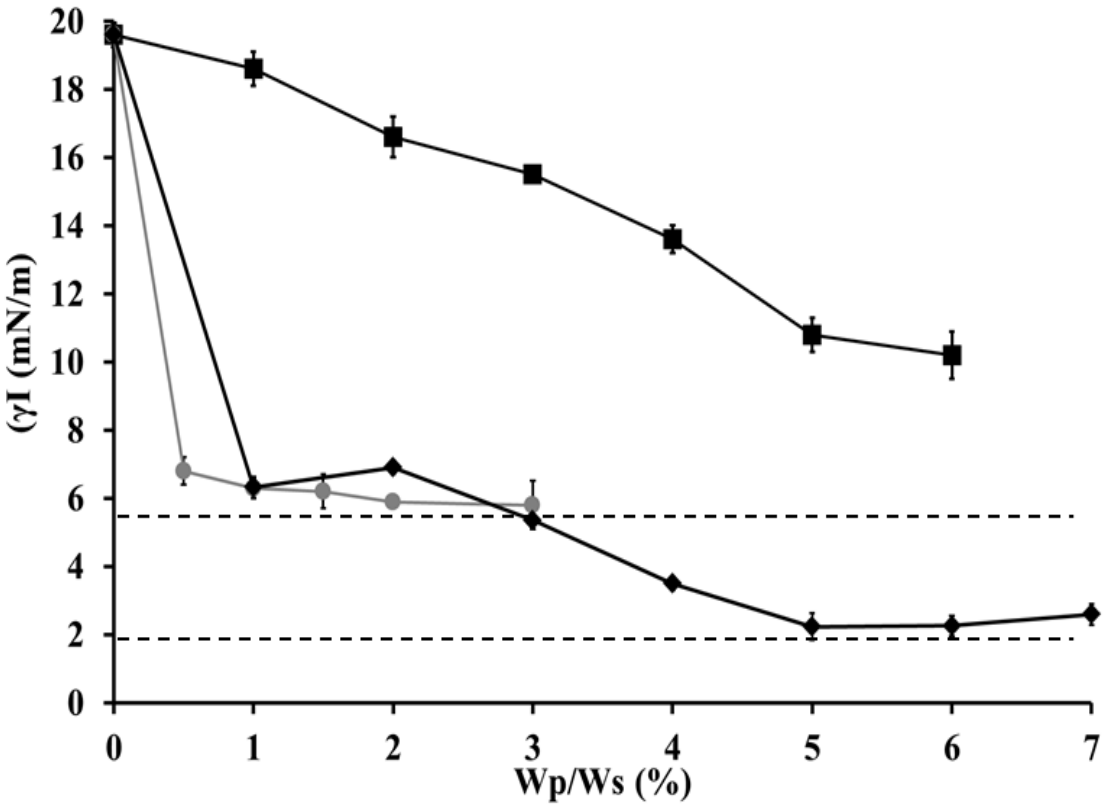

Figure 3.6 *Interfacial tension in weight percentages after 30 min at 60 °C; interfaces are (■) water/(1-6%) phytosterols, (●;0.5-3%) protein/mct and (◆) 1% protein/(1-6% phytosterols). There is a synergistic effect between the protein and phytosterols adsorbed at the oil-water interface which results in a decrease of interfacial tension in mixed interfaces (represented by dashed lines).*

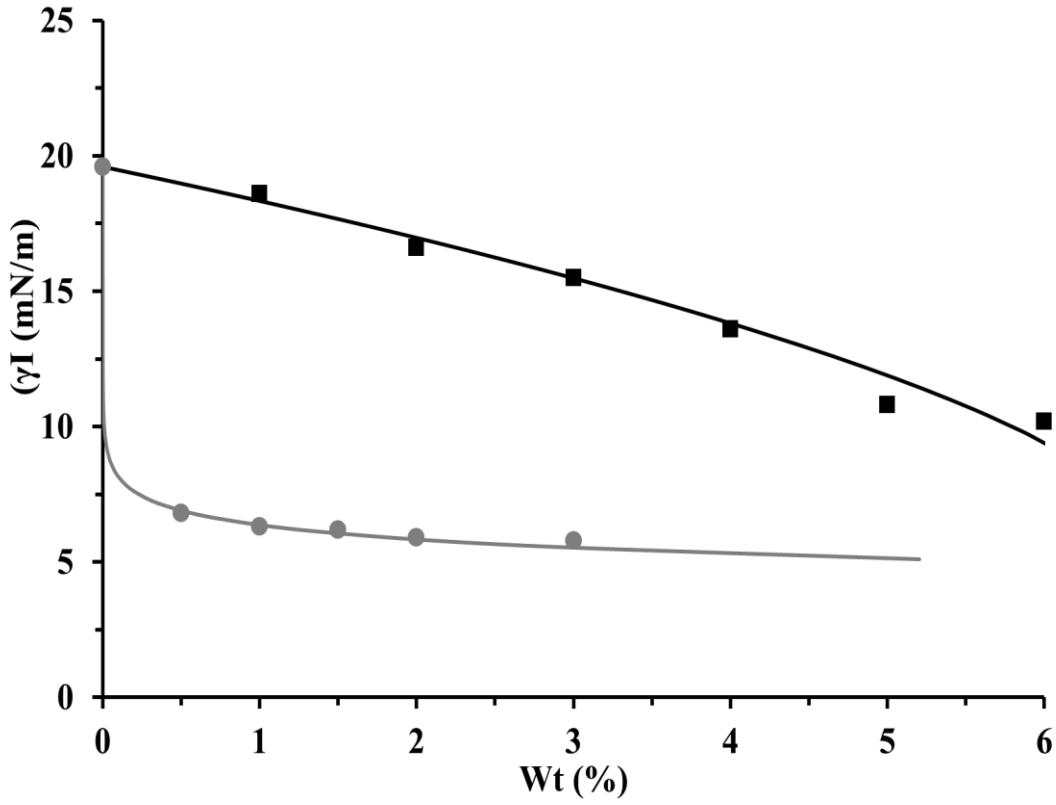

Figure 3.7 *Isotherm fitting to equilibrium interfacial tensions (measured after 30 min at 60 °C). Langmuir and Frumkin isotherms best fit the interfacial tensions for protein(●) and phytosterols(■) respectively. The Langmuir adsorption isotherm was fitted with parameters: adsorption rate constant b = 5.46*10^{7} l/mmol, Area, ω_o = 3.6*10^{6} m^2/mol. Frumkin adsorption isotherm was with parameters: adsorption rate constant b = 9.13*10^{-4} l/mmol, Area, ω_o = 5*10^{4} m^2/mol and interaction parameter α = 2.*

As expected, whey protein, consisting mainly of β-lactoglobulin, was also able to decrease interfacial tension in the absence of phytosterols (Table 1 & Fig. 4). Even with the addition of only 0.5% whey protein, the initial γI significantly decreased, but, unlike phytosterol addition, increasing the concentration of protein (0.5-3%) had little effect on γI values (Table 1). It is hypothesized that whey protein at 0.5% had already saturated the MCT and water interface, and thus increasing protein concentration was not able to significantly further decrease interfacial tension (Dickinson, 1999; McClements, 2004). Whey proteins are comprised of large globular proteins, and the rate at which they absorb at the oil-water interface is limited by their size, compared to other smaller surfactants; however, they have been shown to provide long-term stability to oil-water interfaces (Courthaudon et al., 1991; McClements, 2015). Thus, it not surprising that whey proteins were able to significantly reduce initial γI and over time had a much larger Δ (γI init-γI 30 min), as compared to the phytosterol/water interfaces. Similar interfacial results for whey protein and oil interfaces have been observed previously (Sünder et al., 2001; Drapala et al., 2015; Li et al., 2016).

Most interestingly, the lowest initial γI values came from interfaces containing 3% ≥ phytosterols and whey protein (Table 1) but, as can be noted, all levels of phytosterol concentration influenced interfacial tension in the presence of protein (Fig. 5). In addition, the largest (Δ 0-5 min) value was achieved with the 1.0% protein/4.0% phytosterol interface at 3.2 ± 0.6 mN/m (Table 1). This data suggests that phytosterols and whey protein synergistically reduce interfacial tension and are able to interact at the interface more quickly together than when separated. Thus, the authors believe that whey proteins and phytosterols can be considered to participate in synergism at the emulsion interface. Synergism is defined as "the condition in which the properties of the surfactant mixture are better than those attainable with the individual surfactants by themselves" (Reddy & Ghosh, 2010).

The interaction between phytosterols and whey protein was quantified using RST modified by Rosen and Hua (Rubingh, 1979; Rosen & Hua, 1982). In mixed interfaces with 1% protein and 1-6% phytosterol, the interaction parameter was found to be negative, suggesting that phytosterols and whey protein are interacting at the surface interface (Zhou & Rosen, 2003). Within the bulk system, both the whey protein and phytosterols have negative electric-static charges (Rossi et al., 2010; Zychowski et al.,

2016); however, phytosterols possess a negatively charged hydroxyl group, which most likely interacts at the interface, while the remaining portions of the molecule are relatively neutral. Whey protein has been found previously too complex with nonionic surfactants, such as tween 20; thus, it is very possible that the two compounds, phytosterols and whey protein, are indeed complexing at the surface interface (Wilde & Clark, 1993; Cornec et al., 1998; Demetriades & McClements, 1998).

The interaction parameter reached its most negative result (strongest interaction) at 4% phytosterol and 1% protein, which also coincided with the lower limit of interfacial tension on the tensiometer. Phytosterol levels ≥ 5% resulted in lower levels of protein absorption and higher levels of phytosterol absorption and interaction parameters. In other whey protein-surfactant systems, once protein absorption has been saturated, additional surfactant addition can cause the hydrophilization of any protein surfactant complexes. This leads to decrease in surface activity of the complex and, thus, the complex must compete for the interface with free surfactant molecules (Wüstneck et al., 1996). Results from the previously conducted study by Zychowski et al 2016, found that emulsions, with ≥ 8% phytosterols and 1% protein or phytosterols alone, were not stable and could not be homogenized. This confirms the calculated results suggesting that at a higher concentration of phytosterol enrichment the interfacial composition is dominated by phytosterols. The results calculated *via* RST serve as quantification of the interaction that is occurring between phytosterols and whey proteins at the surface interface.

3.5 Conclusions

Phytosterol crystallization impacts the bioaccessibility of bioactive compounds and can possibly occur at the interface phytosterol-enriched emulsion as demonstrated by confocal, cryo-SEM, and polarized light microscopy. Upon examining the emulsion interface, interfacial tension results demonstrated that both phytosterols and whey proteins were able to lower interfacial tension. However, the combination of phytosterols and whey protein was able to lower interfacial tension to a greater extent than the two components separately, demonstrating synergism between the two compounds. These results were confirmed by interfacial modeling results, suggesting that the two compounds were interacting at the interface. This type of behavior

between phytosterols and whey protein is not well studied and highlights a novel exploitable characteristic of phytosterols, which can be utilized within the functional food industry. Additionally, this work highlights the need to monitor crystallization within and at the surface of the phytosterol enriched matrices to improve bioaccessibility in the final food product.

Acknowledgements

The authors would like to thank the Teagasc Food Research Centre for its support (Teagasc Project RMIS6412) and assistance in organising this collaborative project with Melbourne University. The authors would also like to thank Kamil Drapala for his guidance and help utilising the Kruss Tensiometer at the University College of Cork and Li Day at AgResearch for her assistance. Finally, the authors would like to thank Lisa Blazo from the University of Sheffield for her assistance in editing the manuscript.

References

Acevedo, N. C., & Franchetti, D. (2016). Analysis of co-crystallized free phytosterols with triacylglycerols as a functional food ingredient. *Food Research International, 85*, 104-112. doi:http://dx.doi.org/10.1016/j.foodres.2016.04.012

Andrade, J., & Corredig, M. (2016). Vitamin d3 and phytosterols affect the properties of polyglycerol polyricinoleate (pgpr) and protein interfaces. *Food Hydrocolloids, 54, Part B*, 278-283. doi:http://dx.doi.org/10.1016/j.foodhyd.2015.10.001

Berger, A., Jones, P. J. H., & Abumweis, S. S. (2004). Plant sterols: Factors affecting their efficacy and safety as functional food ingredients. *Lipids Health and Disease, 3*(5), 907-919.

Campbell, S. D., Goff, & Rousseau, D. (2001). Relating bulk-fat properties to emulsified systems: Characterization of emulsion destabilization by crystallizing fats. In N. Widlak, R. Hartel, & S. Narine (Eds.), *Crystallization and solidification properties of lipids.* (pp. 176-189). Champaign, Illinois: AOCS Press.

Carden, T. J., Hang, J., Dussault, P. H., & Carr, T. P. (2015). Dietary plant sterol esters must be hydrolyzed to reduce intestinal cholesterol absorption in hamsters. *The Journal of Nutrition*.

Carr, T. P., Krogstrand, K. L. S., Schlegel, V. L., & Fernandez, M. L. (2009). Stearate-enriched plant sterol esters lower serum ldl cholesterol concentration in normo- and hypercholesterolemic adults. *The Journal of nutrition, 139*(8), 1445-1450.

Cercaci, L., Rodriguez-Estrada, M. T., Lercker, G., & Decker, E. A. (2007). Phytosterol oxidation in oil-in-water emulsions and bulk oil. *Food Chemistry, 102*(1), 161-167.

Chen, X.-W., Guo, J., Wang, J.-M., Yin, S.-W., & Yang, X.-Q. (2016). Controlled volatile release of structured emulsions based on phytosterols crystallization. *Food Hydrocolloids, 56*, 170-179. doi:http://dx.doi.org/10.1016/j.foodhyd.2015.11.035

Clifton, P. (2007). *Plant sterols and stanols as functional ingredients in dairy products* (M. Saarela Ed. Vol. 2). Oxford, UK Elsevier.

Cornec, M., Wilde, P. J., Gunning, P. A., Mackie, A. R., Husband, F. A., Parker, M. L., & Clark, D. C. (1998). Emulsion stability as affected by competitive adsorption between an oil-soluble emulsifier and milk proteins at the interface. *Journal of Food Science, 63*(1), 39-43.

Courthaudon, J.-L., Dickinson, E., Matsumura, Y., & Williams, A. (1991). Influence of emulsifier on the competitive adsorption of whey proteins in emulsions. *Food Structure, 10*(2), 1.

Demetriades, K., & McClements, D. J. (1998). Influence of ph and heating on physicochemical properties of whey protein-stabilized emulsions containing a

nonionic surfactant. *Journal of Agricultural and Food Chemistry, 46*(10), 3936-3942.

Dickinson, E. (1999). *Food emulsions and foams*. Witney, UK: Elsevier Applied Science Publishers Ltd.

Drapala, K. P., Auty, M. A. E., Mulvihill, D. M., & O'Mahony, J. A. (2015). Influence of lecithin on the processing stability of model whey protein hydrolysate-based infant formula emulsions. *International Journal of Dairy Technology, 68*(3), 322-333.

Engel, R., & Schubert, H. (2005). Formulation of phytosterols in emulsions for increased dose response in functional foods. *Innovative Food Science & Emerging Technologies, 6*(2), 233-237.

Heertje, I. (1993). Microstructural studies in fat research. *Food structure, 12*(1), 10.

Henson, S., Cranfield, J., & Herath, D. (2010). Understanding consumer receptivity towards foods and non-prescription pills containing phytosterols as a means to offset the risk of cardiovascular disease: An application of protection motivation theory. *International Journal of Consumer Studies, 34*(1), 28-37.

Herrera, M. L., & Hartel, R. W. (2000). Effect of processing conditions on crystallization kinetics of a milk fat model system. *Journal of the American Oil Chemists' Society, 77*(11), 1177-1188. doi:10.1007/s11746-000-0184-4

Jandacek, R. J., Webb, M. R., & Mattson, F. H. (1977). Effect of an aqueous phase on the solubility of cholesterol in an oil phase. *Journal of lipid research, 18*(2), 203-210.

Jones, P. J. H., & AbuMweis, S. S. (2009). Phytosterols as functional food ingredients: Linkages to cardiovascular disease and cancer. *Current Opinion in Clinical Nutrition & Metabolic Care, 12*(2), 147-151.

Jones, P. J. H., MacDougall, D. E., Ntanios, F., & Vanstone, C. A. (1997). Dietary phytosterols as cholesterol-lowering agents in humans. *Canadian Journal of Physiology and Pharmacology, 75*(3), 217-227. doi:10.1139/y97-011

Jumaa, M., & Müller, B. W. (1998). The effect of oil components and homogenization conditions on the physicochemical properties and stability of parenteral fat emulsions. *International Journal of Pharmaceutics, 163*(1), 81-89.

Li, M., Auty, M. A., O'Mahony, J. A., Kelly, A. L., & Brodkorb, A. (2016). Covalent labelling of β-casein and its effect on the microstructure and physico-chemical properties of emulsions stabilised by β-casein and whey protein isolate. *Food Hydrocolloids*.

Lopez, C., Bourgaux, C., Lesieur, P., & Ollivon, M. (2007). Coupling of time-resolved synchrotron x-ray diffraction and dsc to elucidate the crystallisation properties and polymorphism of triglycerides in milk fat globules. *Le Lait, 87*(4-5), 459-480.

Maher, P. G., Auty, M. A. E., Roos, Y. H., Zychowski, L. M., & Fenelon, M. A. (2015). Microstructure and lactose crystallization properties in spray dried

nanoemulsions. *Food Structure, 3*(0), 11. doi:http://dx.doi.org/10.1016/j.foostr.2014.10.001

Mao, L., Xu, D., Yang, J., Yuan, F., Gao, Y., & Zhao, J. (2009). Effects of small and large molecule emulsifiers on the characteristics of b-carotene nanoemulsions prepared by high pressure homogenization. *Food Technology and Biotechnology, 47*(3), 336-342.

McClements, D. J. (2004). Protein-stabilized emulsions. *Current Opinion in Colloid & Interface Science, 9*(5), 305-313. doi:http://dx.doi.org/10.1016/j.cocis.2004.09.003

McClements, D. J. (2012). Crystals and crystallization in oil-in-water emulsions: Implications for emulsion-based delivery systems. *Advances in Colloid and Interface Science, 174*, 1-30.

McClements, D. J. (2015). *Food emulsions: Principles, practices, and techniques*. Boca Raton, FL: CRC press.

Möbius, D., Miller, R., & Fainerman, V. B. (2001). *Surfactants: Chemistry, interfacial properties, applications* (Vol. 13): Elsevier.

Moruisi, K. G., Oosthuizen, W., & Opperman, A. M. (2006). Phytosterols/stanols lower cholesterol concentrations in familial hypercholesterolemic subjects: A systematic review with meta-analysis. *Journal of the American College of Nutrition, 25*(1), 41-48.

Norton, J. E., & Fryer, P. J. (2012). Investigation of changes in formulation and processing parameters on the physical properties of cocoa butter emulsions. *Journal of Food Engineering, 113*(2), 329-336.

Ostlund, R. E. (2002). Phytosterols in human nutrition. *Annual Review of Nutrition, 22*(1), 533-549.

Ostlund, R. E., Spilburg, C. A., & Stenson, W. F. (1999). Sitostanol administered in lecithin micelles potently reduces cholesterol absorption in humans. *The American Journal of Clinical Nutrition, 70*(5), 826-831.

Pouteau, E. B., Monnard, I. E., Piguet-Welsch, C., Groux, M. J. A., Sagalowicz, L., & Berger, A. (2003). Non-esterified plant sterols solubilized in low fat milks inhibit cholesterol absorption. *European Journal of Nutrition, 42*(3), 154-164. doi:10.1007/s00394-003-0406-6

Pradines, V., Krägel, J. r., Fainerman, V. B., & Miller, R. (2008). Interfacial properties of mixed β-lactoglobulin− sds layers at the water/air and water/oil interface. *The Journal of Physical Chemistry B, 113*(3), 745-751.

Reddy, S., & Ghosh, P. (2010). Adsorption and coalescence in mixed surfactant systems: Water− hydrocarbon interface. *Chemical Engineering Science, 65*(14), 4141-4153.

Rosen, M. J., & Hua, X. Y. (1982). Surface concentrations and molecular interactions in binary mixtures of surfactants. *Journal of Colloid and Interface Science, 86*(1), 164-172.

Rosen, M. J., & Zhou, Q. (2001). Surfactant− surfactant interactions in mixed monolayer and mixed micelle formation. *Langmuir, 17*(12), 3532-3537.

Rossi, L., ten Hoorn, J. W. S., Melnikov, S. M., & Velikov, K. P. (2010). Colloidal phytosterols: Synthesis, characterization and bioaccessibility. *Soft Matter, 6*(5), 928-936.

Rouimi, S., Schorsch, C., Valentini, C., & Vaslin, S. (2005). Foam stability and interfacial properties of milk protein–surfactant systems. *Food Hydrocolloids, 19*(3), 467-478. doi:http://dx.doi.org/10.1016/j.foodhyd.2004.10.032

Rousseau, D. (2000). Fat crystals and emulsion stability — a review. *Food Research International, 33*(1), 3-14. doi:http://dx.doi.org/10.1016/S0963-9969(00)00017-X

Rubingh, D. N. (1979). Mixed micelle solutions *Solution chemistry of surfactants* (pp. 337-354): Springer.

Santas, J., Codony, R., & Rafecas, M. (2013). Phytosterols: Beneficial effects. In K. G. Ramawat & J.-M. Mérillon (Eds.), *Natural products* (pp. 3437-3464): Springer Berlin Heidelberg.

Sünder, A., Scherze, I., & Muschiolik, G. (2001). Physico-chemical characteristics of oil-in-water emulsions based on whey protein–phospholipid mixtures. *Colloids and Surfaces: Biointerfaces, 21*(1–3), 75-85. doi:http://dx.doi.org/10.1016/S0927-7765(01)00186-2

Thivilliers, F., Laurichesse, E., Saadaoui, H., Leal-Calderon, F., & Schmitt, V. (2008). Thermally induced gelling of oil-in-water emulsions comprising partially crystallized droplets: The impact of interfacial crystals. *Langmuir, 24*(23), 13364-13375.

Toro-Vazquez, J. F., Rangel-Vargas, E., Dibildox-Alvarado, E., & Charó-Alonso, M. A. (2005). Crystallization of cocoa butter with and without polar lipids evaluated by rheometry, calorimetry and polarized light microscopy. *European Journal of Lipid Science and Technology, 107*(9), 641-655.

Waninge, R., Walstra, P., Bastiaans, J., Nieuwenhuijse, H., Nylander, T., Paulsson, M., & Bergenståhl, B. (2005). Competitive adsorption between β-casein or β-lactoglobulin and model milk membrane lipids at oil−water interfaces. *Journal of Agricultural and Food Chemistry, 53*(3), 716-724. doi:10.1021/jf049267y

Wilde, P. J., & Clark, D. C. (1993). The competitive displacement of β-lactoglobulin by tween 20 from oil-water and air-water interfaces. *Journal of colloid and interface science, 155*(1), 48-54.

Wüstneck, R., Krägel, J., Miller, R., Wilde, P. J., & Clark, D. C. (1996). The adsorption of surface-active complexes between β-casein, β-lactoglobulin and ionic surfactants and their shear rheological behaviour. *Colloids and Surfaces A: Physicochemical and Engineering Aspects, 114*, 255-265.

Zawistowski, J. (2010). 17 tangible health benefits of phytosterol functional foods. *Functional Food Product Development, 2*.

Zhou, Q., & Rosen, M. J. (2003). Molecular interactions of surfactants in mixed monolayers at the air/aqueous solution interface and in mixed micelles in aqueous media: The regular solution approach. *Langmuir, 19*(11), 4555-4562.

Zychowski, L. M., Logan, A., Augustin, M. A., Kelly, A. L., Zabara, A., O'Mahony, J. A., Conn, C. E., & Auty, M. A. (2016). Effect of phytosterols on the crystallization behavior of oil-in-water milk fat emulsions. *Journal of Agricultural and Food Chemistry, 64*(34), 6546–6554.

Chapter 4

The crystallisation behaviour of phytosterols in bulk milk fat

Lisa M. Zychowski[†§‡#], Amy Logan*[‡], Mary Ann Augustin[‡], Alan L. Kelly[§], James A. O'Mahony[§], Charlotte E. Conn[#], Mark A. E. Auty*[†]

[†] Food Chemistry and Technology Department, Teagasc Food Research Centre, Moorepark, Fermoy, Co. Cork, Ireland

[§] School of Food and Nutritional Sciences, University College Cork, Cork, Ireland

[‡] CSIRO Food and Nutrition, Werribee, Victoria 3030, Australia

[#] School of Applied Science, RMIT University, Melbourne, Victoria 3000, Australia

Abstract

Although the use of phytosterols in dairy based-products is common, limited research has been performed on how phytosterols crystallise within milk fat. In this study, milk fat was enriched with phytosterols at 0, 3, and 6%. These phytosterol-enriched matrices were then studied during the initial crystallisation process, immediately after melting, and being stored for at 4°C for 48 h using synchrotron X-ray diffraction, differential scanning calorimetry, and polarised light microscopy. Phytosterols did not impact milk fat nucleation, but were able to insert themselves within the milk fat triple-chain length (3L) triacylglycerol network during initial crystallisation. After storage, the α network rearranged into a more tightly packed β polymorphic system, and phytosterols were no longer found within the milk fat crystalline network. However, the number and intensity of phytosterol crystalline peaks observed in the X-ray diffraction patterns were greater after storage, and large crystalline structures were observed under polarised light images. This information is useful in understanding the fundamental crystallisation behaviour of phytosterols in milk fat and can be utilised by the functional food industry in the development of phytosterol-enriched dairy systems.

4.1 Introduction

The production of butter dates before the Christian era, making it one of the earlier recorded foods produced by humans (Rodrigues et al., 2007). Even today butter is extremely popular, with large shortages present throughout Europe (Scotti, 2017). Although the majority of butter consumption is through its use in baked goods, butter and butter-based spreads and margarines are an indispensable product in most households. As these spreads are so commonly consumed, it is no surprise that the functional food industry has exploited this matrix for the incorporation of lipophilic ingredients and bioactives (Clifton, 2007). Examples of such products on the market include Smart Balance™ with added omega-3, Melt organics™ probiotic buttery blend, and phytosterol containing spreads such as Benecol™ (Prosperity Organic Foods, 2017). Among these functionalised spreads, the phytosterol-containing products, with their noted ability to lower LDL-cholesterol, are the most popular (Clifton, 2007).

Vegetable-based spreads are often enriched with phytosterols but research has demonstrated that phytosterol enrichment in butter can also lower LDL-cholesterol levels up to 15% (Pelletier et al., 1995). While phytosterol enriched-margarines are common, butter is still considered to have better organoleptic properties (Krause et al., 2007). However, despite popularity and proven effectiveness to lower LDL-cholesterol, there is a limited knowledge regarding the physicochemical behaviour of phytosterols in butter. Thus, this work sought to fill this knowledge gap by evaluating how phytosterols and milk fat crystallise when combined in a bulk form.

As the crystal network structure of butter is dependent on the crystallisation behaviour of the milk fat present, anhydrous milk fat was employed as a model butter-system (Wright & Marangoni, 2006). Phytosterol crystallisation was also examined, as research has demonstrated that solubilised phytosterols are more effective, at lowering LDL-cholesterol levels than crystalline phytosterols (Ostlund et al., 1999; Engel & Schubert, 2005; Shaghaghi et al., 2014). Phytosterol crystallisation was studied within an oil-in-water emulsified milk fat matrix in Chapter 2, but there is limited information characterising phytosterols crystallisation in a milk fat bulk system (Rodrigues et al., 2007).

Hence, this study investigated phytosterol crystallisation in bulk milk fat during immediately after initial crystallisation and after storage. Phytosterol crystallisation was monitored using synchrotron X-ray diffraction, DSC, and polarised light microscopy during the heating and cooling cycle employed in Chapter 2. Bulk milk fat systems, with and without phytosterols, were also studied after storage to understand how the crystallisation behaviour of phytosterols and milk fat combined changes over time.

4.2 Materials and methods

4.2.1 Materials

Crystalline phytosterols were purchased from Sigma Aldrich (Wicklow, Ireland). The main sterol present was β-sitosterol (≥70%) with residual levels of campesterol and β-sitostanol. Commercial grade anhydrous milk fat (AMF) was obtained from Marsh Dairy Products (Appendix 1; Footscray, Australia) for synchrotron and DSC analysis. Milk fat for polarised imaging was procured from Corman Miloko (Tipperary, Ireland).

4.2.2 Methods

The oil phase was prepared by heating AMF to 110˚C with continuous stirring at 300 rpm on a magnetic heating plate. Once reaching 110˚C, crystalline phytosterols were added at 3, and 6% wt/wt and stirred for 2 min, as done previously in Chapters 2 and 3. The oil was then cooled to 80°C and subsequently pipetted into a capillary or pan for synchrotron or DSC analysis, respectively. Samples were then allowed to cool statically and were either held at room temperature (as these were later re-heated to remove the prior thermal history) or stored immediately at 4°C for 48 h.

4.2.2.1 Differential scanning calorimetry

Thermal analysis was conducted on bulk oil samples using a DSC 1 STARe System (Mettler Toledo, Melbourne, Australia) and software (version 14). Approximately 19-21 mg of sample was weighed into a 40 µL aluminium pan (Mettler Toledo, part number ME-27331) and was heated and cooled as outlined in Chapter 2 and Appendix 2 to study the initial crystallisation of the sample. Samples were prepared and analysed by DSC in triplicate on two separate occasions for experimental duplication.

4.2.2.2 Synchrotron X-ray analysis

The Australian Synchrotron SAXS/WAXS beamline was used to perform scattering experiments. The camera length was set at 0.9 m with a photon flux of 14 KeV. Diffraction patterns were recorded in the small-angle ($q = 0.03-1.4$ $Å^{-1}$) and wide-angle regions ($q = 0.9-3.5$ $Å^{-1}$) using a Dectris Pilatus 1 M and a Pilatus 200 K detector, respectively. To capture initial crystallisation, samples were subjected to the cooling and heating profile described in Chapter 2. Synchrotron scans were captured during the temperature profile running for 3 s of live time with a subsequent 7 s of dead time, over a 15 mm gap, to avoid overexposing the sample.

Stored samples were measured after refrigeration at 4 ˚C for 48 h. Samples were analysed using the same camera length and flux but the diffraction patterns were recorded over $q = 0.017-1.18$ $Å^{-1}$ for SAXS measurements and $q = 0.95-3.19$ $Å^{-1}$ for the WAXS. Samples were taken from a refrigeration unit directly into a pre-cooled stage at 4 ˚C, designed by the beamline scientists at the Australian Synchrotron (Fig. 4.1). Samples were allowed to equilibrate at 4 ˚C for 10 min before 3 shots were captured on each capillary over a 15 mm gap on duplicate capillaries. Backline subtraction, Gaussian peak analysis, and the full-width at half-maximum (FWHM) was calculated on all samples as detailed previously in Chapter 2.

4.2.2.3 Polarised light

A 50 µl aliquot of sample was placed on a slide and subjected to the thermal cycle used for DSC and synchrotron diffraction. The calibrated slide was found to have immediate heat transfer and, thus, the exact cooling and heating profiles were recorded. Stored samples were heated from 4-60°C at 2 °C/min using a pre-cooled Linkam LNP heating/cooling stage (Linkam, Surry, UK). Polarised light images were captured using an Olympus BX51 microscope at 20X and using a ProgRes camera (Jenoptik, Wiltshire, UK).

4.2.2.4 Statistical analysis

Results from DSC analysis were analysed for statistical significance utilising SAS® 9.3 Software for Windows. A Post Hoc Tukey's test with a level of probability of $p<0.05$ was set as statistically significant.

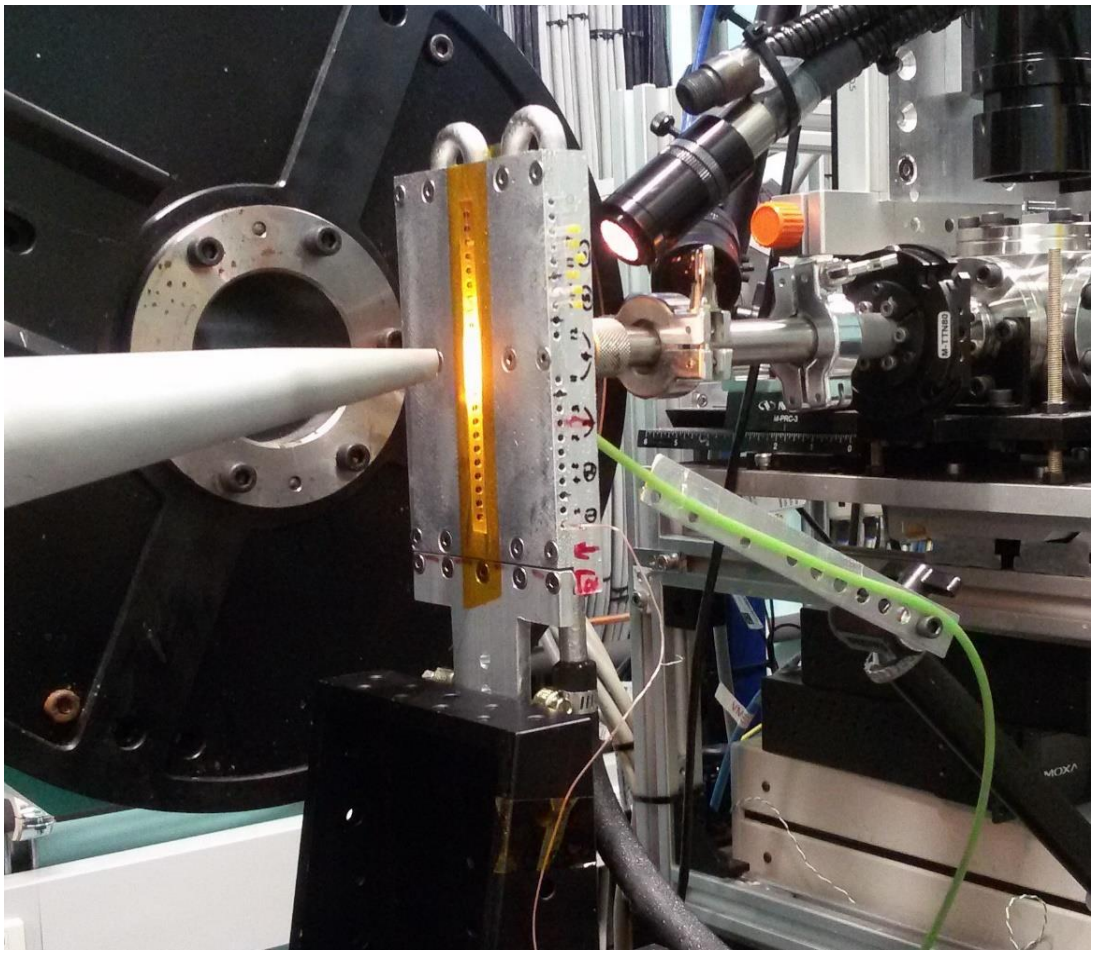

Figure 4.1 *Capillary holding cell designed by staff at the Australian synchrotron cell for temperature control.*

4.3 Results and discussion

The initial crystallisation of bulk milk fat with and without phytosterols was observed utilising synchrotron X-ray diffraction, DSC, and polarised light microscopy. Synchrotron SAXS data provided information on the formation of phytosterol crystals in the milk fat system. Figure 2.6 shows the position of the phytosterol peaks on the SAXS/WAXS diffraction patterns, which were compared against scans of bulk milk fat with and without phytosterol addition during cooling.

Upon cooling to 4 ºC and during the subsequent isothermal period (5 min at 4 ºC), the 6% phytosterol sample developed observable phytosterol crystals at 7.4 and 5.9 Å (Fig. 4.2). These two phytosterol crystals were visible after 2.5 min of holding at 4 ºC and were not seen in the 3% sample throughout the entire holding period (Fig. 4.3). Distinguishable phytosterol crystals were also confirmed during the same thermal

cycle in the emulsified counterpart of the 6% bulk phytosterol-enriched (PE) sample but were found at different positions (17.7 and 5.9 Å; Fig. 2.7 and Fig 4.2). However in the emulsified counterpart, the 3L(4) milk fat reflection was not apparent, as it is in the bulk sample, and thus this milk fat reflection is most likely inhibiting the visualisation of the phytosterol peak at 17.7 Å (Fig 2.7 & Fig. 4.4). This being stated, the phytosterol crystalline peak at 7.4 Å, found during cooling of the bulk phase was visualised in emulsions after 24 hours but was not observed during initial crystallisation in the 0.6% PE emulsion (Fig. 2.5).

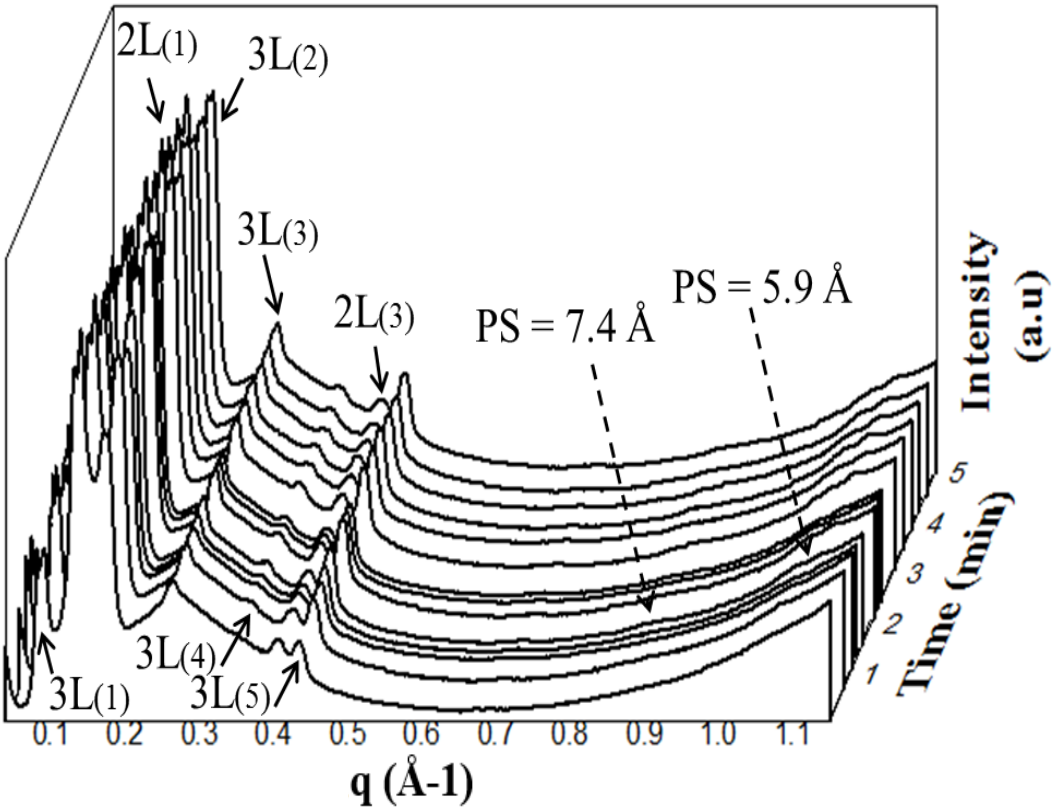

Figure 4.2 *Structural progression of the 6% PE sample during the isothermal holding period at 4 °C after cooling at -3 °C/min. Graph includes SAXS diffraction pattern with WAXS overlap to demonstrate the development of phytosterol crystals.*

The crystal present at 7.4 Å during bulk cooling could be due to the development of different types of β-sitosterol crystals at different rates. The phytosterol powder used in this study contains several β-sitosterol polymorphs, i.e., hemihydrated, anhydrous, and/or monohydrated crystals (von Bonsdorff-Nikander et al., 2003; Moreno-Calvo et al., 2014).There is limited water within the 6% bulk milk fat system, as compared to its emulsified counterpart; thus it is possible this could make the generation of an anhydrous and/or monohydrated phytosterol crystal occur at faster rate than in the emulsified state (Kawachi et al., 2006; Rossi et al., 2010).

Another element that differed from the emulsified state was the lamellar milk fat TAG matrix. In the emulsified state only 3L packing was apparent, but in the bulk state the 3L packing was seen along with a 2L structure. Previous work by others conducted on other milk fat systems also showed development of both the 2L and 3L packing with an α polymorph upon cooling at 1 ºC/min (Lopez et al., 2006). However, this variety of 2L (~45 Å) packing in milk fat is thought to be unstable and this is perhaps explains why this length of 2L packing was not visible during initial emulsion crystallisation, as the 3L packing was favoured (Lopez et al., 2002).

The positions of 3L and 2L peaks were also analysed and calculated, as an average from the 10 synchrotron shots taken at the end of the isothermal period (Table 4.1). In the 3L TAG packing, the addition of phytosterols was found to increase the long spacing or length of the lamellar phase, but did not change the parameters of the overall α polymorph (Fig. 4.3). This increase in 3L packing was also observed in the emulsified counter-part of these bulk systems during initial crystallisation, as described in detail earlier (Fig. 2.7). What is most interesting to note here is that the α 2L lamellar structures did not expand upon phytosterol addition. The FWHM of the first 3L peak increased between the control and PE samples, similar to that viewed within the emulsified system (Table 4.1 & Fig. 2.7); however, the FWHM was broader in the 3% enriched system compared to the 6% system, indicating a more disordered arrangement at lower phytosterol concentration. These trends of milk fat long spacing and FWHM were not observed in the β 2L (~39.5 Å) structure formed after storage (Table 4.1).

Table 4.1 Synchrotron diffraction results as a function of crystallisation treatment and phytosterol enrichment. Bulk milk fat samples were evaluated during initial crystallisation at the end of the isotherm at 4 ºC (Initial cry) or after storage for 48 hr at 4 ºC (After storage).

Sample treatment	Lamellar arrangement	MF long spacing (Å)	FWHM	PS peaks
0% PS Initial cry	$3L_{(1)}$	71.8	7.76E-03	---
	$3L_{(2)}$	35.9	7.85E-03	
	$2L_{(1)}$	45.2	1.09E-02	
3% PS Initial cry	$3L_{(1)}$	72.2	8.28E-03	---
	$3L_{(2)}$	36.1	8.05E-03	
	$2L_{(1)}$	45.0	1.07E-02	
6% PS Initial cry	$3L_{(1)}$	72.4	8.14E-03	6,7
	$3L_{(2)}$	36.2	8.06E-03	
	$2L_{(1)}$	44.8	9.71E-03	
0% PS After storage	$2L_{(1)}$	39.4	1.06E-02	---
3% PS After storage	$2L_{(1)}$	39.5	1.03E-02	2,4,6,7,9,10
6% PS After storage	$2L_{(1)}$	39.5	1.01E-02	1,2,3,4,5,6,7,8,9,10

PS peaks correspond as follows 1=35.6 Å; 2=17.7 Å; 3=11.7 Å; 4=9.67 Å; 5= 8.8 Å; 6=7.4 Å; 7=5.9 Å; 8=5.2; 9=4.8; 10=4.7.

Samples were also measured using DSC during the thermocycle to see if phytosterols influenced milk fat crystalline behaviour in bulk systems. During crystallisation at 3 ºC/min, phytosterols were not found to significantly influence the milk fat crystallisation temperature (Fig. 4.5a & Table 4.2). Unlike in emulsion systems, bulk milk fat systems, with or without added phytosterols, all began crystallisation at ~18 ºC and followed the same pattern throughout. Within the emulsified system, the 0.3% PE crystallised first, followed by the control and then the 0.6% PE emulsion sample (Fig 2.4).

The differences between the phytosterol concentration and order of crystallisation could be driven by two separate mechanisms. Firstly, the type of phytosterols formed initially within the emulsion could be different than what is observed within the bulk phase, as discussed previously. Secondly, dispersing the bulk lipid into an emulsion

droplet decreases the localised volume of lipid with each droplet. Thus, any impurities present within the bulk are now spread between a large quantity of dispersed droplets. Bulk phase impurities could be obscuring any differences in milk fat nucleation patterns resulting from phytosterol addition. Similar results were seen in emulsified and bulk milk fat matrices enriched with β-carotene. Bulk milk fat was found to crystallise at 17.6 ºC regardless of β-carotene addition, but the crystallisation behaviour of the emulsified milk fat containing β-carotene differed between samples and was found to nucleate at different temperatures, depending on β-carotene concentration (Zhang et al., 2013).

The thermal output captured during the isothermal period showed a higher release of energy in both the 3 and 6% PE bulk milk samples compared to the control (Fig. 4.5b). This exothermic event could be due to phytosterol crystal development, although disguisable crystals were not visible in the 3% synchrotron scan, yet this could be due to decreased X-ray diffraction intensity at lower phytosterol concentrations (von Bonsdorff Nikander et al., 2003; Fig. 4.3). During melting, the 6% PE sample had a slightly different DSC pattern compared the 3% PE and control sample, with one less defined peak (peak 3) and had two observable phytosterol peaks present in synchrotron diffraction scans (Fig. 4.4). This confirms that phytosterol crystals formed during the isothermal period within the 6% PE sample and their presence did not influence the nucleation temperature of the bulk milk fat.

A second objective of this study was to evaluate the differences in the PE milk fat matrices after storage, as opposed to immediately after cooling. Upon storage, the bulk milk fat TAG rearranged into more stable β' and β polymorphic forms (Fig. 4.6); this is compared to the predominantly α confirmation found immediately after cooling in the bulk milk fat with and without phytosterol (Fig. 4.3). In addition, only the 2L TAG packing peaks were observed after storage, compared to the 3L and 2L mixture found upon initial crystallisation (Fig 4.6 & Fig. 4.3).

The polymorphs are classified by packing and organisation, with the α polymorph having the largest spaces between repeating units and the most disorganised structure. Conversely, β maintains the tightest packing of the three polymorphs, with β' possessing an intermediate TAG packing (Sato, 2001). The packing density correlates to the Gibbs free energy (*G*) of each polymorph, with the *G* values being the highest

in the α-polymorph. Thus over time, TAG molecule rearrange themselves into a tighter lamellar spacing and polymorphs to produce a more stable system (Sato, 2001; Widlak et al., 2001). Hence, one would expect both β' and β polymorphs to occur in crystallised milk fat upon storage. The observed milk fat polymorphic transformation demonstrated in our work indicates that the presence of phytosterols did not prevent formation of these polymorphs. This is important to note, as the addition of some compounds can slow the development of the β polymorph up to 4 months (Bunjes & Koch, 2005).

To observe how time influenced crystal formation, phytosterol diffraction patterns taken immediately after the sample was cooled to 4 ºC and were compared against samples stored at the same temperature for 48 h (Fig. 4.3 & 4.6). After storage, phytosterol crystals were found to develop into 10 separate disguisable peaks in milk fat at 6% enrichment (compared against the material control). While 10 phytosterol peaks were found in the 6% sample, only 6 out the possible 10 peaks were found to develop in the 3% sample. None of these peaks were evident in the 3% PE milk fat samples immediately upon cooling and only 2 peaks were viewed in the 6% sample, indicating that phytosterol crystal formation is time dependant and will occur at 3% enrichment. Not only was crystal formation observed during synchrotron analysis, but also captured during both initial crystallisation and upon storage using polarised light (Fig 4.7-4.9).

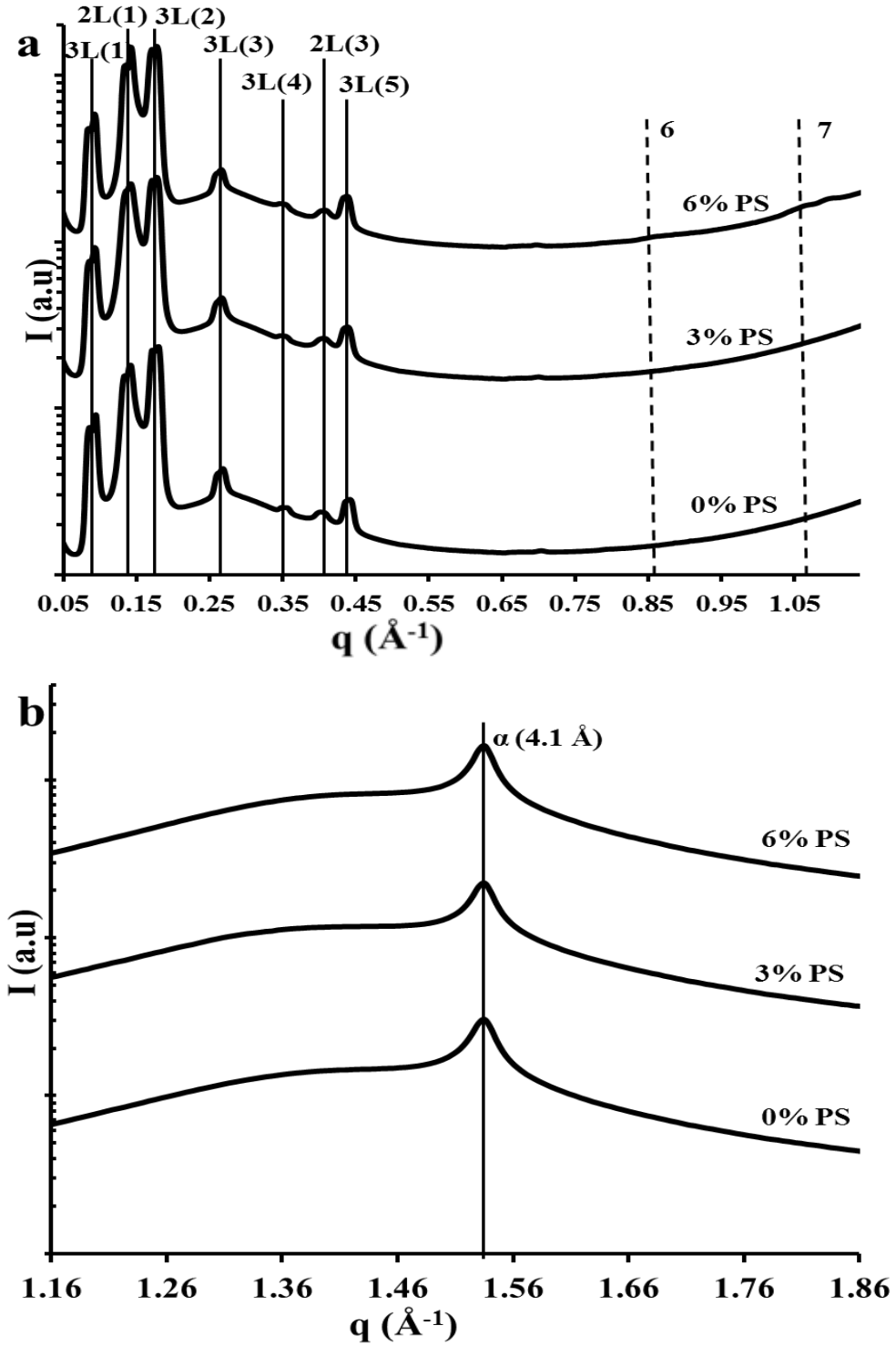

Figure 4.3 *(a) Small and (b) wide-angle synchrotron diffraction patterns captured at 4 °C after cooling at 3 °C/min for the bulk milk fat with and without phytosterol (PS) addition. Values are averaged from the last min of the 5 min isotherm after equilibrium was reached.PS peaks correspond to the following 6=7.4 Å; 7=5.9 Å.*

Table 4.2 Thermal parameters calculated from DSC thermographs during the heating and cooling cycle of bulk milk fat with or without phytosterol (PS)

Sample	Tonset T (˚C)	Peak 1 (˚C)	Peak 2 (˚C)	Peak 3 (˚C)	Endset	Δ H (J g^{-1})
Cooling (-3˚C/min)						
0% PS	19.0 ± 0.1^{a}	16.9 ± 0.2^{a}	9.8 ± 0.2^{ab}	---	---	15.9 ± 0.9^{a}
3% PS	18.1 ± 0.2^{a}	16.7 ± 0.2^{a}	9.6 ± 0.1^{b}	---	---	14.8 ± 1.0^{a}
6% PS	18.7 ± 0.1^{b}	17.2 ± 0.2^{a}	10.1 ± 0.1^{a}	---	---	14.3 ± 0.4^{a}
Heating (10˚C/min)						
0% PS	5.7 ± 0.6^{a}	12.3 ± 0.2^{a}	16.4 ± 0.1^{a}	21.3 ± 0.2^{a}	37.4 ± 0.5^{a}	-38.8 ± 4.6^{a}
3% PS	5.8 ± 1.0^{a}	12.4 ± 0.1^{a}	16.8 ± 0.1^{a}	21.6 ± 0.2^{a}	38.0 ± 0.1^{a}	-38.1 ± 5.2^{a}
6% PS	5.3 ± 0.1^{a}	11.0 ± 0.1^{b}	16.3 ± 0.1^{a}	---	38.2 ± 0.1^{a}	-35.2 ± 0.6^{a}

Tonset corresponds to the start of both crystallisation and melting profiles for emulsions, ΔH corresponds to the total change in enthalpy during the heating or cooling profile, Superscript letters denote significant differences in Tukey's Post Hoc Test with a $p<0.05$

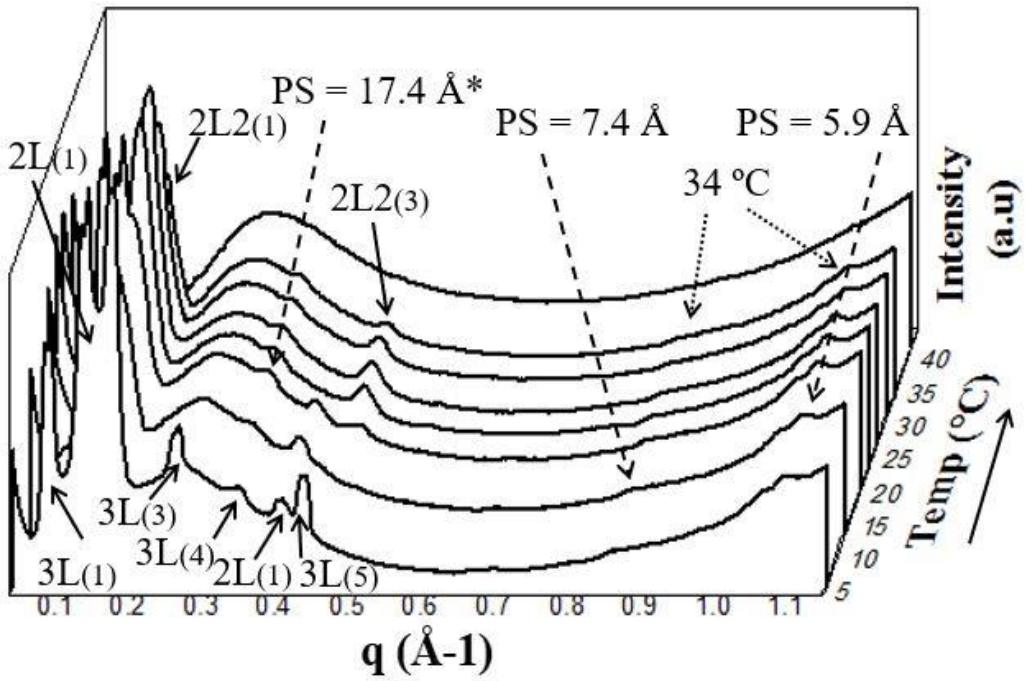

Figure 4.4 Structural evolution of the 6% PE bulk milk sample during the heating ramp from 4 °C. Graph includes SAXS diffraction pattern with WAXS overlap to demonstrate the loss of phytosterol crystallisation peaks at 34 °C.*Represents a possible phytosterol crystalline peak, which was previously hidden by the milk fat 3L(04) before melting.

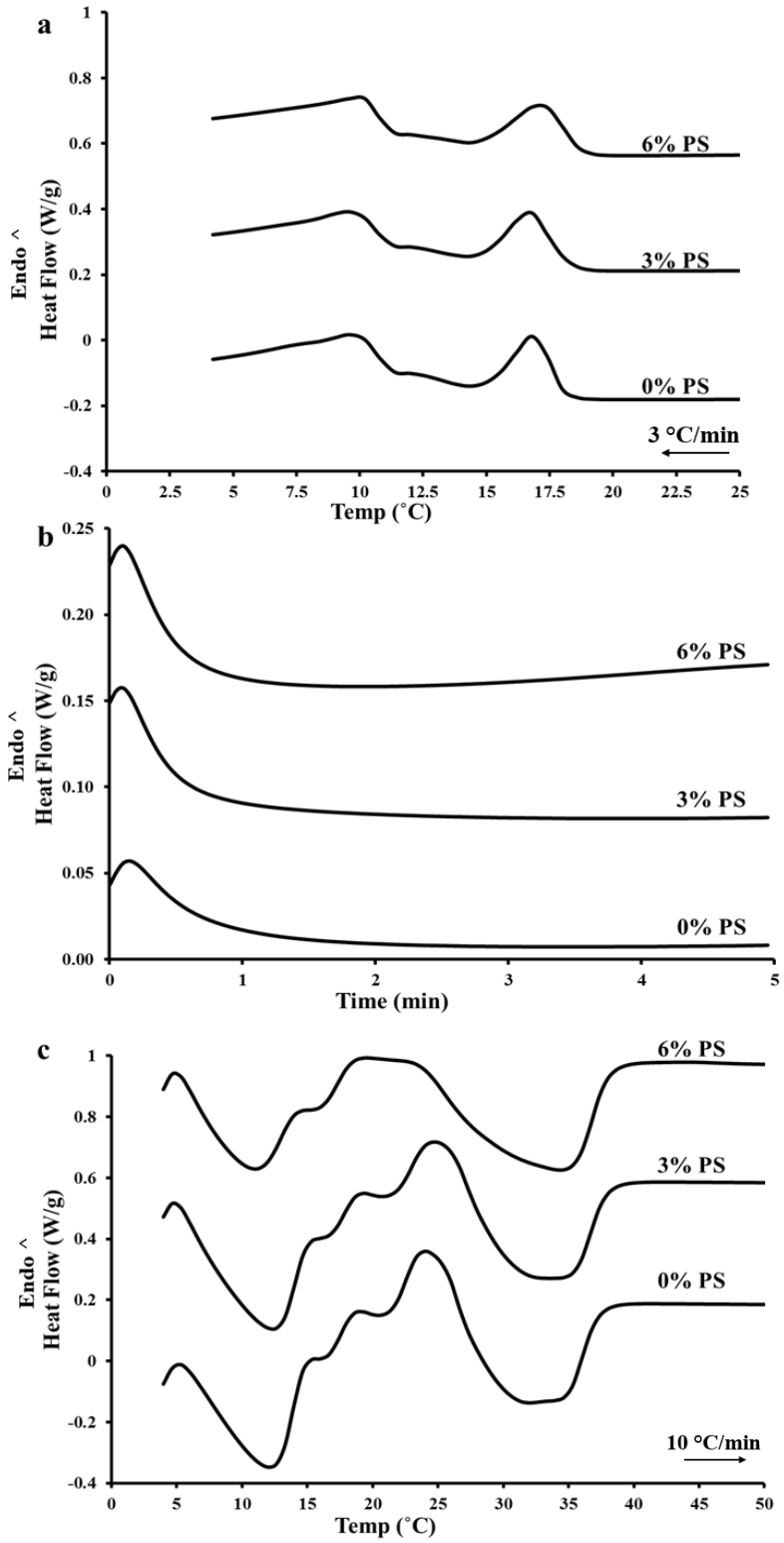

Figure 4.5 *DSC thermographs of bulk milk fat samples with 0, 3, and 6% phytosterol during the (a) cooling, (b) isothermal and (c) heating cycle.*

Micrographs were taken during the cooling process, and all milk fat samples with and without phytosterols were found to crystallize around 18 ºC, as previously observed through the DSC measurements (Table 4.2 & Fig. 4.7). In addition, there were no recognisable difference between the control and phytosterol enriched milk fat systems during initial TAG network crystallisation (Fig 4.7). The network that developed during the initial stages of crystallisation was extremely fine in structure (Fig. 4.7), especially in comparison to the courser and more diffuse crystal network exhibited by the samples that were stored for 48 h (Fig 4.9). After 48 h of storage, large spherulites formed, along with detectable phytosterol crystals in 3 and 6% PE samples (Fig. 4.9). The large spherulites are most likely milk fat TAG, and their change in appearance is due to the TAG crystals having sufficient time to grow and rearrange into more stable microstructures, as described previously (Wright et al., 2000; Wright & Marangoni, 2006). Similar results have been observed in polarised light images of milk fat quenched to 4 °C, opposed to samples crystallised slowly to 25 °C. In this study, samples which had been crystallised at the higher temperature formed larger spherulites, as they had a longer period of time to form into more stable microstructures compared to those rapidly crystallised at 4 °C (Wright et al., 2000).

It is worth highlighting that observed differences in synchrotron diffraction were comparable to the micrographs of phytosterol milk fat networks as a function of temperature. Differences in the melting of phytosterol crystals were observed between the samples heated immediately upon cooling to 4 ºC and those which were held at 4 ºC for 48 h prior to heating. A small amount of birefringence was apparent at 30 ºC in the 6% PE sample heated immediately after the 5 min isothermal period, but by 40 ºC no noticeable crystals were left indicating that the melting of phytosterol crystals was complete prior to 40 ºC (Fig. 4.8). Similar results were observed in the SAXS/WAXS diffraction pattern, where the last phytosterol crystals in the 6% PE bulk sample in the initially crystallised sample were observed at 34 ºC (Fig. 4.4).

On the other hand, SAXS patterns for the 6% phytosterol enriched bulk sample, stored for 48 h, had 10 phytosterol peaks and visible birefringence present in micrographs at ≥ 40 ºC, which finally melted at 55 ºC (Fig 4.9). In the 3% PE sample, fewer phytosterol peaks were diffracted in synchrotron patterns than in the 6% sample, and smaller phytosterol crystals were evident in polarised light images (Fig. 4.6 and Fig. 4.9). Also during melting, no crystals were detectable in the 3% stored bulk sample at

40 ºC (Fig 4.9). Thus, a lower melting temperature was required in the 3% sample (between 20 to 30 ºC) to eliminate birefringence, compared to the 6% sample (between 30 to 40 ºC). This indicates that less energy was required to melt the phytosterol crystals at lower phytosterol concentrations, and thus fewer crystals formed. Similar results were seen by Singh et al. (2009) who evaluated β-sitosterol systems mixed with organzol and found an increase in the melting temperature of the system with phytosterol fraction concentration.

The differences between the stored and initial crystallised phytosterols PE samples demonstrates that the phytosterol crystal network continues to develop further with storage. Furthermore, the quantity of phytosterol peaks present can provide some indication of how developed the phytosterol network is within the TAG system. Phytosterols were not found to interrupt milk fat crystallisation transitions over storage, and phytosterol insertion was found to only occur within the α 3L lamellar spacing and not within the α or β 2L system.

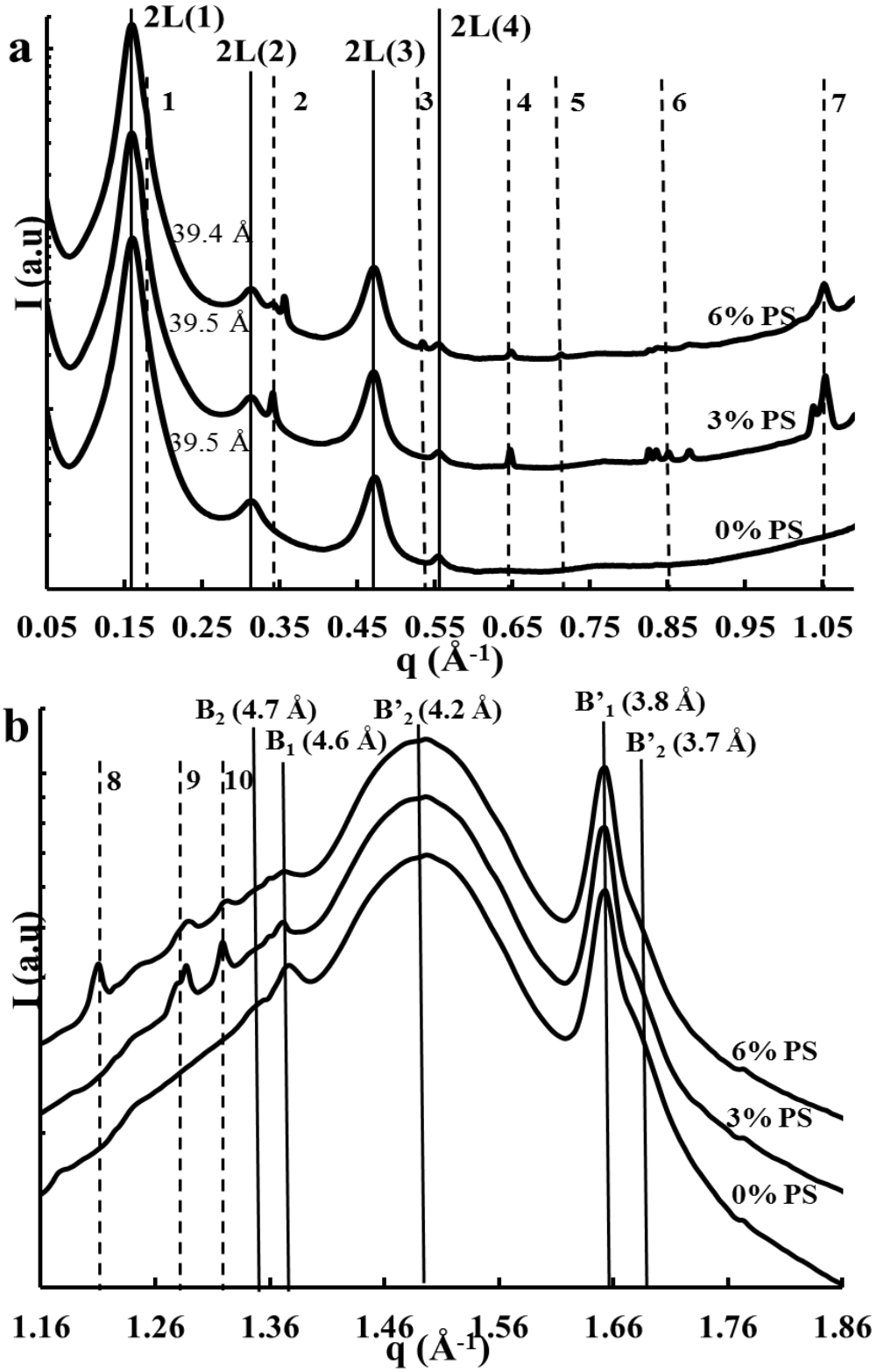

Figure 4.6 *(a) Small and (b) wide-angle synchrotron diffraction patterns of bulk milk fat with 0,3 and 6% PS. Diffraction patterns were captured after 48h of storage at 4 °C. Phytosterol peaks are shown by the dotted lines and correspond to the following distances:1=35.6 Å; 2=17.7 Å; 3=11.7 Å; 4=9.7 Å; 5= 8.8 Å; 6=7.4 Å; 7=5.9 Å; 8=5.2 Å; 9=4.8 Å; 10=4.7 Å.*

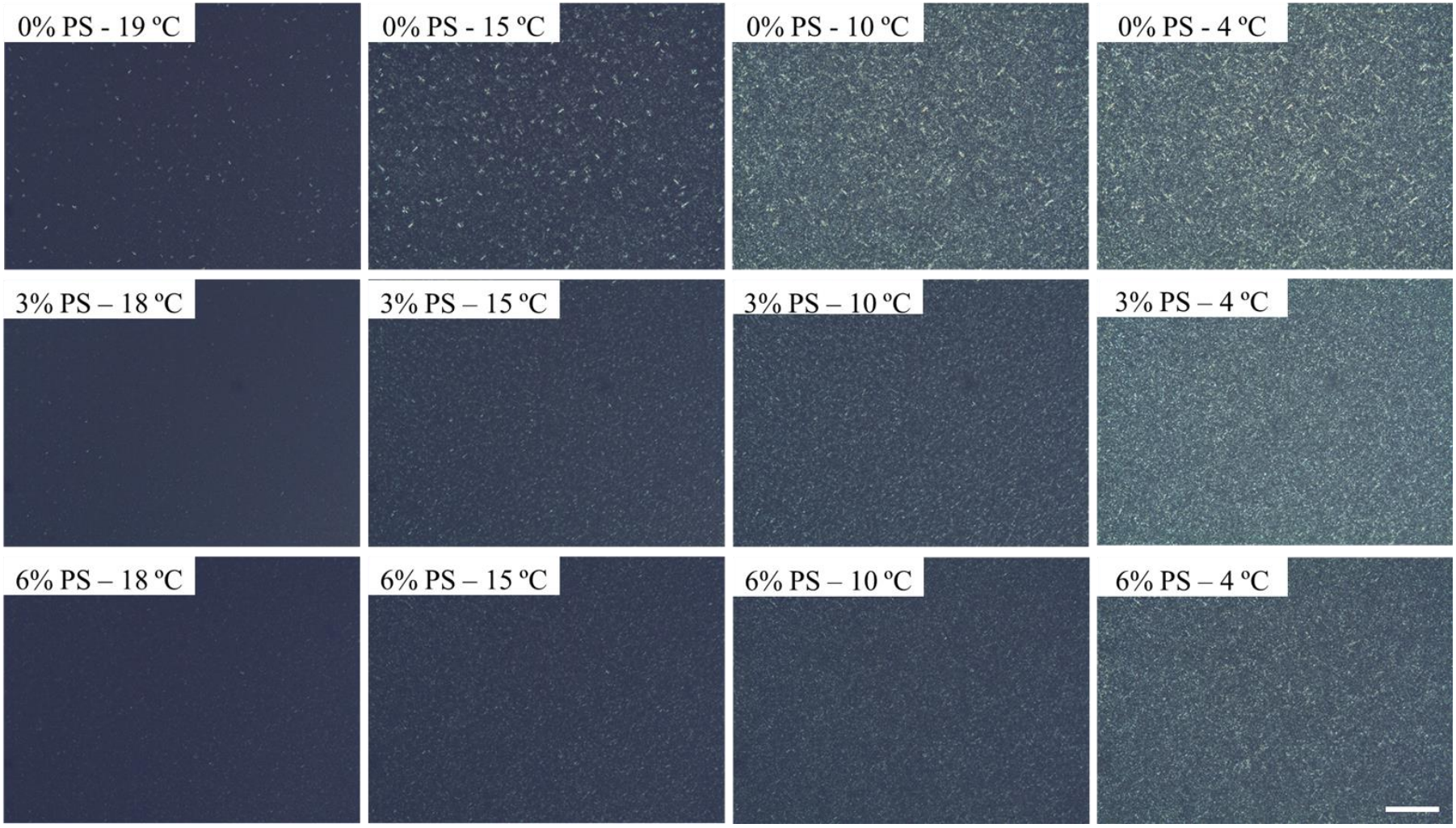

Figure 4.7 *Polarised light micrographs (partially uncrossed polar filters) of bulk milk fat during cooling at 3 ºC/min with 0, 3, and 6% phytosterol (PS). Scale bar=10 µm*

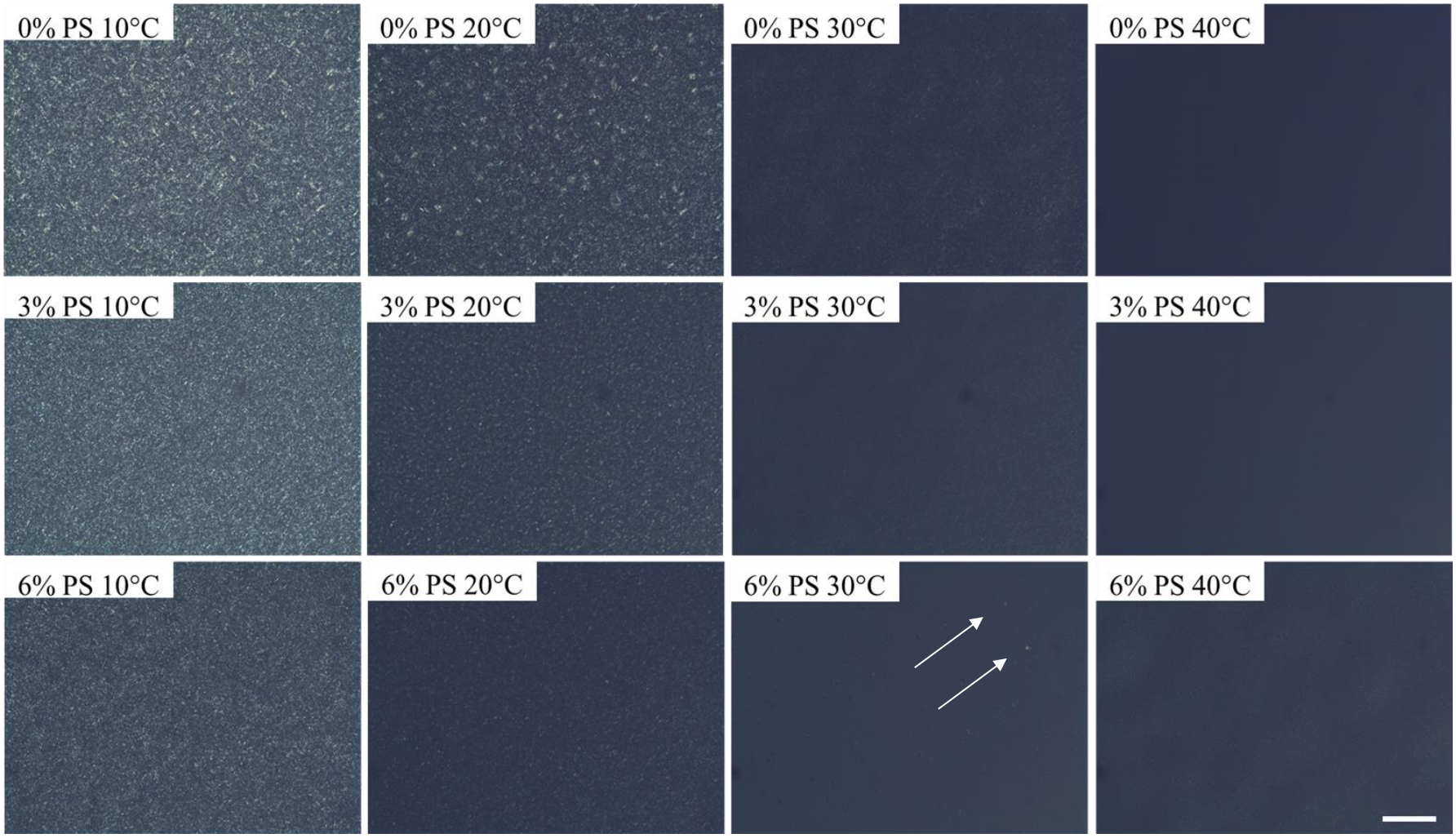

Figure 4.8 *Polarised light micrographs (partially uncrossed polar filters) of bulk milk fat with 0, 3, and 6% phytosterol. Samples are shown during heating at 10 ºC/min after initial crystallisation at -3 ºC /min and a 5 min isothermal hold period. White arrows show residual birefringence present in sample. Scale bar=10 µm*

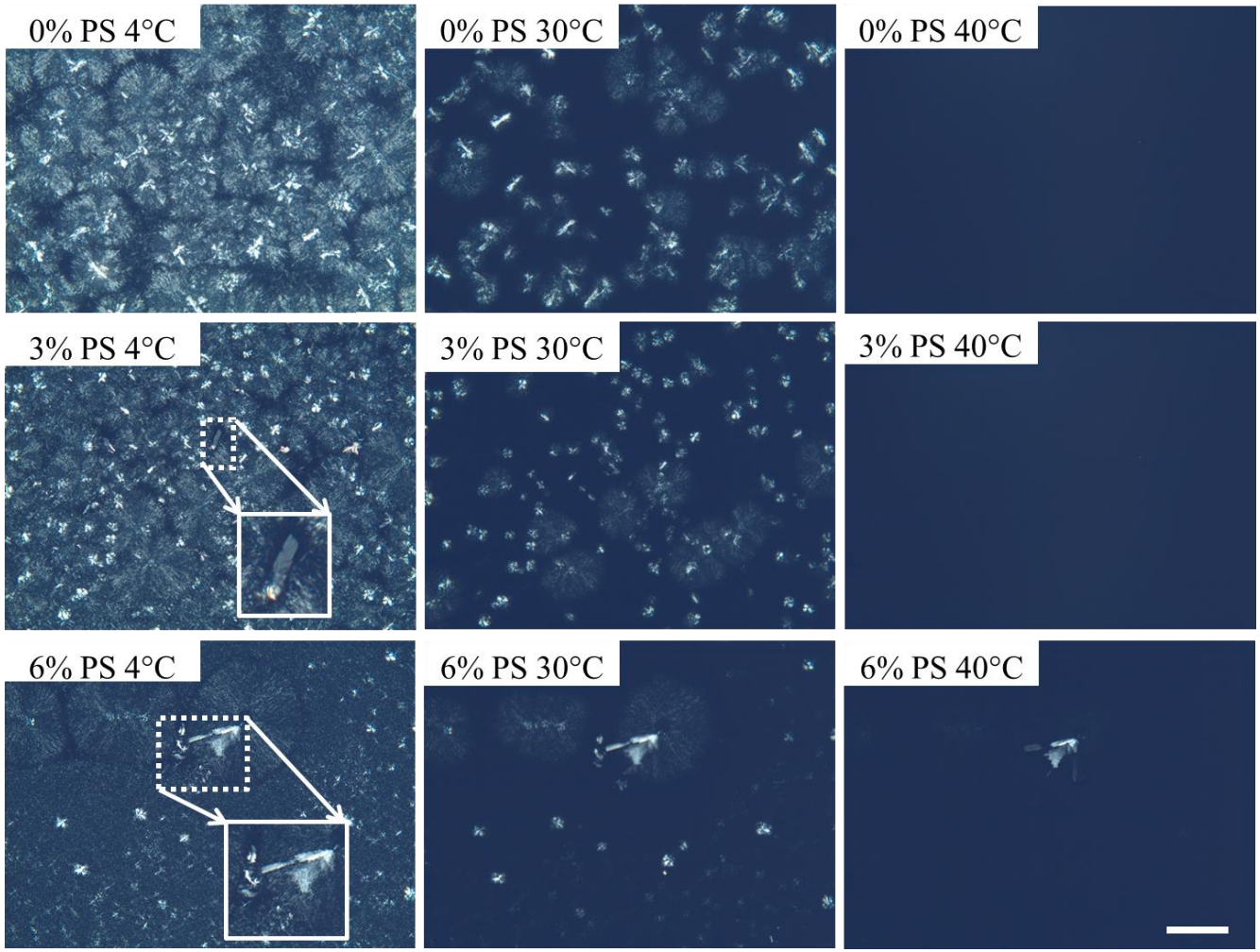

Figure 4.9 Polarised light micrographs (partially uncrossed polar filters) of bulk milk fat with 0, 3, and 6% phytosterol. Samples are shown during heating at 2 ºC/min after 48 h of storage at 4 ºC. White boxes show phytosterol crystals present within the sample. Scale bar=10 µm

4.4 Conclusions

This study examined how phytosterol crystallisation occurs within bulk systems and how it changes with storage. Bulk systems with phytosterols were monitored during initial crystallisation and after storage using DSC, polarised light, and synchrotron X-ray diffraction. Phytosterols were found to insert themselves within the 3L lamellar layer, as seen within the emulsion system, but the change in TAG packing length did not alter the α polymorph. Although phytosterol enrichment was not found to influence the rate of initial nucleation, phytosterol crystals still formed during the cooling process and were able to create a network over time. Phytosterol crystals were found to develop two diffraction peaks within the 6% PE sample during initial crystallisation. After storage, the 6% PE milk fat was found to possess 10 different phytosterol crystalline peaks, compared to the 3% sample which had 6. The 6% PE sample, that was heated immediately after crystallises at 4°C, lost all of its phytosterol and milk fat crystal by 40 °C. However, the 6% sample that had been stored for 48 h still possessed phytosterol crystals at temperatures of ≥ 40 °C. These differences show that the phytosterol crystal network does indeed develop further with storage, as a higher temperature was required to melt the phytosterol crystals present.

References

Bunjes, H., & Koch, M. H. J. (2005). Saturated phospholipids promote crystallization but slow down polymorphic transitions in triglyceride nanoparticles. *Journal of Controlled Release, 107*(2), 229-243. doi:http://dx.doi.org/10.1016/j.jconrel.2005.06.004

Clifton, P. (2007). Plant sterols and stanols as functional ingredients in dairy products. In M. Saarela (Ed.), *Functional Dairy Products* (Vol. 2, pp. 255-261): Woodhead Publishing.

Engel, R., & Schubert, H. (2005). Formulation of phytosterols in emulsions for increased dose response in functional foods. *Innovative Food Science & Emerging Technologies, 6*(2), 233-237.

Kawachi, H., Tanaka, R., Hirano, M., Igarashi, K., & Ooshima, H. (2006). Crystallization of β-sitosterol using a water-immiscible solvent hexane. *Journal of Chemical Engineering of Japan, 39*(8), 869-875.

Krause, A., Lopetcharat, K., & Drake, M. (2007). Identification of the characteristics that drive consumer liking of butter. *Journal of dairy science, 90*(5), 2091-2102.

Lopez, C., Bourgaux, C., Lesieur, P., & Ollivon, M. (2002). Crystalline structures formed in cream and anhydrous milk fat at 4 C. *Le Lait, 82*(3), 317-335.

Lopez, C., Bourgaux, C., Lesieur, P., Riaublanc, A., & Ollivon, M. (2006). Milk fat and primary fractions obtained by dry fractionation: 1. Chemical composition and crystallisation properties. *Chemistry and Physics of Lipids, 144*(1), 17-33. doi:http://dx.doi.org/10.1016/j.chemphyslip.2006.06.002

Moreno-Calvo, E., Temelli, F., Cordoba, A., Masciocchi, N., Veciana, J., & Ventosa, N. (2014). A New Microcrystalline Phytosterol Polymorph Generated Using CO2-Expanded Solvents. *Crystal Growth & Design, 14*(1), 58-68. doi:10.1021/cg401068n

Ostlund, R. E., Spilburg, C. A., & Stenson, W. F. (1999). Sitostanol administered in lecithin micelles potently reduces cholesterol absorption in humans. *The American Journal of Clinical Nutrition, 70*(5), 826-831.

Pelletier, X., Belbraouet, S., Mirabel, D., Mordret, F., Perrin, J. L., Pages, X., & Debry, G. (1995). A diet moderately enriched in phytosterols lowers plasma cholesterol concentrations in normocholesterolemic humans. *Annals of Nutrition and Metabolism, 39*(5), 291-295.

Prosperity Organic Foods, I. (2017). Introducing-new-melt-organic-probiotic-spread. Retrieved from http://www.meltorganic.com/our-products/introducing-new-melt-organic-probiotic-spread/

Rodrigues, J. N., Torres, R. P., Mancini-Filho, J., & Gioielli, L. A. (2007). Physical and chemical properties of milkfat and phytosterol esters blends. *Food research international, 40*(6), 748-755.

Rossi, L., ten Hoorn, J. W. S., Melnikov, S. M., & Velikov, K. P. (2010). Colloidal phytosterols: synthesis, characterization and bioaccessibility. *Soft Matter, 6*(5), 928-936.

Sato, K. (2001). Crystallization behaviour of fats and lipids — a review. *Chemical Engineering Science, 56*(7), 2255-2265. doi:http://dx.doi.org/10.1016/S0009-2509(00)00458-9

Scotti, A. (2017). Butter shortage is a ‘major crisis’ in Europe. *New York Daily News-World*.

Shaghaghi, M. A., Harding, S. V., & Jones, P. J. H. (2014). Water dispersible plant sterol formulation shows improved effect on lipid profile compared to plant sterol esters. *Journal of Functional Foods, 6*, 280-289.

von Bonsdorff-Nikander, A., Karjalainen, M., Rantanen, J., Christiansen, L., & Yliruusi, J. (2003). Physical stability of a microcrystalline β-sitosterol suspension in oil. *European Journal of Pharmaceutical Sciences, 19*(4), 173-179.

Widlak, N., Hartel, R. W., & Narine, S. (2001). *Crystallization and solidification properties of lipids*. Champaign, IL: The American Oil Chemists Society.

Wright, A. J., Hartel, R. W., Narine, S. S., & Marangoni, A. G. (2000). The effect of minor components on milk fat crystallization. *Journal of the American Oil Chemists' Society, 77*(5), 463-475.

Wright, A. J., & Marangoni, A. G. (2006). Crystallization and rheological properties of milk fat *Advanced Dairy Chemistry Lipids* (Vol. 2, pp. 245-291). New York, NY: Springer.

Zhang, L., Hayes, D. G., Chen, G., & Zhong, Q. (2013). Transparent dispersions of milk-fat-based nanostructured lipid carriers for delivery of β-carotene. *Journal of Agricultural and Food Chemistry, 61*(39), 9435-9443.

Chapter 5

Phytosterol crystallisation within bulk and dispersed triacylglycerol matrices as influenced by oil droplet size and low molecular weight surfactant addition

Lisa M. Zychowski[†§‡#], Amy Logan*[‡], Mary Ann Augustin[‡], Alan L. Kelly[§], James A. O'Mahony[§], Charlotte E. Conn[#], Mark A. E. Auty*[†]

[†] Food Chemistry and Technology Department, Teagasc Food Research Centre, Moorepark, Fermoy, Co. Cork, Ireland

[§] School of Food and Nutritional Sciences, University College Cork, Cork, Ireland

[‡] CSIRO Food and Nutrition, Werribee, Victoria 3030, Australia

[#] School of Applied Science, RMIT University, Melbourne, Victoria 3000, Australia

Abstract

Phytosterols can lower LDL-cholesterol and are used by the functional food industry. However, little is known regarding how phytosterol crystallisation can be controlled, despite solubilised phytosterols having improved bioaccessibility. This study investigates crystallisation of phytosterols in model dairy emulsions with whey protein as the primary emulsifier and also in bulk milk fat. Emulsions were studied at two average droplet sizes: 1.0 and 0.2 μm. The effect of lecithin and monoacylglycerol addition phytosterol crystallisation for both emulsion and bulk systems were also evaluated. Results demonstrated that lecithin and monoacylglycerols enrichment into the bulk system minimised phytosterol crystallisation. However, in emulsions, phytosterol crystallisation was mainly influenced by decreasing the droplet size. Smaller emulsion droplets containing lecithin showed the greatest potential for decreasing phytosterol crystallisation and had improved physicochemical stability. Results demonstrate how phytosterol crystallisation can be controlled in future functional food applications.

5.1 Introduction

Phytosterols are natural plant-derived compounds found within nuts, seeds, fruits, and vegetables. Phytosterols, which are found within plant cell membranes, are structurally similar to cholesterol (found in animal cell membranes) only differing in the presence or absence of a double bond and an R group at the twenty-fourth carbon (Ostlund, 2002). The structural similarities between cholesterol and phytosterols allow phytosterols to reduce absorption of cholesterol by competitive solubilisation in the low-density lipoprotein (LDL) chylomicrons, which are absorbed by the enterocyte cells in the small intestine (Rozner & Garti, 2006; Smet, Mensink, & Plat, 2012; Yi et al., 2016). Higher levels of LDL-cholesterol are associated with coronary heart disease, cerebrovascular accidents or strokes, and gallbladder stone disease (Jiang et al., 2004; Moreau, Whitaker, & Hicks, 2002).

While phytosterols have been found to be effective in lowering LDL cholesterol levels, their efficacy is limited by their compositional variety, physical state and dose (Carden, Hang, Dussault, & Carr, 2015; Clifton, 2007; Ostlund, 2002). To detect a significant decrease in LDL cholesterol levels $\geq$ 1.5 g of phytosterols needs to be consumed, which is not possible without the use of medication or functional foods. Due to the low solubility of phytosterols in oil, the hydroxyl group is normally esterified at the third carbon to improve solubility. Although esterified phytosterols are easier to formulate into food products, they have unpredictable absorption rates, leading to variations in finding from human clinical trials (Clifton, Noakes, Ross, & Nestel, 2004; Ling & Jones, 1995; Moruisi, Oosthuizen, & Opperman, 2006). This variation in absorption levels likely reflects the requirement to hydrolyse the esterified phytosterol before absorption. Phytosterol hydrolysis during digestion is subject to inter-individual variability, causing phytosterol absorption rates to vary between 40 and 96% (Carden et al., 2015; Clifton, 2007).

The efficacy of phytosterols is also limited by the physical state in which they are consumed. Solubilised phytosterols have been shown to be more effective than crystalline phytosterols at lowering LDL cholesterol (Engel & Schubert, 2005; Ostlund, Spilburg, & Stenson, 1999; Shaghaghi, Harding, & Jones, 2014). Decreasing the crystal size and degree of crystallinity has been proven to influence phytosterol

bioavailability, yet, limited research has been conducted on how to control phytosterol crystallisation within functional food systems (Ostlund, 2002; Ostlund et al., 1999).

This study seeks to reduce phytosterol crystallisation within a mixed triacylglycerol (TAG) system, which is the typical composition of most food lipids (Akoh & Min, 2008). The model TAG system chosen for the study was milk fat, which forms β polymorphs after cooling and storage. β polymorphic structures are common in foods and occur in other lipids such as palm oil, cocoa, coconut oil, and suet (Akoh & Min, 2008; Widlak, Hartel, & Narine, 2001). The process of digestion is, however, associated with extensive changes to the structure of the milk fat. During digestion the original lamellar packing of milk fat is observed to transition to more complex packings including a bicontinuous cubosome formation. The high surface area associated with these organised lipid structures may improve the bioaccessibility of bioactives dispersed within the lipid matrix (Barauskas, Johnsson, Joabsson, & Tiberg, 2005; Salentinig, Phan, Khan, Hawley, & Boyd, 2013). Promising research has also shown that milk enriched with phytosterols (1.8 g/day) using a proprietary crystal-retardation method can result in a 29.1 ± 4.1% reduction in LDL-cholesterol levels (Pouteau et al., 2003). In Chapter 2 & 4, the underlying mechanism of phytosterol crystallisation within milk fat matrices was examined (Zychowski et al., 2016). However, to date, no work has explored possible ways to decrease phytosterol crystallisation within a milk fat system.

Thus, this work seeks to decrease phytosterol crystallisation in both bulk and emulsified milk fat systems, with a concomitant increase in phytosterol bioaccessibility, by varying the formulation and processing parameters of the PE system. Milk fat formulations were produced with or without added phytosterols and/or low molecular weight surfactants, phospholipids from lecithin or monoacylglycerol (MAG). All lipid formulations were studied in bulk milk fat, and were emulsified with whey protein isolate at two different homogenisation pressures to create droplets approximately 1.0 or 0.2 μm in diameter. Lecithin and MAG were chosen as they have been shown to impact the formation, growth, and location of crystalline compounds within oil-in-water systems (Fredrick, Walstra, & Dewettinck, 2010; Li, Zheng, Xiao, & McClements, 2012; Rousseau, 2000; Sato, 1999). Engel and Schubert (2005) demonstrated that lecithin and MAG decrease phytosterol

crystallisation in both bulk and emulsion systems. However, in this study, detection of crystalline phytosterols was via polarised light microscopy, and their findings may therefore have been limited by the detection limits of the light microscope. As recent studies have demonstrated that phytosterol crystals can be as small as 160 nm in size, higher resolution imaging techniques and analytical tools, such as X-ray diffraction, are required to effectively quantify the level of crystallinity (Rossi, ten Hoorn, Melnikov, & Velikov, 2010).

Droplet size selection (~1.0 and 0.2 μm) was based on previous research demonstrating that milk fat-based, sub-micrometer-sized (<400 nm) emulsion droplets were successful in limiting the crystallisation of β-carotene (Zhang, Hayes, Chen, & Zhong, 2013); Results from this study will increase our fundamental understanding of the impact of droplet size and addition of surfactants on phytosterol crystallisation within bulk and emulsion systems. This information could potentially benefit the food industry in development of functional food products with increased bioaccessibility.

5.2 Materials and methods

5.2.1 Chemicals and ingredients

Crystalline phytosterol consisting of β-sitosterol (≥70%), with residual campesterol and β-sitostanol, was purchased from Sigma Aldrich (Wicklow, Ireland). Glass capillaries with a wall thickness of 0.1 mm were purchased from Charles-Supper (Natick, Massachusetts) for synchrotron analysis. Soy lecithin (Adlec) was kindly donated by Archer Daniels Midland Co. (Chicago, Illinois) and distilled monoglycerides (Dimondan® R-T Pel/B) were purchased from Danisco Australia Pty Ltd. (Banks Meadow, Australia). Whey protein isolate (WPI) (ALACEN© 895, protein content 92.0%) was obtained from Fonterra (Maungaturoto, New Zealand), sodium azide was purchased from Sigma Aldrich (Castle Hill, Australia) and commercial grade anhydrous milk fat was purchased from Marsh Dairy Product (Appendix 1; Footscray, Australia). For polarised images taken in Ireland at the National Imaging Centre, anhydrous milk fat was purchased from Corman Miloko (Carrick on Suir, Ireland).

5.2.2 Preparation of bulk and emulsion samples

Bulk anhydrous milk fat was combined with or without lecithin or MAG at 3 % wt/wt. The bulk mixture was then heated to 110 °C while stirring on a magnetic hot plate at 300 rpm. Once a temperature of 110 °C was achieved, phytosterols were added at 3 and 6% and the mixture was stirred for 2 min. A bulk mixture of each formulation without phytosterols was also made and was subjected to the same thermal and shear treatment. After the holding period, the oil was cooled to 80 °C before loading into capillaries or glass slides for synchrotron analysis or polarised light microscopy, respectively. Samples were then allowed to cool statically to 4 °C and held at this temperature for 48 h.

Oil-in-water emulsions (10% oil: 1% protein: 89% H_20) were prepared by homogenising the described milk fat-based formulations with an aqueous protein phase. The aqueous phase was created by reconstituting whey protein isolate (WPI) at 11.11% protein with stirring at 600 rpm in an ice bath. After 2 h, the solution was then refrigerated at 4 ˚C overnight to allow for complete hydration. Before homogenising the two phases, aliquots of WPI solution were heated to 55 ˚C for 20 min. After heating, the WPI solution was mixed with Milli-Q water at 70 ˚C to create a 1 % protein solution. This process, as employed previously, was utilised to minimise denaturation of the whey protein caused by excessive heating or high temperatures (McClements, 2004; Zychowski et al., 2016).

The two phases were first combined into a pre-emulsion utilising a Silverson rotor-stator mixer set at 3200 rpm for 1 min. The mixture was then homogenised with an EmulsiFlex-C5 (Avestin, Mannheim, Germany) with two different processes. Larger emulsion droplets (~1.0 µm in average diameter) were generated with 1 pass at 300 bar pressure, while smaller droplets (~0.2 µm in average diameter) required 3-5 passes (depending on the formulation) at 1000 bar (Figure 5.1). All emulsions were homogenised at 60 ˚C and then cooled and stored at 4 ˚C. After cooling, 0.02% of sodium azide was added to each emulsion to prevent microbial growth.

5.2.3 Synchrotron X-ray analysis

Scattering experiments were performed on the small- and wide-angle X-ray scattering (SAXS/WAXS) beamline at the Australian Synchrotron (Clayton, Australia) with a camera length of 0.9 m and a beam of wavelength λ= 0.89 Å (14.0 keV). A Dectris Pilatus 1M captured small-angle measurements (q = 0.017-1.18 $Å^{-1}$), while a Pilatus 200K detector recorded wide-angle measurements (q = 0.95-3.19 $Å^{-1}$). Samples were taken from a refrigeration unit directly into a pre-cooled capillary holder at 4 ˚C. Samples equilibrated at 4 ˚C for 10 min before SAXS and WAXS patterns were collected. A series of three, 3 s shots were taken for each emulsion in duplicate capillaries over a 15 mm gap. Snapshots of the material references were also collected on the crystalline phytosterol (with and without MilliQ water), the aqueous phase with WPI, the lecithin and MAG after storage at 4 ˚C for 24 h. The beamline was calibrated using silver behenate and all diffractions patterns of averaged shots were background-subtracted using the Australian Synchrotron SAXS/WAXS software (ScatterBrain, V2.71, Australia). Bulk and emulsion diffraction peaks were analysed utilising Gaussian peak analysis for peak distance and full-width at half-maximum as performed in Chapter 2 and 4.

5.2.4 Differential scanning calorimetry

Thermal analysis of all bulk samples was conducted using a DSC 2 STARe System (Mettler Toledo, Port Melbourne, Australia). Bulk samples were prepared as described above for synchrotron analysis, with ~19-21 mg of sample weighed into a 40 µL aluminium pan (Mettler Toledo, part number ME-27331). All sample pans were hermetically sealed and stored for 48 h at 4 °C. After storage, samples were transferred immediately to a pre-cooled pan holder to maintain temperature and loaded into the DSC chamber set to 4 °C and allowed to equilibrate for 5 min before heating from to 60 °C at 2 °C min^{-1}. This method is similar to a temperature ramp used by Truong et al. (2015), except that the heating rate was slowed from 5 °C to 2 °C min^{-1} to allow for greater resolution during the milk fat melting profile. The DSC STARe software (version 14.0) was employed to calculate the onset temperature (T_{onset}), endset (T_{endset}), along with the maximum values for each peak. The T_{onset} of the last milk fat peak was

also calculated, as it shifted due to differences in formulation. All bulk formulations were prepared and analysed in triplicate.

5.2.5 Polarised light microscopy

Bulk samples were examined using polarised light microscopy on an Olympus BX51 microscope (Olympus Corporation, Tokyo, Japan) with a 20X objective lens. Digital images were captured with ProgRes CT3 camera using Prores 2.7.7 software (Jenoptik, Wiltshire, UK). After cooling to 80 ˚C, bulk fat formulations (50 µl) were pipetted onto a glass slide and allowed to statically cool to room temperature and later stored at 4 ˚C for 48 h. Glass slides were taken directly from storage onto a pre-cooled Linkam LNP heating/cooling stage at 4 ˚C for imaging (Linkam, Surry, UK). After imaging at 4 ˚C, samples were heated at 2 °C min^{-1} to observe the melting profile of the samples. Crystalline material is birefringent under polarised light and appears bright on the micrographs (Li et al., 2012; Maher, Auty, Roos, Zychowski, & Fenelon, 2015).

5.2.6 Particle size

The particle size of the emulsion droplets was evaluated using laser light scattering on a Mastersizer 2000 instrument (Malvern Instruments Ltd., Worcestershire, UK), as described previously in Chapter 2. Particle size analysis was conducted in triplicate for each emulsion formulation.

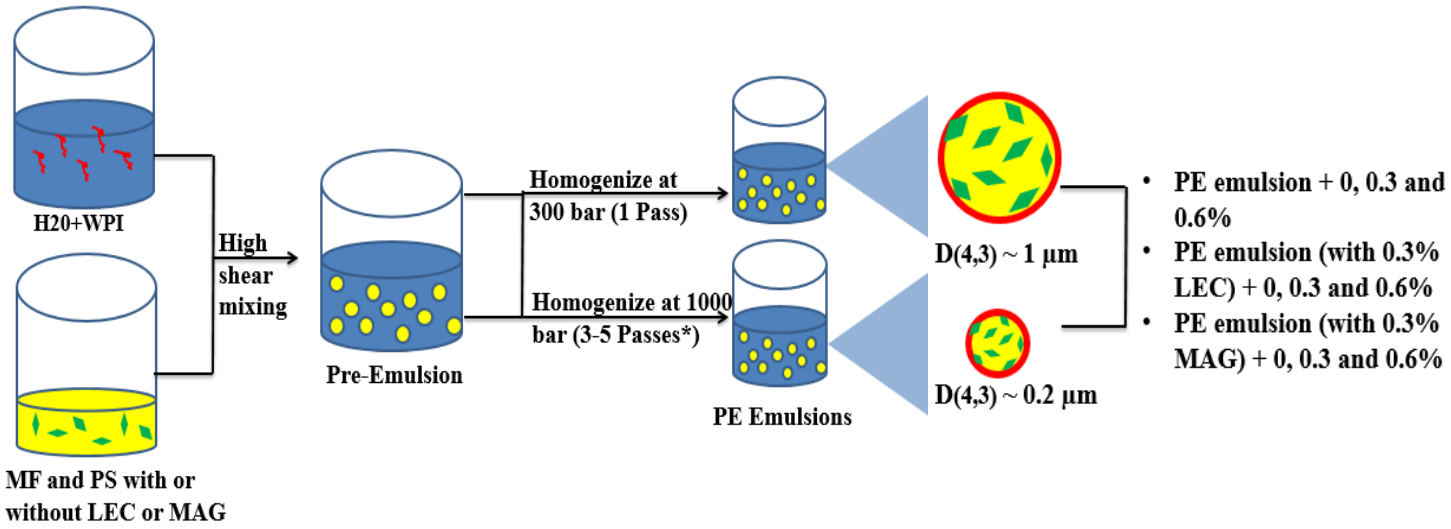

Figure 5.1 *Schematic of phytosterol-enriched (PE) emulsion sample formation (10% oil: 1% WPI: 89% H20). Whey protein (red lines) and phytosterol (PS; green triangles) are highlighted along with the milk fat (yellow). The combination above created 9 different lipid phases at two different* $D_{(4,3)}$ *particle sizes (including controls of each formulation with no phytosterols). All lipid phases were also studied in as bulk systems. *3-5 passes were utilised depending on the compound added to the lipid phase. Emulsions with whey protein, with or without phytosterols, required 4 passes, while emulsions with added lecithin (LEC) required only 3 passes and monoacylglycerol (MAG) addition resulted in 5 passes at 1000 bars to reach a* $D_{(4,3)}$ *of 0.2 µm.*

5.2.7 Optical characterisation of emulsion stability

Emulsion stability was analysed using a light-scattering optical analyser (Turbiscan MA2000, Formulaction, France) as a function of time. After cooling to 4 °C, 6 mL aliquots of each emulsion were pipetted into glass holding cells and measured for backscattering at d 0. Samples were then held at 4 °C and measured after 1-week and 1-month.Optical analysis was performed by backscattering light along the length of the glass holding cell containing the emulsion sample. This scattering data was then interpreted by a near infrared diode for the differences in optical clarity at the bottom and top of the cell, and plotted as backscattering vs. distance in the cell for each sample. Maximum backscattering values for each treatment were compared against those of day 0 to evaluate the change in emulsion stability during storage, as described in Chapter 2.

5.2.8 Statistical analysis

For analysis of emulsion and bulk formulations, mean values ± standard deviations were presented. All results were analysed utilizing SAS® 9.3 software for Windows (Cary, North Carolina). A Tukey's Post Hoc Difference Test with a level of probability at $p<0.05$ was employed to analyse significant differences between treatments.

5.3 Results and Discussion

5.3.1 The effect of lecithin or MAG on phytosterol and milk fat crystallisation within bulk systems

The structural behaviour of different bulk milk fat formulations, with and without phytosterols, was determined using synchrotron SAXS/WAXS, DSC measurements, and polarised light microscopy. Synchrotron SAXS/WAXS data was utilised to assess the presence of phytosterol crystals by comparing diffraction patterns of the bulk milk fat formulations to the crystalline phytosterol and material diffraction patterns (Fig. 5.2). Figure 5.1a shows the SAXS diffraction pattern from the bulk and emulsified milk fat. The spectrum is characteristic of a double lamellar (2L) structure, regardless of whether the milk fat is in a bulk or emulsified form, consistent with previous research (Lopez, Bourgaux, Lesieur, & Ollivon, 2002). The corresponding WAXS

(Fig 5.1b) patterns demonstrate the polymorphic structures formed by the milk fat and will be discussed in more detail below.

Spectra were also collected for phytosterol both as a dry powder and 5% wt/wt aqueous dispersion (Fig 5.2.2a-b). The crystalline phytosterol powder is most likely composed of one or more β-sitosterol polymorphs including hemihydrated, anhydrous, and/or monohydrated crystals, as observed by Moreno-Calvo et al. (2014) for a similar phytosterol mixture. When dispersed in water, fewer diffraction peaks were observed compared to the dry powder (peaks 1, 2, 6 and 7 only). The difference in phytosterol diffraction observed between the dry and aqueous dispersed powder is most likely due to the main phytosterol, β-sitosterol, maintaining only a monohydrated crystal polymorph once in contact with water (Kawachi, Tanaka, Hirano, Igarashi, & Ooshima, 2006; Rossi et al., 2010). Similar results were also observed by Christiansen et al. (2002), where X-ray diffraction patterns of β-sitosterol dispersed within oil were altered by the addition of water to the systems. As the phytosterol powder is a mixture of phytosterols, it is difficult to determine the exact phytosterol crystal varieties present within the system. However, a higher number of phytosterol peaks has previously been found to be related to a higher amount of crystalline phytosterols (von Bonsdorff-Nikander, Karjalainen, Rantanen, Christiansen, & Yliruusi, 2003)

The pure MAG powder was also evaluated to assess the presence of crystalline material within the sample under dry and aqueous dispersed conditions (Fig. 5.1.3a-b). Unlike the powdered phytosterol, the MAG powder was found to produce similar SAXS and WAXS spectra, characteristic of a lamellar phase, under both conditions, consistent with previous research (Qiu & Caffrey, 2000). Lecithin was similarly evaluated (data not shown), but produced no Bragg peaks indicating a lack of long range structural order (Widlak et al., 2001).

For mixtures consisting of milk fat and phytosterol, milk fat peaks dominated the sample spectra. At 6% phytosterol enrichment, 10 separate lattice distances could be detected from phytosterol crystals; 35.6, 17.7, 11.7, 9.7, 8.8, 7.4, 5.9, 5.2, 4.8, and 4.7 Å (Fig. 5.2 & Table 5.1). At 3% phytosterol enrichment in bulk milk fat, only 4 of the 10 phytosterol crystalline peaks observed at 6% enrichment were present, indicating that lower phytosterol concentrations can influence the number and intensity of the

phytosterol crystal peaks, as observed previously (von Bonsdorff-Nikander et al., 2003). Upon addition of both lecithin and MAG, phytosterol crystallisation was suppressed in the 3% enriched formulation, as determined by a reduction in the number and intensity of phytosterol peaks observed (Fig. 5.3). While crystal formation persisted in the 6% sample, only 8 out of the 10 phytosterol diffraction peaks were observed, potentially indicative of a reduction in the amount of crystalline phytosterols (Fig. 5.4).

This high-resolution Synchrotron SAXS data confirms the microscopy observations performed by Engel et al. (2005), which indicated that lecithin (a phospholipid) and MAG could reduce the crystallisation of phytosterols when added to a bulk TAG system by acting as a solubility aid. In nature, phospholipids associate with and help solubilise phytosterols within plant cell membranes, contributing to the fluidity of the membrane (Dufourc, 2008). The affinity of sterols with phospholipids is also applicable to mammalian cells; interactions between cholesterol and phospholipids are necessary for cholesterol solubilisation (Ohvo-Rekilä, Ramstedt, Leppimäki, & Peter Slotte, 2002). Previous work has also shown that sitostanol, the saturated form of sitosterol, can be solubilised within ultrasonicated lecithin micelles. Interestingly, these lecithin-containing sitostanol-micelles were able to reduce cholesterol ~25% more effectively in humans than the powdered crystalline sitostanol, again emphasising the importance of solubilising plant sterols before ingestion (Ostlund et al., 1999).

We suggest that, in addition to phytosterol solubilisation effects, the polar head groups of the phospholipid molecules could have influenced the development of the milk fat TAG network by means of steric hindrance. Previous work on mixtures of milk fat and lecithin demonstrated that lecithin is able to delay the induction of milk fat crystallisation (Vanhoutte, Foubert, Duplacie, Huyghebaert, & Dewettinck, 2002). Vanhoutte et al. (2002) hypothesised that phospholipids incorporate themselves within the crystallisation nuclei during the initial phase of crystallisation, blocking crystal growth, as subsequent TAG attachment is slowed by the physical presence of the bulky phospholipid molecule.

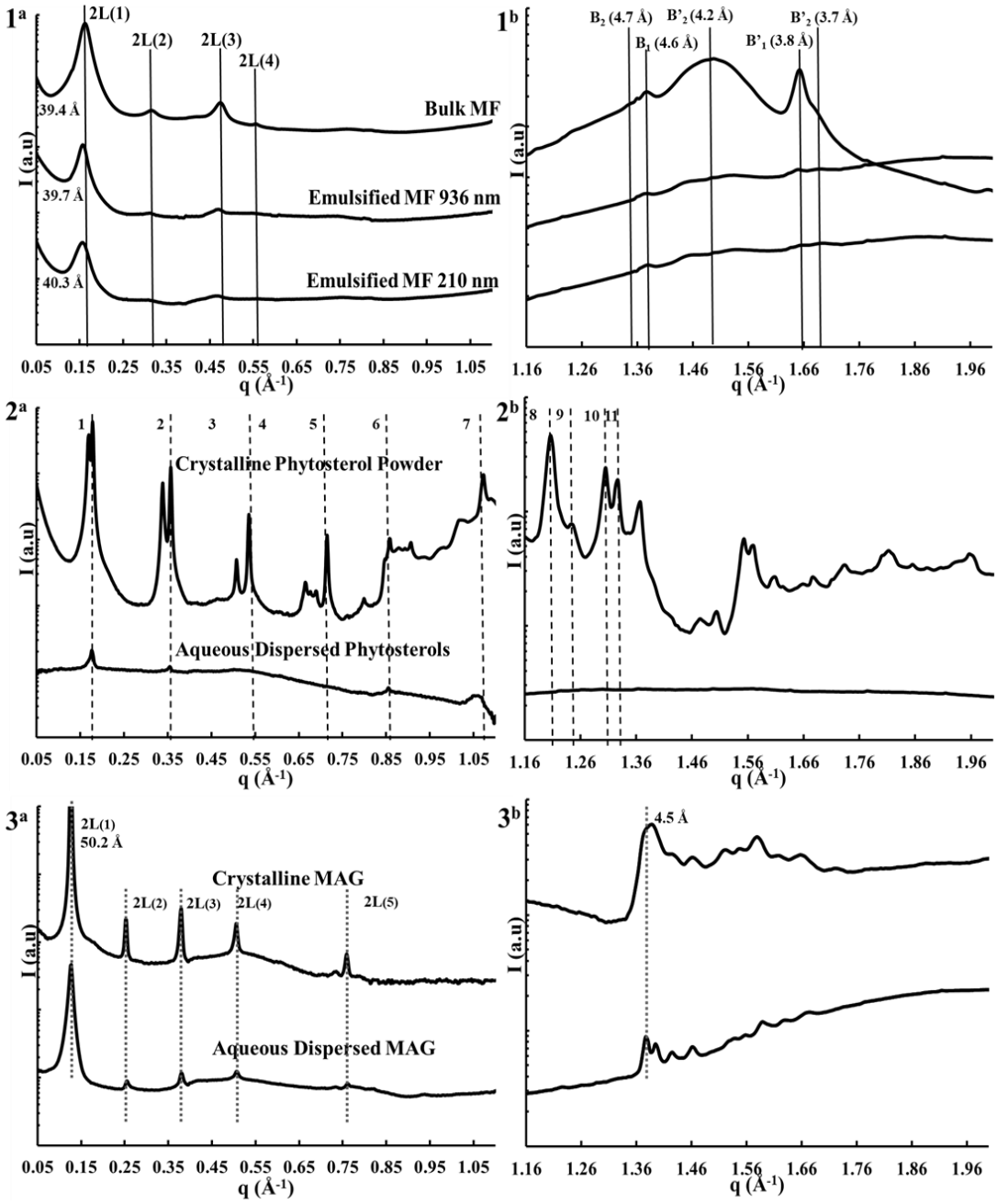

Figure 5.2 *Synchrotron (a) SAXS and (b) WAXS diffraction patterns of material references on a logarithmic scale of intensity after storage 4 °C for 24 h. Samples of (1) milk fat bulk and emulsified are included, along with crystalline and 5% (wt/wt) aqueous dispersed (2) phytosterols and (3) monoacylgylcerols (MAG). Milk fat (solid black lines), phytosterol (dashed black lines), and MAG peaks (small grey dotted lines) are distinguished by different vertical lines. The labelled peaks for phytosterols correspond to the following distances seen within formulations 1=35.6 Å; 2=17.7 Å; 3=11.7 Å; 4=9.7 Å; 5= 8.8 Å; 6=7.4 Å; 7=5.9 Å; 8=5.2 Å; 9=5.1 Å; 10=4.8 Å; 11=4.7 Å.*

Table 5.1. Synchrotron SAXS diffraction results from bulk milk fat (MF) formulations with either added lecithin (LEC), monoacylglycerol (MAG) and/or phytosterols (PS).

Formulation	PS Conc (%)	MF Long Spacing (Å)	PS peaks	T_{onset} Final Peak (°C)	Δ H (Jg^{-1})
Bulk MF	0.0	39.4	---	23.6 ± 0.13^{ab}	-67.4 ± 0.83^{ab}
	3.0	39.5	2,4,6,7	27.3 ± 0.10^{c}	-72.0 ± 3.23^{a}
	6.0	39.5	1,2,3,4,5,6,7,8,10,11	27.2 ± 0.16^{c}	-67.8 ± 0.95^{ab}
Bulk MF + LEC	0.0	39.8	---	23.2 ± 0.08^{b}	-60.7 ± 0.56^{c}
	3.0	39.8	---	22.6 ± 0.19^{d}	-62.3 ± 0.61^{c}
	6.0	39.9	1,2,4,6,7,10,11	23.9 ± 0.16^{a}	-60.4 ± 1.76^{c}
Bulk MF + MAG	0.0	39.9	---	22.6 ± 0.06^{d}	-70.5 ± 0.42^{a}
	3.0	39.7	---	25.8 ± 0.30^{e}	-67.1 ± 1.36^{ab}
	6.0	40.1	1,2,4,6,7,10,11	26.2 ± 0.00^{e}	-68.3 ± 0.64^{ab}

PS peaks correspond as follows 1=35.6 Å; 2=17.7 Å; 3=11.7 Å; 4=9.7 Å; 5= 8.8 Å; 6=7.4 Å; 7=5.9 Å; 8=5.2 Å; 10=4.8 Å; 11=4.7 Å. Superscript letters denote significant differences in Tukey's Post Hoc Test with a $p<0.05$.

Thermal outputs captured from DSC measurements during heating showed a significant ($p < 0.05$) decrease in the melting enthalpy of all samples containing lecithin, with or without added phytosterols (Table 5.1). The energy released during melting demonstrates that some milk fat tended to crystallise upon storage. The decrease in melting enthalpy, however, suggests that the milk fat crystalline network was indeed less developed in samples containing lecithin. In addition, polarised optical microscopy images of bulk milk fat samples enriched with lecithin possessed a less developed and non-homogenous milk fat crystal network compared to the bulk milk fat samples, with larger spherulites present throughout (Fig. 5.5). The difference between the samples with and without lecithin is similar to the difference seen within milk fat samples crystallised at 25 and 4 ºC (Wright, Hartel, Narine, & Marangoni, 2000). At lower temperatures, the critical radius of crystalline milk fat nuclei are smaller than at higher crystallisation temperatures, because of the decreasing solubility of the TAG molecules and the increasing free energy of the system (Wright & Marangoni, 2006). In our study, distinct large spherulites are clearly apparent throughout the samples containing lecithin, suggesting that lecithin influenced the milk fat TAG network growth (Fig. 5.5). Similar results for bulk palm oil were found where the addition of lecithin-derived phospholipids increased the size of the spherulites, while reducing the total amount of palm oil TAG crystals and leading to a loss of interlocking crystals between the palm oil spherulites (Smith, 2000).

Conversely, MAG is known for initiating TAG nucleation. Here, TAG molecules absorb onto the MAG surface and act as catalytic seed crystal impurities (Basso et al., 2010). A larger number of seed crystals leads to the formation of smaller TAG crystals throughout, creating a dense crystalline network. In our work, images taken of samples enriched with MAG after storage show smaller milk fat crystals compared to the control (Fig. 5.5). This is consistent with previous results for other MAG-enriched TAG systems (Basso et al., 2010; Naderi, Farmani, & Rashidi, 2016; Verstringe, Danthine, Blecker, & Dewettinck, 2014; Wassell et al., 2012). Dense crystalline networks are often used in solid-lipid nanoparticle (SLN) technology, where a solid-lipid carrier matrix entraps the bioactive. The entrapment of the bioactive in a crystalline matrix can limit the mobility of the bioactive, preventing its crystallisation and degradation (Bunjes, Drechsler, Koch, & Westesen, 2001; Helgason et al., 2009;

Nik, Langmaid, & Wright, 2012; Weiss et al., 2008). The results suggest that MAG addition seeded the development of a dense milk fat TAG network, which in turn entrapped the phytosterol molecules, preventing crystallisation at 3% phytosterol addition, and reducing the number of crystalline phytosterol peaks in the 6% formulation.

While the MAG and milk fat TAG network entrapped the phytosterols, and lecithin improved their solubilisation, both compounds were able to decrease the number of phytosterol peaks observed in SAXS/WAXS diffraction patterns. Their impact on phytosterol crystallisation was also evident visually. In polarised images, phytosterols appeared as plate-like crystals (outlined in the 3% enriched sample). They can induce crystallisation in the milk fat phase, as seen in the 6% sample (Fig. 5.5), as a finer network is seen when compared to the control milk fat. No distinguishable plate-like phytosterol crystals were observed in samples enriched with either lecithin or MAG, and the milk fat networks look relatively similar between treatments. Upon heating to 40 ºC, the crystalline networks formed within the lecithin and MAG network melted. During this heating process, the 6% phytosterol without lecithin or MAG was the only sample to have noticeable crystals present at temperatures ≥ 40 ºC (Fig 5.7). The networks containing lecithin or MAG were also observed to melt differently compared to the control; at 30 ºC, a much finer crystalline network is observed which displays almost no birefringence, as opposed to the lecithin containing system where large spherulites were still visible.

Regardless of lecithin or MAG addition, bulk milk fat was found to be of a double chain length (2L) configuration with a d-spacing between 39.4 and 40.1 Å after storage at 4 °C for 48 h. Both β and β' polymorphs (Table 5.1 & Fig. 5.2) were observed to be similar to other MF systems (Bugeat, Briard-Bion et al. 2011, Truong, Morgan et al. 2015). Results from Chapter 2 & 4 demonstrated that milk fat forms a more disordered 3L matrix with a loose α-packing during the initial phases of the crystallisation process. This could allow phytosterols to fit inside the milk fat TAG network during the early stages of crystal growth. Over time, the TAG network shifts from the unstable 3L α-packing to a more stable 2L form with β and β' polymorphs.

Table 5.2. Changes in maximum backscattering and synchrotron diffraction results from emulsion (em) formulation (added lecithin (LEC) or monoacylglycerol (MAG) and size

Em	PS Conc (%)	Droplet size ($D_{4,3}$) µm	Δ in BS 1-Week (%)	Δ in BS 1-Month (%)	MF Spacing (Å)	PS peaks
Em WPI	0.0	0.93 ± 0.06^{abc}	8.28 ± 0.85^{a}	10.4 ± 1.07^{a}	39.7	----
	0.3	0.86 ± 0.06^{bcd}	6.49 ± 1.11^{a}	9.5 ± 0.85^{ab}	39.6	6,7,9,10
	0.6	0.73 ± 0.07^{d}	6.64 ± 1.21^{a}	8.7 ± 1.07^{abc}	39.5	1,2,6,7,9,10
Em WPI + LEC	0.0	1.02 ± 0.16^{a}	2.76 ± 0.70^{bc}	10.4 ± 0.59^{a}	39.8	----
	0.3	0.99 ± 0.16^{ab}	3.76 ± 0.99^{b}	9.4 ± 1.13^{ab}	39.8	6,7,9,10
	0.6	0.95 ± 0.13^{abc}	3.69 ± 0.75^{b}	8.3 ± 0.77^{abc}	39.6	1,2,6,7,9,10
Em WPI + MAG	0.0	0.78 ± 0.06^{cd}	3.70 ± 0.97^{b}	7.4 ± 0.50^{bcd}	39.7	----
	0.3	0.79 ± 0.06^{bcd}	3.89 ± 0.47^{b}	8.7 ± 0.30^{abc}	40.0	6,7,9,10
	0.6	0.76 ± 0.05^{cd}	2.14 ± 1.00^{bc}	7.5 ± 0.65^{bcd}	40.0	1,2,6,7,9,10
Em WPI	0.0	0.21 ± 0.00^{e}	----	1.3 ± 0.32^{ef}	40.3	----
	0.3	0.20 ± 0.01^{e}	----	2.3 ± 0.33^{f}	39.9	----
	0.6	2.04 ± 0.01^{e}	----	3.5 ± 0.08^{fg}	39.7	2,6,7,9,10
Em WPI + LEC	0.0	0.18 ± 0.01^{e}	----	2.0 ± 1.19^{ef}	40.1	----
	0.3	0.19 ± 0.01^{e}	----	2.2 ± 0.58^{ef}	39.9	----
	0.6	0.17 ± 0.00^{e}	----	----	39.8	6,7,9,10
Em WPI + MAG	0.0	0.22 ± 0.00^{e}	$1.32 \pm 0.63^{cd*}$	8.8 ± 0.76^{ab}	40.3	----
	0.3	0.22 ± 0.01^{e}	----	5.7 ± 0.32^{dg}	40.2	----
	0.6	0.22 ± 0.02^{e}	----	6.5 ± 1.01^{dc}	40.2	6,7,9,10

All larger (~1.0 µm) milk fat (MF) emulsions were homogenized with 1 pass at 300 bar (top half). The smaller (~0.2 µm; bottom half) emulsion all required homogenization at 1000 bar and either 4, 3, or 5 passes for the WPI, WPI + lec, and WPI + MAG samples, respectively. The difference in backscattering data between day 0 and day 7 or 1-month is denoted as Δ in BS 1-week or Δ in BS 1-month, respectively. Phytosterol (PS) peaks within emulsions correspond as follows 1=35.6 Å; 2=17.7 Å; 3=11.7 Å; 4=9.7 Å; 5= 8.8 Å; 6=7.4 Å; 7=5.9 Å; 8=5.2 Å; 9=5.1 Å; 10=4.8 Å; 11=4.7 Å. *No statistically difference was found between this sample and samples with no change in backscattering (----); samples with no change in backscattering were recorded as 0.00(----) and possessed the statistical label ^{d}. Superscript letters denote significant differences in Tukey's Post Hoc Test with a $p<0.05$.

This is also the case for milk fat with MAG or lecithin, as upon 3% addition of either of these compounds no change in milk fat lamellar spacing was seen within the TAG structure after storage (Table 5.1). Similar results have been seen in a palm oil enriched with the MAG monopalmitin (Verstringe, Dewettinck, Ueno, & Sato, 2014). In their work, palm oil crystallisation was induced by monopalmitin molecules during crystallisation, and monopalmitin crystals were detected at palm oil nucleation sites. However, after 1-week of storage, monopalmitin crystals migrated and crystallised separately in the interstitial spaces between palm oil crystals.

Differential scanning calorimetry was also used to examine the thermal transitions of each bulk sample, with two main differences being observed (Fig. 5.6; Table 5.1). Firstly, phytosterol enrichment significantly ($p < 0.05$) increased the onset temperature (T_{onset}) of the high-melting point milk fat fraction in both the control and in the sample containing MAG. Results from Chapter 2 demonstrated the ability of phytosterol molecules to slow the lamellar devolution of the milk fat network through steric hindrance during melting (Fig. 2.4). No effect on the T_{onset} of the high-melting point fraction was observed for samples containing lecithin. Within the lecithin enriched samples, it is also possible that the lack of milk fat TAG crystal growth minimised the effect of phytosterols on the high-melting point fraction, as an increase in the onset temperature is not distinguishable (Fig. 5.3).

5.3.2 The effect of emulsion droplet size on phytosterol crystallisation

Phytosterol crystallisation within the phytosterol-enriched (PE) emulsion systems was assessed as a function of phytosterol concentration (0.3 and 0.6%) and droplet size ($D_{(4,3)}$ = 0.2 and 1.0 µm average diameter, respectively) using synchrotron SAXS/WAXS (Table 5.2 & Fig. 5.7). Results were compared to the bulk milk fat SAXS/WAXS patterns described earlier (Table 5.1 & Fig. 5.3-5.4); the number of phytosterol peaks was shown to decrease when moving from a bulk to an emulsified state with an average droplet size of 1.0 µm (Tables 5.1 & 5.2). A decrease in the number and intensity of phytosterol crystalline peaks was also observed with decreasing droplet size. For example, for the 0.3% enrichment formulation, no phytosterol peaks were detected in the 0.2 µm emulsions compared to the 4 peaks observed in the 1.0 µm emulsions. To a lesser degree, emulsion size also influenced

the 0.6% enriched emulsion, with the crystalline peak present at 35.6 Å in the 1.0 µm emulsion absent within the smaller sized emulsion.

Dispersing a lipid matrix into an oil-in-water emulsion system results in droplets with a small lipid volume, which limits the number of possible nucleation sites (McClements, 2012). During cooling, the phytosterols would be supersaturated within the bulk milk fat but, without sufficient nuclei in each droplet, the large activation energy required for nucleation can result in a metastable state (Li et al., 2012; McClements, 2012). This metastable, supersaturated state can persist for some time, as a larger activation energy must be overcome before the crystal nuclei can form and grow into crystals. Dispersing the lipid matrix within droplets limits these nucleation sites and is even more pronounced in droplets with a smaller volume (Karadag, Yang, Ozcelik, & Huang, 2013).

Decreased crystallisation of bioactive components when comparing a bulk to an emulsion system has also been observed in other studies, due to this change in activation energy (Bunjes et al., 2001; Oehlke et al., 2014). In addition, as seen within the crystalline phytosterol powder, and its aqueous dispersed form (Fig. 5.1), phytosterols form different crystalline structures in the presence of water (Christiansen et al., 2002). Phytosterols can participate in surface heterogeneous nucleation, and tend to crystallise at the surface of the emulsion droplets (Arima, Ueno, Ogawa, & Sato, 2009; Chen, Guo, Wang, Yin, & Yang, 2016; McClements, 2012; Zychowski et al., 2016).

Crystallisation in emulsion systems may influence the physical stability of the emulsion over time (McClements, 2012). To evaluate stability, emulsions were tested for creaming (Δ backscattering) after 1-week and 1-month storage at 4 ºC, utilising a turbiscan optical analyser (Table 5.1 & Fig. 5.8). No significant change ($p<0.05$) in backscattering was observed after 1-week or 1-month of production between WPI stabilised emulsions with or without phytosterol addition. This is despite the fact that phytosterols were found to be crystalline within these samples (Table 5.2 & Fig. 5.3-5.4). This indicates that, within this system, phytosterol crystallisation does not result in emulsion destabilisation through partial coalescence of the lipid droplets, as observed within other emulsion systems (McClements, 2012). Although

uncharacteristic of emulsified crystalline material, crystalline phytosterols have been previously found to improve emulsion stability. In one such study, performed by Chen et al. (2016), phytosterols were co-crystallised with octenyl succinic anhydride starch at an emulsion interface. The resulting rigid phytosterol complex decreased droplet coalescence and improved the overall stability of the emulsion over time.

Decreasing the droplet size of an emulsion can also greatly improve the thermodynamic stability of the emulsion, and decrease the tendency for an emulsion to phase separate into lipid and aqueous phases (McClements, 2012). As expected, the 0.2 um emulsion showed a dramatic increase in emulsion stability over time at both the 1-week and 1-month mark compared to the 1 μm sample (Table 5.2 & Fig. 5.8). As creaming occurred, emulsion droplets gathered at the top of the tube resulting in a clearing at the bottom. Droplet movement from the bottom of the tube is apparent by increasing line curvature from ~ 7 to 25 mm, while creaming is reflected in the increasing backscattering values at ~ 70 mm (Fig. 5.8a). The 1.0 μm control emulsion was found to be less stable than the control formulation prepared with an average droplet size of 0.2 um. This was evident from larger backscattering values and a higher line curvature at the bottom of the tube (Table 5.2 & Fig. 5.6). Similar results regarding increases in emulsion destabilisation within larger droplet emulsion systems have been observed in other oil-in-water dispersed systems (Abismaïl, Canselier, Wilhelm, Delmas, & Gourdon, 1999; Chanamai & McClements, 2000; Dickinson, Golding, & Povey, 1997). Extreme changes in backscattering between the 1.0 and 0.2 μm PE emulsions demonstrate how emulsion stability is largely affected by droplet size, and independent of phytosterol crystallisation in the emulsion droplets.

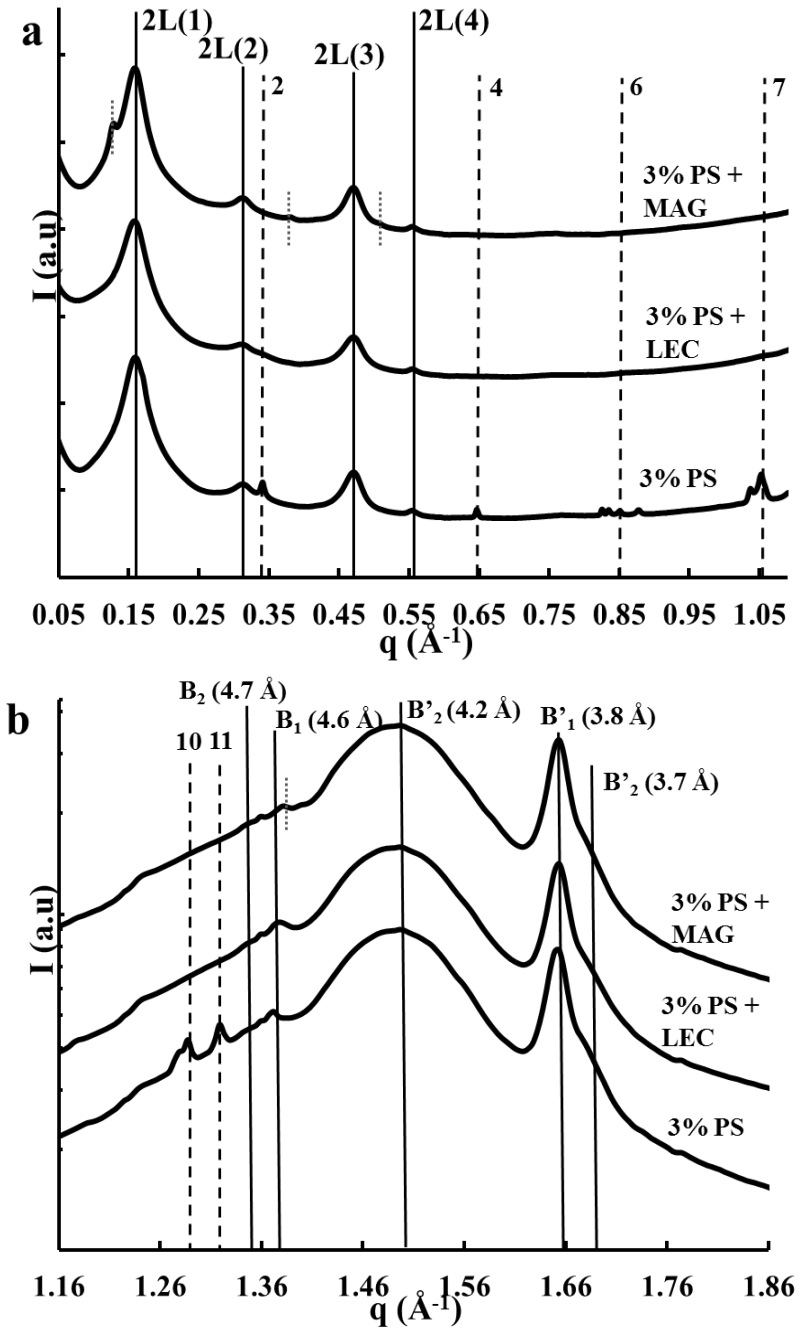

Figure 5.3 *Synchrotron (a) SAXS and (b) WAXS diffraction patterns of bulk milk at 3% (wt/wt) phytosterol (PS) enrichment with or without lecithin (LEC) or monoacylglycerols (MAG). Milk fat (solid black lines), phytosterol (dashed black lines) and MAG peaks (small grey dotted lines) are distinguished by different vertical lines. The labelled peaks for phytosterols correspond to the following distances seen within formulations: 2=17.7 Å; 4=9.7 Å; 6=7.4 Å; 7=5.9 Å; 10=4.8 Å; 11=4.7 Å. It can be noted that no phytosterol peaks were observed in samples containing LEC or MAG in bulk samples at 3% PS enrichment.*

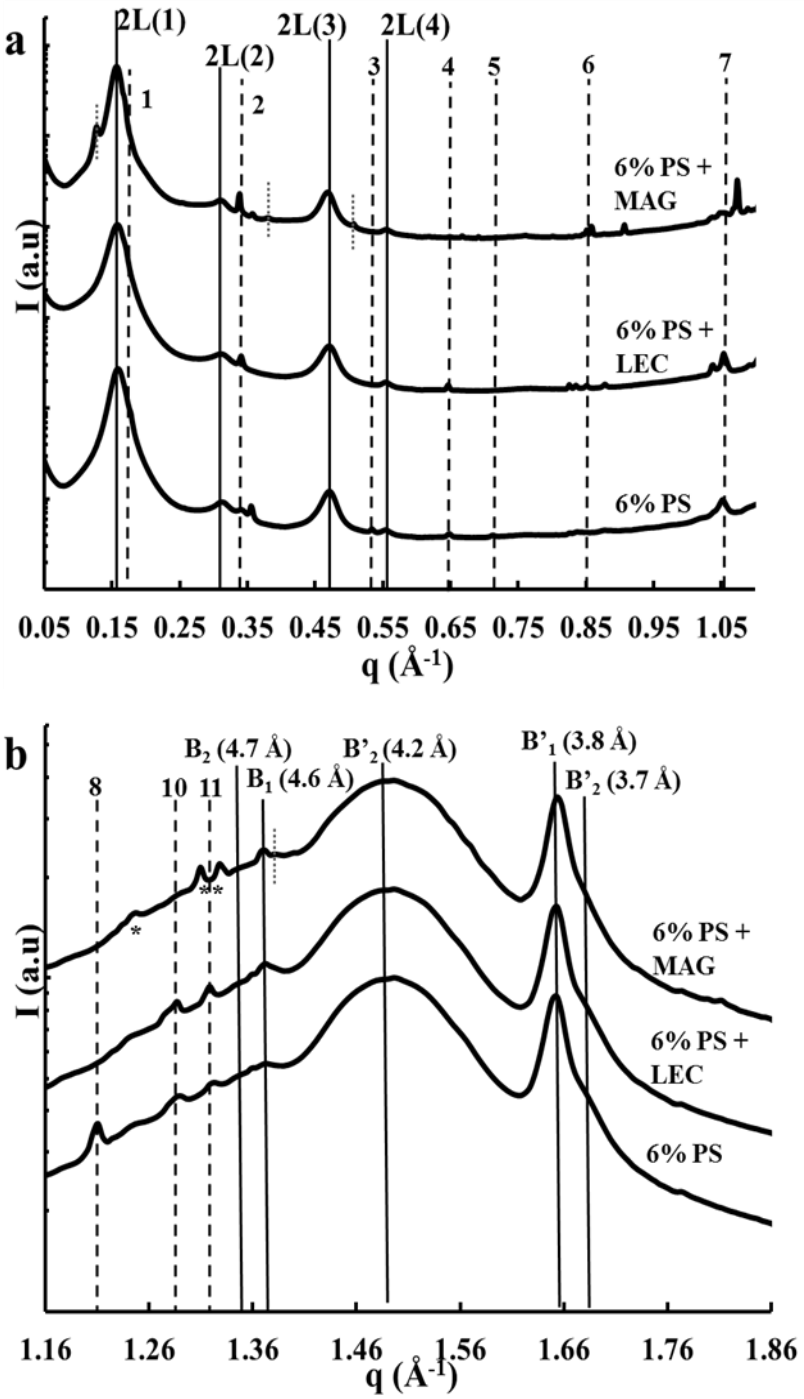

Figure 5.4 *Synchrotron (a) SAXS and (b) WAXS diffraction patterns of bulk milk at 6 % (wt/wt) phytosterol (PS) enrichment with/without lecithin (LEC) or monoacylglycerols (MAG). Milk fat (solid black lines), phytosterol (dashed black lines) and MAG peaks (small grey dotted lines) are distinguished by different vertical lines. The labelled peaks for phytosterols correspond to the following distances seen within formulations: 1=35.6 Å; 2=17.7 Å; 3=11.7 Å; 4=9.7 Å; 5= 8.8 Å; 6=7.4 Å; 7=5.9 Å; 8=5.2 Å; 10=4.8 Å; 11=4.7 Å.*Represents possible peak shift due to MAG crystalline peaks at similar Bragg distances.*

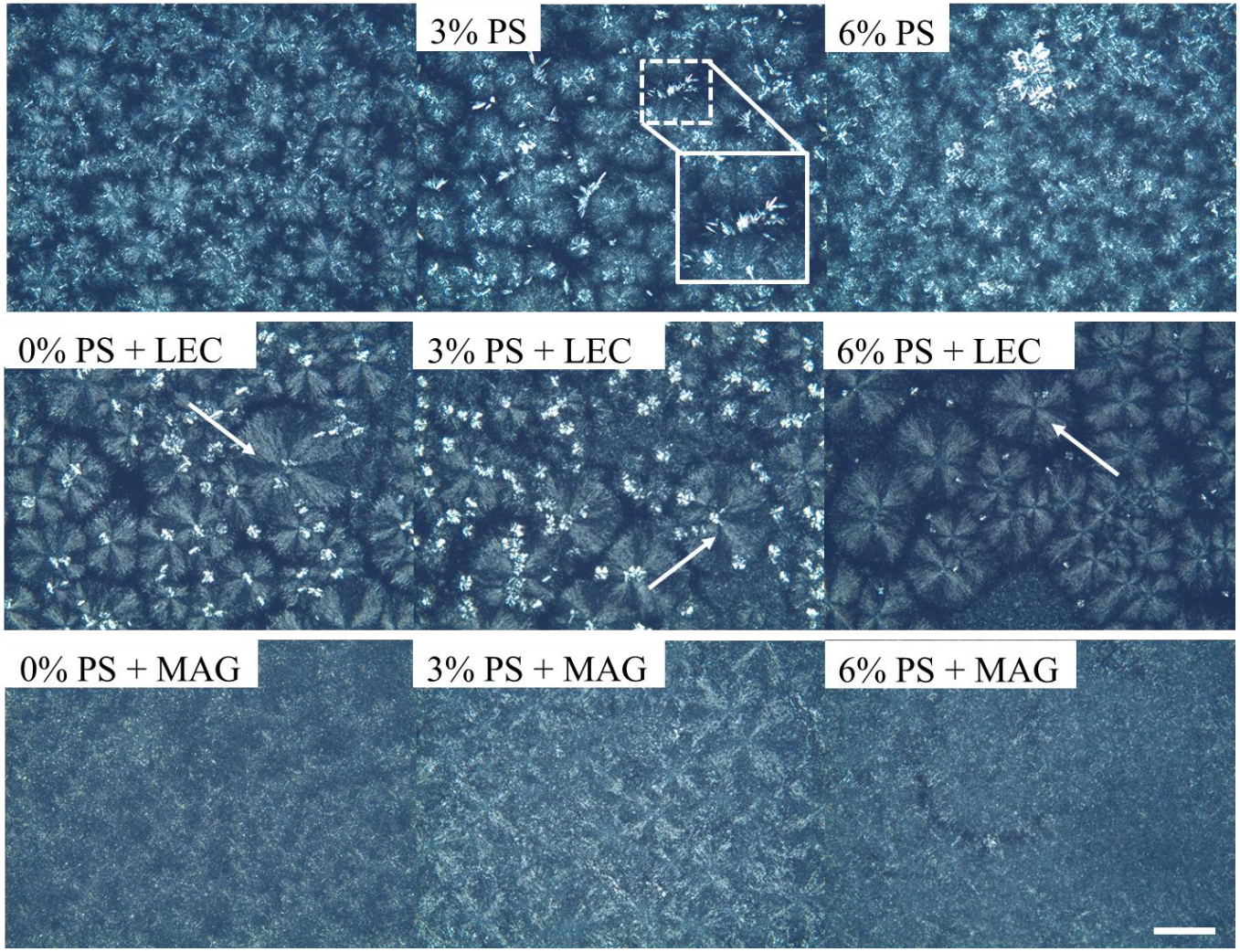

Figure 5.5 *Polarised light micrographs (partially uncrossed polarising filters) of bulk formulations with phytosterols (PS), with or without the addition of lecithin (LEC) or monoacylglycerols (MAG). The enlarged box highlights the presence of phytosterol crystals in the 3% (wt/wt) PS sample. Scale bar = 100 µm. Arrows highlight large milk fat spherulites.*

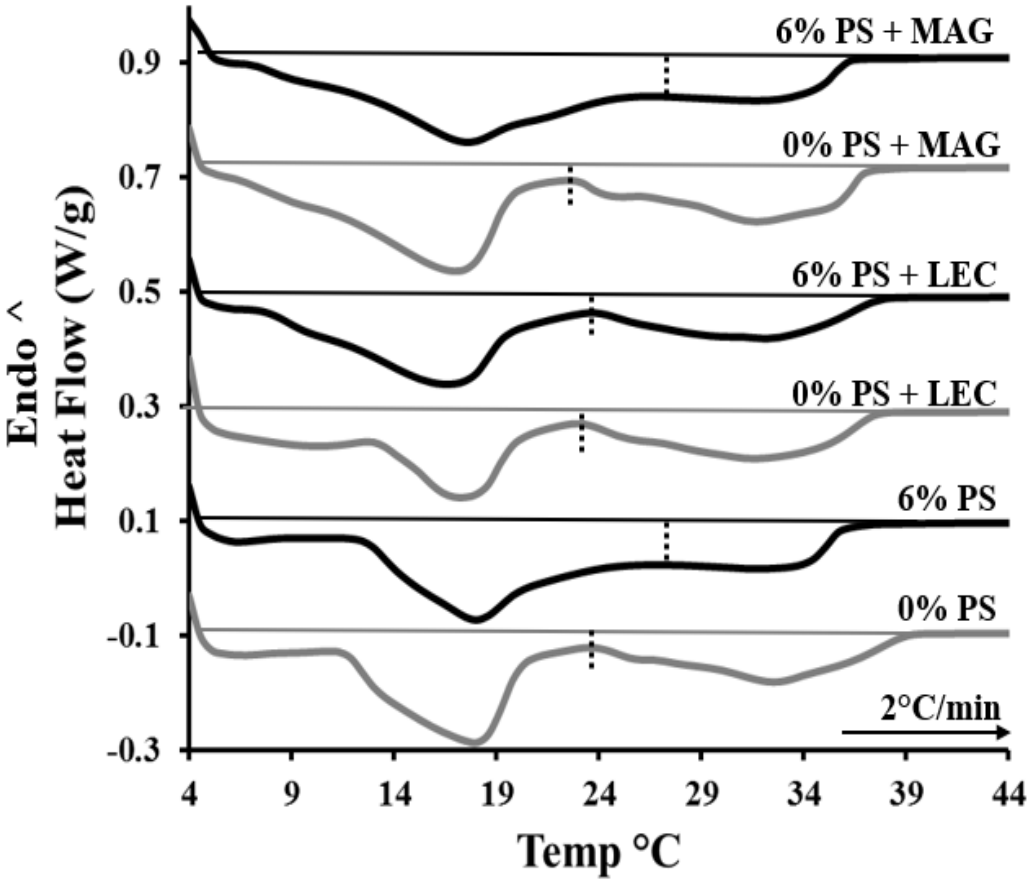

Figure 5.6 DSC thermographs of bulk formulations during heating at 2ºC/min with or without phytosterols (PS) and/or lecithin (LEC) or monoacylgylcerols (MAG). The dashed line represents the start of the last peak (T_{onset}).

5.3.3 The effect of lecithin and MAG on phytosterol crystallisation and emulsion formation and stability

Phytosterol emulsions of 0.2 and 1.0 µm average droplet size were also evaluated for phytosterol crystallisation upon the addition of lecithin and MAG to the dispersed milk fat. Synchrotron SAXS/WAXS patterns demonstrated that there was no difference in the number of crystalline phytosterol peaks in the samples at 1.0 µm, even after the addition of lecithin and MAG (Table 5.2). However, the addition of lecithin and MAG did prevent the phytosterol peak observed at 17.7 Å in the 1.0 µm emulsion from occurring in the 0.2 µm sample at 0.6% enrichment. This minor change indicates that

the most significant reductions in phytosterol crystallisation were due to a decrease in droplet size, as previously discussed (Table 5.2 & Fig 5.7).

The 1.0 µm emulsions prepared with either lecithin or MAG had statistically similar ($p > 0.05$) $D_{(4,3)}$ values between formulations independent of phytosterol concentration, except for the emulsion stabilised by WPI alone, which showed a significant decrease in average droplet size with the addition of 0.6% phytosterol, from 0.93 ± 0.06 to 0.73 ± 0.07 µm. A similar decrease in the droplet size of WPI stabilised emulsions with phytosterol addition has been documented in previous work and is believed to be due to a synergistic interaction between phytosterols and whey protein at the oil-in-water interface. Phytosterol and whey protein can decrease interfacial tension at the oil/water interface of the system to a greater extent together, than each compound can achieve separately (Chapter 3). While all 1.0 µm emulsion droplets required 1 pass at 300 bar to form a stable, monomodal emulsion distribution, the phytosterol emulsion formulations with an average of 0.2 µm sized droplets required homogenisation at 1000 bar and either 4, 3, or 5 passes for the WPI, WPI + lecithin, and WPI + MAG samples, respectively. It is interesting to note that, to create the same sized droplets, lecithin-enriched emulsions required fewer homogenisation passes, while emulsions containing MAG required more than the control stabilized with WPI alone.

During storage, the 1.0 µm WPI stabilized phytosterol emulsions showed a significant increase ($p < 0.05$) in backscattering after 1-week, compared to those stabilized with additional lecithin and MAG (Table 5.2). However, after 1-month, all 1.0 µm emulsions showed relatively similar changes in backscattering. This indicates that in 1.0 µm sized emulsion droplets, lecithin and MAG provided some initial enhanced stability to the system, but over time this advantage was lost. After 1-week of storage at 4 ºC, all of the 0.2 µm emulsions were statistically similar in average droplet size ($p > 0.05$) and stability (Table 5.2 & Fig. 5.9). However, after 1-month, the 0.2 µm emulsions with MAG showed a significant increase ($p < 0.05$) in backscattering compared to all other formulations, and was the least stable.

This trend was not observed within the 1.0 µm PE emulsions, which could be due to the greater levels of surfactant required to stabilize the larger droplet interface in the

0.2 µm, systems, where surface area is inversely related to droplet size (Li et al., 2012). The larger surface area could have encouraged MAG to migrate from the lipid phase to the surface in order to stabilise the emulsion. While MAG can provide stability in some emulsion systems, it is prone to crystallisation at the interface, which in turn can lead to emulsion instability (Mao, Calligaris, Barba, & Miao, 2014; Richards, Golding, Wijesundera, & Lundin, 2011). In addition, previous research has demonstrated that MAG can replace WPI at an emulsion interface, even though this replacement results in a more unstable system (Mao et al., 2014).

Finally, it is interesting to note that the 0.6% PE emulsion with 0.2 µm sized droplets and lecithin was still physically stable after 1-month (Table 5.2). Lecithin can aid solubility of the phytosterol in phospholipid-based membranes, and thus, it is possible that the two amphiphilic compounds could also be interacting at the emulsion interface to provide greater emulsion stability (Cercaci, Rodriguez-Estrada, Lercker, & Decker, 2007; Hąc-Wydro, Wydro, Jagoda, & Kapusta, 2007; Ostlund et al., 1999). Future research could investigate the relationship between the two compounds at the interface, and if higher levels of added lecithin could improve PE emulsion stability.

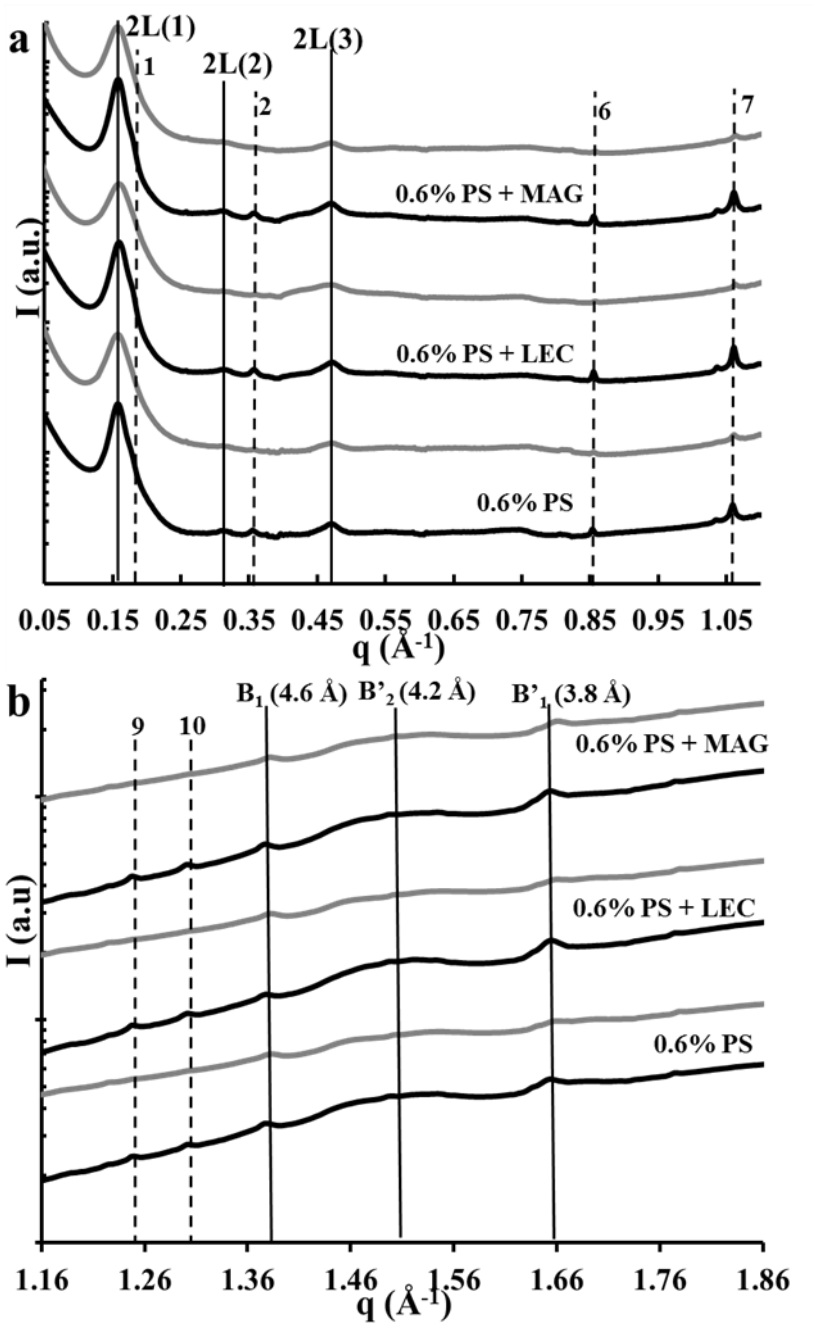

Figure 5.7 *Synchrotron SAXS (a) and WAXS (b) of 0.6% (wt/wt) phytosterol (PS)-enriched emulsions with or without lecithin (LEC) or monoacylglycerols (MAG). The black diffraction patterns corresponds to emulsions with a $D_{(4,3)}$ of 1.0 µm with 0.2 µm shown in grey. Milk fat (solid black lines), phytosterol (dashed black lines), and MAG peaks (small grey dotted lines) are distinguished by different vertical lines. The labelled peaks for phytosterols correspond to the following distances seen within formulations 1=35.6 Å; 2=17.7 Å; 6=7.4 Å; 7=5.9 Å; 9=5.1; 10=4.8.*

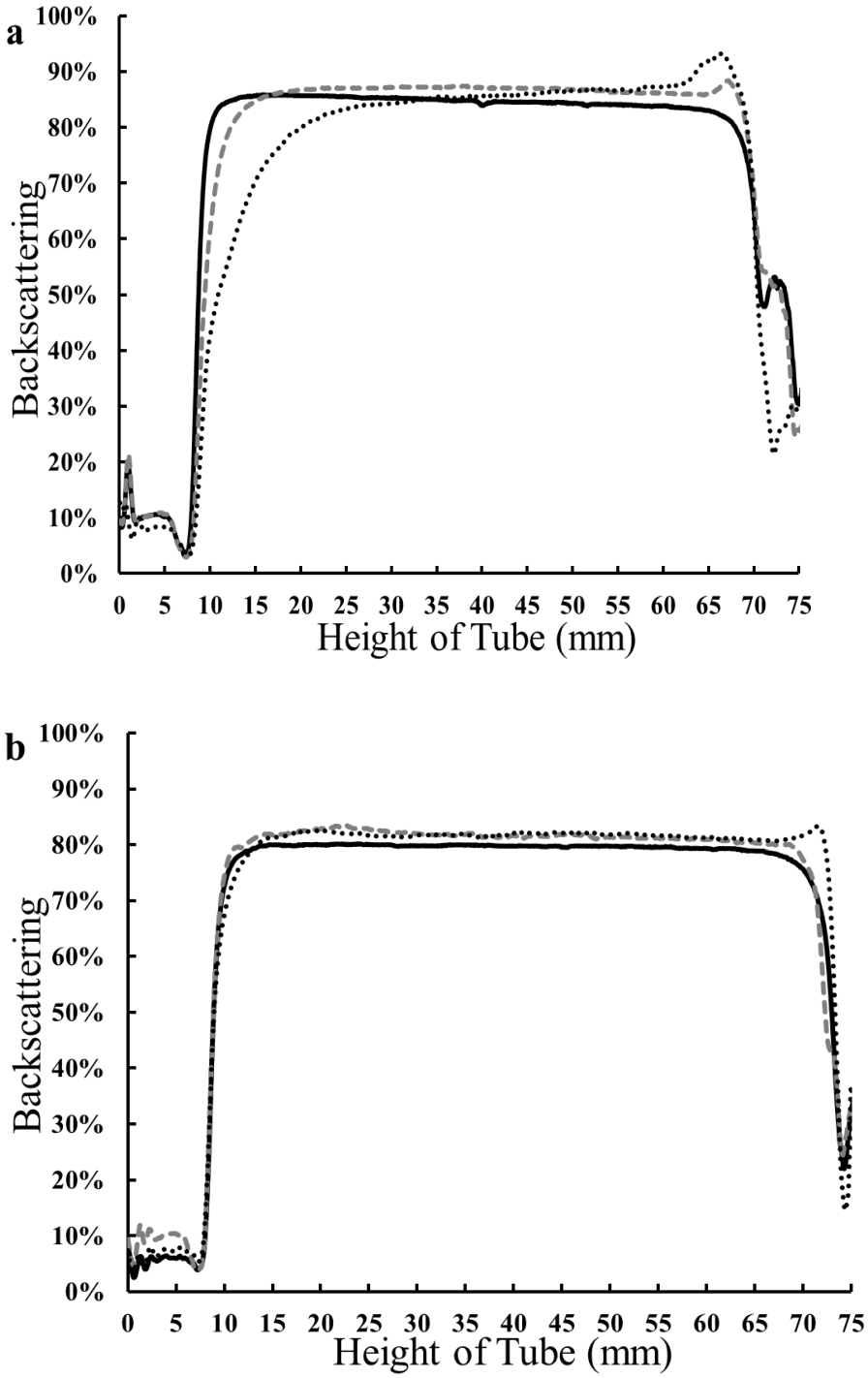

Figure 5.8 *Turbiscan backscattering results of phytosterol-enriched emulsions at (a) 1.0 µm and (b) 0.2 µm ($D_{4,3}$) during stability testing at day 0 (black solid line), day 7 (dashed grey line), and 1-month (dashed black line).*

5.4 Conclusion

This research study sought to understand how crystallisation of phytosterols was impacted by changes within formulation and droplet size. In addition, the systems were analysed for physicochemical changes using DSC, stability testing and polarised light microscopy. In bulk fat systems, the addition of the two surfactants, lecithin and MAG, reduced phytosterol crystallisation through increasing the solubility of the phytosterols and by creating a dense crystalline network entrapping the phytosterol, respectively. Once these formulations were dispersed in emulsion systems, diffraction patterns demonstrated that reductions in phytosterol crystallisation were mostly driven by decreasing the size of the emulsion droplets, not the addition of lecithin or MAG. However, within the smaller PE emulsions with a $D_{(4,3)}$ of 0.2 µm, samples with added MAG were found to be the most unstable, while the 0.6% PE emulsion with lecithin was found to be the most stable over time. This fundamental study is important in understanding how bioactive crystallisation is driven by processing and formulation factors. This information is valuable for the functional food industry to help reduce crystallisation of phytosterols, leading to improved bioaccessibility of the bioactive within the final food product.

Acknowledgements

The authors would like to thank the Teagasc Food Research Centre for assistance in funding this collaborative project (Teagasc Project 6412: “Structured Dairy Emulsions”), and the Australian Synchrotron for beamline access (proposal M10097). The authors would also like to thank the Australian Research Council, as Dr. Charlotte Conn is the recipient of a DECRA Fellowship DE160101281.We would also like to thank Nigel Kirby (Australian Synchrotron, Melbourne, Australia) for his invaluable guidance in setting up the synchrotron experiment. In addition, we thank Tamar Greaves (RMIT, Australia), Stephan Homer (CSIRO, Australia), and Lisa Blazo (University of Sheffield) for their assistance with this project.

References

Abismaïl, B., Canselier, J. P., Wilhelm, A. M., Delmas, H., & Gourdon, C. (1999). Emulsification by ultrasound: drop size distribution and stability. *Ultrasonics Sonochemistry, 6*(1–2), 75-83. doi:http://doi.org/10.1016/S1350-4177(98)00027-3

Akoh, C. C., & Min, D. B. (2008). *Food Lipids: Chemistry, Nutrition, and Biotechnology*: CRC press.

Arima, S., Ueno, S., Ogawa, A., & Sato, K. (2009). Scanning microbeam small-angle X-ray diffraction study of interfacial heterogeneous crystallization of fat crystals in oil-in-water emulsion droplets. *Langmuir, 25*(17), 9777-9784.

Barauskas, J., Johnsson, M., Joabsson, F., & Tiberg, F. (2005). Cubic phase nanoparticles (cubosome†): principles for controlling size, structure, and stability. *Langmuir, 21*(6), 2569-2577.

Basso, R. C., Ribeiro, A. P. B., Masuchi, M. H., Gioielli, L. A., Gonçalves, L. A. G., Santos, A. O. d., . . . Grimaldi, R. (2010). Tripalmitin and monoacylglycerols as modifiers in the crystallisation of palm oil. *Food Chemistry, 122*(4), 1185-1192. doi:http://doi.org/10.1016/j.foodchem.2010.03.113

Bunjes, H., Drechsler, M., Koch, M. J., & Westesen, K. (2001). Incorporation of the Model Drug Ubidecarenone into Solid Lipid Nanoparticles. *Pharmaceutical Research, 18*(3), 287-293. doi:10.1023/A:1011042627714

Carden, T. J., Hang, J., Dussault, P. H., & Carr, T. P. (2015). Dietary plant sterol esters must be hydrolyzed to reduce intestinal cholesterol absorption in hamsters. *The Journal of Nutrition*.

Cercaci, L., Rodriguez-Estrada, M. T., Lercker, G., & Decker, E. A. (2007). Phytosterol oxidation in oil-in-water emulsions and bulk oil. *Food Chemistry, 102*(1), 161-167.

Chanamai, R., & McClements, D. J. (2000). Dependence of creaming and rheology of monodisperse oil-in-water emulsions on droplet size and concentration. *Colloids and Surfaces A: Physicochemical and Engineering Aspects, 172*(1–3), 79-86. doi:http://doi.org/10.1016/S0927-7757(00)00551-3

Chen, X.-W., Guo, J., Wang, J.-M., Yin, S.-W., & Yang, X.-Q. (2016). Controlled volatile release of structured emulsions based on phytosterols crystallization. *Food Hydrocolloids, 56*, 170-179. doi:http://dx.doi.org/10.1016/j.foodhyd.2015.11.035

Christiansen, L. I., Rantanen, J. T., von Bonsdorff, A. K., Karjalainen, M. A., & Yliruusi, J. K. (2002). A novel method of producing a microcrystalline β-sitosterol suspension in oil. *European Journal of Pharmaceutical Sciences, 15*(3), 261-269.

Clifton, P. (2007). Plant sterols and stanols as functional ingredients in dairy products. In M. Saarela (Ed.), *Functional Dairy Products* (Vol. 2, pp. 255-261): Woodhead Publishing.

Clifton, P., Noakes, M., Ross, D., & Nestel, P. (2004). High dietary intake of phytosterol esters decreases carotenoids and increases plasma plant sterol levels with no additional cholesterol lowering. *Journal of Lipid Research, 45*(8), 1493-1499.

Dickinson, E., Golding, M., & Povey, M. J. W. (1997). Creaming and Flocculation of Oil-in-Water Emulsions Containing Sodium Caseinate. *Journal of Colloid and*

Interface Science, 185(2), 515-529. doi:http://dx.doi.org/10.1006/jcis.1996.4605

Dufourc, E. J. (2008). Sterols and membrane dynamics. *Journal of Chemical Biology, 1*(1-4), 63-77.

Engel, R., & Schubert, H. (2005). Formulation of phytosterols in emulsions for increased dose response in functional foods. *Innovative Food Science & Emerging Technologies, 6*(2), 233-237.

Fredrick, E., Walstra, P., & Dewettinck, K. (2010). Factors governing partial coalescence in oil-in-water emulsions. *Advances in Colloid and Interface Science, 153*(1), 30-42.

Hąc-Wydro, K., Wydro, P., Jagoda, A., & Kapusta, J. (2007). The study on the interaction between phytosterols and phospholipids in model membranes. *Chemistry and Physics of Lipids, 150*(1), 22-34. doi:https://doi.org/10.1016/j.chemphyslip.2007.06.211

Helgason, T., Awad, T. S., Kristbergsson, K., Decker, E. A., McClements, D. J., & Weiss, J. (2009). Impact of Surfactant Properties on Oxidative Stability of β-Carotene Encapsulated within Solid Lipid Nanoparticles. *Journal of Agricultural and Food Chemistry, 57*(17), 8033-8040. doi:10.1021/jf901682m

Jiang, Z.-Y., Han, T.-Q., Suo, G.-J., Feng, D.-X., Chen, S., Cai, X.-X., . . . Jiang, Y. (2004). Polymorphisms at cholesterol 7α-hydroxylase, apolipoproteins B and E and low density lipoprotein receptor genes in patients with gallbladder stone disease. *World Journal of Gastroenterology, 10*(10), 1508.

Karadag, A., Yang, X., Ozcelik, B., & Huang, Q. (2013). Optimization of preparation conditions for quercetin nanoemulsions using response surface methodology. *Journal of Agricultural and Food Chemistry, 61*(9), 2130-2139.

Kawachi, H., Tanaka, R., Hirano, M., Igarashi, K., & Ooshima, H. (2006). Crystallization of β-sitosterol using a water-immiscible solvent hexane. *Journal of Chemical Engineering of Japan, 39*(8), 869-875.

Kirby, N. M., Mudie, S. T., Hawley, A. M., Cookson, D. J., Mertens, H. D., Cowieson, N., & Samardzic-Boban, V. (2013). A low-background-intensity focusing small-angle X-ray scattering undulator beamline. *Journal of Applied Crystallography, 46*(6), 1670-1680.

Li, Y., Zheng, J., Xiao, H., & McClements, D. J. (2012). Nanoemulsion-based delivery systems for poorly water-soluble bioactive compounds: Influence of formulation parameters on polymethoxyflavone crystallization. *Food Hydrocolloids, 27*(2), 517-528.

Ling, W., & Jones, P. (1995). Dietary phytosterols: a review of metabolism, benefits and side effects. *Life Sciences, 57*(3), 195-206.

Lopez, C., Bourgaux, C., Lesieur, P., & Ollivon, M. (2002). Crystalline structures formed in cream and anhydrous milk fat at 4 C. *Le Lait, 82*(3), 317-335.

Maher, P. G., Auty, M. A. E., Roos, Y. H., Zychowski, L. M., & Fenelon, M. A. (2015). Microstructure and lactose crystallization properties in spray dried nanoemulsions. *Food Structure, 3*(0), 11. doi:http://dx.doi.org/10.1016/j.foostr.2014.10.001

Mao, L., Calligaris, S., Barba, L., & Miao, S. (2014). Monoglyceride self-assembled structure in O/W emulsion: formation, characterization and its effect on emulsion properties. *Food Research International, 58*, 81-88.

McClements, D. J. (2004). Protein-stabilized emulsions. *Current Opinion in Colloid & Interface Science, 9*(5), 305-313. doi:http://dx.doi.org/10.1016/j.cocis.2004.09.003

McClements, D. J. (2012). Crystals and crystallization in oil-in-water emulsions: Implications for emulsion-based delivery systems. *Advances in Colloid and Interface Science, 174*, 1-30.

Moreau, R. A., Whitaker, B. D., & Hicks, K. B. (2002). Phytosterols, phytostanols, and their conjugates in foods: structural diversity, quantitative analysis, and health-promoting uses. *Progress in Lipid Research, 41*(6), 457-500. doi:http://dx.doi.org/10.1016/S0163-7827(02)00006-1

Moreno-Calvo, E., Temelli, F., Cordoba, A., Masciocchi, N., Veciana, J., & Ventosa, N. (2014). A New Microcrystalline Phytosterol Polymorph Generated Using CO2-Expanded Solvents. *Crystal Growth & Design, 14*(1), 58-68. doi:10.1021/cg401068n

Moruisi, K. G., Oosthuizen, W., & Opperman, A. M. (2006). Phytosterols/Stanols Lower Cholesterol Concentrations in Familial Hypercholesterolemic Subjects: A Systematic Review with Meta-Analysis. *Journal of the American College of Nutrition, 25*(1), 41-48. doi:10.1080/07315724.2006.10719513

Naderi, M., Farmani, J., & Rashidi, L. (2016). Structuring of Chicken Fat by Monoacylglycerols. *Journal of the American Oil Chemists' Society, 93*(9), 1221-1231.

Nik, A. M., Langmaid, S., & Wright, A. J. (2012). Nonionic surfactant and interfacial structure impact crystallinity and stability of β-carotene loaded lipid nanodispersions. *Journal of Agricultural and Food Chemistry, 60*(16), 4126-4135.

Oehlke, K., Adamiuk, M., Behsnilian, D., Gräf, V., Mayer-Miebach, E., Walz, E., & Greiner, R. (2014). Potential bioavailability enhancement of bioactive compounds using food-grade engineered nanomaterials: a review of the existing evidence. *Food & function, 5*(7), 1341-1359.

Ohvo-Rekilä, H., Ramstedt, B., Leppimäki, P., & Peter Slotte, J. (2002). Cholesterol interactions with phospholipids in membranes. *Progress in Lipid Research, 41*(1), 66-97. doi:https://doi.org/10.1016/S0163-7827(01)00020-0

Ostlund, R. E. (2002). Phytosterols in human nutrition. *Annual Review of Nutrition, 22*(1), 533-549.

Ostlund, R. E., Spilburg, C. A., & Stenson, W. F. (1999). Sitostanol administered in lecithin micelles potently reduces cholesterol absorption in humans. *The American Journal of Clinical Nutrition, 70*(5), 826-831.

Pouteau, E. B., Monnard, I. E., Piguet-Welsch, C., Groux, M. J. A., Sagalowicz, L., & Berger, A. (2003). Non-esterified plant sterols solubilized in low fat milks inhibit cholesterol absorption. *European Journal of Nutrition, 42*(3), 154-164. doi:10.1007/s00394-003-0406-6

Qiu, H., & Caffrey, M. (2000). The phase diagram of the monoolein/water system: metastability and equilibrium aspects. *Biomaterials, 21*(3), 223-234. doi:http://dx.doi.org/10.1016/S0142-9612(99)00126-X

Richards, A., Golding, M., Wijesundera, C., & Lundin, L. (2011). The influence of secondary emulsifiers on lipid oxidation within sodium caseinate-stabilized oil-in-water emulsions. *Journal of the American Oil Chemists' Society, 88*(1), 65-73.

Rossi, L., ten Hoorn, J. W. S., Melnikov, S. M., & Velikov, K. P. (2010). Colloidal phytosterols: synthesis, characterization and bioaccessibility. *Soft Matter, 6*(5), 928-936.

Rousseau, D. (2000). Fat crystals and emulsion stability — a review. *Food Research International, 33*(1), 3-14. doi:http://dx.doi.org/10.1016/S0963-9969(00)00017-X

Rozner, S., & Garti, N. (2006). The activity and absorption relationship of cholesterol and phytosterols. *Colloids and Surfaces A: Physicochemical and Engineering Aspects, 282*, 435-456.

Salentinig, S., Phan, S., Khan, J., Hawley, A., & Boyd, B. J. (2013). Formation of highly organized nanostructures during the digestion of milk. *American Chemical Society Nano, 7*(12), 10904-10911.

Sato, K. (1999). Solidification and phase transformation behaviour of food fats—a review. *European Journal of Lipid Science and Technology, 101*(12), 467-474.

Shaghaghi, M. A., Harding, S. V., & Jones, P. J. H. (2014). Water dispersible plant sterol formulation shows improved effect on lipid profile compared to plant sterol esters. *Journal of Functional Foods, 6*, 280-289.

Smet, E. D., Mensink, R. P., & Plat, J. (2012). Effects of plant sterols and stanols on intestinal cholesterol metabolism: suggested mechanisms from past to present. *Molecular Nutrition & Food Research, 56*(7), 1058-1072.

Truong, T., Morgan, G. P., Bansal, N., Palmer, M., & Bhandari, B. (2015). Crystal structures and morphologies of fractionated milk fat in nanoemulsions. *Food Chemistry, 171*, 157-167.

Vanhoutte, B., Foubert, I., Duplacie, F., Huyghebaert, A., & Dewettinck, K. (2002). Effect of phospholipids on isothermal crystallisation and fractionation of milk fat. *European Journal of Lipid Science and Technology, 104*(11), 738-744.

Verstringe, S., Danthine, S., Blecker, C., & Dewettinck, K. (2014). Influence of a commercial monoacylglycerol on the crystallization mechanism of palm oil as compared to its pure constituents. *Food Research International, 62*, 694-700. doi:http://doi.org/10.1016/j.foodres.2014.04.049

Verstringe, S., Dewettinck, K., Ueno, S., & Sato, K. (2014). Triacylglycerol crystal growth: templating effects of partial glycerols studied with synchrotron radiation microbeam X-ray diffraction. *Crystal Growth & Design, 14*(10), 5219-5226.

von Bonsdorff-Nikander, A., Karjalainen, M., Rantanen, J., Christiansen, L., & Yliruusi, J. (2003). Physical stability of a microcrystalline β-sitosterol suspension in oil. *European Journal of Pharmaceutical Sciences, 19*(4), 173-179.

Wassell, P., Okamura, A., Young, N. W. G., Bonwick, G., Smith, C., Sato, K., & Ueno, S. (2012). Synchrotron Radiation Macrobeam and Microbeam X-ray Diffraction Studies of Interfacial Crystallization of Fats in Water-in-Oil Emulsions. *Langmuir, 28*(13), 5539-5547. doi:10.1021/la204501t

Weiss, J., Decker, E., McClements, D. J., Kristbergsson, K., Helgason, T., & Awad, T. (2008). Solid Lipid Nanoparticles as Delivery Systems for Bioactive Food Components. *Food Biophysics, 3*(2), 146-154. doi:10.1007/s11483-008-9065-8

Widlak, N., Hartel, R. W., & Narine, S. (2001). *Crystallization and solidification properties of lipids*. Champaign, IL: The American Oil Chemists Society.

Wright, A. J., Hartel, R. W., Narine, S. S., & Marangoni, A. G. (2000). The effect of minor components on milk fat crystallization. *Journal of the American Oil Chemists' Society, 77*(5), 463-475.

Wright, A. J., & Marangoni, A. G. (2006). Crystallization and rheological properties of milk fat *Advanced Dairy Chemistry Lipids* (Vol. 2, pp. 245-291). New York, NY: Springer.

Yi, J., Knudsen, T. A., Nielsen, A.-L., Duelund, L., Christensen, M., Hervella, P., . . . Mouritsen, O. G. (2016). Inhibition of cholesterol transport in an intestine cell model by pine-derived phytosterols. *Chemistry and Physics of Lipids, 200*, 62-73. doi:http://doi.org/10.1016/j.chemphyslip.2016.06.008

Zhang, L., Hayes, D. G., Chen, G., & Zhong, Q. (2013). Transparent dispersions of milk-fat-based nanostructured lipid carriers for delivery of β-carotene. *Journal of Agricultural and Food Chemistry, 61*(39), 9435-9443.

Zychowski, L. M., Logan, A., Augustin, M. A., Kelly, A. L., Zabara, A., O'Mahony, J. A., . . . Auty, M. A. (2016). Effect of Phytosterols on the Crystallization Behavior of Oil-in-Water Milk Fat Emulsions. *Journal of Agricultural and Food Chemistry, 64*(34), 6546–6554.

Chapter 6

Grazing-incidence small-angle X-ray scattering on oil-in-water droplet array crystallisation

Lisa M. Zychowski[†§‡#], Amy Logan*[‡], Mary Ann Augustin[‡], Alan L. Kelly[§], James A. O'Mahony[§], Charlotte E. Conn[#], Mark A. E. Auty*[†]

[†] Food Chemistry and Technology Department, Teagasc Food Research Centre, Moorepark, Fermoy, Co. Cork, Ireland

[§] School of Food and Nutritional Sciences, University College Cork, Cork, Ireland

[‡] CSIRO Food and Nutrition, Werribee, Victoria 3030, Australia

[#] School of Applied Science, RMIT University, Melbourne, Victoria 3000, Australia

Declaration: Grazing-incidence small angle X-ray scattering was performed by the first author, Jamie Strachan and Haitao Yu with the assistance of the Charlotte E. Conn, Xuehua Zhang, and the Australian beam line scientists. Droplet arrays were made by Shuhua Peng and DSC bulk powders runs were performed by Amy Logan. Experimental and cell design was carried out as a collaborative effort by the first author, Xuehua Zhang, Charlotte E. Conn, Amy Logan, and Nigel Kirby. All experimental results were analysed by the first author. The chapter written by the first author and edited by the co-authors.

Abstract

Droplets arrays are employed for study a wide range of biological, physical, and chemical processes. Limited research has been performed on the crystallisation of these droplets, which offers the unique opportunity to study a colloid-like system without the presence of a surfactant. Droplets arrays were created in this study by the solvent exchange of two different lipids; trimyristin and trilaurin. Droplets and bulk samples were subjected to a temperature ramp and studied utilising synchrotron grazing-incidence small-angle X-ray scattering. The creation of a customised cell along with the angled grazing-incidence beam allowed for the visualisation of lipid crystallisation within the systems. Trimyistin was found to have a higher longitudinal spacing and to crystallise before trilaurin. Synchrotron results for bulk lipids correspond well to data captured using differential scanning calorimetry, demonstrating the accuracy of the Grazing-Incidence Small-Angle Scattering measurements. The development of this methodology allows for future studies to investigate other oil-and-water interfaces and could be potentially utilised to study interfacial phytosterol crystallisation.

6.1 Introduction

Droplet arrays are commonly used within microfluidics to study a wide variety of different topics such a thermodynamics or biological processes (Bao, Rezk, Yeo, & Zhang, 2015; Bao, Werbiuk, Lohse, & Zhang, 2016; Flaim, Chien, & Bhatia, 2005; Li et al., 2015; Ziauddin & Sabatini, 2001). A droplet array is comprised of a surface containing a series of closely packed droplets. Although difficult to generate, droplet arrays offer the unique possibility of studying a segregated droplet system. Droplet array generation through solvent exchange can deposit lipid droplets at fixed distances; this offers the possibility of not only studying a surfactant-less lipid-droplet system but also of potentially quantifying the influence of different droplet array spacings on lipid crystallisation kinetics (Dyett, Yu, & Zhang, 2017).

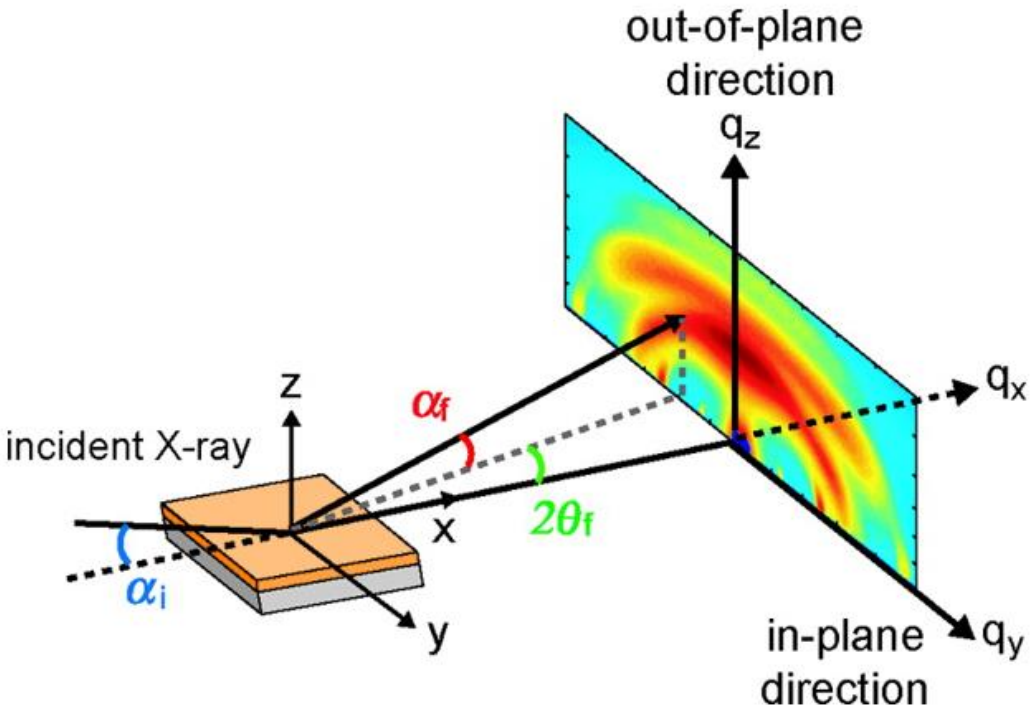

Figure 6.1 *Grazing-Incidence Small-Angle X-ray Scattering configuration, which demonstrates how the X-ray beam impinges on surface, allowing for quantification of film-like samples (Wakita, Jin, Shin, Ree, & Ando, 2010)*

Measuring lipid crystallisation within these lipid-droplet arrays has been difficult due to the presence of the array attached to the bottom of each droplet. The development of synchrotron grazing-incidence small-angle x-ray scattering (GISAXS; Fig. 6.1), however, enables the quantification of ordered structures on a surface. The angled beam employed in GISAXS is commonly used to study surfaces, monolayers, and

ultrathin films (Dutta, 2000). Currently, no known research has been performed utilising this system to study crystallisation within a lipid-droplet array. Thus, the objective of this study was to develop a method to quantify droplet TAG structure and development during the lipid crystallisation process.

Two lipids, trimyristin (C45) and Trilaurin (C39; Fig. 6.2), were selected for the study as they possess different crystallisation temperatures and parameters (Takeuchi, Ueno, & Sato, 2003). Additionally, both lipids are present within milk fat and thus are applicable to previous research performed on milk fat systems (Chapter 2-5; Jensen, 2002; Markiewicz-Kęszycka et al., 2013). Additionally, C45 and C39 have been used as the lipid base in solid lipid nanoparticles, which are emulsions with a dispersed solid lipid phase (Bunjes, Westesen, & Koch, 1996). Solid lipid structures have been extensively studied for functional applications, as they have been found to protect bioactives from degradation and can prevent bioactive crystallisation (Aditya et al., 2014; Torre & Pinho, 2015). Thus, the development of this GISAXS technology to observe lipid droplet crystallisation on an array can be applicable not only to phytosterol crystallisation within milk fat but could also be applied to other lipophilic bioactive systems employing solid lipid systems.

In order to study droplet array crystallisation a new GISAXS cell was developed by the beam line scientists at the Australian Synchrotron and the cell was fitted with the GISAXS beam. Crystallisation of the two lipids was monitored during the heating and cooling cycle. These results were compared against DSC data as a means of quantifying the temperature accuracy of the developed GISAXS system. This newly developed system offers the possibility of studying diverse lipid droplet systems and to understand the influence of surfactant and droplet spacing on crystallisation. Results from this study can be employed not only in the functional food industry but also in other applications such as photonics, near-field imaging, and biomolecular tissue analysis.

6.2 Materials and methods

6.2.1 Materials

Trimyristin (C45;≥99%;), Trilaurin (C39;≥99%), ethanol (≥99%) and octadecyltrimethylchlorosilane (OTS; >90%) were all purchased from Sigma Aldrich (St.Louis, MO). The silicon material utilised to produce patterned strips was procured from University Wafer Inc. (Boston, MA). The photoresist material spun onto silicon wafer was made from AZ1512HS (MicroChemicals GmbH, Ulm, Germany). Acetone and isopropyl alcohol in analytical grade were purchased from Chem-Supply Pty Ltd (Gillman, Australia).

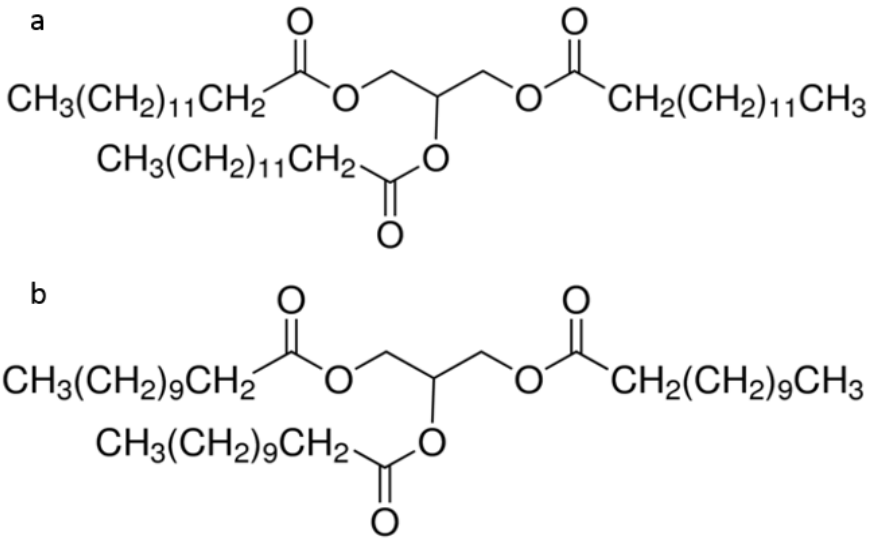

Figure 6.2 *Chemical formulae of Trimyristin (*$C_{45}H_{86}O_6$*;C45) and Trilaurin (C39;* $C_{39}H_{74}O_6$*;C39)*

6.2.2 Methods

6.2.2.1 Preparation of droplet array

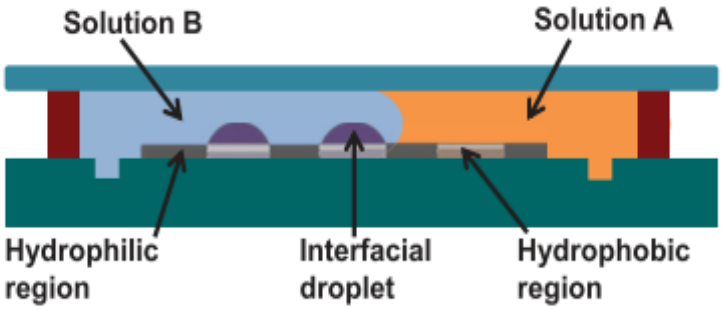

Figure 6.3 *Schematic, illustrating droplet creation through solvent exchange in a fluid tight system. Solution A consists of the ethanol and lipid mixture (2%), while solution B is water. The bottom plate is substrate used to create the droplet array. Taken from Bao et al. (2015).*

Droplets were created by solvent exchange on pre-patterned silicon wafer (Fig. 6.3). Circular hydrophobic patches with a diameter of 5 µm were created by first spinning AZ1512HS photo-resistor material onto the silicon wafer (Fig. 6.4). Afterwards, the wafer was exposed to UV light through a photomask and subsequently washed with developer solution AZ 400K (diluted with water in 1:4 ratio). The silicon was then treated with chemical vapour deposition, which transformed the unprotected circular domains into a hydrophobic area while the protected area remained hydrophilic. Further washing with acetone, isopropyl alcohol and ethanol was then performed to wash away any remaining photo resistant material.

Solvent exchange was conducted at 60°C, with all syringes and solutions preheated accordingly. After heating, the lipid and ethanol solution were inserted into a custom-designed fluid cell for solvent exchange, as employed previously (Bao et al., 2016; Lessel et al., 2015). After 10 min of equilibration at the target temperatures, a 2% lipid (C39 or C45) and ethanol solution was inserted into one end of the cell. To prevent leaks between solutions or air contamination, a gas-tight syringe was employed along with a luer lock and Teflon tubing. After flooding the cell with the lipid solution, the syringe was exchanged for the second liquid, water. The pre-

heated water was pumped at 500 µL/min and slowly displaced the solvent and lipid mixture. The exchange of a "good solvent" consisting of ethanol by a "poor solvent" composed of water induced heterogenous nucleation on the hydrophobic patches of silicone (Fig. 6.3; Bao, Rezk, Yeo, & Zhang, 2015). Imaging of nanodroplets was performed before and after solvent exchange using optical microscopy in reflection mode (Huvitz HRM-300, Gunpo, South Korea). Images were also captured after the temperature cycle and with/without synchrotron radiation.

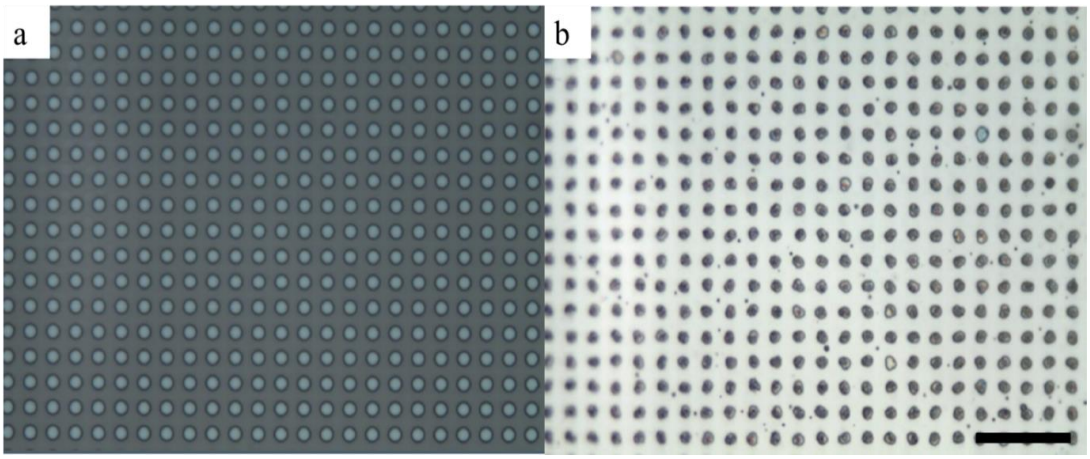

Figure 6.4 *Bright-field microscopy of silicon pattern surface (a) before and (b) after solvent liquid exchange. *Scale bar = 40µm*

6.2.2.2 Synchrotron grazing incident X-ray scattering analysis

Grazing incident small-angle X-ray scattering (GISAXS) measurements were carried at the SAXS/WAXS beamline in Clayton, Australia. A monochromatised X-ray radiation at a diameter of 250 µm, with a 15 keV radiation source, was employed at 0.03-0.6 $Å^{-1}$, along with a Pilatus 1M detector. The sample-to-detector distance was 0.96 m. The beam was aligned with a custom-made cell fitted with temperature control (Fig. 6.5). The cell was equipped with a 4x1x11 mm well to hold the silicon wafer samples in place for GISAXS analysis (Fig. 6.5b).

For analysis, silicon wafers containing the lipid droplets or bulk lipid sample, were inserted into the cell, and covered with de-gassed milli-Q water. The calibrated cell was then heated to 60°C until a liquid lamellar state was achieved. After heating, the cell was cooled at 1°C/min and then held at 4°C for 5 min. GISAXS shots were taken before, during, and after cooling in a gapless mode with a 3 s exposure time. After 5 min of holding at 4°C, the stage was re-equilibrated to room temperature before loading the next sample. The beam was calibrated using silver behenate. Baseline correction and Gaussian peak analysis were performed on diffraction patterns as described in chapter 2. Unfortunately, due to slight variations in the beam angle between samples, total background subtraction of the Kapton tape was not possible and Kapton peaks are hence visible on GISAXS diffraction patterns.

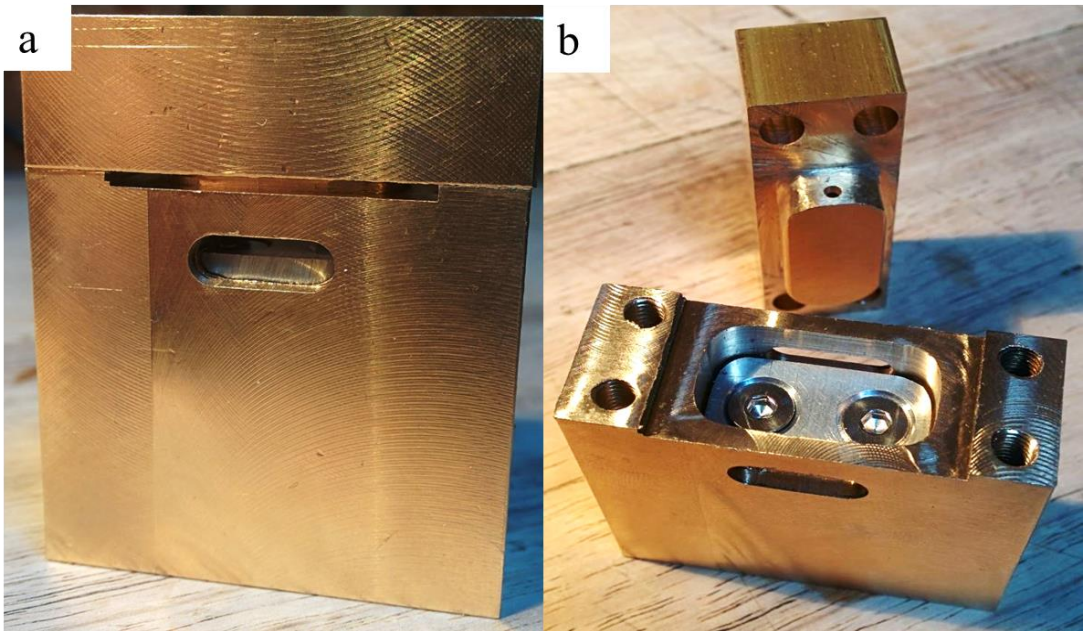

Figure 6.5 *Grazing-Incidence Small-Angle X-ray Scattering (GISAXS) cell designed by the staff at the Australian synchrotron cell for evaluating lipid droplet array during crystallisation. Images include (a) side angle of closed cell with GISAXS widow and (b) overhead view of opened cell*

6.2.2.3 Differential scanning calorimetry

Thermal analysis of all bulk samples was conducted on samples using a DSC 1 STARe System (Mettler Toledo, Port Melbourne, Australia) equipped with software (version 14.0). C39 and C45 lipid samples were melted and quantities of ~19-21 mg

were weighed into 40 µL aluminium pans (Mettler Toledo, part number ME-27331). Samples were then stored at room temperature for over 48 h before analysis, as done for synchrotron samples. After storage, pans containing C39 and C45 were heated in the DSC chamber to 60 and 70°C, respectively, and held there for 5 min. After heating the sample, DSC analysis began as the sample was cooled to 0°C at 1°C/min. After cooling, the sample was held at 0°C for 10 min before being re-heated to 60°C at 1°C/min. The DSC STARe software calculated the onset temperature of each peak (T_{onset}) and end set (T_{endset}), along with the maximum values for each peak.

6.3 Results and discussion

6.3.1 Synchrotron grazing-incidence small-angle X-ray scattering

Bulk and droplet lipid samples were monitored using synchrotron GISAXS during the cooling cycle from 60 to 4 ºC at 1ºC/min. The C45 bulk sample was found to crystallise first at 37 ºC, followed by the C45 droplet sample at 35 ºC (Table 6.1 & Fig. 6.6-6.9). The bulk C39 sample crystallised at a lower temperature of 23 ºC, with the droplets crystallising at 22 ºC. As this cooling cycle was only performed on one sample for each lipid system, due to time constraints, thus it cannot be determined if the differences in crystallisation temperature between the bulk and the droplets was significant. However, nucleation theory explains that, due to the smaller quantity of impurities within droplets, as opposed to bulk systems, nucleation should be delayed (Herhold, Ertaş, Levine, & King Jr, 1999; McClements, 2012).

These catalytic impurities found within lipids, such as dust or reverse micelles, can result in nucleation of a bulk lipid system, as only one impurity is needed to nucleate crystallisation within the system. Thus, if those impurities are limited to a select number of droplets, crystallisation is delayed, and the amount of super-cooling required to imitate nucleation is greater (Günther, Schmid, Mehling, Hiebler, & Huang, 2010; Herhold et al., 1999; McClements, 2012). Previous experimental results of bulk and emulsified systems have also shown that crystallisation occurred first within the bulk system and was subsequently delayed within the dispersed system (Lopez et al., 2002; Lopez, Bourgaux, Lesieur, Riaublanc, & Ollivon, 2006; Montenegro, Antonietti, Mastai, & Landfester, 2003). It can also be noted that the two lipid varieties were drastically different in crystallisation Tonset, which will be discussed in detail in the DSC section below.

Table 6.1 Synchrotron diffraction results as a function of sample preparation. Position and full width at half maximum (FWHM) values are taken from an average of 2 shots taken at 4 ºC

Sample	Crystallisation Temp (°C)	Position (Å)	FWHM ($Å^{-1}$)
C45 Bulk	37	36.8	2.9E-03
C45 Droplets	35	37.1	5.5E-03
C39 Bulk	23	32.5	3.0E-03
C39 Droplets	22	32.7	4.2E-03

Synchrotron diffraction peaks correspond to the longitudinal spacing of the triacylglycerol (TAG) molecules of the lipid (Widlak, Hartel, & Narine, 2001). The sample peak of the bulk C45 sample was recorded at 36.8 Å, while the bulk 39 sample was at 32.5 Å (Table 6.1 & Fig. 6.6-6.9). The C45 and C39 droplets were very similar in position to the bulk samples at 37.1 and 32.7 Å, respectively. All lipid samples crystallised in a 2L structure, meaning a double chain length arrangement of the TAG molecules (Lopez, Bourgaux, Lesieur, & Ollivon, 2007). The differences in 2L length were expected, as the C45 TAG molecule is composed of a glycerol backbone with three 14-carbon chain moieties attached, opposed to C39 with 12-carbon chain moieties (Fig. 6.2). Thus, as the TAG molecules arranged into a double-chain length configuration, more space was required as the carbon chains were larger in size (Widlak et al., 2001). These results were confirmed by the study from Takeuchi et al. (2003), who evaluated the lattice parameters and longitudinal spacing of C39, C45, tripalmitin (C51) and tristearin (C57). As the carbon number of the moieties increased, so did the packing parameters of the lipid matrix. There were more polymorphs observed within this study, due to the creation of unstable intermediates from rapid cooling (100°C/min); nevertheless, the C39 sample had a 2L peak corresponding to 32 Å, while that of the C45 was observed at 37 Å. Wide angle X-ray measurements from this study confirmed that these lamellar distances corresponded to a β' lattice parameter. These results demonstrate that GISAXS data taken from our cell, which was specifically designed for this study, correspond well to those from traditional SAXS measurements.

Table 6.2 Thermal parameters calculated from DSC thermographs recorded during the cooling and heating cycle

Sample	Tonset (°C)	peak (°C)	endset (°C)	ΔH (J g^{-1})
		Cooling (crystallisation)		
Bulk C45	36.9 ± 0.2[a]	34.3 ± 0.4[a]	32.1 ± 0.3[a]	56.9 ± 30.9[a]
Bulk C39	24.8 ± 0.2[b]	23.1 ± 0.7[b]	22.2 ± 0.7[b]	40.2 ± 7.1[a]
		Heating (peak 1; crystallisation)		
Bulk C45	37.0 ± 0.3[a]	38.8 ± 0.2[a]	40.8 ± 0.3[a]	14.6 ± 8.4[a]
Bulk C39	19.6 ± 1.0[b]	22.9 ± 0.2[b]	24.1 ± 1.0[b]	5.8 ± 2.6[a]
		Heating (peak 2; melting)		
Bulk C45	56.8 ± 0.1[a]	57.3 ± 0.0[a]	56.6 ± 1.8[a]	-78.8 ± 43.2[a]
Bulk C39	45.8 ±0.1[b]	46.2 ± 0.0[b]	45.7 ± 1.4[b]	-57.0 ± 10.7[a]

Subscript lower-case letters denote significant differences in a Tukey's post-hoc test with a $p < 0.05$.

The full width at half maximum (FWHM) was also calculated, as this gives information regarding the level of ordering within a TAG system (Lopez et al., 2002). The results showed that a greater amount of disorder was observed within the droplets as compared to the bulk samples. Similarly, milk fat, during cooling at 1 ºC/min, has been recorded to have a FWHM of 0.6 X 10^{-2} $Å^{-1}$, while droplets of 1.3 µm in size cooled at the same rate had a FWHM of 0.4 X 10^{-2} $Å^{-1}$(Lopez et al., 2002; Lopez et al., 2006). This discrepancy between results could be due to the loss of shape observed within C45 and C39 droplets after the heating and cooling cycles (Fig. 6.10 a-b). While some droplets were found to be intact, many coalesced and/or spread out onto the silicone sheet. This was not found to be due to the GISAXS cycle, but due to the presence of water during the temperature cycle. Thus, the differences within the FWHM could be driven by the differences in crystallisation patterns, as the large bulk samples stayed affixed to the hydrophobic silicon wafer (not shown). It should also be noted that research preformed after this experiment demonstrated that droplets created at a slower deposition time (200 µl/min) maintained shape after the thermal cycle and would be recommended for future studies (Fig. 6.10 c-d).

6.3.2 Differential scanning calorimetry

Bulk lipid samples were also subjected to the heating and cooling regime utilising DSC analysis. After holding at 60 ºC, samples were cooled at 1 ºC/min to reach 4 ºC. During cooling, both the C45 and C39 lipids were found to have a significantly different ($p<0.05$) crystallisation peak at 32.3 ± 0.2 and 23.1 ± 0.7, respectively (Table 6.2 & Fig. 6.11). Proportionately, all T_{onset} and T_{endset} values were also different and in accordance with the recorded peaks. The order of crystallisation of the peaks agree with what was observed utilising GISAXS diffraction (Table 6.1). The differences in crystallisation between the C45 and C39 are due to the quantity of hydrophobic interaction present within the different TAG systems.

As the carbon chain-length increased, so did the surface area of the molecule; this allowed for more intermolecular forces (i.e. hydrophobic and van Der Waals) to occur and thus a greater number of interactions resulted in a larger exothermic heat release during crystallisation (Damodaran, Parkin, & Fennema, 2007; Widlak et al., 2001). The larger amount of interactions also means that higher hydrocarbon TAG will crystallise and melt at higher temperatures, as confirmed by the differences observed between the C45 and C39 system and results from other studies (Cebula & Smith, 1991; Lutton & Fehl, 1970).

Interestingly, our lipid samples crystallised during cooling but then had another exothermic event upon heating (Table 6.2 & Fig. 6.11). This recrystallisation was due to the melting of the metastable β', which firstly crystallises into the β polymorph before completely melting (Kellens, Meeussen, Hammersley, & Reynaers, 1991; Widlak et al., 2001). Similar results were observed in other C45 and C39 mixes, in which two endotherms were observed during the heating cycle at 1.25 ºC/min (Kellens et al., 1991). Although β' melting been observed with the DSC Chapter 4 (Fig. 5.6), the endothermic event was not evident during heating, as this was negated by the large exothermic release from the diverse TAG system present.

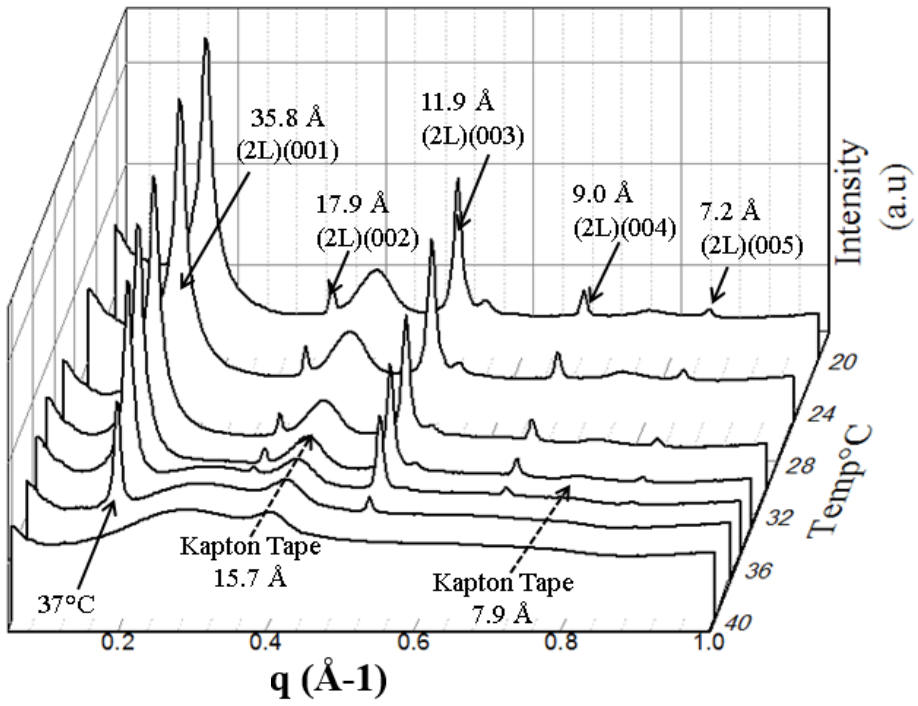

Figure 6.6 *Trimyristin bulk lipid sample during crystallisation from 60 to 4 ºC at 1 ºC/min.*

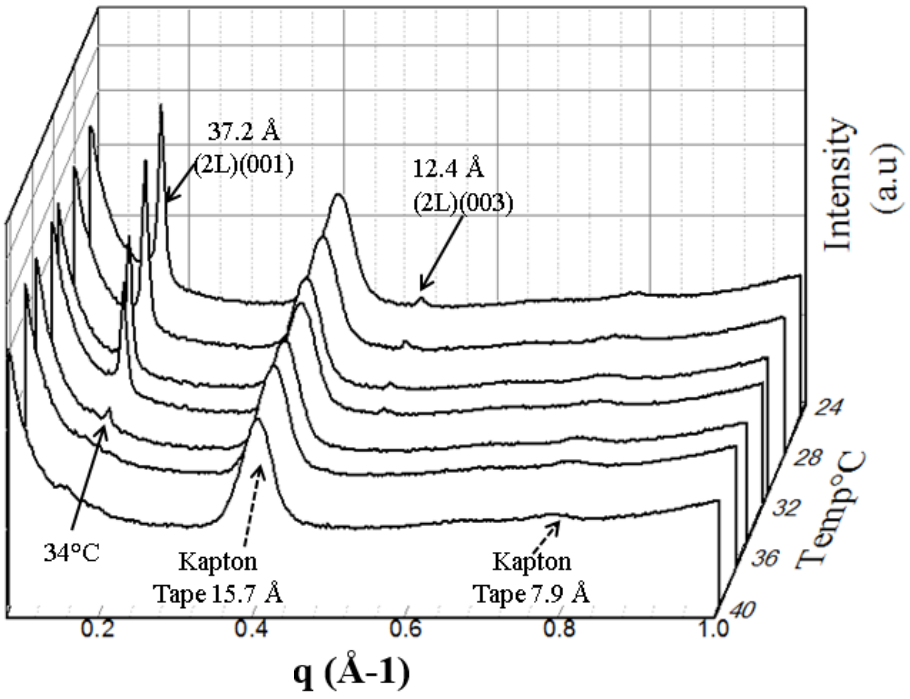

Figure 6.7 *Trimyristin droplet lipid sample during crystallisation from 60 to 4 ºC at 1 ºC/min.*

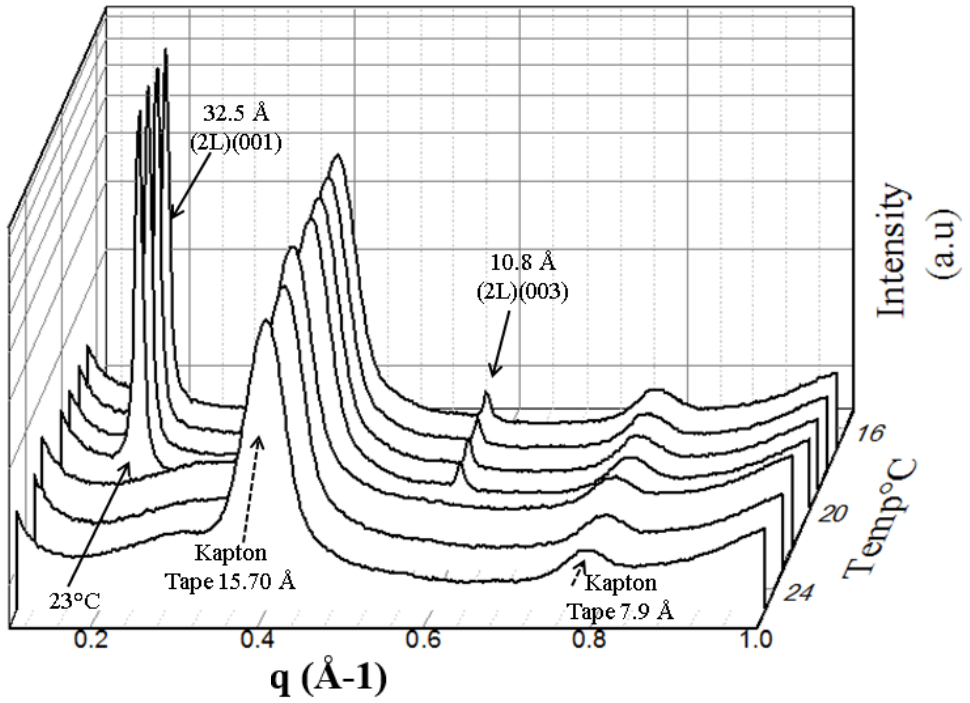

Figure 6.8 *Trilaurin bulk lipid sample during crystallisation from 60 to 4 ºC at 1 ºC/min.*

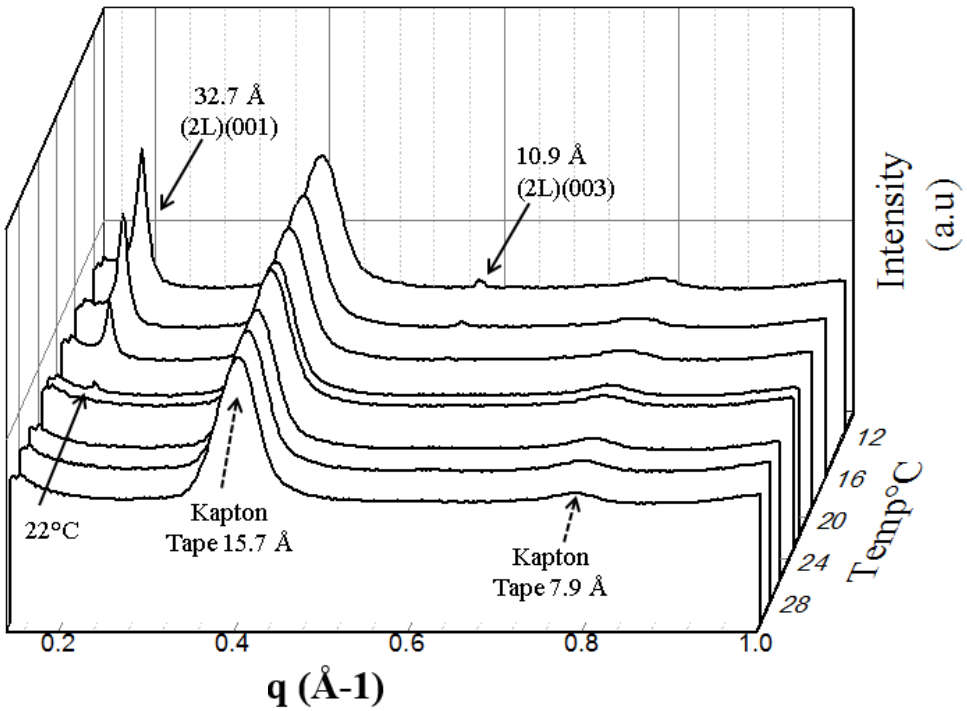

Figure 6.9 *Trilaurin droplet lipid sample during crystallisation from 60 to 4 ºC at 1 ºC/min.*

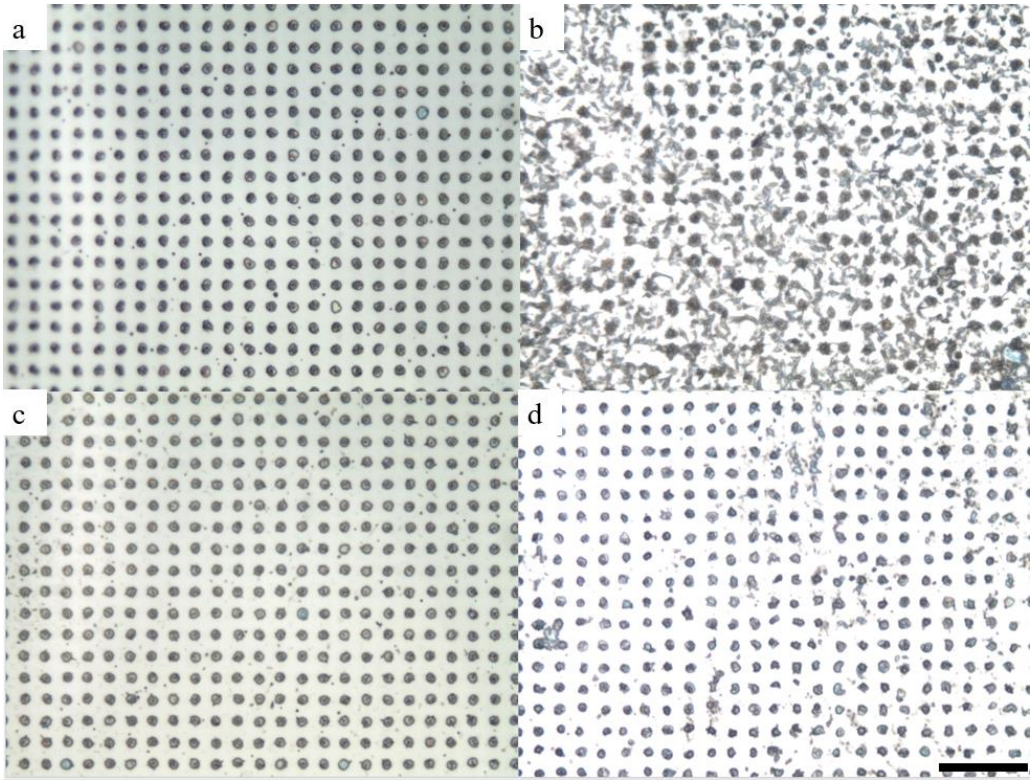

Figure 6.10 *The Trimyristin droplets deposited at 500 µl/min (a) before and (b) after the heating/cooling cycle. The droplets formed at 200 µl/min exhibited less coalesced and are shown (c) before and (d) after the temperature ramp.*

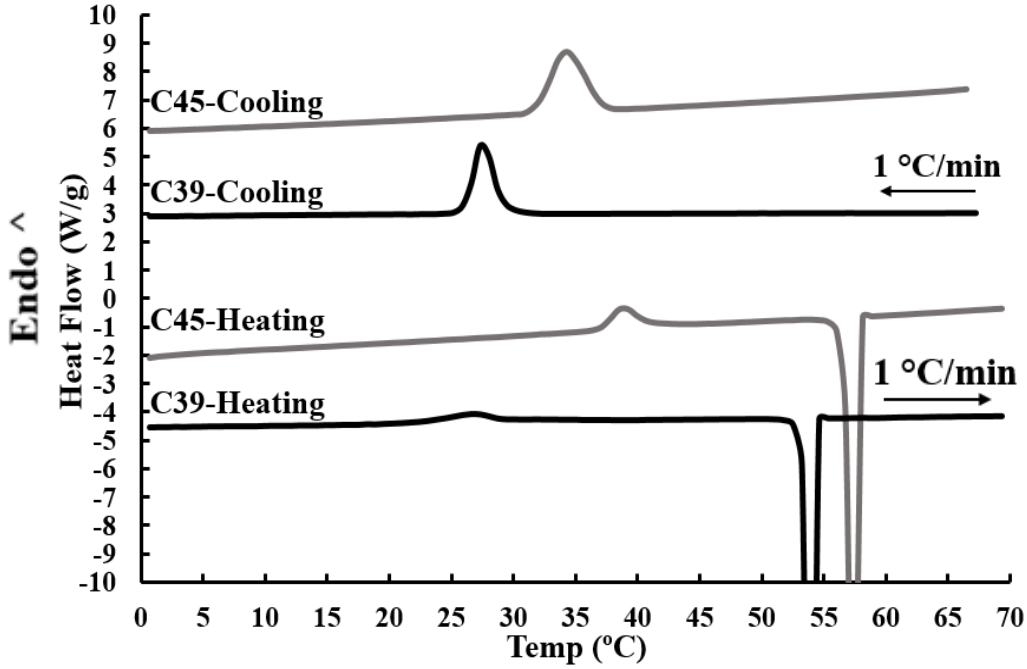

Figure 6.11 *Differential scanning calorimetry thermographs of the C45 and C39 bulk samples during the cooling and heating cycle.*

6.4 Conclusions

Results from this study have demonstrated the possibility of performing GISAXS measurements on two different lipid droplet arrays. Droplets and bulk crystallisation was detectable using GISAXS and results showed an increase in the packing parameter with carbon chain length and an increase in the FWHM in droplet samples. Bulk crystallisation temperatures measured utilising DSC correspond well to synchrotron measurements. Further research should be conducted on more slowly dispositioned droplets and measuring the crystallisation kinetics within these lipid systems. The development of this system allows phytosterols to be observed on a droplet array without the presence of surfactants. Studying this unique system could lead to an increased understanding of how phytosterol crystallisation is influenced by the presence of an oil-and-water interface and by droplet-droplet interactions.

References

Aditya, N. P., Macedo, A. S., Doktorovova, S., Souto, E. B., Kim, S., Chang, P.-S., & Ko, S. (2014). Development and evaluation of lipid nanocarriers for quercetin delivery: A comparative study of solid lipid nanoparticles (SLN), nanostructured lipid carriers (NLC), and lipid nanoemulsions (LNE). *LWT - Food Science and Technology, 59*(1), 115-121. doi:http://dx.doi.org/10.1016/j.lwt.2014.04.058

Bao, L., Rezk, A. R., Yeo, L. Y., & Zhang, X. (2015). Highly ordered arrays of femtoliter surface droplets. *Small, 11*(37), 4850-4855.

Bao, L., Werbiuk, Z., Lohse, D., & Zhang, X. (2016). Controlling the growth modes of femtoliter sessile droplets nucleating on chemically patterned surfaces. *The Journal of Physical Chemistry Letters, 7*(6), 1055-1059.

Bunjes, H., Westesen, K., & Koch, M. H. J. (1996). Crystallization tendency and polymorphic transitions in triglyceride nanoparticles. *International Journal of Pharmaceutics, 129*(1–2), 159-173. doi:http://dx.doi.org/10.1016/0378-5173(95)04286-5

Cebula, D. J., & Smith, K. W. (1991). Differential scanning calorimetry of confectionery fats. Pure triglycerides: Effects of cooling and heating rate variation. *Journal of the American Oil Chemists' Society, 68*(8), 591-595.

Damodaran, S., Parkin, K. L., & Fennema, O. R. (2007). *Fennema's food chemistry*. Boca Raton, FL: CRC press.

Dutta, P. (2000). Grazing incidence X-ray diffraction. *Curr. Sci, 2000*, 1478-1483.

Dyett, B., Yu, H., & Zhang, X. (2017). Formation of surface nanodroplets of viscous liquids by solvent exchange. *The European Physical Journal E, 40*, 1-6.

Flaim, C. J., Chien, S., & Bhatia, S. N. (2005). An extracellular matrix microarray for probing cellular differentiation. *Nature Methods, 2*(2), 119.

Günther, E., Schmid, T., Mehling, H., Hiebler, S., & Huang, L. (2010). Subcooling in hexadecane emulsions. *International Journal of Refrigeration, 33*(8), 1605-1611.

Herhold, A. B., Ertaş, D., Levine, A. J., & King Jr, H. (1999). Impurity mediated nucleation in hexadecane-in-water emulsions. *Physical Review E, 59*(6), 6946.

Jensen, R. G. (2002). The Composition of Bovine Milk Lipids: January 1995 to December 2000. *Journal of Dairy Science, 85*(2), 295-350. doi:http://dx.doi.org/10.3168/jds.S0022-0302(02)74079-4

Kellens, M., Meeussen, W., Hammersley, A., & Reynaers, H. (1991). Synchrotron radiation investigations of the polymorphic transitions in saturated monoacid triglycerides. Part 2: Polymorphism study of a 50:50 mixture of tripalmitin and tristearin during crystallization and melting. *Chemistry and Physics of Lipids, 58*(1), 145-158. doi:http://dx.doi.org/10.1016/0009-3084(91)90120-Z

Lessel, M., Bäumchen, O., Klos, M., Hähl, H., Fetzer, R., Paulus, M., . . . Jacobs, K. (2015). Self- assembled silane monolayers: an efficient step- by- step recipe for high- quality, low energy surfaces. *Surface and Interface Analysis, 47*(5), 557-564.

Li, H., Yang, Q., Li, G., Li, M., Wang, S., & Song, Y. (2015). Splitting a Droplet for Femtoliter Liquid Patterns and Single Cell Isolation. *ACS Applied Materials & Interfaces, 7*(17), 9060-9065. doi:10.1021/am509177s

Lopez, C., Bourgaux, C., Lesieur, P., Bernadou, S., Keller, G., & Ollivon, M. (2002). Thermal and structural behavior of milk fat: 3. Influence of cooling rate and droplet size on cream crystallization. *Journal of Colloid and Interface Science, 254*(1), 64-78. doi:http://dx.doi.org/10.1006/jcis.2002.8548

Lopez, C., Bourgaux, C., Lesieur, P., & Ollivon, M. (2007). Coupling of time-resolved synchrotron X-ray diffraction and DSC to elucidate the crystallisation properties and polymorphism of triglycerides in milk fat globules. *Le Lait, 87*(4-5), 459-480.

Lopez, C., Bourgaux, C., Lesieur, P., Riaublanc, A., & Ollivon, M. (2006). Milk fat and primary fractions obtained by dry fractionation: 1. Chemical composition and crystallisation properties. *Chemistry and Physics of Lipids, 144*(1), 17-33. doi:http://dx.doi.org/10.1016/j.chemphyslip.2006.06.002

Lutton, E., & Fehl, A. (1970). The polymorphism of odd and even saturated single acid triglycerides, C8–C22. *Lipids, 5*(1), 90-99.

Markiewicz-Kęszycka, M., Czyżak-Runowska, G., Lipińska, P., & Wójtowski, J. (2013). Fatty acid profile of milk-a review. *Bulletin of the Veterinary Institute in Pulawy, 57*(2), 135-139.

McClements, D. J. (2012). Crystals and crystallization in oil-in-water emulsions: Implications for emulsion-based delivery systems. *Advances in Colloid and Interface Science, 174*, 1-30.

Montenegro, R., Antonietti, M., Mastai, Y., & Landfester, K. (2003). Crystallization in miniemulsion droplets. *The Journal of Physical Chemistry B, 107*(21), 5088-5094.

Takeuchi, M., Ueno, S., & Sato, K. (2003). Synchrotron Radiation SAXS/WAXS Study of Polymorph-Dependent Phase Behavior of Binary Mixtures of Saturated Monoacid Triacylglycerols. *Crystal Growth & Design, 3*(3), 369-374. doi:10.1021/cg025594r

Torre, L. G., & Pinho, S. C. (2015). Lipid Matrices for Nanoencapsulation in Food: Liposomes and Lipid Nanoparticles. In H. Hernández-Sánchez & G. F. Gutiérrez-López (Eds.), *Food Nanoscience and Nanotechnology* (pp. 99-143). New York, NY: Springer International Publishing.

Widlak, N., Hartel, R. W., & Narine, S. (2001). *Crystallization and solidification properties of lipids*. Champaign, IL: The American Oil Chemists Society.

Ziauddin, J., & Sabatini, D. M. (2001). Microarrays of cells expressing defined cDNAs. *Nature, 411*(6833), 107-110. doi:http://www.nature.com/nature/journal/v411/n6833/suppinfo/411107a0_S1.html

Chapter 7

General discussion and recommendations for future research

Lisa M. Zychowski[†§]

[†] Food Chemistry and Technology Department, Teagasc Food Research Centre, Moorepark, Fermoy, Co. Cork, Ireland

[§] School of Food and Nutritional Sciences, University College Cork, Cork, Ireland

7.1 Overview of findings

As phytosterols and milk fat have not been studied extensively together, it was necessary to establish how the two components influenced the crystallisation behaviour of each separate component (Chapters 2 & 4). This theme is related to the physicochemical properties of the system, i.e., droplet size, emulsion stability, and droplet morphology (Chapters 2, 4, & 5). Low molecular weight surfactants were also studied in this context, as both phytosterol crystallisation and the physiochemical properties of the system were investigated (Chapter 5). Finally, the influence of the o/w interface on crystallisation was also focused on during the study, as it also relates to the final physiochemical properties of the system (Chapters 3 & 6). The following themes are depicted schematically in Figure 7.1 and are explained in detail in the following subsections.

7.1.1 The effect of phytosterols on the crystallisation behaviour of milk fat

The influence of phytosterol crystallisation on the behaviour of milk fat was studied in both bulk and emulsified matrices in this thesis (Chapters 2 & 4). Upon cooling, the 0.3% PE emulsion was the first to start crystallising, which was then followed by the control emulsion and then the 0.6% PE sample. The 0.6% PE emulsion should have nucleated before the 0.3% PE emulsion, due to the higher concentration of impurities, but the delayed nucleation is hypothesised to be due to how the phytosterols crystallised within the milk fat.

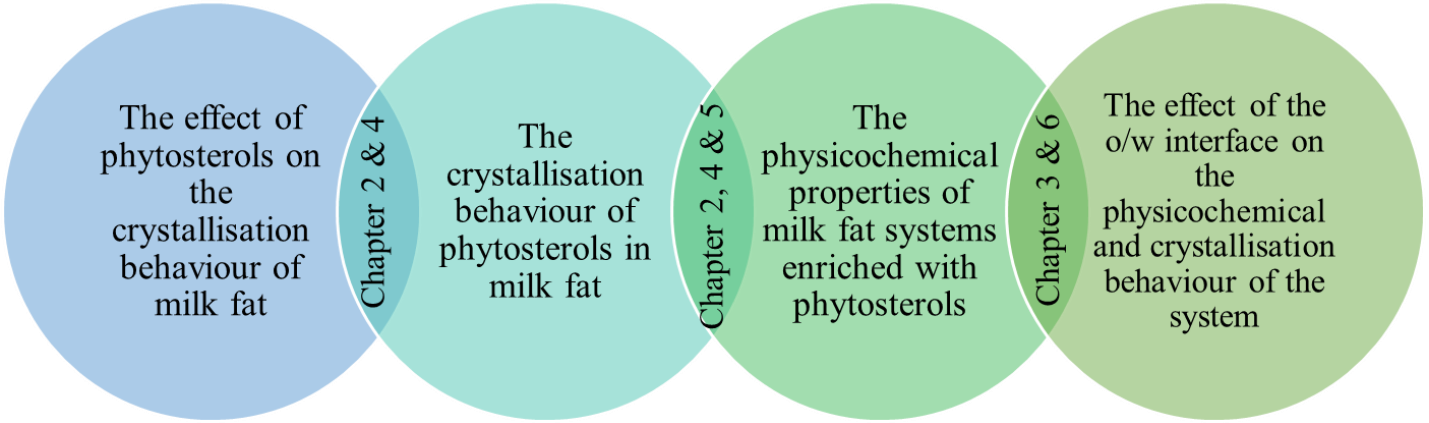

Figure 7.1 *Schematic representation of the associations between the core themes investigated in this thesis*

As detected by Synchrotron SAXS/WAXS analysis, 0.3% PE samples had an increased TAG lamellar spacing, due to phytosterol insertion. In the 0.6% PE sample, a further increase in the lamellar spacing of milk TAG network was found, along with detectable phytosterol crystals. Thus, the delayed nucleation was believed to be due to the supercooling required for the phytosterol crystals to form in emulsified milk fat. Similar results were found in previous studies with lecithin at 0.03, 0.06, and 0.09% wt/wt in palm oil, where blends with the lowest concentration promoted crystallisation and, conversely, higher concentration blends (0.6-0.9%) decreased crystallisation (Miskandar et al., 2006). In bulk milk fat systems enriched with phytosterols (Chapter 4), no difference in nucleation temperature was detected, interestingly similar results have been seen in milk fat bulk and emulsified systems enriched with β-carotene (Zhang et al., 2013).

Regarding the morphology of the emulsified milk fat, phytosterol enrichment was found to increase the lamellar spacing of the milk fat TAG network in the observed 3L spacing. However, the distances within the α polymorph remained the same. This indicated that phytosterols could insert themselves within the milk fat TAG network but did not impact the spacing between the repeating lattice units.

In Chapter 4, the bulk milk fat TAG structure was examined during the initial crystallisation process, as employed in Chapter 2, and after storage at 4 ºC for 48 h. In bulk milk fat, both 2L and 3L packing were detected during the initial crystallisation process. Interestingly, phytosterol insertion into the milk fat TAG packing was observed but only in the 3L spacing and not within the 2L spacing. This is most likely due to the stability and size constrictions of the 2L packing, as 3L packing is more unstable and tends to have a looser configuration (Widlak et al., 2001). After storage, the bulk and emulsified milk fat TAG network rearranged into more stable β’ and β polymorphs (Chapters 2 & 5). Upon TAG restructuring, phytosterols were no longer found to influence the lamellar spacing, which is most likely due to the loss of the loose 3L structure in the more stable TAG configuration.

7.1.2 The crystallisation behaviour of phytosterols in milk fat

During the initial crystallisation process in milk fat, phytosterols crystalline development was investigated in both bulk and emulsified systems (Chapters 2 & 4). In emulsified systems, phytosterol crystals were only found in 0.6% PE samples at

two different diffractions peaks (Chapter 2). Similarly, in bulk milk fat systems, phytosterol crystalline development was only seen in the 0.6% sample; however, the crystals were observed at different Bragg peak distances than in the emulsified sample. This was also noticeable when comparing phytosterol crystals in the two systems after storage (Chapters 4 & 5). In the emulsified system, fewer crystalline peaks were apparent from SAXS/WAXS data and were recorded at different distances, than what was seen in bulk phytosterol-enriched systems. Differences in phytosterol crystalline behaviour are most likely due to the presence of water in the emulsified system as β-sitosterol, the main phytosterol in the mixture used in the study, can only maintain a monohydrated crystal polymorph once in contact with water (Kawachi et al., 2006; Rossi et al., 2010).

Information regarding how phytosterols crystallise in milk fat systems was then utilised to study if the crystalline behaviour of phytosterols could be changed by the addition of low molecular weight surfactants and by changing the droplet size (Chapter 5). Lecithin and MAG were found to significantly decrease phytosterol crystallisation in the bulk phase with no phytosterol crystals detectable in the 3% sample and a smaller number of SAXS/WAXS peaks in the 0.6% sample, as compared to the sample without low molecular weight surfactants. In the emulsion system, phytosterol crystallisation was influenced more by changes in the droplet size than by phytosterol addition. However, the smaller droplet PE emulsions containing lecithin demonstrated the greatest potential for decreasing phytosterol crystallisation among the evaluated systems.

7.1.3 The physicochemical properties of milk fat systems enriched with phytosterols

Phytosterols in milk fat matrices influenced more physicochemical properties of the system, than just crystallisation behaviour. In Chapters 2 and 5, phytosterols were found to be able to decrease the average droplet size of a milk fat emulsion with whey protein alone as the emulsifier, and this was found to be due to synergistic interaction between the two compounds (Chapter 3). However, this change in droplet size did not significantly change the creaming behaviour of the system, as emulsions were found to be equally unstable with and without phytosterols after 1 week and 1 month (Chapters 2 & 5). Interestingly, bioactive crystallisation in an emulsion

system typically causes instability but this was not seen in the studied PE emulsions. Although bioactive crystallisation normally destabilises emulsions, another study found that phytosterols, which had co-crystallised with octenyl succinic anhydride at the o/w interface, had improved emulsion stability and minimised droplet coalescence (Chen et al., 2016).

The PE emulsions were then evaluated for changes in emulsion stability in Chapter 5, upon the addition of MAG or lecithin and by decreasing the droplet size. Decreasing the droplet size was found to significantly improve PE emulsion stability, as seen in previous studies (Dickinson et al., 1997; Abismaïl et al., 1999; Chanamai & McClements, 2000). In PE emulsions with smaller sized droplets, MAG was found to progressively destabilise emulsion systems over time, which is believed to be due to MAG crystallisation. Conversely, PE emulsions containing lecithin with an average droplet size of 0.2 μm had the best emulsion stability over time. As phytosterols typically interact with phosolipids in plant membranes, it is possible that an interaction between these two compounds could be aiding in emulsion stability (Hąc-Wydro et al., 2007).

7.2.4 The effect of the oil-in-water interface on the physicochemical and crystallisation behaviour of the system

The presence of an o/w interface influences the crystallisation behaviour of a system. Supercooling, along with the influence of interfacial components interacting with the lipid phase, can impact the physicochemical and crystallisation properties of the system. In Chapters 2 and 3, phytosterol crystallisation was observed at the o/w interface of 0.6% PE emulsions. This was visualised using polarised light microscopy, CSLM, and Cryo-SEM. Phytosterol enrichment impacted the morphology of emulsion droplets, as some droplets had a rigid edge, suggesting that phytosterol crystallisation could occur at the interface.

There has been very limited research investigating if, and how, phytosterols interact at the interface. Thus, in Chapter 3, phytosterols were studied in a model o/w system using dynamic interfacial tension measurements. These results showed that phytosterols can lower interfacial tension and when combined with whey protein, can lower interfacial tension to a greater extent than when separated. Interfacial data collected and results generated from interfacial models, suggested that phytosterols

are surface active and can participate in a synergistic interaction with whey protein. This synergistic interaction at the o/w interface could explain the decrease in droplet size with phytosterol enrichment, and it is also possible that this interaction is what facilitated the PE emulsions in remaining stable over time.

Finally, in Chapter 6, a system was developed to see if the interface of o/w droplets can be studied without the presence of a surfactant or emulsifier. Solvent exchange was employed on two different TAG lipids found in milk fat in order to create droplets on a substrate. In this study, GISAXS was used, along with a customised cell, to see if the droplets could be detected during the crystallisation and melting processes in the presence of water. Measurements collected quantified the different crystallisation patterns of the lipids, but more work is needed, as droplets were too large and were not significantly different than what was observed in the bulk phase. However, with continued development of the method, droplet array crystallisation could be very interesting in terms of increasing our fundamental understanding of o/w interfacial crystallisation.

7.3 Recommendations for future work

7.3.1 Characterise the relationship between phytosterols and lecithin

In the work conducted in Chapter 5, PE emulsions with lecithin were found to have a smaller number of observed phytosterol peaks, as well as improved emulsion stability. In nature, phosolipids, as present in lecithin, interact with phytosterols in the plant cell membrane (Hąc-Wydro et al., 2007). In addition, lecithin has been known to be able to solubilise phytosterols in micelle systems (Ostlund et al., 1999); however, this relationship has not been well-studied in food systems. Further work could be conducted in this area to characterise how phytosterols and lecithin interact at the o/w interface. It would be worth investigating this by using dynamic interfacial tension measurements in a mixed system, as done in Chapter 3. In addition, it would also be worth examining if a higher concentration of lecithin could increase the loading capacity of the system. Emulsion formulations in this study had a low loading capacity, as emulsions with $\geq 0.8\%$ phytosterol separated immediately and could not be homogenised.

7.3.2 Studies of phytosterols in food emulsion systems

In this system, phytosterols were studied in emulsions with whey protein functioning as the main emulsifier. However, it would be worth examining how caseinate, or even hydrolysed protein, interact with phytosterols. Caseinates are commonly used in the food industry and can migrate to the o/w interface more quickly than whey proteins during emulsion formation (McClements, 2004). They are also more stable to heat than whey proteins, and can have improved stability in processes such as spray drying (Sliwinski et al., 2003). It is possible that caseinate might not interact with phytosterols at the interface, as seen with WPI, but it would be interesting to investigate how phytosterols would behave in other food emulsions.

7.3.3 *In vitro/in vivo* studies

Finally, *in vitro* and *in vivo* studies need to be carried out on the emulsion structures created in this thesis. In Appendix 3, a method is presented for how to carry out an *in vitro* examination of the PE emulsions using a simulated human digestion system. However, only one emulsion system was tested due to time constraints. The emulsion tested also dissolved quite fast in the system used and it would be worth testing if bulk lipid added into the digestion system would give a better indication of phytosterol solubility in the system. *In vivo* studies could also be carried out on the emulsions formulated in Chapter 5. However, as milk fat has been found to naturally form bicontinuous cubosomes during digestion, it would be worth assessing against appropriate control systems with vegetable oil to see how milk fat influences phytosterol absorption between different lipid matrices (Salentinig et al., 2013).

References

Abismaïl, B., Canselier, J. P., Wilhelm, A. M., Delmas, H., & Gourdon, C. (1999). Emulsification by ultrasound: Drop size distribution and stability. *Ultrasonics Sonochemistry, 6*(1–2), 75-83. doi:http://doi.org/10.1016/S1350-4177(98)00027-3

Chanamai, R., & McClements, D. J. (2000). Dependence of creaming and rheology of monodisperse oil-in-water emulsions on droplet size and concentration. *Colloids and Surfaces A: Physicochemical and Engineering Aspects, 172*(1–3), 79-86. doi:http://doi.org/10.1016/S0927-7757(00)00551-3

Chen, X.-W., Guo, J., Wang, J.-M., Yin, S.-W., & Yang, X.-Q. (2016). Controlled volatile release of structured emulsions based on phytosterols crystallization. *Food Hydrocolloids, 56*, 170-179. doi:http://dx.doi.org/10.1016/j.foodhyd.2015.11.035

Dickinson, E., Golding, M., & Povey, M. J. W. (1997). Creaming and flocculation of oil-in-water emulsions containing sodium caseinate. *Journal of Colloid and Interface Science, 185*(2), 515-529. doi:http://dx.doi.org/10.1006/jcis.1996.4605

Hąc-Wydro, K., Wydro, P., Jagoda, A., & Kapusta, J. (2007). The study on the interaction between phytosterols and phospholipids in model membranes. *Chemistry and Physics of Lipids, 150*(1), 22-34. doi:https://doi.org/10.1016/j.chemphyslip.2007.06.211

Kawachi, H., Tanaka, R., Hirano, M., Igarashi, K., & Ooshima, H. (2006). Crystallization of β-sitosterol using a water-immiscible solvent hexane. *Journal of Chemical Engineering of Japan, 39*(8), 869-875.

Khan, J., Hawley, A., Rades, T., & Boyd, B. J. (2015). In situ lipolysis and synchrotron small- angle x- ray scattering for the direct determination of the precipitation and solid- state form of a poorly water- soluble drug during digestion of a lipid- based formulation. *Journal of Pharmaceutical Sciences*.

McClements, D. J. (2004). Protein-stabilized emulsions. *Current Opinion in Colloid & Interface Science, 9*(5), 305-313. doi:http://dx.doi.org/10.1016/j.cocis.2004.09.003

Miskandar, M., Che Man, Y., Abdul Rahman, R., Nor Aini, I., & Yusoff, M. (2006). Effects of emulsifiers on crystallization properties of low-melting blends of palm oil and olein *Journal of Food Lipids, 13*(1), 57-72.

Ostlund, R. E. (2002). Phytosterols in human nutrition. *Annual Review of Nutrition, 22*(1), 533-549.

Ostlund, R. E., Spilburg, C. A., & Stenson, W. F. (1999). Sitostanol administered in lecithin micelles potently reduces cholesterol absorption in humans. *The American Journal of Clinical Nutrition, 70*(5), 826-831.

Rossi, L., ten Hoorn, J. W. S., Melnikov, S. M., & Velikov, K. P. (2010). Colloidal phytosterols: Synthesis, characterization and bioaccessibility. *Soft Matter, 6*(5), 928-936.

Rozner, S., Popov, I., Uvarov, V., Aserin, A., & Garti, N. (2009). Templated cocrystallization of cholesterol and phytosterols from microemulsions.

Journal of Crystal Growth, 311(16), 4022-4033. doi:http://dx.doi.org/10.1016/j.jcrysgro.2009.06.027

Salentinig, S., Phan, S., Khan, J., Hawley, A., & Boyd, B. J. (2013). Formation of highly organized nanostructures during the digestion of milk. *American Chemical Society Nano, 7*(12), 10904-10911.

Sliwinski, E., Lavrijsen, B., Vollenbroek, J., Van der Stege, H., Van Boekel, M., & Wouters, J. (2003). Effects of spray drying on physicochemical properties of milk protein-stabilised emulsions. *Colloids and Surfaces B: Biointerfaces, 31*(1), 219-229.

Widlak, N., Hartel, R. W., & Narine, S. (2001). *Crystallization and solidification properties of lipids*. Champaign, IL: The American Oil Chemists Society.

Zhang, L., Hayes, D. G., Chen, G., & Zhong, Q. (2013). Transparent dispersions of milk-fat-based nanostructured lipid carriers for delivery of β-carotene. *Journal of Agricultural and Food Chemistry, 61*(39), 9435-9443.

Appendix 1

FAMES data for milk fat

Declaration: FAMES data was collected and analysed by Shen Zhiping.

A1.1 Method

The fatty acid methyl esters (FAMES) were prepared from the total lipids using a modified method (Shen et al., 2011). A subsample (50 μL) of melted MF was dissolved in hexane (4 mL) in a glass tube. Two molar KOH in methanol (300 μL) was added into the glass tube and the tube capped after being blanketed under argon, was placed on a Ratek Platform Mixer and shaken at 160 rpm for 20min at room temperature. The solution was then neutralized with 2 M HCl in water (300 μL) containing trace methyl orange indicator. The solution was left to settle for 30 min before the top layer was withdrawn and injected into the GC (1 μL).

The GC analysis was performed using a 6890A GC system (Agilent Technologies Australia Pty Ltd, Mulgrave, Australia), equipped with a SP-2560 fused silica column (100 m, 0.25 mm id and 0.20 μm films, Sigma-Aldrich, Sydney, Australia) and a AOC 5000 autosampler (Shimadzu, Melbourne, Australia). The split ratio was 50:1 and oven temperature was isothermal at 180 °C for 60 mins. Both the injector and detector (FID) temperature were held at 250 °C. Agilent Chemstation software was used to integrate GC area counts. Identification of fatty acid methyl esters were referenced with the published results from the same type of column and temperature programme (Ratnayake et al., 2006) using anhydrous MF (previous internal lab identification)

A1.2 Results

Table A.1 Fatty acid methly esters (FAMES) composition of milk fat utilised in synchrotron and DSC studies.

FAMES	Average (% wt/wt)
C4:0	2.09 ± 0.02
C6:0	1.52 ± 0.02
C8:0	1.10 ± 0.01
C9:0	0.05 ± 0.0
C10:0	2.87 ± 0.03
C10:1(ω1)	0.27 ± 0.0
C12:0	3.74 ± 0.01
C13:0	0.09 ± 0.0
C12:1 (ω9)	0.15 ± 0.01
c13:0	0.10 ± 0.01
C14:0	12.11 ± 0.06
C15:0	2.45 ± 0.01
C14:1 (ω5)	0.93 ± 0.0
C16:0	29.06 ± 0.05
C17:0	0.80 ± 0.03
C16:1 (C 7)	0.25 ± 0.0
C16:1 (C 9)	1.75 ± 0.01
C17:0	0.64 ± 0.01
C17:1 (9C)	0.09 ± 0.0
C17:1 (11C)	0.22 ± 0.01
C18:0	11.36 ± 0.04
C18:1 9t	0.31 ± 0.0
C18:1 (10-11t)	3.77 ± 0.01
C18:1 (12-14t+6-8c)	0.29 ± 0.01
C18:1 (9c+15t+6-10c)	18.07 ± 0.06
18:1 (11c)	0.44 ± 0.02
C18:1 (12c)	0.14 ± 0.0
18:1 (13c)	0.07 ± 0.0
18:1 (16t+14c)	0.63 ± 0.01
C18:1 (15C)	0.28 ± 0.0
18:2 (9t,12t)	0.41 ±0.01
C18:2 ω6(11t, 15c)	0.49 ± 0.01
C18:2 ω6(total) cis-cis	1.12 ± 0.0
C20:0	0.18 ± 0.0
C18:3 (c,c,c)	0.64 ± 0.0
CLA	1.37 ± 0.01

C=cis conformation T=trans conformation ω=double bond iso=isomer CLA=conjugated linoleic acid

References

Ratnayake, W. N., Hansen, S. L., & Kennedy, M. P. (2006). Evaluation of the cp-sil 88 and sp-2560 gc columns used in the recently approved aocs official method ce 1h-05: Determination of cis-, trans-, saturated, monounsaturated, and polyunsaturated fatty acids in vegetable or non-ruminant animal oils and fats by capillary glc method. *Journal of the American oil Chemists' Society, 83*(6), 475-488.

Shen, Z., Apriani, C., Weerakkody, R., Sanguansri, L., & Augustin, M. A. (2011). Food matrix effects on in vitro digestion of microencapsulated tuna oil powder. *Journal of Agricultural and Food Chemistry, 59*(15), 8442-8449.

Appendix 2

Thermal behaviour of phytosterols

A2.1. Introduction

The following experiment was conducted to confirm if the thermal crystal history of the phytosterol was erased in bulk milk fat by using the heating ramp employed in Chapter 2 and 4.

A2.1 Materials and methods

A2.2.1 Chemical and ingredients

Crystalline phytosterol, a mixture of β-sitosterol (≥70%) with residuals of campesterol and β-sitostanol, was purchased from Sigma Aldrich (Wicklow, Ireland). Commercial grade anhydrous milk fat was obtained from Corman Miloko (Carrick on Suir, Ireland).

A2.2.2 DSC

To determine if the phytosterol had been dissolved in the milk fat, DSC data was recorded for the phytosterol powder and with the highest level of phytosterol used within milk fat at 6% (wt/wt). Analysis was only conducted on the bulk sample as temperatures above 100 ˚C are not recommended for emulsion-type samples, due to the boiling of the aqueous phase (Dumas et al., 1994). The samples were prepared by heating AMF to 110 ˚C with continuous stirring at 300 rpm on a magnetic heating plate. Upon reaching 110 ˚C, the phytosterol powder was added to the milk fat at 6% and was withheld in the control sample. Samples were then stirred for 2 min, as done in Chapters 2-5. The oil was then cooled to 80°C and subsequently ~19-21 mg was pipetted into a 40 μL aluminium pan for DSC analysis, as done in Chapters 2, 4 and 5. Samples were then allowed to cool statically and were held at room temperature for 24 h. Due to the lower density of the bulk phytosterol powder, only 11-13 mg could be measured within the pan.

Milk fat samples were then placed onto the DSC (Mettler-Toledo DSC 821e, Schwerzenbach, Switzerland) and were heated from 25-60 °C at 10 °C/min, as done within Chapters 2 and 4. After 5 min of holding at 60 °C, the samples were then ramped to 155 °C at 10°C/min to see if a phytosterol peak could be observed within the phytosterol-enriched (PE) bulk milk fat samples.The bulk phytosterol powder

was simply heated from 25-155 ℃ at 10 ℃/min to observe its general melting profile.

A2.2.3 Synchrotron SAXS/WAXS

Phytosterol-enriched bulk milk fat samples were prepared as described in the DSC section above. However, after mixing, the milk fat was placed into a quartz capillaries of 1.5 mm diameter (GLAS Muller, Berlin, Germany) and held at room temperature for 48 hrs. Samples were placed onto adapted Linkham microscope stage for heating and cooling with a steel holder designed to hold the capillary upright in the X-ray beam. Samples were heated from 25° C to above 60 ℃ at 10 ˚C/min and held at that temperature for 5 min. Scattering data was collected during the at the end of the holding period, as described in Chapter 2.

A.2.3 Results and discussion

The DSC data demonstrated that the phytosterol (PS) powder used throughout the thesis melted from ~125-142 ℃ (Fig. A.2.1). Similar results have been observed with other phytosterol blends (Vaikousi et al., 2007). In addition, after the holding period, PE milk fat was found not to possess a phytosterol melting peak. However, phytosterols were found to change the normal melting profile of milk fat (Figure A.2.1 & Fig. 5.6), which could be from the melting of the phytosterols. Several possibilities could exist as to why the thermal behaviour of the phytosterols changes so dramatically once mixed with the milk fat.

As suggested by Acevedo & Franchetti (2016), phytosterols can co-crystallise with other food TAG. Results from the mentioned study demonstrated that phytosterols melt at much lower temperatures when combined with soy bean oils, as compared to the bulk phytosterol powder. For example, the β-sitosterol used in this experiment melted at 137.78 ± 0.79 ℃. However, when this was mixed with soy bean oil, the melting temperature changed to 63.02 ± 2.00 ℃ (Fig. A.2.2). In addition, it could be possible that the phytosterol crystals are co-crystallising with the cholesterol present in milk, as this too has been found to change the thermal properties of the phytosterols (Rozner et al., 2009).

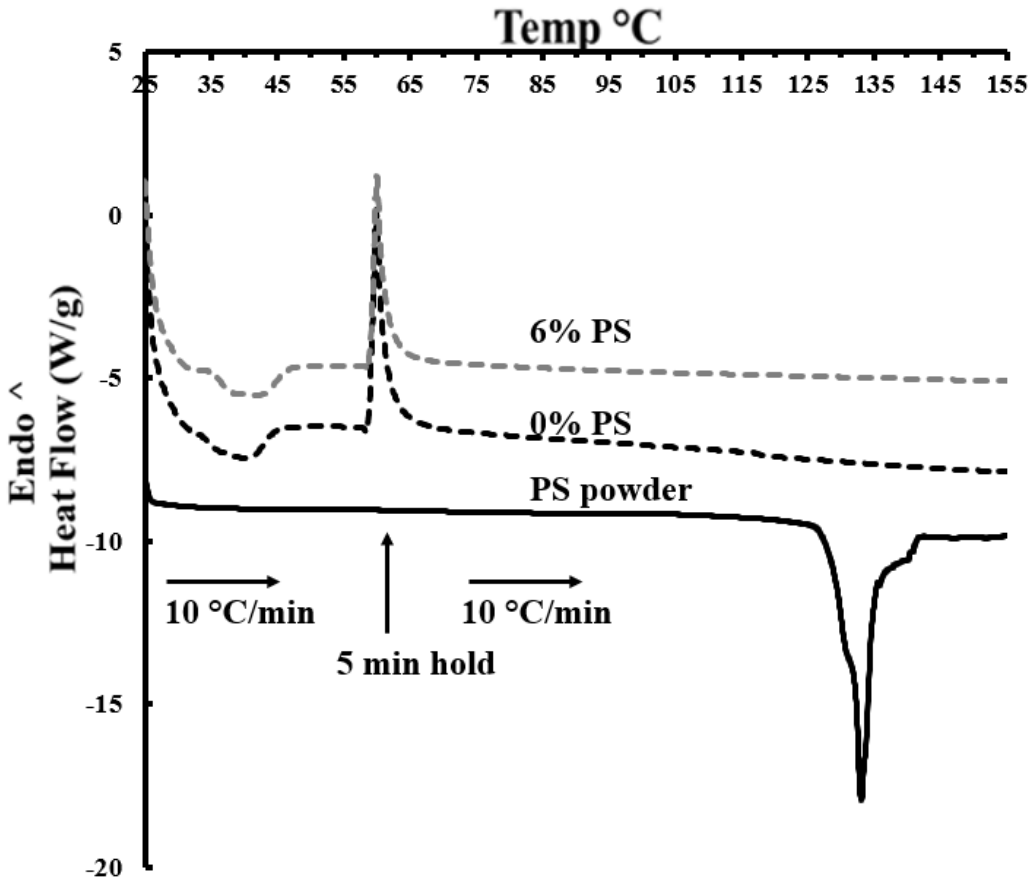

.

Figure A.2.1 *DSC thermographs of phytosterol (PS) powder and phytosterol enriched bulk milk fat at 0 and 6% (wt/wt) during the heating ramp used in Chapter 2 and 4. After the holding period, an additional heating step to 155 °C was employed in the bulk milk fat samples. Note that the PS powder was not held at 60 °C.*

Beyond the DSC data, synchrotron results captured at the end of the hold time at 60 °C also demonstrated a lack of long-range order and did not record the presence of any phytosterol crystals (Fig. A.2.3). In addition, images captured using a slower heating process (2 °C/min instead of 10 °C/min) in Chapter 4 also showed phytosterol crystal melting at temperatures below 60 °C (Fig. 4.9).

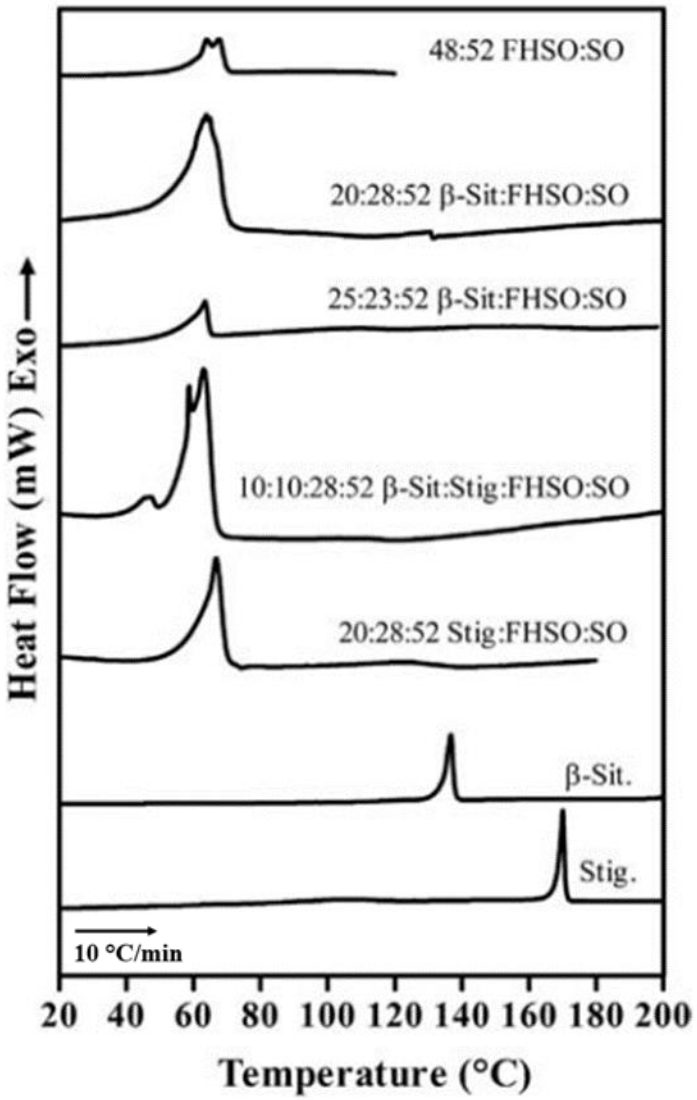

Figure A.2.2 *DSC thermograms of fully-hydrogenated soy bean oil (FHSO) blended with soy bean oil (SO) with or without β-sitosterol (β-Sit.) and/or stigmasterol (Stig.; Acevedo & Franchetti, 2016).*

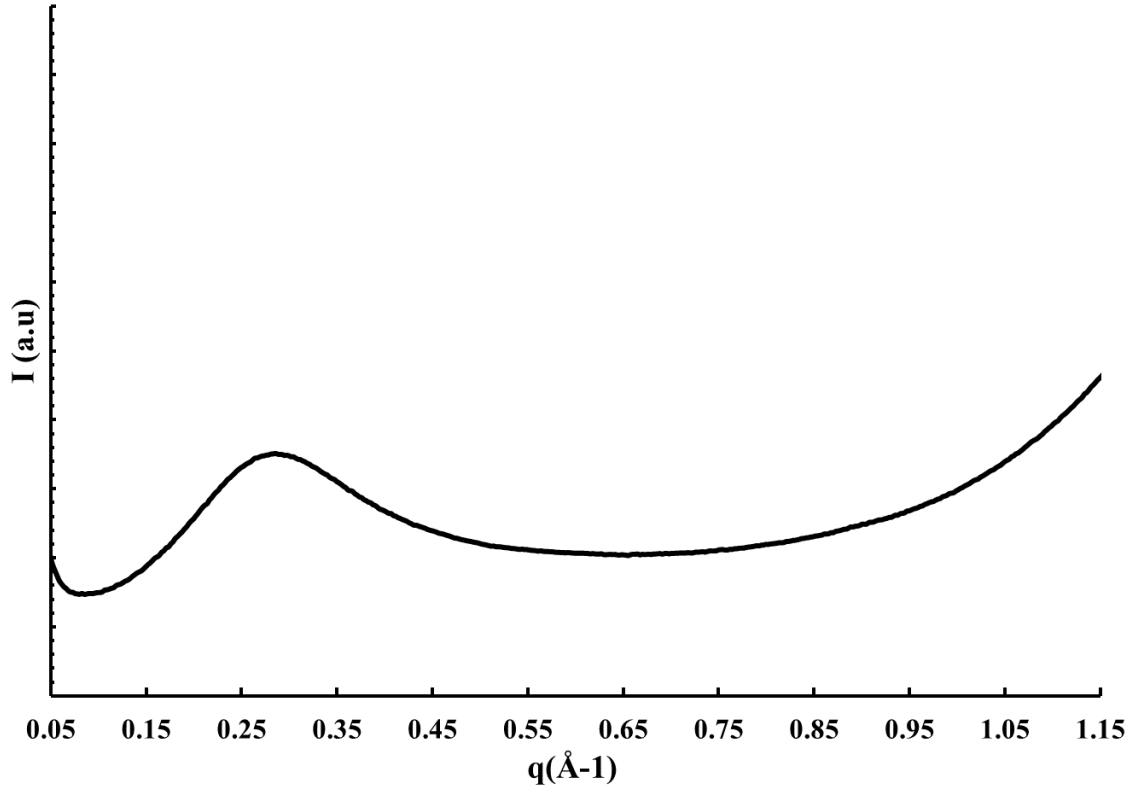

Figure A.2.3 *Synchrotron diffraction pattern of 6% phytosterol-enriched bulk milk sample after the holding period at 60 °C for 5 min. Graph includes SAXS diffraction pattern with WAXS overlap to demonstrate the lack of both phytosterol and milk fat crystals. Standard milk fat and phytosterol peaks can be located on Figure 5.1.*

A.2.4 Conclusion

The heating ramp from Chapter 2 and 4 was employed in the 6% PE bulk milk fat sample. As indicated by synchrotron and DSC data, the sample was found to have its thermal crystal history erased, and no phytosterols crystals were observed.

References

Acevedo, N. C., & Franchetti, D. (2016). Analysis of co-crystallized free phytosterols with triacylglycerols as a functional food ingredient. *Food Research International, 85*, 104-112. doi:http://dx.doi.org/10.1016/j.foodres.2016.04.012

Dumas, J. P., Zeraouli, Y., & Strub, M. (1994). Heat transfer inside emulsions. Determination of the dsc thermograms. Part 2. Melting of the crystallized droplets. *Thermochimica Acta, 236*(Supplement C), 239-248. doi:https://doi.org/10.1016/0040-6031(94)80272-6

Rozner, S., Popov, I., Uvarov, V., Aserin, A., & Garti, N. (2009). Templated cocrystallization of cholesterol and phytosterols from microemulsions. *Journal of Crystal Growth, 311*(16), 4022-4033. doi:http://dx.doi.org/10.1016/j.jcrysgro.2009.06.027

Vaikousi, H., Lazaridou, A., Biliaderis, C. G., & Zawistowski, J. (2007). Phase transitions, solubility, and crystallization kinetics of phytosterols and phytosterol−oil blends. *Journal of Agricultural and Food Chemistry, 55*(5), 1790-1798. doi:10.1021/jf0624289

Appendix 3

Method and data for human *in vitro* digestion system

Method and data for human *in vitro* digestion system

A3.1. Introduction

The following experiment is included as information for future *in vitro* studies on different PE emulsions (Chapter 7.3). As only one emulsion was studied here, this data is not complete but is detailed as a design concept.

A3.2 Materials and methods

A3.2.1 Materials

In this study milk fat was purchased from Marsh Dairy Product (Footscray, Australia) and WPI (ALACEN© 895, protein content 92.0%) was sourced from Frontera (Maungaturoto, New Zealand). For the digestion buffer tris maleate (reagent grade), bile salt (sodium taurodeoxycholate, >95%), and 4-bromophenylboronic acid (4-BPBA, >95%) were obtained from Sigma-Aldrich (St. Louis, Missouri). Calcium chloride dihydrate (>99%) was purchased from Ajax Finechem (Seven Hills, Australia). Sodium chloride (>99%) was sourced from Chem Supply (Gillman, Australia).

A3.2.2 Methods

A PE emulsion was prepared as an outline in Chapter 2 at 0.6% phytosterol enrichment. The emulsion was stored at 4°C for 48 h before 13 ml of the emulsion was dispersed into 14 ml of the fabricated human bile salts, as prepared previously (Khan et al.,2015). This level was chosen as it corresponded to the quantity of milk fat digested in a previous study (Salentinig et al., 2013). The emulsion was then added into a jacketed digestion vessel at 37 °C. The glass vessel was manually titrated to a pH of 6.5 ± 0.003 and allowed to equilibrate for 5 min with stirring. The vessel was equipped with a stirrer (801 Stirrer MetrohmR, Switerland) and a pH-stat apparatus attached to a glass pH electrode (iUnitrode, MetrohmR, Switerland) for recording (Fig. A3.1). After equilibration, 5 g of lipase was added to the vessel to begin lipolysis. As free fatty acids were released, a 0.6 M solution of NaOH was used to bring the pH back to 6.5. The pH was set at 6.5, as it falls between the recommended pH ranges for pancreatic lipase activity (pH 6–10) and duodenal pH (5.9–6.5; Khan et al.,2015). Samples were run until the pH stat reached equilibrium, in approximately ≥ 30 min, signaling the completion of lipolysis. SAXS data was

collected during digestion using the Australian SAXS/WAXS beamline. The synchrotron was arranged as detailed in Khan et al. (2015) but with a q range of 0.03-1.4 $Å^{-1}$.

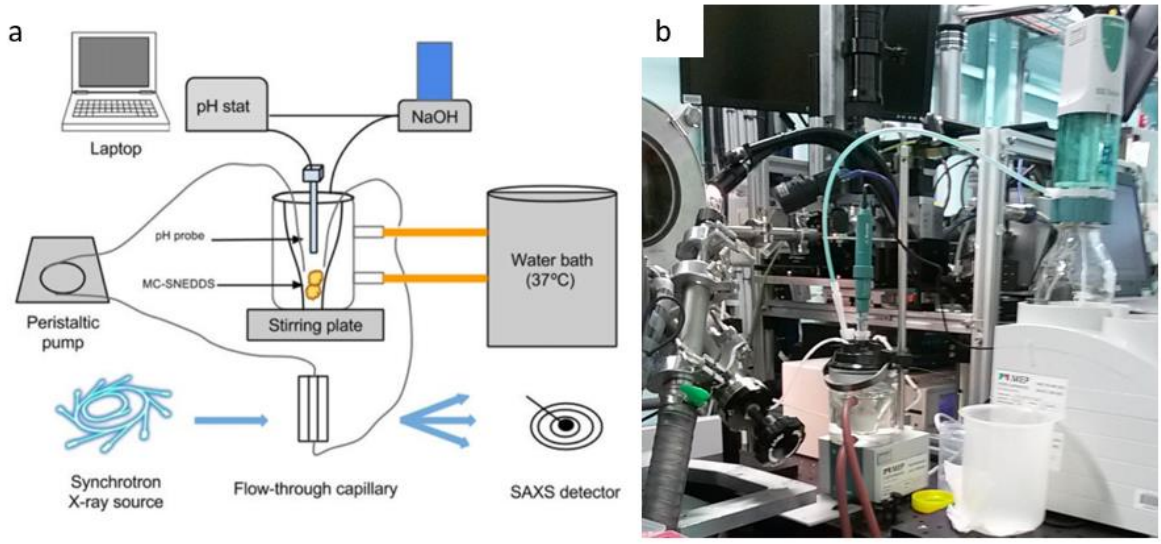

Figure A3.1 *(a) Configuration of the system for in situ lipolysis used for PE digestion. (b) Picture of the digestion vessel on the Australian SAXS/WAXS beamline.*

A3.3 Results and discussion

After addition into the bile salts, only two out of the potential 4 peaks seen in Chapter 5 were observed (Fig. A3.2). However, as the measurement system is dynamic, it is hard to distinguish if this result was due to the bile salt, temperature change, or background, as the liquid was constantly flowing through the measurement cell. The *in situ* digestion of the PE emulsion showed that, at 240 s the phytosterol peaks were no longer detectable. We could also see that, at even higher Bragg distances, another peak was developing; this was most likely a lamellar milk fat arrangement, as milk assembles into this first during digestion before more complex formations (Salentinig et al., 2013). The loss of noticeable phytosterol crystals was very rapid, as the total digestion lasted for 30 min. At this time, it is

unclear if this result was what should have been observed or if the phytosterol crystalline peaks were too small against the background.

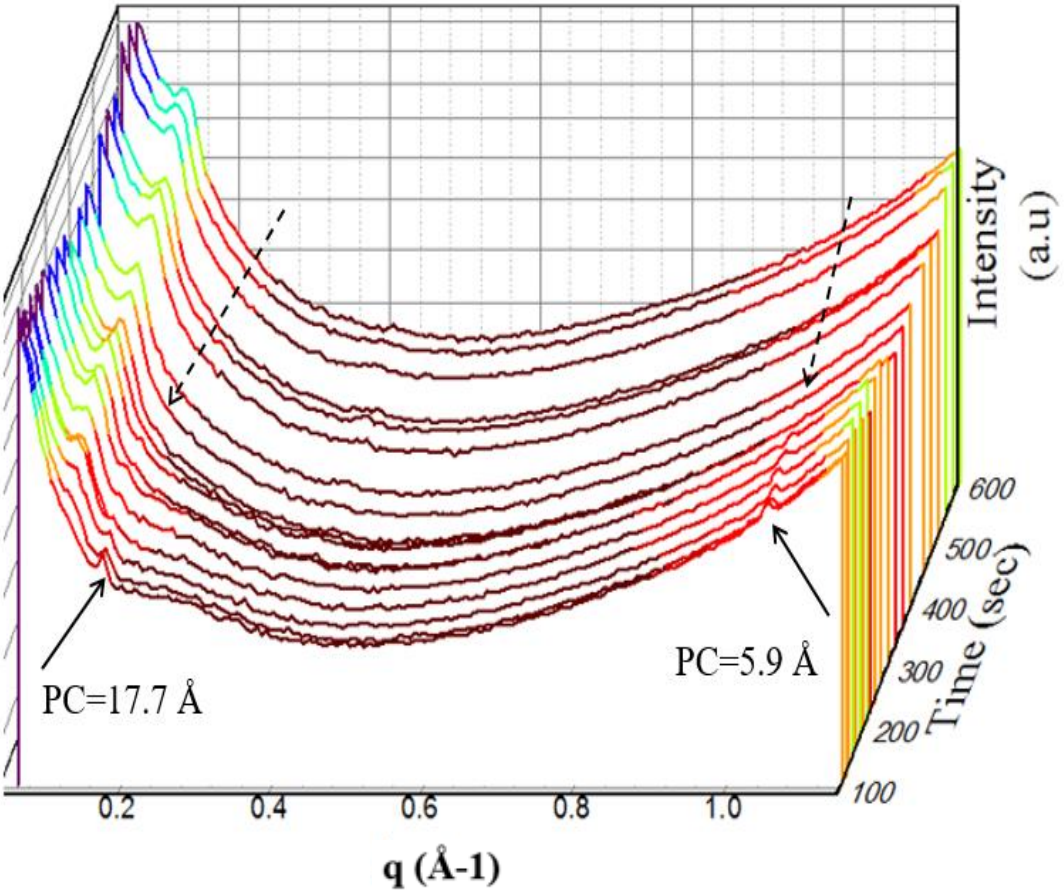

Figure A.3.2 *Structural evolution of 0.6% PE emulsion during the in situ digestion process at 37°C after cooling at -3 °C/min. Graph includes SAXS diffraction pattern with slightly longer distances to demonstrate the presence of phytosterol crystals. The solid arrows are used to highlight phytosterol crystals before digestion. After the first diffraction pattern, lipase was added and digestion began. The dotted arrows show when phytosterol crystals are no longer observed after 240 s. PC=Phytosterol crystal*

For future studies, it is recommended to try using higher quantities of PE emulsions into the bile salt mixtures before addition into the digestion cell, as intensity of the phytosterol peaks in this sample were low compared to the background of the cell. If it is not possible to achieve the level of diffraction necessary to visualise the phytosterols in an emulsion system, it would be worth examining the different bulk formulations. For example, as lecithin was seen to decrease phytosterol

crystallisation in the bulk system, it would be interesting to see if the phosolipids were able to influence *in situ* digestion at all.

A3.4 Conclusion

By employing dynamic SAXS measurements, a PE emulsion was digested using an *in situ* configuration. The emulsion dissolved after 240 s, but these results have not been confirmed. Further development work needs to be performed on the system and more PE emulsions should be examined.

References

Khan, J., Hawley, A., Rades, T., & Boyd, B. J. (2015). In situ lipolysis and synchrotron small-angle x-ray scattering for the direct determination of the precipitation and solid-state form of a poorly water-soluble drug during digestion of a lipid-based formulation. *Journal of Pharmaceutical Sciences*.

Salentinig, S., Phan, S., Khan, J., Hawley, A., & Boyd, B. J. (2013). Formation of highly organized nanostructures during the digestion of milk. *American Chemical Society Nano, 7*(12), 10904-10911.

Appendix 4

Published works

JOURNAL OF AGRICULTURAL AND FOOD CHEMISTRY

Article

pubs.acs.org/JAFC

Effect of Phytosterols on the Crystallization Behavior of Oil-in-Water Milk Fat Emulsions

Lisa M. Zychowski,[†,§,Δ,#] Amy Logan,[*,Δ] Mary Ann Augustin,[Δ] Alan L. Kelly,[§] Alexandru Zabara,[#] James A. O'Mahony,[§] Charlotte E. Conn,[#] and Mark A. E. Auty[*,†]

[†]Food Chemistry and Technology Department, Teagasc Food Research Centre, Moorepark, Fermoy, County Cork, Ireland

[§]School of Food and Nutritional Sciences, University College Cork, Cork, Ireland

[Δ]CSIRO Food and Nutrition, Werribee, Victoria 3030, Australia

[#]School of Applied Science, RMIT University, Melbourne, Victoria 3000, Australia

ABSTRACT: Milk has been used commercially as a carrier for phytosterols, but there is limited knowledge on the effect of added plant sterols on the properties of the system. In this study, phytosterols dispersed in milk fat at a level of 0.3 or 0.6% were homogenized with an aqueous dispersion of whey protein isolate (WPI). The particle size, morphology, ζ-potential, and stability of the emulsions were investigated. Emulsion crystallization properties were examined through the use of differential scanning calorimetry (DSC) and Synchrotron X-ray scattering at both small and wide angles. Phytosterol enrichment influenced the particle size and physical appearance of the emulsion droplets, but did not affect the stability or charge of the dispersed particles. DSC data demonstrated that, at the higher level of phytosterol addition, crystallization of milk fat was delayed, whereas, at the lower level, phytosterol enrichment induced nucleation and emulsion crystallization. These differences were attributed to the formation of separate phytosterol crystals within the emulsions at the high phytosterol concentration, as characterized by Synchrotron X-ray measurements. X-ray scattering patterns demonstrated the ability of the phytosterol to integrate within the milk fat triacylglycerol matrix, with a concomitant increase in longitudinal packing and system disorder. Understanding the consequences of adding phytosterols, on the physical and crystalline behavior of emulsions may enable the functional food industry to design more physically and chemically stable products.

KEYWORDS: *phytosterols, plant sterols, synchrotron, crystallization, emulsion, milk fat, delivery systems, bioactive, functional foods*

INTRODUCTION

Phytosterols are naturally occurring compounds found in cereals, nuts, vegetables, and fruits. There are over 200 identified types of phytosterols, the most abundant being β-sitosterol, campesterol, and stigmasterol.[1] They are chemically similar to human cholesterol, differing only in the presence or absence of a double bond and a side chain at the C-24 position.[2] This similarity enables phytosterols to effectively reduce serum cholesterol by preventing its absorption in the intestinal tract. Mechanistically, this is achieved through competitive solubilization between cholesterol and plant sterols in the bile salt and acid micelles. The result is an increase in endogenous cholesterol synthesis, which mediates removal of low-density lipoproteins (LDL) from the blood.[3−7]

To significantly lower LDL-cholesterol levels, it is recommended to consume >1.5 g of plant sterols daily.[8] To achieve these levels, dietary supplementation is needed, as the average intake of plant sterols is between 160 and 400 mg per day.[9] Due to a global rise in diet-related chronic diseases, there has been an increased interest in using phytosterols in functional foods. However, successful incorporation of these molecules within food matrices has been challenging because of their low solubility, lipophilic nature, and high melting point.[10−12]

To overcome these challenges, the functional food industry traditionally esterified phytosterols to solubilize them into high-fat matrices such as plant margarines. Although esterified phytosterols are more soluble in oil than their nonesterified counterparts, their application is not preferred due to higher processing costs and unpredictable adsorption rates.[10,13] Ester varieties need to be hydrolyzed prior to absorption, which is subject to interindividual variability among human digestive systems, resulting in absorption rates varying between 40 and 96%.[5,10,14−16] To enhance the solubility of unesterified phytosterols, emulsion-based delivery systems have been employed and proven successful in lowering LDL-cholesterol.[17−20]

Although phytosterol-enriched emulsion systems are effective at lowering LDL-cholesterol, their success is still highly dependent upon the physical state and location of the phytosterols in the emulsion system. It has been demonstrated that solubilized phytosterols are more effective at lowering LDL-cholesterol levels than dispersed nonsolubilized phytosterols.[19,21−23] In the design of an appropriate carrier matrix, functional performance of the bioactive in the chosen matrix is crucial to ensuring the success of the final functional food.[24]

In this study, a milk fat-based emulsion was chosen as the carrier matrix. Milk has become a popular carrier for phytosterols, as it has been reported to be more effective at lowering LDL-cholesterol than bread or cereals.[25] In a previous

Received: April 15, 2016
Revised: June 21, 2016
Accepted: July 30, 2016
Published: July 30, 2016

DOI: 10.1021/acs.jafc.6b01722
J. Agric. Food Chem. 2016, 64, 6546−6554

study, a 29.1 ± 4.1% reduction in LDL-cholesterol levels was observed when subjects ingested milk enriched with emulsified phytosterols using a proprietary crystal-retardation method.[22] In addition, the diverse blend of triacylglycerols (TAG) in milk fat has been found to be more effective than soybean oil for the encapsulation of the bioactive β-carotene.[26] Milk fat contains up to 400 different types of fatty acids, which generates a complex crystalline TAG network upon cooling.[27] Milk fat has the potential to encapsulate other types of bioactives, but limited knowledge exists about how the physical and chemical properties of the milk fat are affected by this or what type of compounds can be incorporated.

Thus, this study aimed to develop knowledge regarding the use of milk fat-based emulsions for the delivery of phytosterols. The crystallization and melting properties of phytosterols within emulsified milk fat systems was investigated through thermal and structural analysis. The stability, particle size, and ζ-potential of the emulsions were also monitored to understand how phytosterol incorporation affects the physical properties and stability of the emulsion systems. This knowledge will enable the functional food industry to optimize the bioaccessibility and functional performance of phytosterol-enriched dairy products.

MATERIALS AND METHODS

Chemicals and Ingredients. Crystalline phytosterol, a mixture of β-sitosterol (≥70%) with residuals of campesterol and β-sitostanol, was purchased from Sigma-Aldrich (Wicklow, Ireland). Commercial grade anhydrous milk fat was obtained from Marsh Dairy Products (Footscray, Australia). Whey protein isolate (WPI) (ALACEN 895, protein content = 92.0%) was purchased from Fronterra (Maungaturoto, New Zealand). Sodium azide was purchased from Sigma-Aldrich (Castle Hill, Australia). Emulsions prepared for imaging in Ireland utilized anhydrous milk fat purchased from Corman Miloko (Carrick on Suir, Ireland) and WPI (BiPro protein content = 92.7%) sourced from Danisco Food International (Eden Prairie, MN, USA).

Preparation of Emulsions. Oil-in-water emulsions (10% oil/1% protein/89% H_20) were prepared on a wt %/wt basis with or without added phytosterols in the oil fraction (0.3 or 0.6 wt %/wt). The aqueous phase was prepared by reconstituting WPI at 11.11% protein for 2 h in an ice bath with Milli-Q water. The solution was then stored overnight at 4 °C to allow for complete hydration. Before homogenization, aliquots of WPI solution needed to create 1% protein in the final emulsion were removed and heated to 55 °C for 20 min. After heating, the WPI solution was diluted with distilled water at 70 °C and then subsequently added to the oil phase. This process was employed to minimize denaturation of the whey protein by high temperatures or excessive heat exposure.[28]

The oil phase was prepared by heating the milk fat to 110 °C and holding the sample at this temperature for 2 min with stirring on a magnetic hot plate at 300 rpm. If phytosterols were added, they were included at the start of the 2 min hold time. After the hold time, the oil phase was added to the aqueous phase, and the mixture was sheared with a Silverson rotor-stator mixer for 1 min at 3200 rpm and 65 °C to form a pre-emulsion. The pre-emulsion was then homogenized using an EmulsiFlex-C5 (Avestin, Mannheim, Germany) operating at 300 bar pressure at 60 °C in a single pass. The control emulsion (without added phytosterol) and phytosterol-enriched (PE) emulsions were then statically cooled and stored at 25 °C. After cooling, 0.01% sodium azide was added to prevent microbial growth during storage, and samples were analyzed within 24 h of production.

In total, three different levels of enrichment were chosen for the PE emulsions: 0.0, 0.3, and 0.6%. The 0.0% PE emulsion functions as the control sample as it contains only milk fat in the dispersed phase. The next two levels of enrichment, 0.3 and 0.6%, are expressed in this study based on the weight by weight percentage of total phytosterol in the emulsion. The 0.6% PE emulsion was chosen as the highest level of enrichment, as the emulsion at 0.8% enrichment was not stable and separated immediately upon prehomogenization. It can be noted that all formulated emulsions had a pH of 6.8, independent of phytosterol enrichment.

Particle Size. The particle size of the emulsions was measured by laser light scattering using a Mastersizer 2000 instrument (Malvern Instruments Ltd., Worcestershire, UK). The emulsions were measured at room temperature in a Hydro SM cell with an obscuration of ∼10%. A differential refractive index of 1.095 (1.462 for milk fat/1.33 for water) and an absorption of 0.001 were used as optical parameters for the measurements. Particle size distributions and volume-weighted mean diameters ($D_{4,3}$)

$$D_{4,3}\left(= \sum n_i d_i^4 / \sum n_i d_i^3 \right) \quad (1)$$

were calculated on the basis of spherical geometry, where *ni* is the number of droplets with diameter *di* (eq 1). Measurements were averaged from two replicates, and trials were repeated in triplicate.

Emulsion ζ-Potential. The ζ-potential of each emulsion was determined using a Malvern Nano ZS. Before analysis, each emulsion was diluted to 1:200 in Milli-Q water. An electric field was then applied to each sample in a folded capillary cell held at 25 °C. Using the Smoluchowski model, the direction and velocity of the droplet was used to calculate the ζ-potential of the particles present. The results and standard deviations are reported as the average of two measurements on three individual emulsion preparations.

Optical Characterization of Emulsion Stability. Emulsion stability was assessed using a light-scattering optical analyzer (Turbiscan MA2000, Formulaction, France) as a function of time. After cooling, 6 mL of emulsion samples were placed into glass holding cells to be measured at day 0. Samples were then held at 25 °C and measured again on days 1, 3, 5, and 7 to compare the amount of destabilization between treatments. Maximum backscattering values for each treatment were used to compare the percentage difference between days 0 and 7 during storage. Light photons were backscattered along the length of the tube containing a near-infrared diode. Scattering data was then collected and interpreted for emulsion destabilization.

Differential Scanning Calorimetry. Thermal analysis of onset temperatures and peaks was conducted on emulsion samples using a DSC 1 STARe System (Mettler Toledo, Port Melbourne, Australia) and software (version 12.10). Samples were stored at room temperature prior to analysis, for which aliquots (∼19−21 mg) were weighed into a 40 μL aluminum pan (Mettler Toledo, part no. ME-27331) and hermetically sealed. Milli-Q was used in the reference pan. Thermal history of the phytosterols and milk fat was found to be erased by heating samples from 25 to 60 °C at 10 °C/min and holding the samples at this temperature for 5 min. After holding, the samples were cooled from 60 to 4 °C at a rate of 3 °C/min and held at 4 °C for 5 min. Samples were then heated to 60 °C at a rate of 10 °C/min. Analysis was conducted in triplicate.

Synchrotron X-ray Analysis. The Australian Synchrotron SAXS/WAXS beamline in Clayton, Australia, was used to perform scattering experiments at a flux of 14 keV and a camera length of 0.9 m. Diffraction patterns were recorded in the small-angle (q = 0.03−1.4 $Å^{-1}$) and wide-angle regions (q = 0.9−3.5 $Å^{-1}$) using a Dectris Pilatus 1 M and a Pilatus 200 K detector, respectively. Detailed information regarding the beamline systems and parameters can be found elsewhere.[29] Emulsion samples of 20 μL were decanted into quartz capillaries of 1.5 mm diameter (GLAS Muller, Berlin, Germany) and subjected to a temperature ramp. The heating/cooling element for the melting and cooling stages was an adapted Linkham microscope stage with a steel holder designed to hold the capillary upright in the X-ray beam. Samples were heated from 25 to >60 °C at 10 °C/min and held at that temperature for 5 min. All samples were found to be in a liquid crystalline lamellar state prior to cooling. Cooling was conducted at 3 °C/min until 4 °C was reached. Small-angle X-ray scattering (SAXS) and wide-angle X-ray scattering (WAXS) patterns were collected once the sample reached the isothermal period. The machine scanned for 3 s of live time with a subsequent 7 s of dead time over a 15 mm gap in

DOI: 10.1021/acs.jafc.6b01722
J. Agric. Food Chem. 2016, 64, 6546−6554

series to avoid overexposing the sample. After 5 min of holding at 4 °C, the stage was re-equilibrated to room temperature before the next sample was loaded. SAXS and WAXS snapshots of material references were collected on the crystalline phytosterol, with and without Milli-Q water, and the aqueous phase with WPI after storage at 4 °C for 24 h.

Baseline correction was performed using the Australian Synchrotron SAXS/WAXS software (ScatterBrain, V2.71, Australia). Diffraction peaks were analyzed, as a function of time and phytosterol concentration, in terms of the maximum intensity and the full-width at half-maximum (fwhm) using MatLab (Math Works Inc., Matlab R2014b, USA). The Gaussian peak analysis

$$f(x) = a\, e^{-(x-b)^2/2c^2} \quad (2)$$

function (eq 2) was used to analyze the multiple peaks in each pattern. In this equation a is the height of the diffracted peak, b is the center position of the peak, and c is the peak's full width at half of its maximum intensity. The fwhm can provide structural information on the level of ordering within a TAG system.[30]

Confocal Laser Scanning Microscopy. Visualization of the emulsion droplets was carried out at the National Food Imaging Centre at Teagasc (Fermoy, Ireland). Emulsions were prepared in the same manner and at the same pressure but utilized an APV1000 homogenizer instead (SPX flow, Germany). Imaging was carried out using a Leica TCS SP5 confocal laser scanning microscope (CLSM; Leica Microsystems CMS GmbH, Wetzlar, Germany) using a 63× oil immersion objective at 3 and 5 times zoom factors. Dual confocal illumination was created by using an argon laser at 488 nm and a helium/neon laser at 633 nm to show lipids and proteins, respectively. Samples were prepared for imaging by adding 10 μL of Nile Blue (0.1 g/100 μL) into 1 mL of emulsion and vortexing for 10 s. Approximately 50 μL of labeled emulsion was placed on a microscope slide and a coverslip placed on top. Images (8-bit, 512 × 512 pixels) were obtained using simultaneous dual-channel imaging and were pseudocolored to show protein (red) and lipids (green). Emulsions were evaluated 24 h after preparation to evaluate the microstructure of the droplets after equilibration.

Statistical Analysis. Mean values ± standard deviations were reported for each employed treatment. Results were analyzed for statistical significance utilizing SAS 9.3 software for Windows. A Tukey's post hoc difference test with a level of probability at $p < 0.05$ was utilized to analyze significant differences between treatments.

RESULTS

Physical Properties of Emulsions. Particle sizes were expressed as the volume-weighted distributions of emulsions made with various amounts of phytosterol added to the fat phase (0.0, 0.3, and 0.6 wt %/wt). The droplet distribution of the PE emulsions ranged from 0.035 to 28.25 μm and was visualized on a logarithmic scale (Figure 1). Phytosterol addition resulted in a shift in the droplet size distribution and a reduction in the mean droplet diameter, reflected in the ($D_{4,3}$) values (Table 1). The particle size decreased significantly ($p < 0.05$) from an average of 1.17 ± 0.13 μm for the control emulsion to 0.99 ± 0.07 and 0.90 ± 0.04 μm for the 0.3 and 0.6% PE emulsions, respectively.

Emulsions (pH 6.8) were found to range in ζ-potential from −53.62 ± 4.53 to −47.34 ± 1.78 mV (Table 1), in agreement with previous research utilizing whey protein at an oil-in-water interface.[31,32] Emulsions were not found to have statistically different ζ-potential values ($p > 0.05$) following the addition of phytosterols, but these values tended to be less negative with phytosterol addition.

Emulsion stability was examined by assessment of creaming as a function of time. Droplet creaming is demonstrated by a decrease in the initial slope of the pattern and an increase in the backscattering at the top of the tube (Figure 2). Creaming was

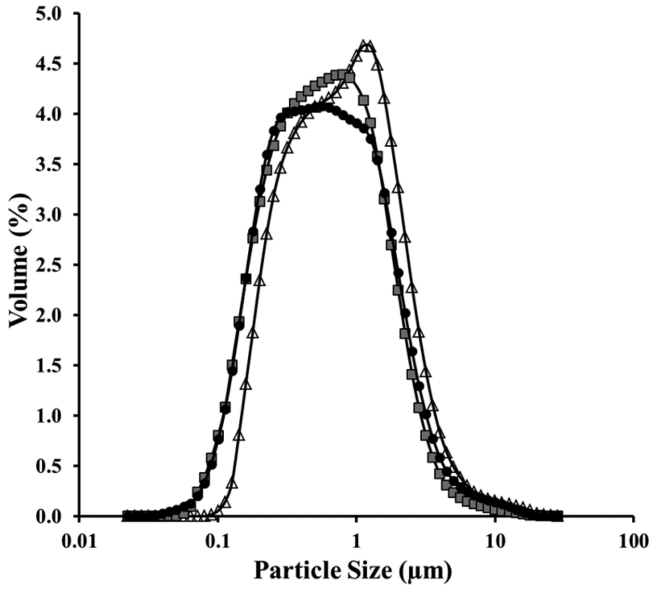

Figure 1. Particle size distribution of 10% milk fat/1% protein/89% H_2O emulsions with different phytosterol enrichment (PE) levels: (triangles) 0.0% PE emulsion (the control); (squares) 0.3% PE emulsion; (circles) 0.6% PE emulsion.

Table 1. Volume-Weighted Mean Diameters of Emulsions ($D_{4,3}$), ζ-Potentials, and Changes in Maximum Backscattering Percentages on Days 0 and 7 as a Function of Phytosterol Enrichment (PE) Level[a]

formulation	$D_{4,3}$ (μm)	ζ-potential (mV)	Δ in BS[b] (%)
0.0% PE emulsion	1.17 ± 0.13a	−53.62 ± 4.53a	8.28 ± 1.11a
0.3% PE emulsion	0.99 ± 0.07b	−51.07 ± 3.24a	7.48 ± 1.79a
0.6% PE emulsion	0.90 ± 0.04b	−47.34 ± 1.78a	6.80 ± 2.04a

[a]Lower case letters denote significant differences in Tukey's post hoc test with a $p < 0.05$. [b]Δ in BS = difference between backscattering maximums between days 0 and 7.

observed in all samples, increasing over time from days 1 to 7. Samples did not differ greatly between each other in terms of destabilization with the addition of phytosterols (Figure 2). The extent of creaming was quantified by subtracting the maximum backscattering percentages between days 0 and 7; the difference in percentage is reported as an absolute value in Table 1 and was not significantly different ($p > 0.05$) between treatments.

The microstructures of the emulsions were recorded using confocal laser scanning microscopy (CSLM) within 24 h of homogenization (Figure 3). All of the emulsions contained relatively small droplets with a range of different diameters ($d \approx 0.1-10$ μm), consistent with the particle size measurements (Table 1) and distributions shown in Figure 1. There were no visible differences between the control and the 0.3% PE emulsion at 3× and 5× magnification. However, in the 0.6% PE emulsion, visible crystals were present in larger droplets by negative contrast, creating an altered interface on the droplets and changing their shape (Figure 3).

Crystallization Properties. *Differential Scanning Calorimetry.* Emulsion samples consisting of different levels of phytosterol enrichment were heated to erase the previous thermal history and subjected to cooling at 3 °C/min until holding at 4 °C. During cooling, the start of crystallization (T_{onset}) differed significantly ($p < 0.05$) between all PE

DOI: 10.1021/acs.jafc.6b01722
J. Agric. Food Chem. 2016, 64, 6546−6554

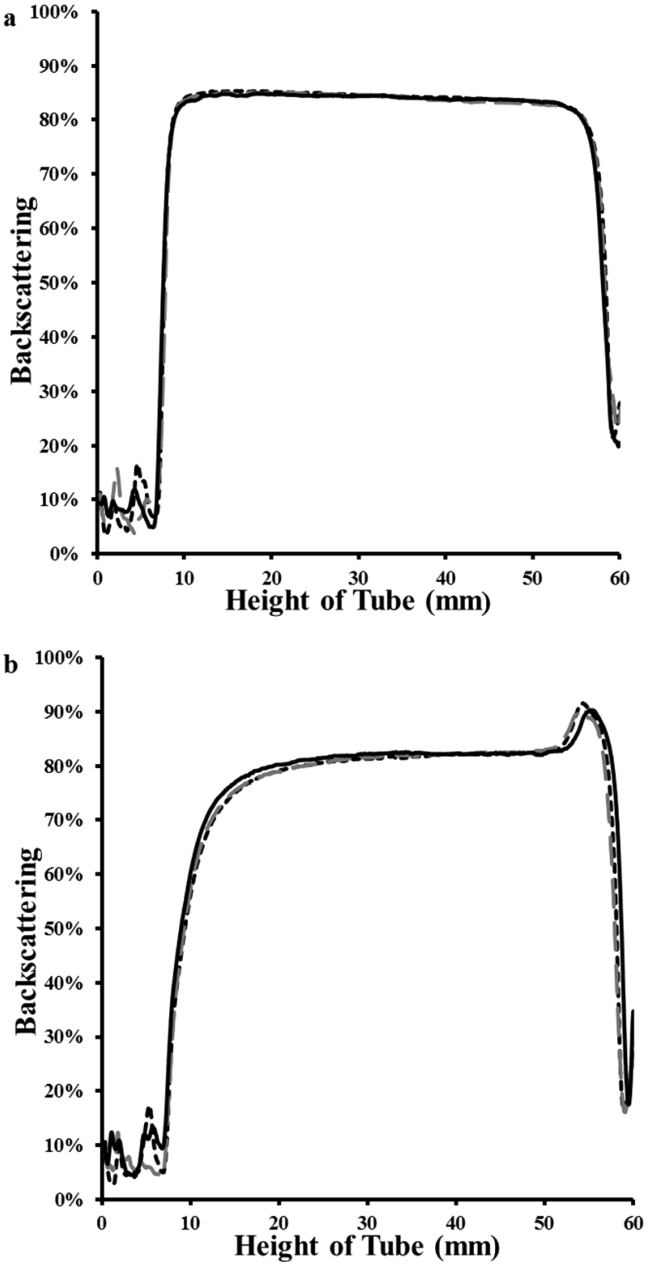

Figure 2. Turbiscan backscattering results of phytosterol-enriched (PE) emulsions during stability testing on (a) day 0 and (b) day 7. Emulsions are depicted as (dashed black line) 0.0% PE emulsion (the control), (gray dashed line) 0.3% PE emulsion, and (solid black line) 0.6% PE emulsion.

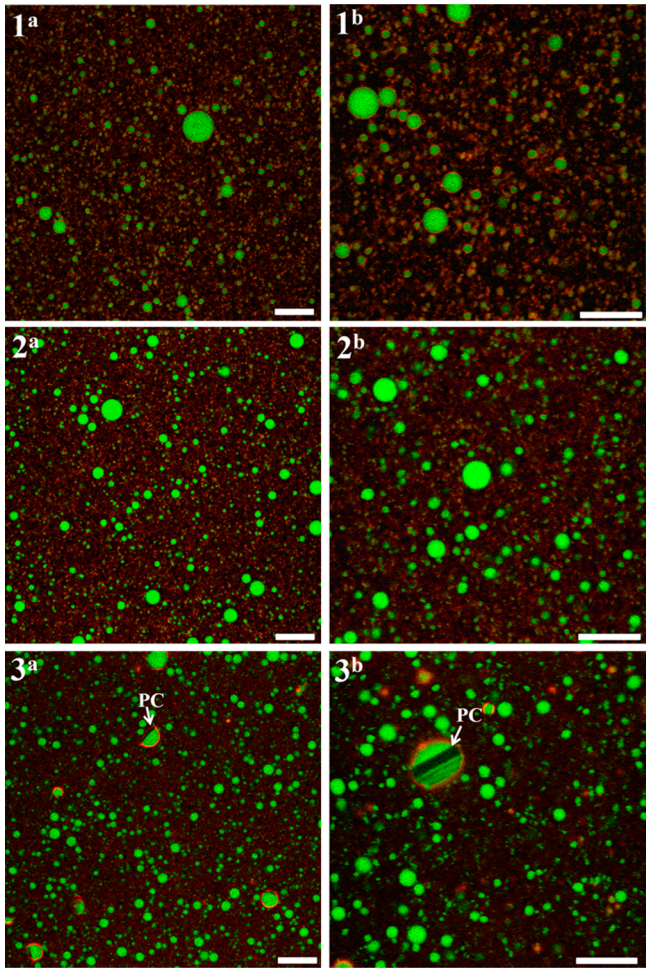

Figure 3. Confocal laser scanning micrographs of phytosterol-enriched (PE) emulsions at 3 and 5 times magnification superscripted as "a" and "b", respectively. Emulsions are labeled as (1) 0.0% PE emulsion (the control), (2) 0.3% PE emulsion, and (3) 0.6% PE emulsion. Micrographs show size distribution of milk fat droplets with fat represented in green and protein in red. Scale bar = 10 μm. Crystalline phytosterols both at the interface and within fat droplets are made visible by negative contrast (white arrows). PC = phytosterol crystal.

emulsions. The 0.3% PE emulsion nucleated first at 14.92 ± 0.12 °C (Figure 4a and Table 2). The control emulsion began crystallizing at 13.35 ± 0.16 °C followed by the 0.6% sample at 11.36 ± 0.03 °C. Subsequently, the thermal output of each emulsion peaked at significantly ($p < 0.05$) different temperatures in the same order as initial nucleation.

During heating at 10 °C/min, the T_{onset} or melting of 0.3% PE sample began at 7.06 ± 0.60 °C (Figure 4b and Table 2). This was followed by the control at 8.16 ± 0.52 °C and the 0.6% PE emulsion at 8.84 ± 0.16 °C. The order of melting between samples was similar to the exhibited T_{onset} order during cooling. During melting, the 0.3% PE emulsion peaked first at 12.22 ± 0.09 °C and then exhibited a second peak at 17.33 ± 0.17 °C to create a different pattern from the other two samples.

Thermodynamic changes in enthalpy were also measured during the heating and cooling regimes. During cooling, the change in enthalpy between emulsions was not significantly different between the 0.0, 0.3, and 0.6% PE emulsions. However, it should be noted that the 0.6% emulsion released 1.36 ± 0.02 J g^{-1}, even though its nucleation temperature was lower than that of the other PE emulsions. In addition, during the isothermal period, the 0.6% PE emulsion released more energy than both the control and the 0.3% PE emulsions to reach equilibrium at 4 °C (Figure 5b). During melting, there was no significant difference in the change in enthalpy among the samples.

Synchrotron SAXS and WAXS. Synchrotron X-ray scattering data, obtained under isothermal conditions, measured at small (SAXS) and wide (WAXS) angles, provided structural information such as the lamellar spacing, polymorphic forms, and the presence of phytosterol crystals adopted by the PE emulsions after cooling at −3 °C/min. The isothermal evolution at 4 °C for 5 min of the 0.6% PE emulsion is

DOI: 10.1021/acs.jafc.6b01722
J. Agric. Food Chem. 2016, 64, 6546−6554

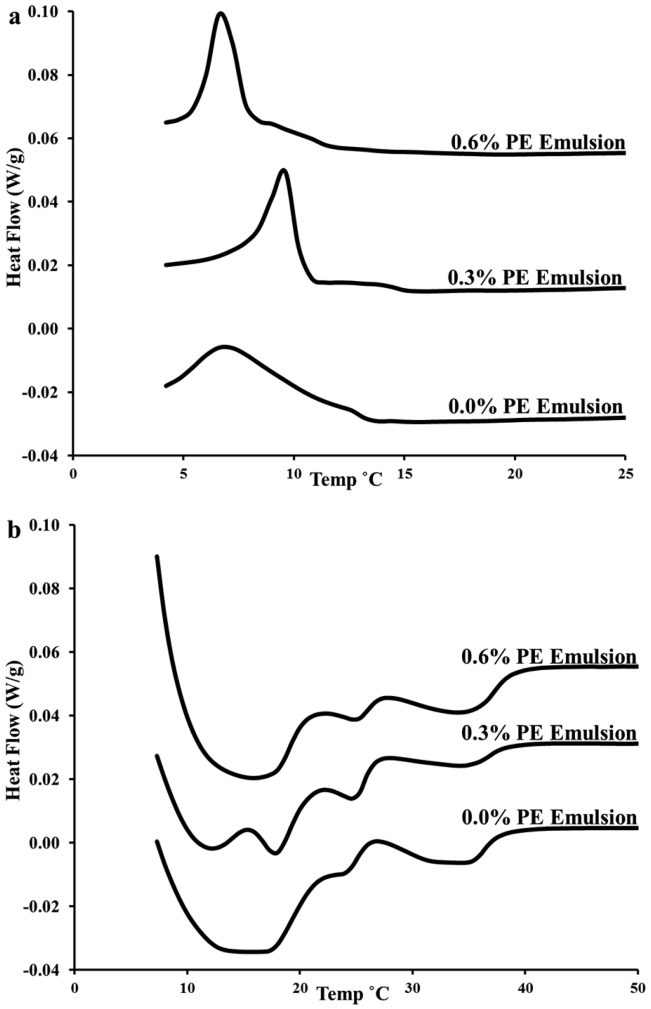

Figure 4. DSC thermographs of PE emulsions during (a) the cooling cycle at −3 °C/min and (b) the heating cycle at 10 °C/min.

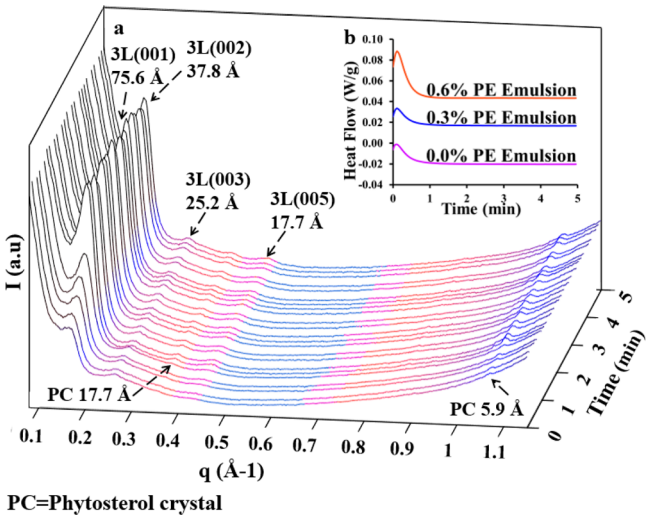

Figure 5. Structural evolution of 0.6% PE emulsion during the isothermal holding period at 4 °C after cooling at −3 °C/min. Graph includes SAXS diffraction pattern with WAXS overlap to demonstrate the development of phytosterol crystals (a). Corresponding DSC recordings during the 5 min hold are plotted with all of the PE emulsions to demonstrate the differences in thermal responses (b). PC = phytosterol crystal.

shown in Figure 5a. The triple-chain length (3L) second and third reflections, denoted 3L(002) and 3L(003), were observed first, which is expected as these are typically the most intense peaks.[30] After 1 min, the 3L(001) peak at 76.6 Å appears, along with the 3L(005) reflection at 15.1 Å. This transition is not a 2L to 3L transition, due to the early peak heights matching those of scans taken at the end of the isotherm; this has also been observed in other dispersed milk fat systems.[33] During the isotherm of the 0.6% sample, development of the phytosterol crystals can be observed (Figure 5a). At 0 min, the smaller phytosterol crystals at 5.9 Å are already present, but the larger crystals at 17.7 Å began to develop only after 1 min of holding at 4 °C. This crystal formation is accompanied by a large exothermic release in the DSC results (Figure 5b). The occurrence of phytosterol crystals was confirmed by diffraction patterns corresponding to the material references of the dry and aqueous dispersed phytosterol crystalline powder (Figure 6).

It can also be noted that the lamellar phase of the dispersed milk fat in the 0.0 and 0.3% samples developed identically to that in the 0.6% sample, but no additional crystal presence was recorded (data not shown).

Averaged diffraction patterns and values of the last 10 scans of all PE emulsions at the end of the isothermal period are displayed in Figure 7. The first, second, third, and fifth reflections of a characteristic lamellar phase were observed for all three samples. The lamellar packing of the emulsified milk fat crystals in the 0.0 and 0.3% PE emulsions was within the range of 55−75 Å, consistent with a 3L structure.[34,35] The 0.6% PE emulsion falls slightly outside this generally accepted range (75.6 Å), but is still considered to be a 3L system, as seen previously in milk fat with added polyunsaturated fatty acids.[36] All PE emulsions contained the characteristic 3L reflections at approximately 37, 25, and 14 Å, denoted 3L(002), 3L(003),

Table 2. Thermal Parameters Calculated from DSC Thermographs Recorded during Heating and Cooling Cycles of Phytosterol-Enriched (PE) Emulsions[a]

temp cycle	sample	T_{onset} (°C)	peak 1 (°C)	peak 2 (°C)	peak 3 (°C)	peak 4 (°C)	ΔH (J g^{-1})
cooling	0.0% PE emulsion	13.35 ± 0.16a	7.08 ± 0.03a				1.39 ± 0.04a
	0.3% PE emulsion	14.92 ± 0.12b	9.57 ± 0.09b				1.32 ± 0.04a
	0.6% PE emulsion	11.36 ± 0.03c	6.80 ± 0.08c				1.36 ± 0.02a
heating	0.0% PE emulsion	8.16 ± 0.52ab		16.60 ± 0.54a	21.88 ± 0.82a	34.50 ± 0.01a	−2.93 ± 0.74a
	0.3% PE emulsion	7.06 ± 0.60a	12.22 ± 0.09	17.33 ± 0.17b	24.72 ± 0.09a	34.38 ± 0.49a	−2.95 ± 0.35a
	0.6% PE emulsion	8.84 ± 0.16b		15.96 ± 0.29a	24.86 ± 0.10b	34.13 ± 0.34a	−3.22 ± 0.42a

[a] T_{onset} corresponds to the start of both crystallization and melting profiles for emulsions, ΔH corresponds to the total change in enthalpy during the heating or cooling profile. Lower case letters denote significant differences in Tukey's post hoc test with a $p < 0.05$.

DOI: 10.1021/acs.jafc.6b01722
J. Agric. Food Chem. 2016, 64, 6546−6554

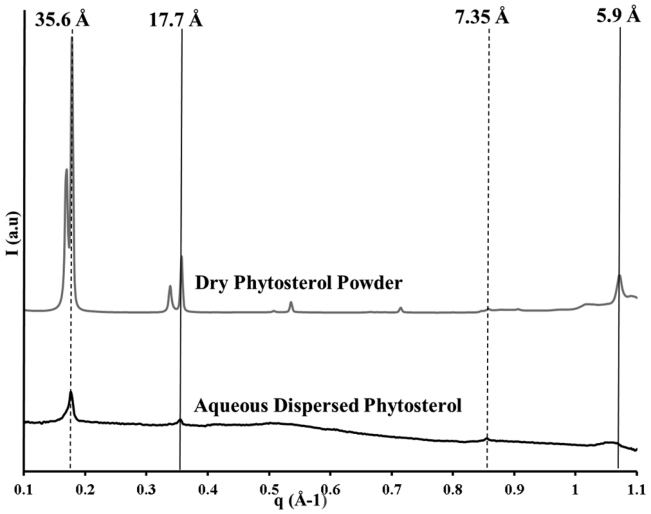

Figure 6. Diffraction patterns of material references: 5 wt %/wt phytosterol dispersed in water and dry phytosterol powder after storage at 4 °C for 24 h. Graph includes SAXS with WAXS overlap to show the phytosterol crystals present within both references. The solid line represents phytosterol peaks present in the PE emulsions after crystallization and are used for comparison. The dashed line marks phytosterol peaks that appear only after 24 h at 4 °C and are therefore not relevant.

and 3L(005), respectively. The 3L(004) reflection was absent as it is mainly observable within bulk milk fat systems.[36] The TAG lamellar spacing of the milk fat increased with higher levels of phytosterols in the emulsion. The control had the smallest 3L(001) *D*-spacing among samples at 74.0 Å, with the 0.3% sample and the 0.6% PE emulsion swelling to 74.9 and 75.6 Å, respectively (Figure 7a).

The largest and most intense reflection, 3L(002), was evaluated for its full-width at half-maximum (fwhm) expressed as $Å^{-1}$). The fwhm provides an indication of the level of disorder within the lamellar phase.[30] Here as phytosterol was added, the fwhm increased from 0.013 $Å^{-1}$ in the control sample to 0.014 $Å^{-1}$ in the 0.3% PE sample, and widened further to 0.016 $Å^{-1}$ in the 0.6% PE sample (Figure 7a). This is indicative of increased disorder within the lamellar structure as the phytosterol was incorporated. An α-packing type was observed throughout the samples at the same short spacing distance of 4.1 Å.[37] Phytosterols also crystallized separately in the 0.6% sample and were identified in both SAXS and WAXS patterns at 17.7 and 5.9 Å, respectively (Figure 7).

DISCUSSION

Influence of Physical Properties on the Emulsion System. Particle size, ζ-potential, stability, and confocal micrographs were used to evaluate the effect of phytosterol addition on the emulsion's physical properties. The particle size and appearance of the PE emulsion droplets were altered after phytosterols were dispersed within the lipid phase, whereas emulsion stability and ζ-potential were not affected. Phytosterols dispersed with a nonionic surfactant at a similar pH have been reported to have a ζ-potential of −45 mV, but in this system the protein's electrostatic repulsion at the droplet interface might have been too strong for the phytosterols to significantly influence the system.[38] The addition of phytosterols also did not contribute to creaming or destabilization within the emulsion systems.

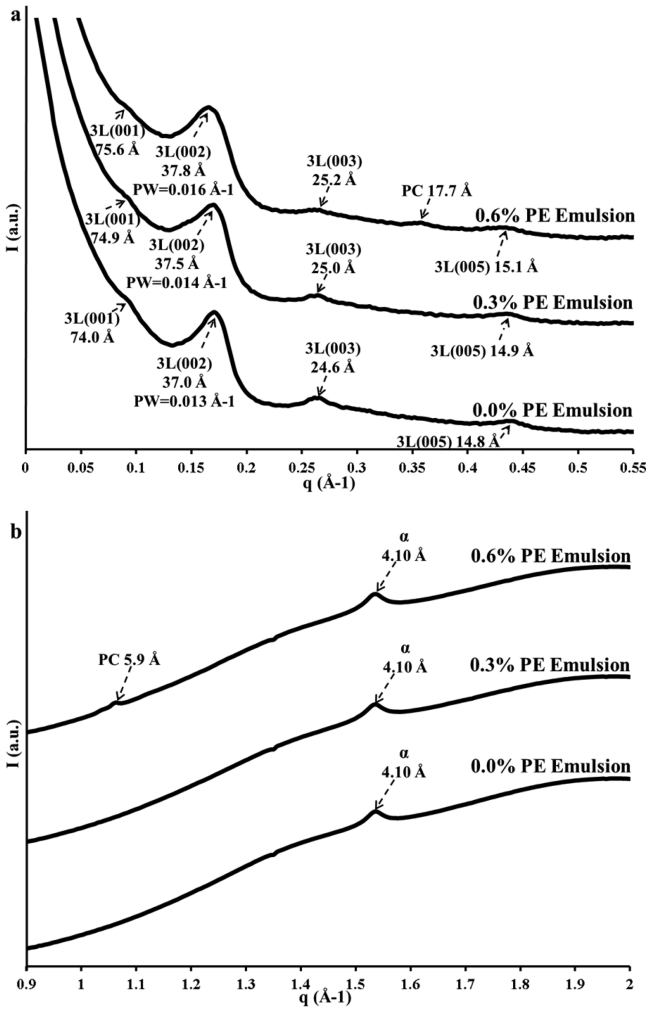

Figure 7. (a) Small and (b) wide-angle Synchrotron diffraction patterns captured at 4 °C after cooling at −3 °C/min. Values are averaged from the last minute of the 5 min isotherm after equilibrium was reached. PC = phytosterol crystal.

Phytosterol addition decreased the $D_{4,3}$ of the emulsion droplets and the appearance of droplets at 0.6% enrichment. It has been found previously that phytosterols possess the ability to lower interfacial tension and can pack together tightly at an oil−water interface.[39] The presence of water has been found to produce large monohydrated needle-shaped phytosterol crystals.[40] Thus, it is hypothesized that the elongated shapes observed in the confocal micrographs of our work were phytosterol crystals. This confirmation of an interfacial presence and crystallization supports the possibility that interfacial phytosterol interactions occurred within the emulsion systems. It is theorized that these surface interactions resulted in the decreased particle size observed within the 0.3 and 0.6% PE emulsions. To confirm these findings, more work is needed to characterize this type of interfacial phytosterol behavior in dispersed systems.

Thermal Analysis of Phytosterol-Enriched Emulsions. Differences in the thermal profiles of PE emulsions may be explained by understanding the concentration-dependent mechanism of phytosterol crystallization within the milk fat TAG matrix. In both the 0.3 and 0.6% PE emulsions, the dispersed phytosterols acted as an impurity, forming nucleation sites within the oil droplets; this resulted in volume-

DOI: 10.1021/acs.jafc.6b01722
J. Agric. Food Chem. 2016, 64, 6546−6554

heterogeneous nucleation. Volume-heterogeneous nucleation describes an emulsion with a higher number of impurities than available droplets. These impurities function as nuclei during cooling and thus initiate the crystallization of the dispersed fat.[41−44] In accordance with this mechanism, crystallization occurred in the 0.3% PE emulsion at 14.92 ± 0.12 °C, before the control at 13.35 ± 0.16 °C, as expected.

Thus, the 0.6% PE emulsion should have nucleated before the 0.3% PE emulsion, due to the higher concentration of impurities. It is hypothesized that the delayed nucleation was a result of the differences between how the phytosterols were partitioned between the 0.3 and 0.6% PE emulsions. In the 0.6% PE emulsion, separate phytosterol crystals formed and 3L longitudinal packing increased (Figure 7). Additional evidence for crystal formation was demonstrated by the higher energy released during the isothermal period in the 0.6% PE emulsion (Figure 5b). The phytosterols within 0.3% PE emulsion inserted themselves within the milk fat TAG network, but no large phytosterol crystals were detected (Figure 7). It is hypothesized that the higher activation energy observed within the 0.6% PE emulsion is the result of phytosterol crystal formation. Thus, supercooling is required to overcome this activation energy, which in turn delays the overall nucleation in the 0.6% PE emulsion. This type of concentration-dependent crystalline behavior has been observed in other systems with catalytic impurities, such as phospholipid-based lecithin. In an earlier study by Miskandar et al., soy lecithin was dispersed into palm oil blends at 0.03, 0.06 and 0.09 wt %/wt and monitored for solid fat content through nuclear magnetic resonance; the blends with the lowest concentration of soy lecithin, at 0.03%, were found to promote crystallization, through an increase in the solid fat content of the palm oil blends, compared to blends with 0.06−0.09% lecithin.[45,46]

Similarly, during the heating cycle, the 0.6% PE emulsion began melting (T_{onset}) at a higher temperature than both the control and the 0.3% PE emulsion. This can possibly be explained by the higher energy required to melt the phytosterol crystals formed during the isothermal holding period (Figure 5b). Additionally, the presence of these phytosterol crystals may have slowed the lamellar devolution of the TAG matrix through steric hindrance.[46,47] A similar response can be seen in delayed transitions between polymorphic phases such as α, β, and β' when different additives have been incorporated into the lipophilic carriers.[46,48−50] This was also supported by the Synchrotron results, where the highest amount of disorder was observed in samples with added phytosterols (Figure 7a). These results will be further discussed in the following section on emulsion crystallization.

Crystalline Structures and Morphologies of Phytosterol-Enriched Emulsions. Milk fat is composed of a complex mixture of TAG and can adopt lamellar structures in either 3L or 2L configurations.[30,36,51] All emulsions were found to demonstrate 3L crystalline packing, which is well recognized in dispersed milk fat systems cooled at 3 °C/min (Figure 7a).[30,34,36] The 0.6% PE emulsion is graphed for reference, during the isothermal evolution at 4 °C for 5 min, to exhibit the development of the milk fat TAG lamellar structure within the PE emulsions (Figure 5a). A 3L lamellar structure is observed within the sample, with the 3L(002) and 3L(003) diffracting first, followed by less intense reflections at 3L(001) and 3L(005). These results indicate that 3L packing had already developed within the dispersed phase at the start of the isothermal period, and the increase in intensity over time confirms these findings. Similar studies on milk fat have also recorded a slight delay between the development of all the 3L reflections.[33,52]

Most importantly, during the isothermal evolution of the 0.6% sample, it is possible to observe the development of the phytosterol crystals (Figure 5a). The graph includes a slight overlap with the WAXS region, allowing the presence of phytosterol crystals in the WAXS region at 5.9 Å at time zero to be clearly seen. After 1 min of holding at 4 °C, the second phytosterol crystal peak became apparent in the SAX region at 17.7 Å. As discussed previously, this development was accompanied by a large exothermic event in the 0.6% sample (Figure 5b). The 0.6% PE sample had a large heat of fusion during cooling as well, even though it crystallized later than the control and 0.3% PE samples. It is possible that the development of these phytosterol crystals would have required a large activation energy. Thus, delayed nucleation was observed as more energy was needed for crystallization of the phytosterols.

Differences were observed in the internal packing of the 3L crystal structures in the PE emulsions, which relates to the thickness of the laminar layers (Figure 7a). As such, an increase in long-spacing indicates that the distance between the repeated TAG units, that is, the spacing within the 3L laminar layers, is larger. The control sample had the shortest long-spacing at 74.0 Å. In contrast, the 3L structures of the 0.3 and 0.6% PE samples had thicknesses of 74.9 and 75.6 Å, respectively. This progressive increase in long-spacing suggests that, during lipid crystallization, phytosterols are able to incorporate themselves within the complex milk fat TAG matrix. This insertion enlarges the internal spacing between the laminar layers, but does not affect the spacing between the individual 3L units; thus, the same α-packing is retained throughout the samples. The 0.3 and 0.6% PE emulsions both influenced the lamellar packing of the milk fat TAG, but the 0.6% PE emulsion contains additional separate crystal peaks at 17.7 and 5.9 Å. These separate crystals could be within the TAG matrix or outside α-repeating units, but have been shown to affect both the TAG packing and thermal patterns of the emulsion matrices. A potential model for this system is demonstrated in Figure 8, which depicts how the phytosterols might be incorporated into the system.

Similar changes in the lamellar thickness have been seen in studies with different milk fat compositions.[36] An increase in the unsaturated fatty acids content of milk has been shown to result in an augmentation of long-spacing, similar to the observations from our work with phytosterol addition.[36] Upon

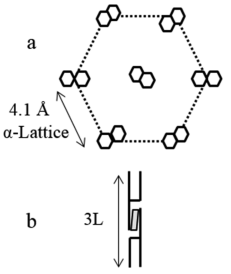

Figure 8. Lamellar structures of the dispersed fat phase in phytosterol-enriched PE emulsions, detailing the lateral chain packing in image a. Image b details the 3L structure of the TAG molecules. The tilted box represents a phytosterol crystal in its proposed position between TAG units.

DOI: 10.1021/acs.jafc.6b01722
J. Agric. Food Chem. 2016, 64, 6546−6554

adding polyunsaturated fatty acids into the bovine diet, Lopez et al. showed that there was an increase in the 3L(001) spacing in milk fat from 71.5 to 75.5 Å. The bent-chain morphology of the unsaturated fatty acids within the TAG matrix of the enriched samples expanded the long-spacing during crystallization, but did not change the initial α-packing at 4.10 Å.[36]

The fwhm of the diffracted Synchrotron peaks can be an additional tool to understand the lamellar packing, indicating the internal organization of the system. In milk fat systems a larger fwhm is associated with a higher degree of disorder within the 3L or 2L TAG packing.[30] Larger fwhm values have been shown previously in milk fat fractions with a greater diversity of fatty acids. For example, Lopez and Ollivon reported that the olein milk fat fraction, consisting of more unsaturated fatty acids but with a lower diversity of TAG, has a smaller fwhm than that of unfractionated milk fat.[52] Similarly, in the conducted study, the control emulsion had the smallest fwhm at 0.013 $Å^{-1}$. When phytosterol concentration increased, so did the fwhm, to 0.014 $Å^{-1}$ in the 0.3% PE emulsion and to 0.016 $Å^{-1}$ in the 0.6% PE emulsion. In the emulsion, the insertion of phytosterol molecules into the dispersed phase further disordered the already complex TAG matrix, which in turn increased the fwhm.

The use of phytosterols in milk fat emulsions is of significant interest in the dairy and functional food industries. In this study, the physical, thermal, and structural consequences of adding these bioactives into dispersed milk fat systems were examined. These results demonstrated that phytosterols can be added at levels up to 0.6% with little impact on the emulsion stability or ζ-potential. The addition of these molecules into a dispersed system was found to decrease the average mean particle size and distribution along with changing the physical appearance of some droplets, with large phytosterol crystals forming near the droplet interface at 0.6% enrichment. Phytosterol addition was also found to affect crystallization properties of the system and was concentration dependent. In the 0.6% PE emulsion, nucleation was delayed and a larger amount of energy was released during the cooling and isothermal period, as compared to the control and 0.3% emulsions. These DSC results coincided with the formation of nonsolubilized phytosterol crystal growth. Phytosterol enrichment in emulsions also changed the long-spacing of the observed lamellar structure, expanding the structure, but not changing the overall α-packing of this system. This indicates that, during crystallization, whereas phytosterols could integrate between TAG units, they could not influence the polymorphic form created. Little work has been done to characterize milk fat emulsions enriched with bioactive compounds. Thus, the results of this fundamental study can be used to further develop this area of research, as well as provide valuable information to the functional food industry regarding the effects of phytosterol addition on milk fat systems.

AUTHOR INFORMATION

Corresponding Authors

*(A.L.) Phone/fax: +61 (0)3 9731 3478. E-mail: Amy.Logan@csiro.au.

*(M.A.E.A.) Phone/fax: +353 (0)25 42442. E-mail: mark.auty@teagasc.ie.

Funding

We thank the Teagasc Food Research Centre for its support (Teagasc Project RMIS6412).

Notes

The authors declare no competing financial interest.

ACKNOWLEDGMENTS

We thank the Teagasc Food Research Centre for assistance in organizing this collaborative project and the Australian Synchrotron for beamline access (proposal no. M8476). We also thank Christelle Lopez (INRA Rennes, France) and Nigel Kirby (Australian Synchrotron, Melbourne, Australia) for invaluable guidance in setting up the Synchrotron experiment. Additionally, we thank Mi Xu, Sofia Oiseth, and Li Day (CSIRO, Melbourne, Australia) and Dale Osborn and Tamar Greaves (RMIT, Australia) for their assistance in this project.

ABBREVIATIONS USED

PE, phytosterol-enriched; TAG, triacylglycerol; $D_{4,3}$, volume-weighted mean diameters; DSC, differential scanning calorimetry; SAXS, small-angle X-ray scattering; WAXS, wide-angle X-ray scattering; fwhm, full-width at half-maximum; 3L, triple-chain length; 2L, double-chain length

REFERENCES

(1) Berger, A.; Jones, P.; Abumweis, S. S. Plant sterols: factors affecting their efficacy and safety as functional food ingredients. *Lipids Health Dis.* **2004**, *3*, 907−919.

(2) MacKay, D.; Jones, P. Phytosterols and cardiovascular disease. *Bioactive Food as Dietary Interventions for Cardiovascular Disease*; Elsevier: 2013; p 171.

(3) Plat, J.; Mackay, D.; Baumgartner, S.; Clifton, P. M.; Gylling, H.; Jones, P. J. H. Progress and prospective of plant sterol and plant stanol research: report of the Maastricht meeting. *Atherosclerosis* **2012**, *225*, 521−533.

(4) Plat, J.; Mensink, R. P. Plant stanol and sterol esters in the control of blood cholesterol levels: mechanism and safety aspects. *Am. J. Cardiol.* **2005**, *96*, 15−22.

(5) Smet, E. D.; Mensink, R. P.; Plat, J. Effects of plant sterols and stanols on intestinal cholesterol metabolism: suggested mechanisms from past to present. *Mol. Nutr. Food Res.* **2012**, *56*, 1058−1072.

(6) Ostlund, R. E., Jr. Phytosterols in human nutrition. *Annu. Rev. Nutr.* **2002**, *22*, 533−549.

(7) Rozner, S.; Aserin, A.; Wachtel, E. J.; Garti, N. Competitive solubilization of cholesterol and phytosterols in nonionic micro-emulsions. *J. Colloid Interface Sci.* **2007**, *314*, 718−726.

(8) Cusack, L. K.; Fernandez, M. L.; Volek, J. S. The food matrix and sterol characteristics affect the plasma cholesterol lowering of phytosterol/phytostanol. *Adv. Nutr.* **2013**, *4*, 633−643.

(9) Lagarda, M. J.; García-Llatas, G.; Farré, R. Analysis of phytosterols in foods. *J. Pharm. Biomed. Anal.* **2006**, *41*, 1486−1496.

(10) Clifton, P. Plant sterols and stanols as functional ingredients in dairy products. In *Functional Dairy Products*; Saarela, M., Ed.; Woodhead Publishing: 2007; Vol. 2, pp 255−261.

(11) Dickinson, E.; Leser, M. E. *Food Colloids: Self-Assembly and Material Science*; Royal Society of Chemistry: 2007; Vol. 308.

(12) Vaikousi, H.; Lazaridou, A.; Biliaderis, C. G.; Zawistowski, J. Phase transitions, solubility, and crystallization kinetics of phytosterols and phytosterol−oil blends. *J. Agric. Food Chem.* **2007**, *55*, 1790−1798.

(13) Franchetti, D. Analysis of co-crystallized free phytosterols with triacylglycerols as a functional food ingredient. *Food Res. Int.* **2016**, *85*, 104−112.

(14) Mattson, F. H.; Grundy, S. M.; Crouse, J. R. Optimizing the effect of plant sterols on cholesterol absorption in man. *Am. J. Clin. Nutr.* **1982**, *35*, 697−700.

(15) Carden, T. J.; Hang, J.; Dussault, P. H.; Carr, T. P. Dietary plant sterol esters must be hydrolyzed to reduce intestinal cholesterol absorption in hamsters. *J. Nutr.* **2015**, *145*, 1402−1407.

DOI: 10.1021/acs.jafc.6b01722
J. Agric. Food Chem. 2016, 64, 6546−6554

(16) Lubinus, T.; Barnsteiner, A.; Skurk, T.; Hauner, H.; Engel, K.-H. Fate of dietary phytosteryl/-stanyl esters: analysis of individual intact esters in human feces. *Eur. J. Nutr.* **2013**, *52*, 997−1013.
(17) Rondanelli, M.; Monteferrario, F.; Faliva, M. A.; Perna, S.; Antoniello, N. Key points for maximum effectiveness and safety for cholesterol-lowering properties of plant sterols and use in the treatment of metabolic syndrome. *J. Sci. Food Agric.* **2013**, *93*, 2605−2610.
(18) Gremaud, G.; Dalan, E.; Piguet, C.; Baumgartner, M.; Ballabeni, P.; Decarli, B.; Leser, M.; Berger, A.; Fay, L. Effects of non-esterified stanols in a liquid emulsion on cholesterol absorption and synthesis in hypercholesterolemic men. *Eur. J. Nutr.* **2002**, *41*, 54−60.
(19) Ostlund, R. E.; Spilburg, C. A.; Stenson, W. F. Sitostanol administered in lecithin micelles potently reduces cholesterol absorption in humans. *Am. J. Clin. Nutr.* **1999**, *70*, 826−831.
(20) Alexander, M.; Acero Lopez, A.; Fang, Y.; Corredig, M. Incorporation of phytosterols in soy phospholipids nanoliposomes: Encapsulation efficiency and stability. *Food Sci. Technol.* **2012**, *47*, 427−436.
(21) Shaghaghi, M. A.; Harding, S. V.; Jones, P. J. Water dispersible plant sterol formulation shows improved effect on lipid profile compared to plant sterol esters. *J. Funct. Foods* **2014**, *6*, 280−289.
(22) Pouteau, E. B.; Monnard, I. E.; Piguet-Welsch, C.; Groux, M. J. A.; Sagalowicz, L.; Berger, A. Non-esterified plant sterols solubilized in low fat milks inhibit cholesterol absorption. *Eur. J. Nutr.* **2003**, *42*, 154−164.
(23) Engel, R.; Schubert, H. Formulation of phytosterols in emulsions for increased dose response in functional foods. *Innovative Food Sci. Emerging Technol.* **2005**, *6*, 233−237.
(24) McClements, D. J. Enhancing nutraceutical bioavailability through food matrix design. *Curr. Opin. Food Sci.* **2015**, *4*, 1−6.
(25) Clifton, P. M.; Noakes, M.; Sullivan, D.; Erichsen, N.; Ross, D.; Annison, G.; Fassoulakis, A.; Cehun, M.; Nestel, P. Cholesterol-lowering effects of plant sterol esters differ in milk, yoghurt, bread and cereal. *Eur. J. Clin. Nutr.* **2003**, *58*, 503−509.
(26) Zhang, L.; Hayes, D. G.; Chen, G.; Zhong, Q. Transparent dispersions of milk-fat-based nanostructured lipid carriers for delivery of β-carotene. *J. Agric. Food Chem.* **2013**, *61*, 9435−9443.
(27) MacGibbon, A.; Taylor, M. Composition and structure of bovine milk lipids. In *Advanced Dairy Chemistry: Lipids*; Springer: 2006; Vol. 2, pp 1−42.
(28) McClements, D. J. Protein-stabilized emulsions. *Curr. Opin. Colloid Interface Sci.* **2004**, *9*, 305−313.
(29) Kirby, N. M.; Mudie, S. T.; Hawley, A. M.; Cookson, D. J.; Mertens, H. D.; Cowieson, N.; Samardzic-Boban, V. A low-background-intensity focusing small-angle X-ray scattering undulator beamline. *J. Appl. Crystallogr.* **2013**, *46*, 1670−1680.
(30) Lopez, C.; Bourgaux, C.; Lesieur, P.; Bernadou, S.; Keller, G.; Ollivon, M. Thermal and structural behavior of milk fat: 3. Influence of cooling rate and droplet size on cream crystallization. *J. Colloid Interface Sci.* **2002**, *254*, 64−78.
(31) Mao, L.; Calligaris, S.; Barba, L.; Miao, S. Monoglyceride self-assembled structure in O/W emulsion: formation, characterization and its effect on emulsion properties. *Food Res. Int.* **2014**, *58*, 81−88.
(32) Ye, A.; Lo, J.; Singh, H. Formation of interfacial milk protein complexation to stabilize oil-in-water emulsions against calcium. *J. Colloid Interface Sci.* **2012**, *378*, 184−190.
(33) Lopez, C.; Bourgaux, C.; Lesieur, P.; Bernadou, S.; Keller, G.; Ollivon, M. Thermal and structural behavior of milk fat: 3. Influence of cooling rate and droplet size on cream crystallization. *J. Colloid Interface Sci.* **2002**, *254*, 64−78.
(34) Lopez, C.; Bourgaux, C.; Lesieur, P.; Ollivon, M. Coupling of time-resolved synchrotron X-ray diffraction and DSC to elucidate the crystallisation properties and polymorphism of triglycerides in milk fat globules. *Lait* **2007**, *87*, 459−480.
(35) Widlak, N.; Hartel, R. W.; Narine, S. *Crystallization and Solidification Properties of Lipids*; American Oil Chemists' Society: 2001.
(36) Bugeat, S.; Perez, J.; Briard-Bion, V.; Pradel, P.; Ferlay, A.; Bourgaux, C.; Lopez, C. Unsaturated fatty acid enriched vs. control milk triacylglycerols: solid and liquid TAG phases examined by synchrotron radiation X-ray diffraction coupled with DSC. *Food Res. Int.* **2015**, *67*, 91−101.
(37) Lopez, C.; Bourgaux, C.; Lesieur, P.; Ollivon, M. Crystalline structures formed in cream and anhydrous milk fat at 4°C. *Lait* **2002**, *82*, 317−335.
(38) Rossi, L.; ten Hoorn, J. W. S.; Melnikov, S. M.; Velikov, K. P. Colloidal phytosterols: synthesis, characterization and bioaccessibility. *Soft Matter* **2010**, *6*, 928−936.
(39) Cercaci, L.; Rodriguez-Estrada, M. T.; Lercker, G.; Decker, E. A. Phytosterol oxidation in oil-in-water emulsions and bulk oil. *Food Chem.* **2007**, *102*, 161−167.
(40) Christiansen, L. I.; Rantanen, J. T.; von Bonsdorff, A. K.; Karjalainen, M. A.; Yliruusi, J. K. A novel method of producing a microcrystalline β-sitosterol suspension in oil. *Eur. J. Pharm. Sci.* **2002**, *15*, 261−269.
(41) McClements, D. J.; Decker, E. A.; Weiss, J. Emulsion-based delivery systems for lipophilic bioactive components. *J. Food Sci.* **2007**, *72*, R109−R124.
(42) Coupland, J. N. Crystallization in emulsions. *Curr. Opin. Colloid Interface Sci.* **2002**, *7*, 445−450.
(43) Skoda, W.; Van den Tempel, M. Crystallization of emulsified triglycerides. *J. Colloid Sci.* **1963**, *18*, 568−584.
(44) Fredrick, E.; Van de Walle, D.; Walstra, P.; Zijtveld, J. H.; Fischer, S.; Van der Meeren, P.; Dewettinck, K. Isothermal crystallization behaviour of milk fat in bulk and emulsified state. *Int. Dairy J.* **2011**, *21*, 685−695.
(45) Miskandar, M.; Che Man, Y.; Abdul Rahman, R.; Nor Aini, I.; Yusoff, M. Effects of emulsifiers on crystallization properties of low-melting blends of palm oil and olein. *J. Food Lipids* **2006**, *13*, 57−72.
(46) Ribeiro, A. P. B.; Masuchi, M. H.; Miyasaki, E. K.; Domingues, M. A. F.; Stroppa, V. L. Z.; de Oliveira, G. M.; Kieckbusch, T. G. Crystallization modifiers in lipid systems. *J. Food Sci. Technol.* **2015**, *52*, 3925−3946.
(47) Aronhime, J. S.; Sarig, S.; Garti, N. Mechanistic considerations of polymorphic transformations of tristearin in the presence of emulsifiers. *J. Am. Oil Chem. Soc.* **1987**, *64*, 529−533.
(48) Sato, K.; Kuroda, T. Kinetics of melt crystallization and transformation of tripalmitin polymorphs. *J. Am. Oil Chem. Soc.* **1987**, *64*, 124−127.
(49) Bunjes, H.; Koch, M. H.; Westesen, K. Effects of surfactants on the crystallization and polymorphism of lipid nanoparticles. In *Molecular Organisation on Interfaces*; Springer: 2002; pp 7−10.
(50) Joseph, S.; Rappolt, M.; Schoenitz, M.; Huzhalska, V.; Augustin, W.; Scholl, S.; Bunjes, H. Stability of the metastable α-polymorph in solid triglyceride drug-carrier nanoparticles. *Langmuir* **2015**, *31*, 6663−6674.
(51) Cisneros, A.; Mazzanti, G.; Campos, R.; Marangoni, A. G. Polymorphic transformation in mixtures of high-and low-melting fractions of milk fat. *J. Agric. Food Chem.* **2006**, *54*, 6030−6033.
(52) Lopez, C.; Bourgaux, C.; Lesieur, P.; Riaublanc, A.; Ollivon, M. Milk fat and primary fractions obtained by dry fractionation: 1. Chemical composition and crystallisation properties. *Chem. Phys. Lipids* **2006**, *144*, 17−33.

DOI: 10.1021/acs.jafc.6b01722
J. Agric. Food Chem. 2016, 64, 6546−6554